# Self-Assembly of Bay-Substituted Perylene Bisimides by Ligand-Metal Ion Coordination

Dissertation zur Erlangung
des naturwissenschaftlichen Doktorgrades der Julius-Maximilians-Universität Würzburg

vorgelegt von
Vladimir Stepanenko
aus Makinsk

Würzburg 2008

Eingereicht am: 19. November 2008
bei der Fakultät für Chemie und Pharmazie

1. Gutachter: Prof. Dr. Frank Würthner
2. Gutachter: Prof. Dr. Dirk Kurth

der Dissertation

1. Prüfer: Prof. Dr. Frank Würthner
2. Prüfer: Prof. Dr. Dirk Kurth
3. Prüfer: Prof. Dr. Anke Krüger

des öffentlichen Promotionscolloquiums

Tag des öffentlichen Promotionscolloquiums: 17. Dezember 2008

Doktorurkunde ausgehängt am: _____

*für meine Familie*

## Acknowledgment / Danksagung

Ich bedanke mich bei allen, die zum Gelingen dieser Arbeit beigetragen haben. Mein besonderer Dank gilt:

Meinem Doktorvater, Herrn Prof. Dr. Frank Würthner, für die sehr interessante und vielfältige Themenstellung und die Förderung dieses Themas durch zahlreiche wertvolle Anregungen und Diskussionen sowie für seine uneingeschränkte Unterstützung und die exzellenten Arbeitsbedingungen in seinem Arbeitskreis.

Der Deutschen Forschungsgemeinschaft (DFG) und Volkswagen Stiftung für die finanzielle Unterstützung.

Herrn Dr. Chantu Saha-Möller für seine exzellente und zuverlässige Überarbeitung von Manuskripten, Postern und Teilen der vorliegenden Doktorarbeit.

Herrn Dr. Rainer Dobrawa, Herrn Dipl.-Chem. Theo Kaiser, Herrn Dr. Peter Osswald, Herrn Dr. Zhijian Chen, Herrn Dipl.-Chem. Volker Dehm, Frau Dr. Catharina Hippius and Frau Dipl.-Chem. Stefanie Rehm für die hervorragende Zusammenarbeit, unzählige Diskussionen und Unterstützung im Labor.

Frau Dr. Marina Knoll (Lysetska) für die Einführung in die AFM-Nanowelt, die gute Zusammenarbeit und das sehr gute und freundschaftliche Arbeitsklima im AFM-Labor.

Frau Dr. Shinobu Uemura für ihr Engagement, die gute Zusammenarbeit und angenehme Zeit im AFM-Labor.

Frau Manuela Deppisch für die tatkräftige Unterstützung im Labor so wie ihre Engagement bei Freizeitunternehmungen und ihre immerwährende gute Laune.

Herrn Joachim Bialas für seine Hilfsbereitschaft im Labor.

Frau Ana-Maria Krause für die Durchführung der Cyclovoltammetriemessungen und ihre stete Hilfsbereitschaft während der gesamten Zeit.

Frau Christiana Toussaint und Herrn Dr. Chantu Saha-Möller für ihre schnelle und kompetente Hilfe bei Formalitäten und organisatorischen Angelegenheiten sowie für ihr Engagement für den Arbeitskreis in jeder Hinsicht.

Herrn Dr. Matthias Grüne und Frau Elfriede Ruckdeschel für die motivierte und kompetente Messung der NMR-Spektren.

Herrn Dr. Michael Büchner und Herrn Fritz Dadrich für die Aufnahme der Massenspektren.

Herrn Dipl.-Ing. Bernd Brunner für die kompetente Hilfe bei allen Computerfragen.

Allen aktuellen und ehemaligen Mitarbeitern des AK Würthner für die schöne Zeit, die gute Zusammenarbeit und das freundschaftliche Arbeitsklima.

Und zuletzt aber allen voran danke ich mich bei Euch, Svetlana und Oleg, für eure unschätzbare Unterstützung und die aufgebrachte endlose Geduld.

## List of Abbreviation

| | |
|---|---|
| AFM | Atomic Force Microscopy |
| BChl | Bacteriochlorophyll |
| Chl | Chlorophyll |
| COSY | Correlation Spectroscopy |
| DMF | *N,N′*-Dimethylformamide |
| DOSY | Diffusion Ordered Spectroscopy |
| ESI | Electrospray Ionization |
| FAB | Fast Atom Bombardment |
| HOPG | Highly Ordered Pyrolytic Graphite |
| HRMS | High Resolution Mass Spectrometry |
| LH | Light-harvesting |
| MALDI-TOF | Matrix-Assisted Laser Desorption Injection Time-of-Flight |
| MS | Mass Spectrometry |
| Mp | Melting Point |
| NMR | Nuclear Magnetic Resonance |
| PBI | Perylene Bisimide |
| ppm | parts per million |
| TMS | Tetramethylsilane |
| tpy | Terpyridine |
| UV/Vis | Ultraviolet/Visible |

## Table of Contents

**Introduction and Aim of This Thesis** **1**

**Chapter 1: Metallosupramolecular Dye Assemblies: Cycles and Polymers (-A Literature Survey -)** **5**

Cyclic Metallosupramolecular Dye Assemblies **6**

Cyclic Dye Assemblies by Coordination to External Metal Ion **7**

Cyclic Dye Assemblies by Coordination to Metallochromophore **17**

Metallosupramolecular Polymers **26**

Conclusion **36**

References **37**

**Chapter 2: Synthesis and Characterization of Regioisomerically Pure 1,7-Disubstituted Perylene Bisimide Dyes** **43**

Introduction **44**

Results and Discussion **46**

Synthesis **46**

Optical and Electrochemical Properties **51**

Conclusion **54**

Experimental Section **56**

References **65**

**Chapter 3: Metal-Ion Mediated Self-Assembly of Terpyridine-anchored Perylene Bisimides into Extended Rigid Polymers** **71**

Introduction **72**

Results and Discussion **75**

Synthesis of Tpy-anchored PBI Ligands **75**

Complexation of Monotopic Ligands with Zn(II) Ion **76**

Supramolecular Polymerization of Ditopic Ligands by Zn(II) Ion Coordination **79**

$^{1}$H DOSY NMR Investigations **82**

Optical Properties **83**

AFM Investigation of Coordination Polymers **87**

Electrostatic Self-Assembly of Coordination Polymers **92**
Conclusions **95**
Experimental Section **96**
References **104**

**Chapter 4: Honeycomb-Structured 2D Nanopatterns by Metal-Ion Directed Hierarchical Self-Assembly of Perylene Dyes** **109**
Introduction **110**
Results and Discussion **113**
Synthesis **113**
Study of Complexation Reaction of Ligand with Zn(II) Ion **113**
$^{1}$H DOSY NMR Investigations **115**
MALDI-TOF Mass Spectrometry **117**
Optical Properties **118**
AFM Investigation **119**
Conclusion **122**
Experimental Section **123**
References **126**

**Chapter 5: Summary** **129**

**Chapter 6: Zusammenfassung (Summary in German)** **135**

**Appendix** **143**

**List of Publications** **155**

# Introduction and Aim of this Thesis

One of the major focuses of modern supramolecular chemistry[1] is the organization of functional molecular building blocks by noncovalent interactions such as hydrogen bonding, π-π-interactions, dipolar and solvophobic interactions, and metal-ligand coordination.[2] The functional self-assembled architectures have found applications in catalysis,[3] data storage devices,[4] as photonic[5] and electronic[6] materials as well as sensors.[7]

Coordination bonds are highly directional and significantly stronger than other noncovalent interactions; moreover, thermodynamic and kinetic stability of such bonds can be fine-tuned by choosing a proper combination of ligand types and metal ions. Metal ion-ligand interaction provides excellent means for the fabrication of supramolecular systems which possess functionality like light harvesting and excitation energy transfer, and charge or ion transport. In the past decade, significant progress has been made in the area of functional metallosupramolecular architectures such as coordination polymers[8] and small discrete assemblies.[9]

The major aim of this thesis is the design and synthesis of novel perylene bisimide (PBI) building blocks and their metal-ion-induced self-assembly into metallosupramolecular architectures, in particular coordination polymers and metallomacrocyclic arrays that exhibit excellent photoluminescent properties and are stable in solution. Further, objective of this thesis is the construction of 2D nanopatterns on surfaces by metal-ion-directed hierarchical self-assembly of PBI dyes functionalized with appropriate receptors. 2,2′:6′,2″-Terpyridine (tpy) is chosen as receptor unit since tpy ligands are easily accessible by conventional synthetic methods and they possess defined complexation behavior with various transition metal ions. The present work reveals that the structural properties of PBI-based metallosupramolecular architectures can be tailored by structural variation of tpy ligand as supramolecular polymers are obtained by using linear bis(tpy) PBI ligands, while metallocycles are created from angular bis(tpy) PBI ligands.

***Chapter 1*** gives a brief overview on metal ion-directed self-assembly of dyes into macrocyclic and polymeric architectures and their functional aspect are discussed as well.

In ***Chapter 2***, the synthesis of regioisomerically pure 1,7-dibromoperylene bisimide and the nucleophilic replacement of bromine atoms by pyrrolidinyl groups that affords pure 1,7-difunctionalized mono and bisimide chromophores with optical properties reminiscent of those of chlorophyll *a* are described.

In ***Chapter 3***, the synthesis of novel red and green tpy-functionalized PBI building blocks and their metal-ion-directed self-assembly into coordination polymers are presented. The supramolecular coordination polymers have been studied in detail by $^{1}$H NMR, DOSY NMR, and UV/Vis spectroscopy. The polymer formation is visualized by atomic force microscopy (AFM) and the self-organization of PBI-based coordination polymers on surfaces has been explored by AFM. In this Chapter, the formation of alternate multilayer films of coordination polymers with different optical properties by electrostatic self-assembly using layer-by-layer technique is also described.

***Chapter 4*** reports the formation of honeycomb-structured 2D nanopatterns by metal-ion-directed hierarchical self-assembly of angular tpy-anchored PBI ligands. The formation of supramolecular metallomacrocycles was established by $^{1}$H NMR titration and DOSY experiments. The structural characterization of macrocycles was achieved by MALDI-TOF MS providing expected mass peak of the macrocycle and additional peaks of the multi-charged fragments. The optical properties of ditopic PBI ligand and cyclic trimer in DMF have been explored by UV/Vis absorption and fluorescence spectroscopy. AFM studies reveal the honeycomb-structured 2D assemblies of metallomacrocycles that cover the HOPG surface up to several square micrometers.

The thesis concludes with summaries in English (**Chapter 5**) and in German (***Chapter 6***).

## References

[1] a) J.-M. Lehn, *Supramolecular Chemistry: Concept and Perspectives*, VCH-Weinheim, **1995**; b) J.-M. Lehn, *Proc. Natl. Acad. Sci. U.S.A*. **2002**, *99*, 4763-4768; c) G. M. Whitesides, M. Boncheva, *Proc. Natl. Acad. Sci. U.S.A*. **2002**, *99*, 4769-4774; d) J.-M Lehn, *Chem. Soc. Rev.* **2007**, *36*, 151-160.

[2] a) J. A. A. W. Elemans, A. E. Rowan, R. J. M. Nolte, *J. Mater. Chem.* **2003**, *13*, 2661-2670; b) H. M. Keizer, R. P. Sijbesma, *Chem. Soc. Rev*. **2005**, *34*, 226-234; c) F. J. M. Hoeben, P. Jonkheijm, E. W. Meijer, A. P. H. J. Schenning, *Chem. Rev*. **2005,** *105*, 1491-1546; d) J. A. A. W. Elemans, R. van Hameren, R. J. M. Nolte, A. E. Rowan, *Adv. Mater.* **2006**, *18*, 1251-1266; e) T. Rehm, C, Schmuck, *Chem. Commun.* **2007**, 801-813.

[3] a) P. J. Stang, B. Olenyuk, *Angew. Chem.* **1996**, *108*, 797-802; *Angew. Chem. Int. Ed. Engl.* **1996**, *35*, 732-736; b) M. L. Merlau, M. P. Mejia, S. T. Nguyen, J. T. Hupp, *Angew. Chem.* **2001**, *113*, 4369-4372; *Angew. Chem.* **2001**, *40*, 4239-4242; c) V. F. Slagt, P. Kaiser, A. Berkessel, M Kuil, A. M. Kluwer, P. W. N. M. van Leeuwen, J. N. H. Reek, *Eur. J. Inorg. Chem.* **2007**, *29*, 4653–4662; d) C. G. Oliveri, P. A. Ulmann, M. J. Wiester, C. A. Mirkin, *Acc. Chem. Res*. **2008**, *DOI: 10.1021/ar800025w*; e) A. C. Laungani, J. M. Slattery, I. Krossing, B. Breit, *Chem. Eur. J.* **2008**, *14*, 4488-4502.

[4] a) P. L. Anelli, N. Spencer, J. F. Stoddart, *J. Am. Chem. Soc.* **1991**, *113*, 5131-5133; b) Y. Q. Wen, Y. L. Song, G. Y. Jiang, D. B. Zhao, K. Ding, W. F. Yuan, X. Lin, H. J. Gao, L. Jiang, D. B. Zhu, *Adv. Mater.* **2004**, *16*, 2018-2021; c) J. E. Green, J. W. Choi, A. Boukai, Y. Bunimovich, E. Johnston-Halperin, E. DeIonno, Y. Luo, B. A. Sheriff, K Xu, Y. S. Shin, H.-R. Tseng, J. F. Stoddart, J. R. Heath, *Nature* **2007**, *445*, 414-417.

[5] a) F. Würthner, *Chem. Commun.* **2004**, *14*, 1564-1579; b) F. Würthner, Z. Chen, F. J. M. Hoeben, P. Osswald, C.-C. You, P. Jonkheijm, J. von Herrihuyzen, A. P. H. J. Schenning, P. P. A. M. van der Schoot, E.W. Meijer, E. H. A. Beckers, S. C. J. Meskers, R. A. J. Janssen, *J. Am. Chem. Soc.* **2004**, *126*, 10611-10618; c) Z. Chen, V. Stepanenko, V. Dehm, P. Prins, L. D. A. Siebbeles, J. Seibt, P. Marquetand, V. Engel, F. Würthner, *Chem. Eur. J.* **2007***, 13,* 436-449; d) A. Ajayaghosh, A. K. Praveen, *Acc. Chem. Res.* **2007,** *40,* 644–656; e) M. W. Cooke, G. S. Hanan, *Chem. Soc. Rev.* **2007**, *36*, 1466-1476.

[6] a) F. Würthner, *Angew. Chem.* **2001**, *113*, 1069-1071; *Angew. Chem. Int. Ed. Engl.* **2001**, *40*, 1037-1039; b) K. Nørgaard, T, Bjørnholm, *Chem. Commun.* **2005**, 1812-1823; c) A. P. H. J. Schenning, E. W. Meijer, *Chem. Commun.* **2005**, 3245-3258; d) K. S. Chichak, A. Star, M. V. P. Altoé, J. F. Stoddart,

*Small* **2005**, *4*, 452-461 ; e) K. Tashiro, T. Aida, *Chem. Soc. Rev.* **2007**, *36*, 189-197.

[7] a) B. Valeur, I, Leray, *Coord. Chem. Rev.* **2000**; *205*, 3-40; b) D. T. McQuade, A. E. Pullen, T. M. Swager, *Chem. Rev.* **2000,** *100,* 2537-2574; c) L. Prodi, F. Bolletta, M. Montalti, N. Zaccheroni, *Coord. Chem. Rev.*, **2000**, *205*, 59-83; d) W. A. Alves, P. A. Fiorito, S. I. Córdoba de Torresi, R. M. Torresi, *Biosens. Bioelectr.* **2006**, *22*, 298–305; e) E. V. Anslyn, *J. Org. Chem.* **2007**, *72*, 687-699; f) M. Burnworth, S. J. Rowan, C. Weder, *Chem. Eur. J.* **2007**, *13*, 7828-7836.

[8] a) U. S. Schubert, C. Eschbaumer, *Angew. Chem.* **2002**, *114*, 3016-3050; *Angew. Chem. Int. Ed.* **2002**, *41*, 2892-2926; b) R. Knapp, S. Kelch, O. Schmelz, M. Rehahn, *Macromol. Symp.* **2003**, *204*, 267-286; c) R. Dobrawa, F. Würthner, *J. Polym. Sci. Part A: Polym. Chem.* **2005**, *43*, 4981-4995; d) D. G. Kurth, M. Higuchi, *Soft Matter* **2006**, *2*, 915-927; e) M. Burnworth, D. Knapton, S. J. Rowan, C. Weder, *J. Inorg. Org. Polym. Mater.* **2007**, *17*, 91-103; f) D. G. Kurth, *Sci. Technol. Adv. Mater.* **2008**, *9*, 014103.

[9] a) S. Leininger, B. Olenyuk, P. J. Stang, *Chem. Rev.* **2000**, *100*, 853-908; b) G. F. Swiegers, T. J. Malefetse, *Chem. Rev.* **2000**, *100*, 3483-3537; c) F. Würthner, C.-C. You, C. R. Saha-Möller, *Chem. Soc. Rev.* **2004**, *33*, 133-146; d) Y. Kobuke, *Eur. J. Inorg. Chem.* **2006**, *12*, 2333-2351; e) C. H. M. Amijs, G. P. M. van Klink, G. van Koten, *Dalton Trans.* **2006**, 308-327; f) S. J. Lee, J. T. Hupp, *Coord. Chem. Rev.* **2006**, *250*, 1710-1723; g) J. R. Nitschke, *Acc. Chem. Res.* **2007**, *40*, 103-112; h) M. W. Cooke, D. Chartrand, G. S. Hanan, *Coord. Chem. Rev.* **2008**, *252*, 903-921.

# Chapter 1

## Metallosupramolecular Dye Assemblies: Cycles and Polymers

### - A Literature Survey -

**Abstract**: Cyclic metallosupramolecular dye assemblies have become a focus of interest due to their resemblance to natural light harvesting photosynthetic complexes. In the past decade, numerous structurally impressive and novel macrocyclic dye architectures based on coordinative ligand-metal ion interaction have been designed and investigated. This chapter gives a brief overview on the current development in the field of metal-ion-directed self-assembly of dyes into macrocyclic and polymeric architectures. Functional aspects of such supramolecular dye assemblies have also been discussed.

## Cyclic Metallosupramolecular Dye Assemblies

One of the most important processes in nature is the photosynthesis.[1] It is the physico-chemical process by which plants, algae and photosynthetic bacteria convert solar energy into electrochemical energy and chemical potential energy is stored in carbohydrates and other organic compounds. The oxidation processes of carbohydrates supply energy to the living organisms. Photosynthesis starts with the absorption of photons by light-harvesting (LH) systems that consist of hundreds of pigment molecules (mainly chlorophyll (Chl) or bacteriochlorophyll (BChl) and carotenoids) anchored to proteins within the photosynthetic membrane and serve a specialized protein complex known as a reaction center. This process is followed by efficient energy migration within the light-harvesting systems until a reaction center is encountered.[1]

Since recent studies on native photosynthetic bacterial membranes using crystallography[2] and AFM measurement[3] (see Figure 1) have provided insight into cyclic arrangements of BChl in light-harvesting complexes, the investigation of well-designed cyclic metal-ion-directed self-assemblies of functional chromophores has

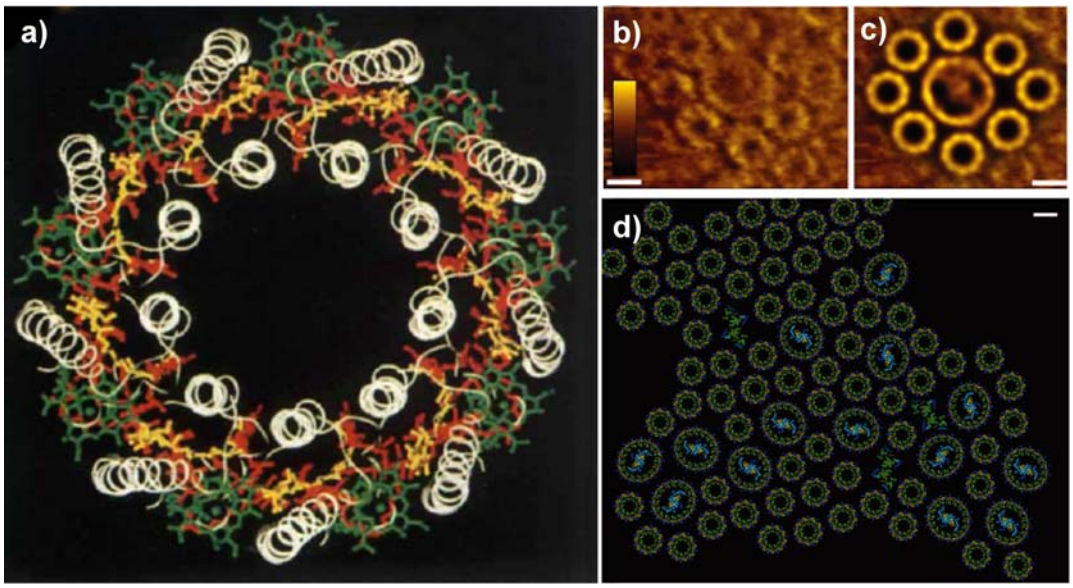


***Figure 1.*** Molecular organization of a photosynthetic apparatus: (a) The nanomeric complex viewed from the cytoplasmic side of the membrane. Protein units are presented as white, B800 BChl *a* green, B850 BChl *a* red, and carotenoids yellow. (Reprinted with permission from ref. 2a. Copyright (1995) Nature Publishing Group). (b) Raw-data AFM topograph of a native chromophore membrane, *z* scale is 3 nm; (c) fitting of the LH2 and core-complex averages corresponding to the relative position and orientation in the topograph; (d) core-complex model of LH2; bars are 5 nm. (Reprinted with permission from ref. 3b. Copyright (2004) The National Academy of Science, U.S.A.)

become increasingly more important and gained recognition as a topical field in supramolecular chemistry.[4]

The development and investigation of artificial model systems of LH complexes based on cyclic dye architectures is of significant importance to acquire knowledge on harvesting and conversion of solar energy and for exploring potential application of such artificial systems in molecular energy conversion devices. Properly designed supramolecular dye assemblies have not only potential to be used as artificial LH systems, but also for applications in the fields of molecular recognition, sensing and supramolecular catalysis. In the past years, several reviews were published on cyclic coordination architectures created by self-assembly of suitably designed ligands and specific metal ions.[5] Cyclic chromophore arrays with cavities of variable sizes and shapes are accessible upon formation of macrocycles. By spontaneous reaction between properly predesigned ligands and metal ions, desirable self-assembled architectures may be obtained. Triangular, square, pentagonal and hexagonal assemblies can be produced by coordination reactions of ligands and metal corner units with 60°, 90°, 108°, and 120° angles, respectively.[5]

**Cyclic Dye Assemblies by Coordination to Metal Ions.** As one of the early examples, Fujita and co-workers reported the self-assembly of (ethylenediamine)palladium(II) dinitrate [enPd$(NO_3)_2$] or Pt(II) salt with 4,4′-bipyridine in methanol-water solution in 1990.[6] This self-assembly led to the formation of a kinetically stable planar square **1**, which was obtained in high yield under the conditions of thermodynamic control proved by $^1$H NMR spectroscopy. Meanwhile, several other groups led by Stang[7], Würthner,[8] and Hupp[9] used the concept of metal-ligand interactions in order to construct well-defined square architectures. Stang and co-workers improved the structure of square **1**, where the organic soluble phosphine derivative was used as metal corner unit. The highly soluble metallosupramolecular squares **2** were investigated by X-Ray analysis that revealed a high degree of $\pi$-stacking between one of the phenyl groups of the phosphine ligand and the pyridine rings. This imposes considerable rigidity on the corner unit and fixes the angle between the two adjacent coordination sites.

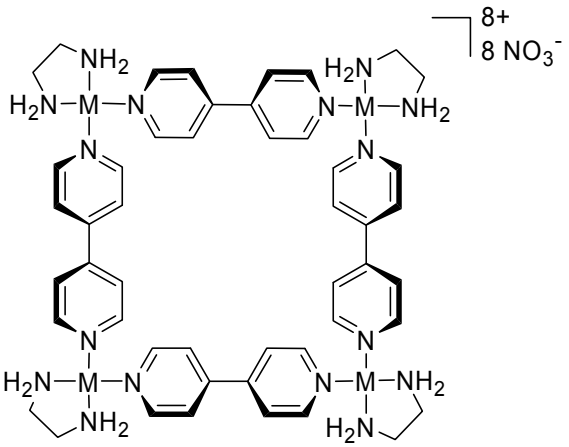


**1**

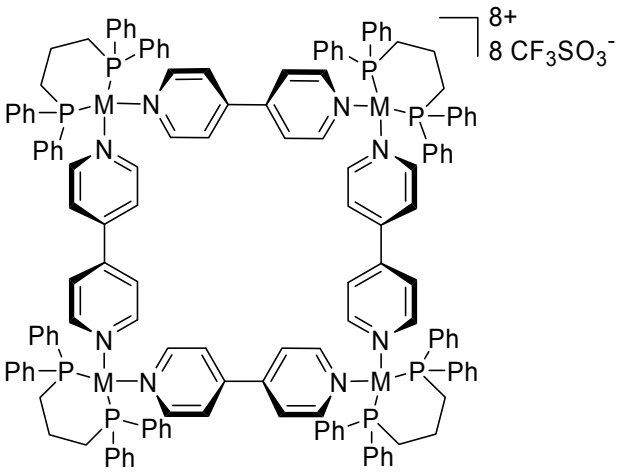


**2**

The use of phosphine groups as metal corner units significantly extended the chemistry of square compounds. Thus, molecular squares with variety of ditopic ligands, *e.g.*, dicyanobiphenyl, dicyanobenzene, diazapyrene, diazabenzoperylene (square **3**), and 2,6-diazaanthracene (square **4**), were synthesized by metal-ion-mediated self-assembly with the square-planar *cis*-bis(phosphine) Pt and Pd bis(triflate) complexes in organic solvents.[7]

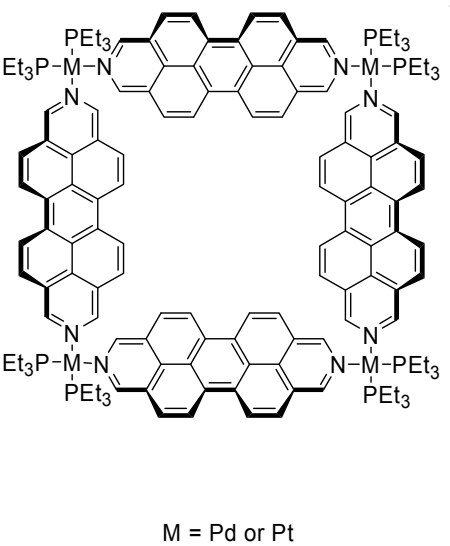


**3**

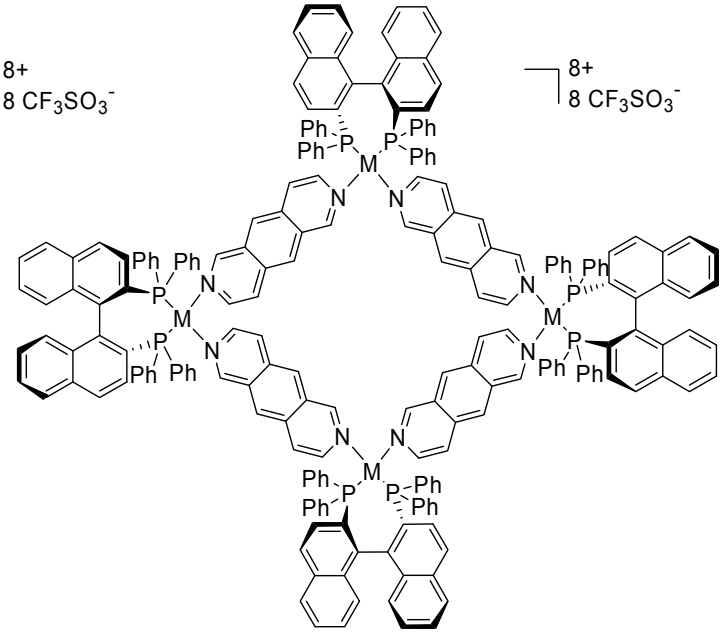


**4**

Despite of their size and multiple charges, these unique macrocyclic molecular squares are remarkably soluble in many common organic solvents and were fully characterized by $^{19}F$, $^{31}P$ and $^{13}C$ NMR technique, and elemental analysis, with the

exception of **3**, which was obtained as impure material in lower yields. Furthermore, the molecular squares **4** that are chiral due to molecular helicity, can be constructed by self-assembly between the chiral square-planar Pd(II) and Pt(II) bisphosphane triflate complexes and appropriate achiral bidentate diaza ligands as building blocks. These chiral molecular squares can be used for asymmetric catalysis and as model systems in biomimetic studies.[7c]

Würthner and co-workers have prepared a series of high fluorescent tetraphenoxy-substituted diazadibenzoperylene ligands.[8a,b] The complex dynamic equilibria between molecular triangles **5** and molecular squares **6** in solution were observed, when twisted fluorescent dyes were used as bridging ligands. Both macrocyclic assemblies can co-exist in solution, however, bulky *tert*-butylphenoxy substituents (p-*t*BuPh) shift the equilibrium towards square **6** due to the sterical obstruction for triangular species **5**. A similar self-assembly strategy was employed by Würthner's group for the preparation of perylene bisimide-based squares **7** that exhibit fluorescent properties.[8c-g] Because the pyridyl units in ditopic ligands are located at the imide position of the perylene core, where nodes exist in the HOMO and LUMO orbitals, the excellent fluorescent properties of uncomplexed chromophores remained unchanged in the metal-ion-assembled superstructures.

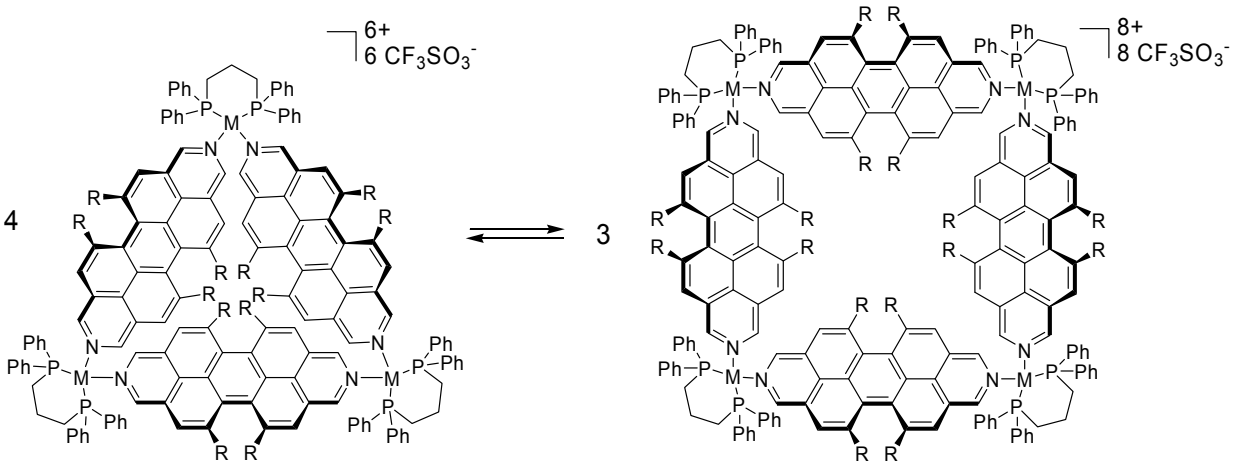


M = Pd or Pt, R = p-*t*BuPhO

**5**

M = Pd or Pt, R = p-*t*BuPhO

**6**

Further decoration of perylene bisimide (PBI) chromophores with functional scaffold, e.g. with 16 pyrene or 4-dimethylamino-1,8-naphthalimide dye units, led to the multichromophoric squares **7b** and **7c** which are reminiscent of cyclic dye assemblies in native LH systems.

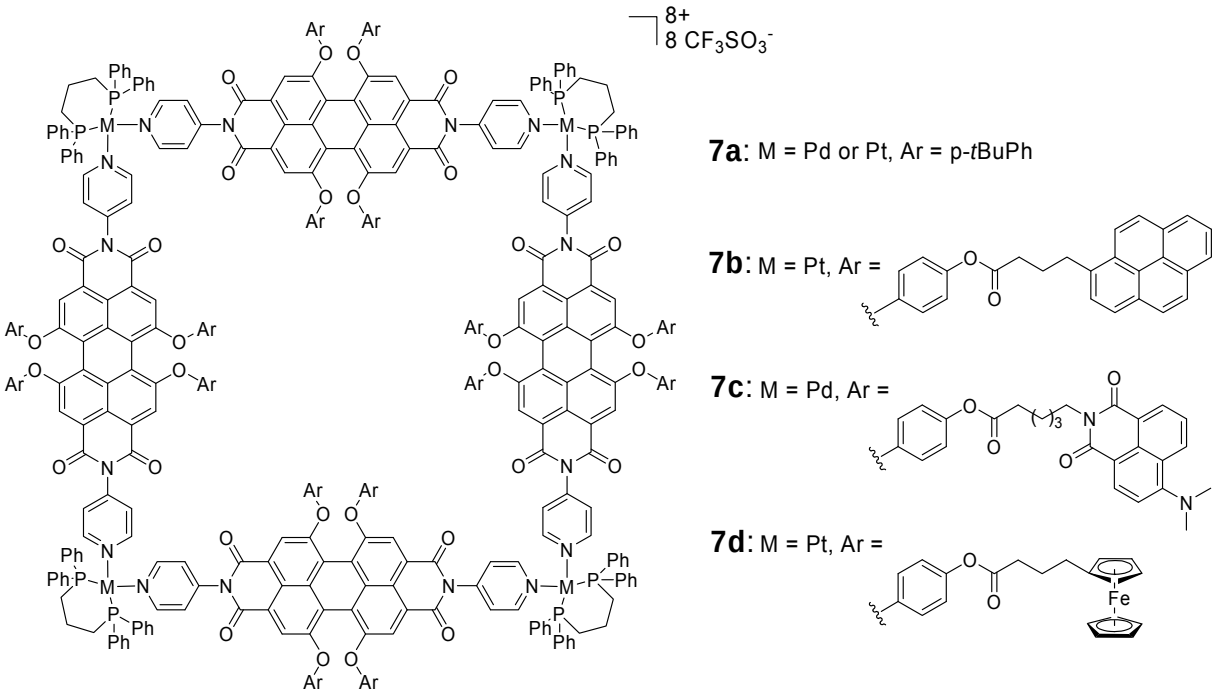


**7**

Steady-state and time-resolved fluorescence investigations showed that the energy absorbed by the peripheral dye units can be efficiently transferred to the core perylene bisimide dyes through a fluorescent resonance energy transfer (FRET) mechanism.[8g,h] For example, the pyrene-containing molecular square **7b** is an artificial light-harvesting system that combines a fast ($k_{en}$ = 5.0×10$^9$ s$^{-1}$) and efficient (90%) energy transfer with a very fast and even more efficient (>94%) electron-transfer process with rates of 5×10$^{11}$ to 43×10$^{11}$ s$^{-1}$ upon visible excitation.

When perylene bispyridyl imides were modified with four ferrocenyl moieties, the molecular squares **7d** containing 20 redox active units could be organized through metal-ion-mediated self-assembly.[8f] However, two reversible four-electron reductive processes for the inner four perylene bisimides could be observed by cyclic voltammetry. Thus, these are little influenced by the supramolecular arrangement. On the other hand, the redox properties of the 16 peripheral ferrocenyl groups are strongly affected by the sterical constraints which are imposed by the core square superstructure. In addition, the chemical oxidation of ferrocene-functionalized perylene bisimides could be realized by thianthrenium pentachloroantimonate and the redox process could be conveniently monitored by spectrophotometry. It was shown that metal-ion-directed self-assembly of square nanostructures can be used to organize redox active functional units in three-dimensional space.[8f]

The Pt(II) and Pd(II) bisphosphane complexes as metal corners could be successful used for the preparation of porphyrin squares **8** reported by Stang and co-workers.[10] The porphyrin and its Zn complex were chosen for this study because of their relatively straightforward preparation and, most important, their electron transfer, redox, and photoactivity properties. Incorporation of these species into multicomponent arrays revealed to be an attractive strategy for the construction of functional arrays, e.g. artificial LH systems. Moreover, high solubility of porphyrin dyes into common organic solvents facilitates the self-assembly process. Interaction of linear ditopic porphyrin ligands with the reactive Pt(II) or Pd(II) complexes in dichloromethane at room temperature results in the formation of the desired tetranuclear complexes **8** in excellent isolated yields. The square structures were confirmed by $^{1}H$ and $^{31}P$ NMR spectroscopy, elemental analysis, and mass spectrometry.

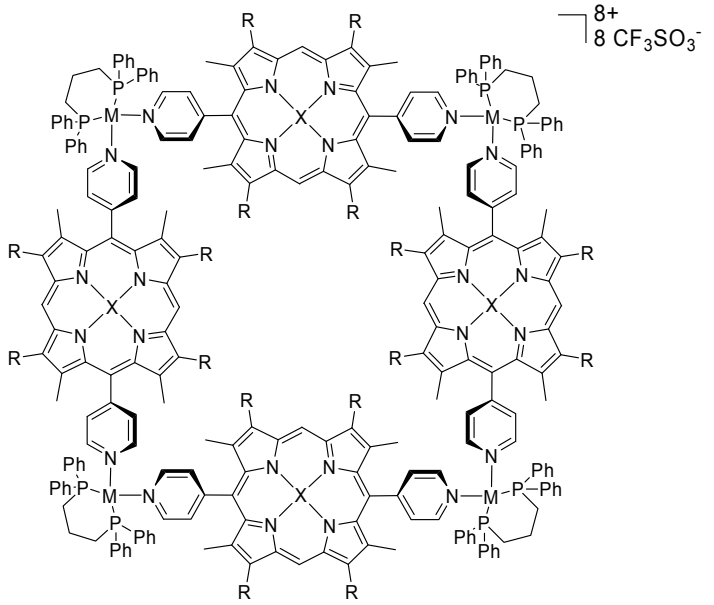


**8**

M = Pd or Pt, R = *n*-$C_6H_{13}$, X = 2H or Zn

Other approach to the design of porphyrin cyclic arrays was employed by Drain and Lehn.[11] Stable tetramers were synthesized by the ligation of *meso*-pyridylporphyrins or the corresponding zinc complexes to *cis* and *trans* square-planar Pt(II) and Pd(II) arrays. The 90° angle between the pyridyl groups in 5,10-dipyridylporphyrins or its zinc complexes and a trans substitution of Pd led to the formation of closed structure **9**. A similar trend was observed for the formation of isomeric Pt-based square compounds **10** from 5,15-dipyridylporphyrins and

corresponding zinc complexes. The photochemical properties of porphyrins impart a functionality to such assemblies that facilitates their characterization and yields insight into the structural and physico-chemical features of larger organized structures.

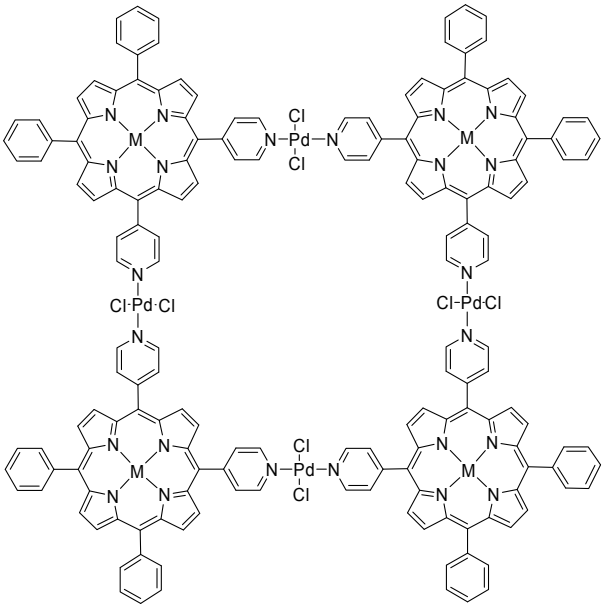

**9**

M = 2H or Zn

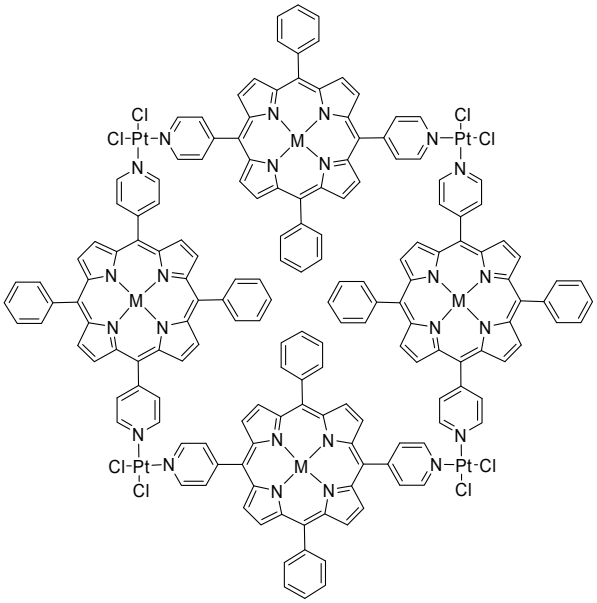

**10**

M = 2H or Zn

Molecular square **11** with the same framework as **10**, constructed by *trans*-substituted porphyrins and Re(I) corners, was reported by Hupp and co-workers.[9] The porhyrin-walled squares **11** were obtained in nearly quantitative yield and fully characterized by $^{1}$H NMR spectroscopy, elemental analysis, and mass spectrometry. The kinetically inert Re-N bond excludes the exchange of ligands in solution at room temperature, but at elevated temperature the square is formed apparently through thermodynamic control. The dimensions, pre-organization, and multiple binding site availability of tetrazinc(II)-metalated square **11** suggest the possibility of strong host-guest complex construction. Thus, the application of molecular square **11** as an encapsulant for manganese porphyrin epoxidation catalysts with enhanced catalyst lifetime and substrate selectivity was also described. Hupp's group was able to increase the binding constant for 4-(phenyl)pyridine to square **11** from $1.5\times10^{4}$ $M^{-1}$ to $1.4\times10^{5}$ $M^{-1}$ by discarding alkyl substituents in **12** and adding perfluorophenyl groups (values in dichloromethane).[9c] Since the perfluorinated substituents are strongly

electron withdrawing, the Lewis acidity of the Zn(II) sites is significantly increased, that strengthen the Zn-N interactions, leading to higher binding constant.

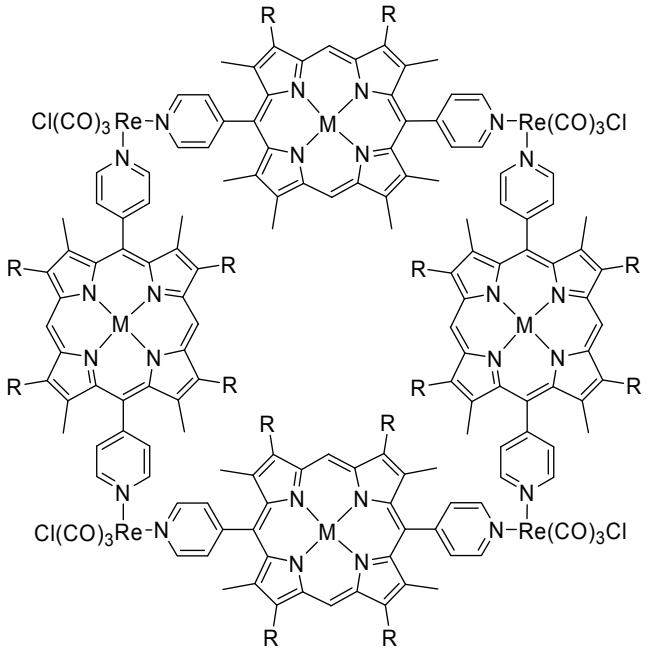

**11**

M = 2H or Zn, R = *n*-$C_4H_9$

Alessio and co-workers reported about the synthesis and characterization of 2+2 homometallic molecular squares of porphyrins obtained by self-assembly of 5,10-dipyridylporphyrin with neutral Ru(II) octahedral complexes.[12] Compared with the most of the previous examples of porphyrin-based molecular squares, which used square planar charged Pt(II) and Pd(II) complexes as structural units, the metallocyclic species **12** are neutral, thus providing greater solubility in organic solvents. Due to the inertness of the Ru-pyridyl bond, which provides kinetic stability to the molecular squares **12**, the authors could show that these discrete units, after metalation of the porphyrins, are suitable building blocks for the construction of more elaborate assemblies of higher order by axial coordination of bridging ligands. Using zinc porphyrin metallacycles **12**•$Zn_2$ as rigid building blocks, the construction of discrete supramolecular assemblies of porphyrins with cavities of well-defined shape and size was introduced. The perpendicular arrangement of chromophores in the molecular box **12a**[12c] consisting of two zinc-porphyrin metallacycles connected by two free-base 4′-*trans*-dipyridylporphyrins axially coordinated to the zinc centers bears a resemblance to that of bacteriochlorophylls in natural LH complexes.

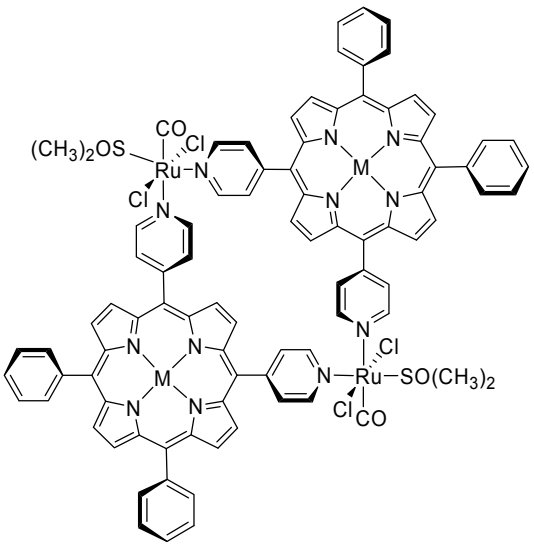


M = 2H or Zn

**12**

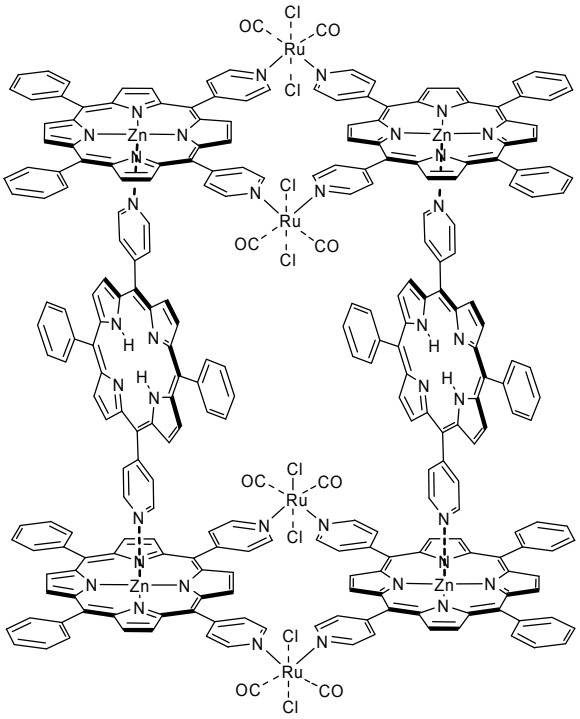


**12a**

Terpyridine (tpy) acts as π-acceptor to stabilize various metal oxidation states and exhibits strong chelating affinity with many transition metals.[13] Thus, tpy is one of the most widely-used ligands in metallosupramolecular chemistry. A series for heterometallic molecular squares was prepared by self-assembly of pyridine-modified tpy with Ru(II) salts, and Pd (II) bisphosphane complex by Sun and Lees.[14] Ferrocene units have been positioned at metal corner and applied as linker to achieve the redoxactive nanosize assembly **13**. This heterometallic square incorporating four redoxactive terpyridyl metal complexes as bridging ligands in addition to four ferrocene units is an attractive assembly for electrochemical sensing.

The terpyridine unit was successful used for the construction of triangle arrays such as **14** by Ziessel's group.[15] The geometric constraints built into the preorganized ligand based on 1,10-phenanthroline with an angle of 60° facilitated the formation of a cyclic trimer **14** upon complexation with Fe(II) ion. The triangular structure was confirmed by $^{1}H$ and $^{13}C$ NMR spectroscopy, and mass spectrometry.

A similar self-assembly strategy was employed by Newkome and co-workers for the preparation of cyclic terpyridine-based discrete structures. The cyclic architectures composed of di-, tri-, penta-, and hexa-nuclear bis(terpyridine)-metal units were prepared using appropriately designed angular ditopic bis(terpyridyl) ligands assembled by Fe(II), Ru(II), or Zn(II) ions coordination.[16]

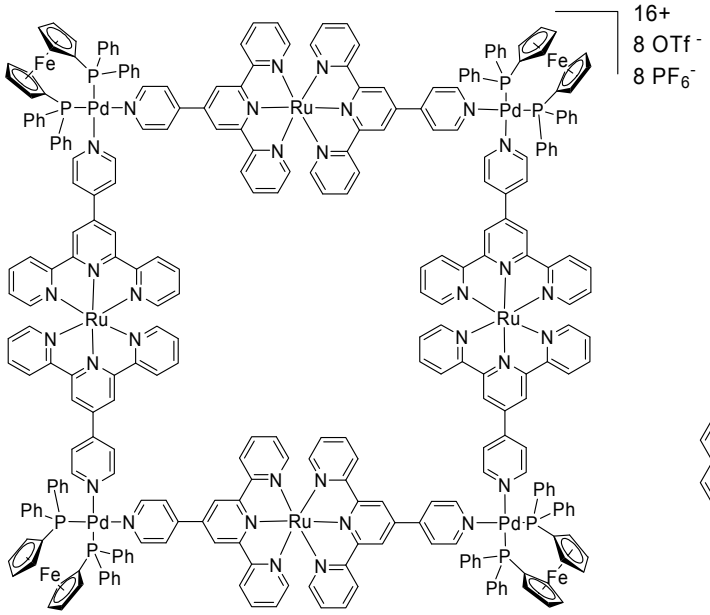


**13**

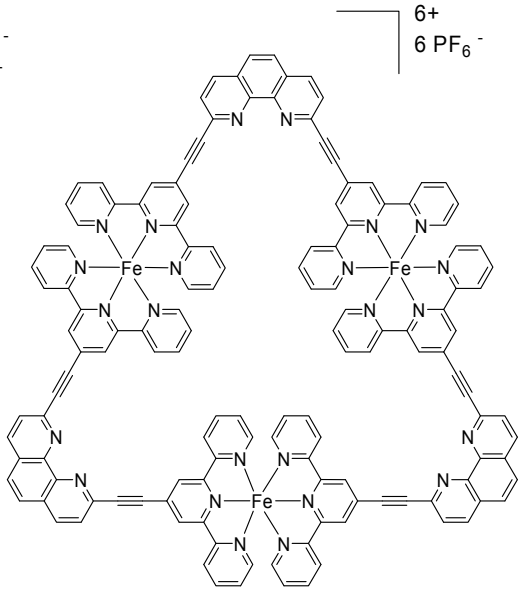


**14**

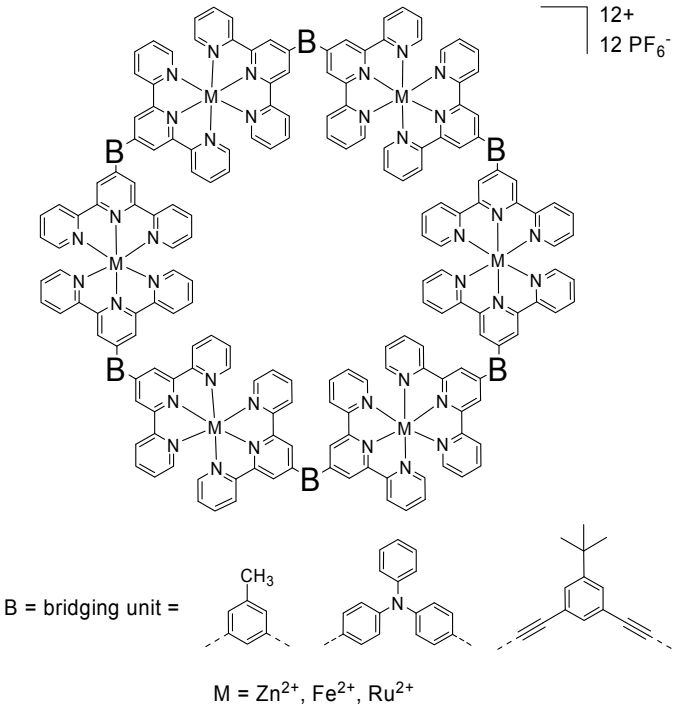


**15**

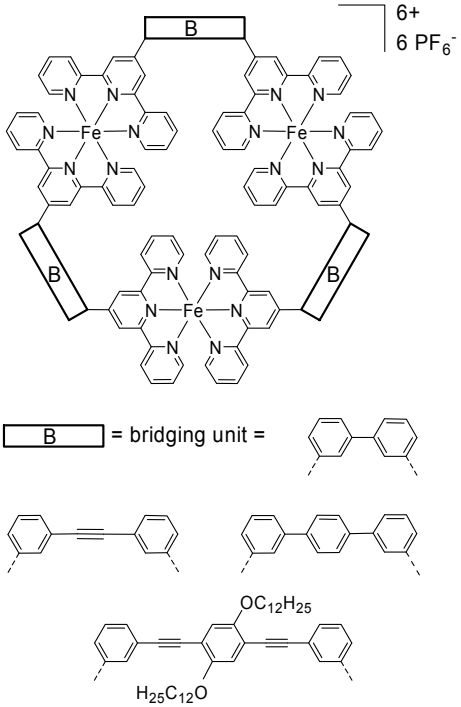


**16**

Heteronuclear hexameric metallomacrocycles **15**,[16a,b,d] which employ both Ru- and Fe-connectivity, was achieved by employing stepwise construction principle. This principle allows the specific introduction of different metal centers, coupled with the

ability to tailor the periphery of hexamacrocycles, and affords entry into novel shape-persistent architectures and cores for dendritic constructions. The characterization of the metallomacrocycles was carried out by $^{1}H$, $^{13}C$ NMR, UV spectroscopy, and mass spectrometry, as well as electrochemistry. The reversible redox characteristics of molecular assemblies **15** suggest that they are potential candidates for energy storage and release, as well as nanoscale molecular electronic and magnetic devices.[16b,d] Family of pentameric metallomacrocycles based on a carbazol unit as bridging ligand was also reported by Newkome and co-workers.[16c] The macropentacyclic complexes were used for coating of nanocrystalline $TiO_2$ in a Grätzel-type solar cell device. In the recent past, novel shape-persistent hexagonal macrocycles **16** could supplement the library of cyclic metal-ion-mediated supramolecular architectures.[16g] The complexation between bis(tpy) ligands and Fe(II) ion produced trimeric metallomacrocycle possessing hexagonal motif. The structures of complexes **16** were elucidated by $^{1}H$, $^{13}C$ NMR spectroscopy, and mass spectrometry. Their optical and electrochemical properties were also characterized.[16g]

Fascinate cyclic architectures were reported by Lehn and co-workers.[17] The self-assembly of circular helices whose frameworks are templated by counter anions of metal ions yields pentanuclear and hexanuclear complexes **17** and **18**, respectively. The complexation of tris-bipyridine ligand with $FeCl_2$ salts results first in a kinetic polymeric product. This progressively converts into the thermodynamic pentanuclear cyclic array which incorporates a chloride ion in the cavity as evidenced by X-ray analysis. In contrast, the self-assembly of the same ligand with $FeSO_4$ and $Fe(BF_4)_2$ gives hexanuclear complex. Two levels of self-assembly can be distinguished in the present system. First, the organization of the ligands around the metal ions, which results in a helical architecture. Second, the ring closure into a torus of defined size.

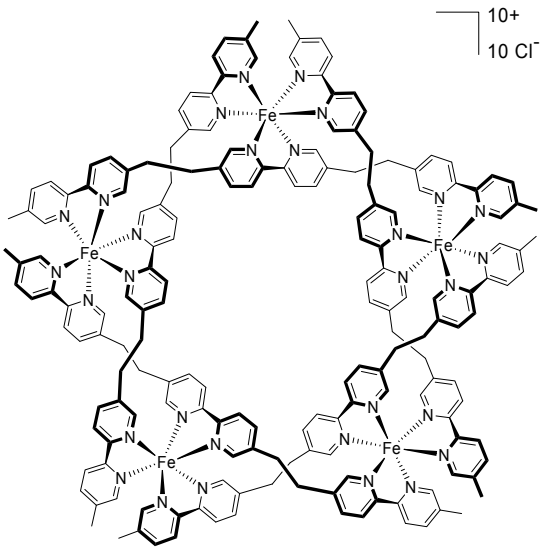


**17**

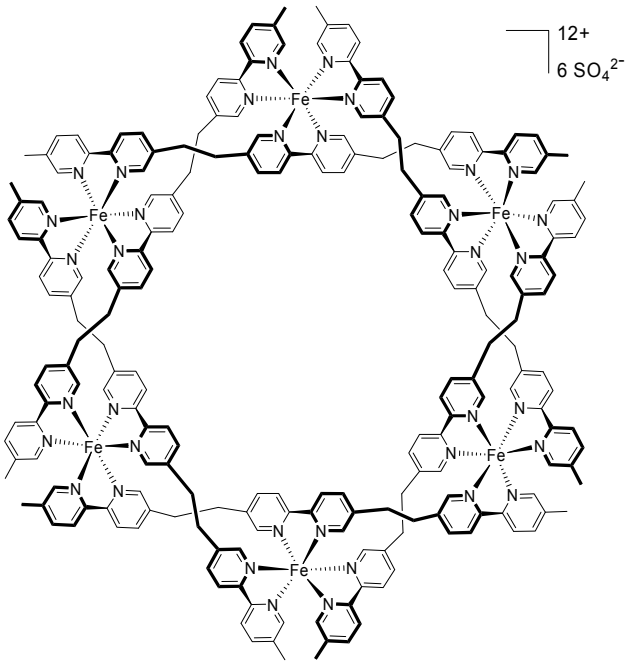


**18**

**Cyclic Dye Assemblies by Coordination to Metallochromophore.** Chromophores containing own metal ions such as metalloporphyrin and metallophthalocyanine have been widely used for metal-ion-directed self-cyclization approach. Central metals accommodated in the macrocyclic structures permit one or two axial coordinations of ligand depending on the metal ion species. The smallest macrocyclic assemblies by this strategy are cofacially coordinated porphyrin dimers **19** reported by Kobuke and co-workers.[18] They proposed the idea of complementary coordination of an imidazolyl substituent of one porphyrin to the $Zn^{2+}$ center of another porphyrin, whose imidazolyl coordinated back to $Zn^{2+}$ in the first porphyrin.[18] The dimer **19** is stabilized through coordinative as well as π-π-stacking interactions and their stability constant reaches $10^{11}$ $M^{-1}$ in nonpolar solvent at lower concentrations. In the recent past, novel porphyrin-phthalocyanine cyclic dimer **20** organized by self-complementary imidazolyl-to-zinc coordination was reported.[19] The association constant in toluene for coordination reached ever $10^{14}$ $M^{-1}$, which was much higher that those for the coordination homodimers **19**. Due to close contact of the porphyrin and phthalocyanine planes, a strong shielding of the cofacial protons was observed. The stacked dimers possessed unique optical properties due to strong exciton coupling and charge-transfer between the porphyrin and phthalocyanine units.

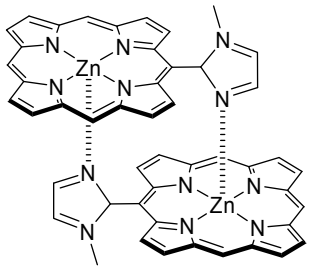

**19**

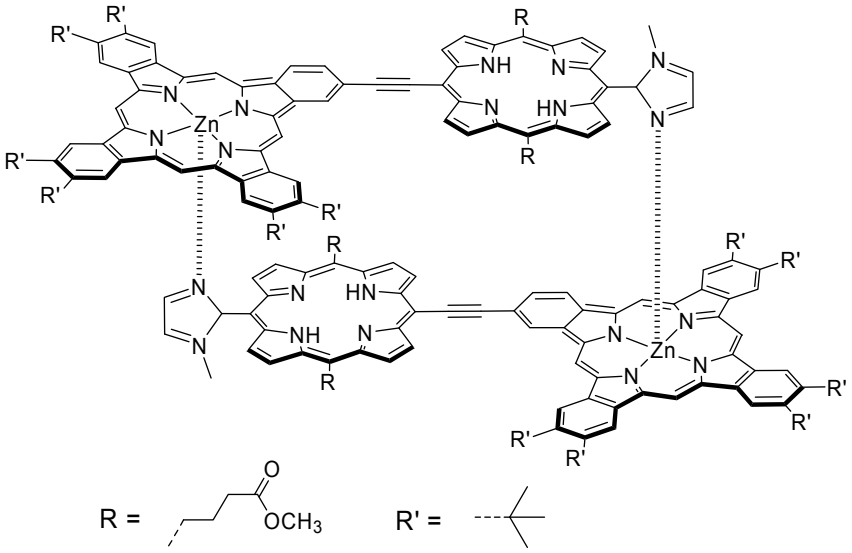

**20**

A series of isomeric pyridine-functionalized tetraphenylporphyrins, where a pyridyl function is perpendicular to the porphyrin plane, and investigation of their self-assembly properties in solution and in the solid state was reported by Hunter and co-workers.[20] These functionalized zinc porphyrin dyes afford self-cyclized assemblies **21** at diluted conditions with an association constant of $10^8$ $M^{-1}$ in dichloromethane. The self-assembly process is thermodynamically controlled, thus macrocyclization was quantitative.[20a]

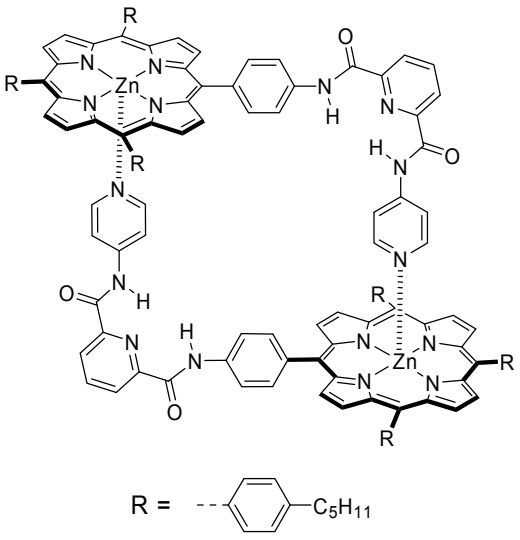

**21**

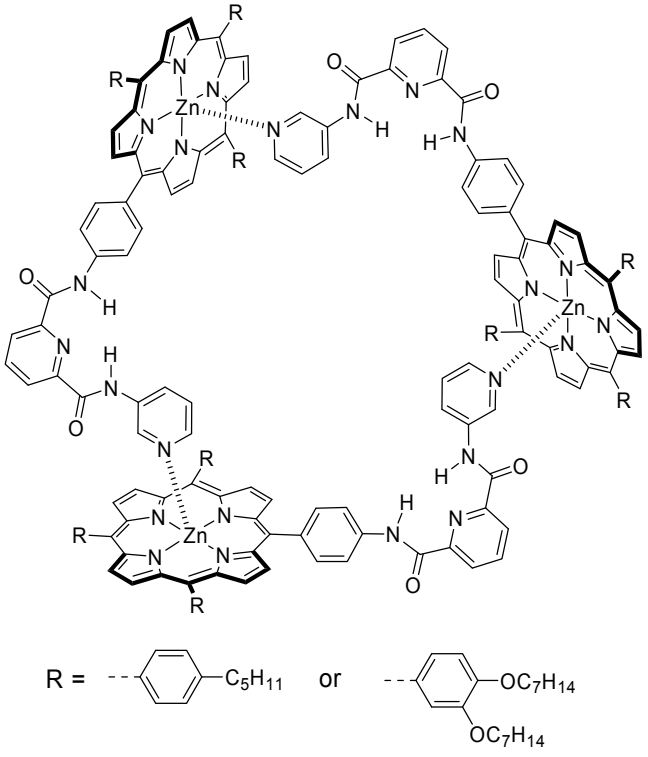

**22**

Self-assembly of dimer **21** generates a macrocyclic complex containing a spacious cavity with inwardly directed hydrogen-bond recognition sites. Thus, this functionalized macrocycle with cavities is utilizable for selective molecular recognition and can encapsulate amide guests of suitable size and shape to form host-guest complexes.[20a,d,e] The self-assembly properties of cyclic architectures depend on the covalent structure of the monomers. Increasing the angle between the plane of the porphyrin and the orientation of the pyridine ligand from 90° in monomers, which are used for construction of **21**, to 150° should favor the formation of a trimeric macrocycle **22**, while the square tetramer **23** was formed predominantly when this angle was 180°.[20b,c] The concentration-dependent UV/Vis experiments in dichloromethane indicated that self-assembly is taking place between $10^{-7}$ and $10^{-5}$ M. The stability constants of the resultant assemblies **21**-**23** in dichloromethane are as high as $10^{12}$ $M^{-2}$.

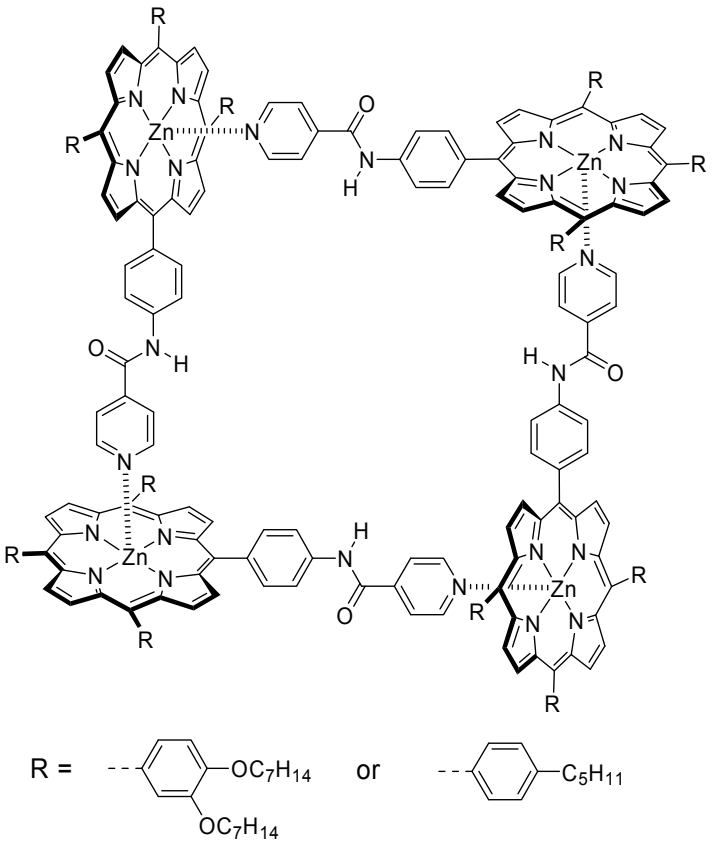


**23**

The preparation of cyclic porphyrin assemblies **24a** and **24b** and studies of their photoinduced energy and electron transfer were also reported by Hunter's group.[21] Free porphyrins with two pyridyl groups at the end of the two *trans-meso* positions

coordinate to zinc-porphyrin dimers, which contain a naphthalenediimide or terephthaloyl diamide unit as the bridging group, to afford the complexes **24a** and **24b**. The cyclic dimer **24a** has a naphthalenediimide group as linker that can act as an electron acceptor in photoinduced electron-transfer reaction with porphyrins.[21] The dimer complex **24b** contains a terephthaloyl diamide and this cannot act as an electron acceptor, it behaves rather as an inert spacer. The stability constant of these self-assembled complexes is $3\times10^8$ $M^{-1}$ in dichloromethane, which is very close to the value reported for cyclic dimer **21**.[20a] The spectroscopic investigations indicated that both cyclic dye assemblies **24a** and **24b** dissociate at a concentration about $10^{-8}$ M; however, remain fully assembled down to concentration below $10^{-7}$ M.

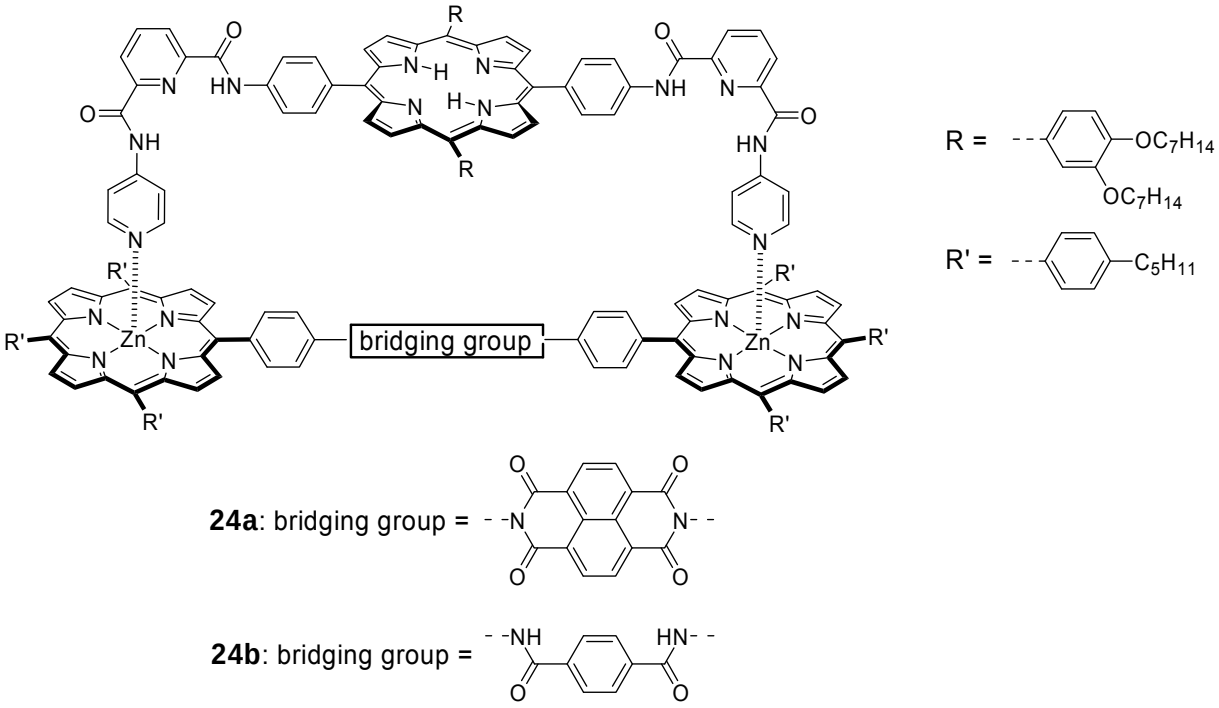


The weak fluorescent emission of zinc-porphyrin dimer containing a naphthalenediimide linker is not significantly changed upon complexation to **24a**, which implies that fast electron transfer from the zinc porphyrin to the naphthalenediimide also takes place in the complex. In contrast, in **24b** the intensity of the fluorescence emission of the Zn(II) part is significantly reduced by the energy transfer from the zinc-porphyrin to free-porphyrin part.

The self-assembly of zinc porphyrins bearing a pyrazole substituent was reported by Ikeda and co-workers.[22] The ability of pyrazole-substituted zinc-porphyrin chromophores **25a** to self-assemble in solution into cyclic trimer **26** was explored by UV/Vis absorption and $^1$H NMR spectroscopy, and vapor pressure

osmometry. However, the self-cyclization of zinc porphyrin **25b** resulted in a tetrameric species. Theoretical calculations of a model system revealed that the coordination angle, which is defined as the angle between the porphyrin mean plane and the CH bond at position 3 in an axially coordinated pyrazole ring, is 59° for an unsubstituted pyrazole ligand **25a** and 65° for 3,5-dimethylpyrazole ligand **25b**. Thus, the formation of a tetrameric assembly in the case of ligand **25b** can be explained in terms of steric repulsion imposed by the methyl groups.

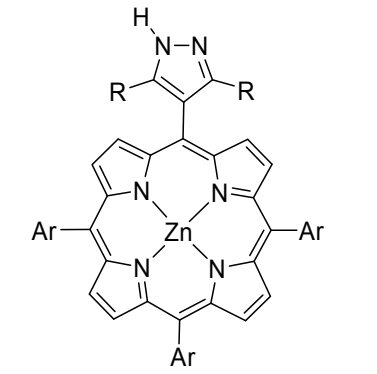


**25a**: R = H

**25b**: R = Me

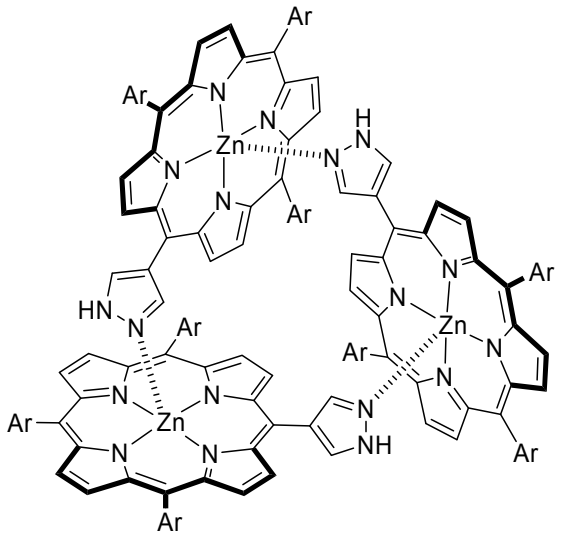


R = H

**26**

Imamura and co-workers have reported the cyclic ruthenium porphyrin tetramers **27a-c**.[23a,b] The tetrameric architecture of these cyclic assemblies was elucidated by variable temperature $^1$H NMR spectroscopy. The presence of excitonic interactions between cofacially arranged ruthenium porphyrin units in these cyclic molecules was revealed by electrochemical analysis.[23a] The self-assembled rhodium(III) porphyrin complex **27d** was also investigated by Imamura and co-workers.[23c] The cyclic structure of this complex was confirmed by X-ray analysis. The tetramer in the solid state deviates from ideal $C_{4h}$ symmetric structure, in which the pyridyl groups would be coordinated vertically to the neighboring porphyrin units. The dihedral angles of coordinating pyridyl groups and rhodium porphyrins in cyclic complex **27d** are 87.8° and 108.6°.

A perfect symmetric structure was observed for a zinc-porphyrin tetramer system by Osuka's group.[24] The X-ray analysis of this zinc-porphyrin tetramer

confirmed the square structure with the dihedral angles between porphyrin mean planes of 89.1° and 90.9°.

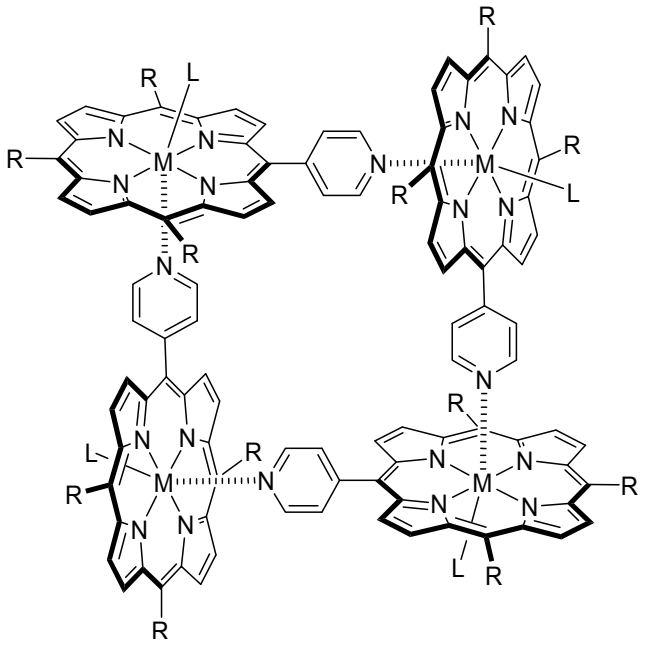

**27a**: M = Ru, L = CO, R = Ph

**27b**: M = Ru, L = CO, R = *p*-MePh

**27c**: M = Ru, L = Py, R = *p*-MePh

**27d**: M = Rh, L = Cl, R = *p*-*t*BuPh

Changing the geometry of the monomer unit can have dramatic effect on the structure and self-assembly properties of porphyrin arrays. Hunter and co-workers have designed two different cobalt porphyrins. One, the compound **28a**, which is symmetrically substituted with two identical ligand side arms forms linear polymers.[25a] Other ligand **28b** which is unsymmetrically functionalized with complementary but different ligand side arms self-assembles into macrocyclic dodecamer **29** over the concentration range of 5-500 μM.[25b] The formation of proposed macrocycle was substantiated by gel permeation chromatography (GPC) and molecular modeling studies. With increasing concentration, higher molecular weight polymers begin to emerge. The chromophores in cyclic dodecamer **29** are too far apart to show strong excitonic coupling in the UV/Vis absorption spectrum and, unfortunately, cobalt quenches the porphyrin fluorescence, which makes any analysis of the energy transfer and excitonic coupling properties of this synthetic analogue of bacterial light-harvesting complexes problematic.

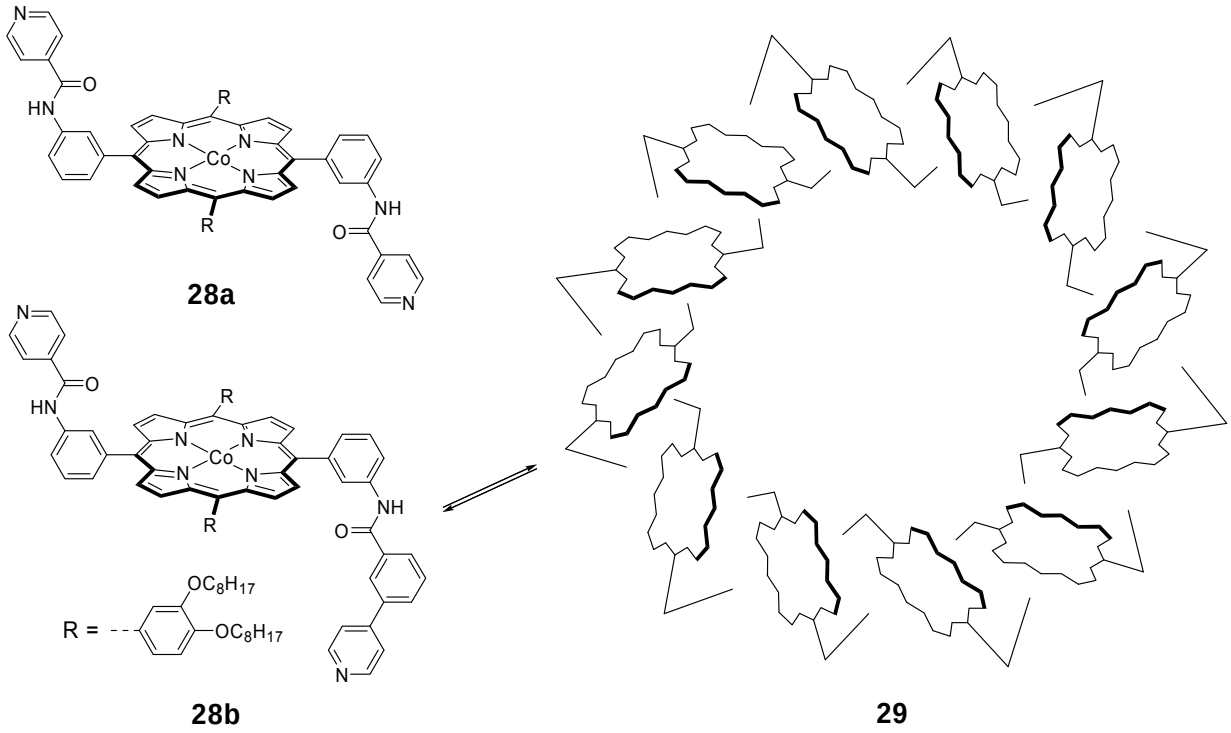


The synthesis of zinc-porphyrin-based supramolecular macrocyclic arrays as mimics of photosynthetic LH antennae was reported by Kobuke and co-workers. [26,27] Pentameric and hexameric macrocyclic porphyrin architectures were constructed by complementary coordination of bis(zinc-imidazolporphyrins). The size of the macrocycles can be controlled by the angle between the two connecting bonds of porphyrin units to the spacer. Thus, the *m*-phenylene-linked bis(imidazolyl-zinc-porphyrin) building blocks **30** were successfully used to form entropically favorable pentameric (**31**, n = 0, substituents R are not shown) and enthalpically favorable hexameric (**31**, n = 1, substituents R are not shown) supramolecular macrocycles.[26a-c] Using covalent connection, in particular by ring-closing metathesis, it was possible to permanently fix the macrocyclic arrays and to enable spectroscopic studies in various solvents at different concentrations. The covalently linked species were separated by GPC and characterized by MALDI-TOF mass spectrometry and small-angle X-ray scattering measurements. The cyclic porphyrin arrays did not show any fluorescence quenching by assembly formation and represent a good model artificial light-harvesting complexes.

Kobuke's group also reported the supramolecular formation of cyclic pentamers and hexamers from bis(zinc-imidazolylporphyrin) linked by a *m*-bis(ethynyl)phenylene spacer.[26d,e] Introduction of the ethyne units between porphyrin

and phenylene in **32** allows free rotation along the ethyne axis. Thus, an electronic communication among porphyrins is feasible due to the coplanar conformation. Using the exciton-exciton annihilation and anisotropy depolarization times, the excitation energy hopping times in macrocyclic pentameric (**33**, n = 0) and hexameric (**33**, n = 1) systems were obtained as 21 ps and 12.8 ps, respectively. Furthermore, pentameric and hexameric porphyrin arrays could be visualized by ultrahigh vacuum scanning tunneling microscopy (UHV-STM) on Au(111) surface.[26d] The slipped-cofacial arrangement was clearly observed and assigned by comparison with the disassociated structure obtained at submolecular resolution. The STM measurements indicated that the slipped-cofacial dimer plane laid horizontally on the gold surface.

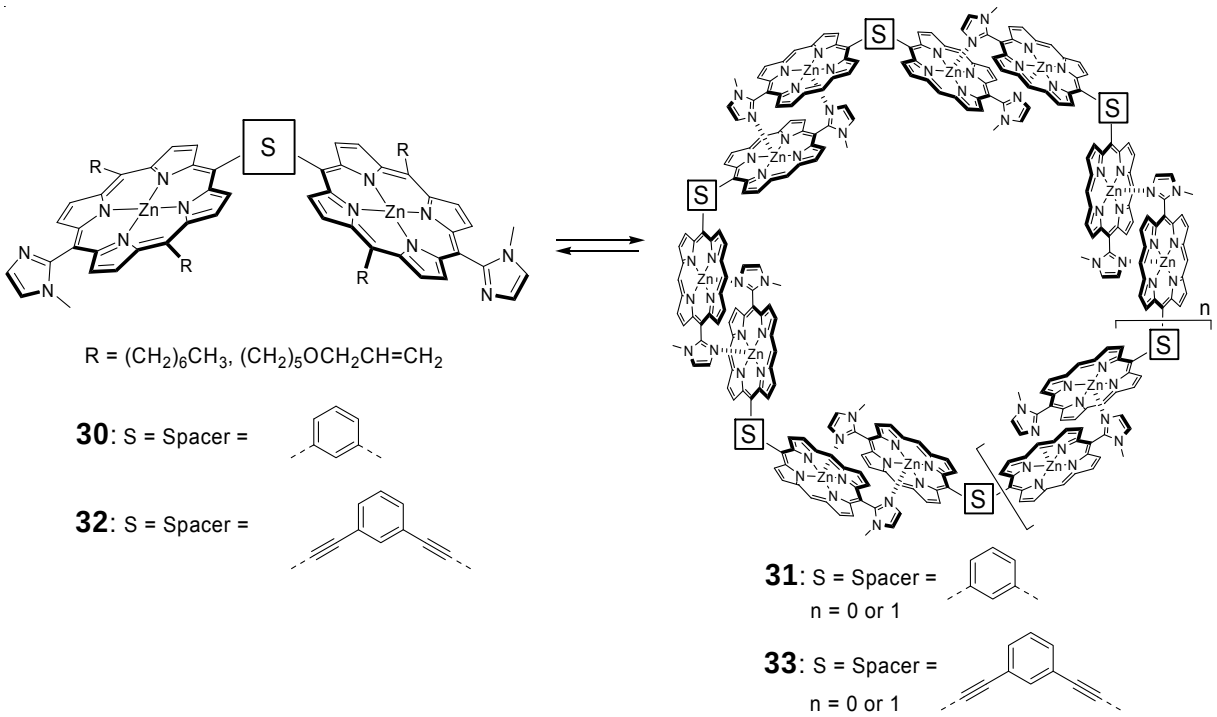


When three porphyrins are connected through *m*-phenylene spacer and imidazolyl groups are appended at molecular terminals as in **34**, the self-assembly results in a macrocyclic trimer **35**.[27a,c] The macrocyclic trimeric assembly **35** contains three coordination-free zinc-porphyrin and can accommodate tripodal ligand in its hole by multitopic and cooperative coordination. The modification of the ligand with energy and electron acceptors and further coordination with **35** seems to be an interesting way to construct LH systems.

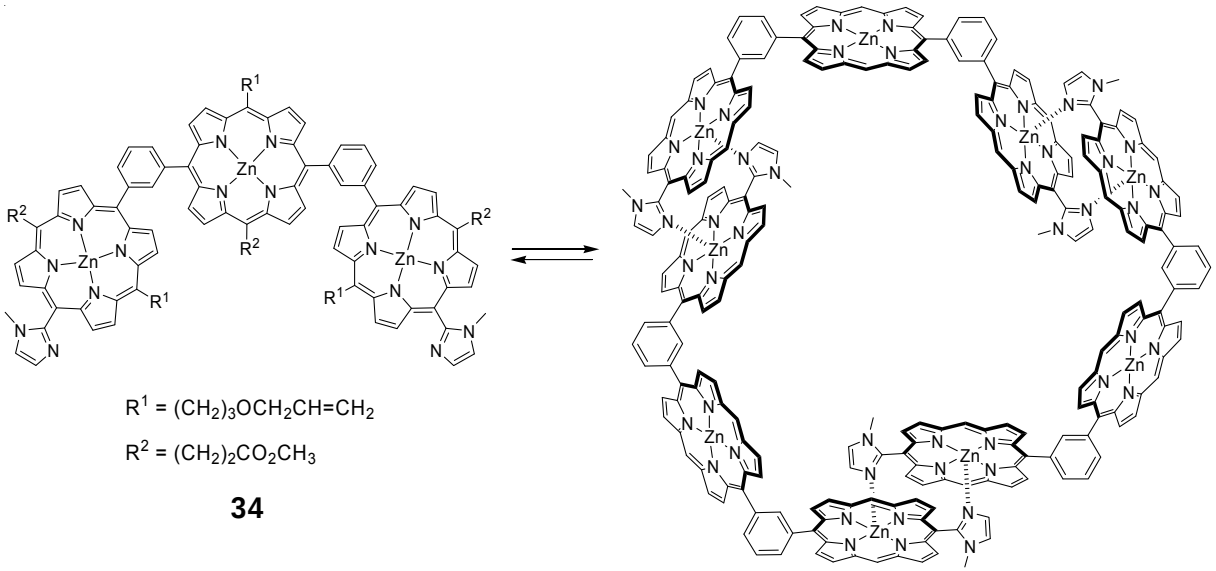


**34** **35**

A series of macrocycles from trimer to decamer self-assembled from ferrocene-bridged trisporphyrin **36** was also reported by Kobuke and co-workers.[27b,d] Trisporphyrin **36** spontaneously generates the dimeric assembly **37** upon Zn(II) ion addition.

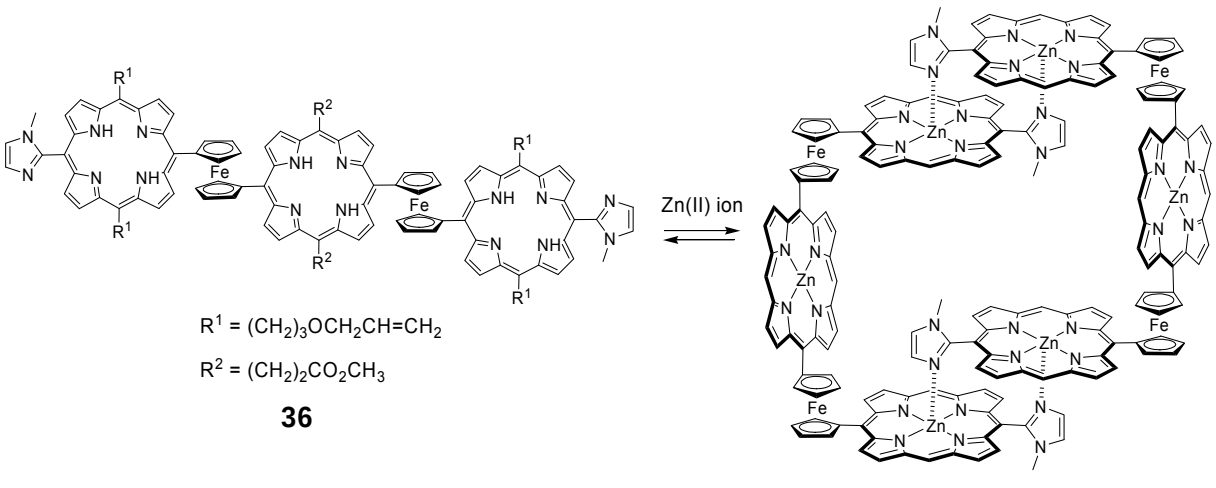


**36** **37**

Taking advantage of the hinge-like flexibility of ferrocene, the dimer ring **37** was transformed into a mixture of porphyrin macrocycles by reorganizing the structures cleaved once by solvent. Macrocycles were stable in the absence of coordinating solvent and could be easily transformed to initial dimeric complex in the present of coordinating solvent such as methanol. This transformation is completely reversible and can be controlled by the choice of solvent system. Flexible and large molecular cavities with multiple coordination sites make these macrocycles versatile hosts for a

wide variety of guest molecules. The unique photo and electronic properties of porphyrin and ferrocene emphasize the attractiveness of these cyclic architectures for use in molecular recognition and artificial LH complexes.

## Metallosupramolecular Polymers

Metallosupramolecular polymers play a significant role in supramolecular chemistry as it is the case for cyclic self-assemblies described before. Introduction and definition of supramolecular coordination polymers as well as the basic correlations between the resulting polymer chain length, complex binding constant, and concentration have been described comprehensively in a recent review by Dobrawa and Würthner[28] and in the PhD thesis of R. Dobrawa (Universität Würzburg **2004**).[29] Therefore, these aspects of metallosupramolecular polymers are not repeated here.

The wide range of readily available metal ions and ligand units provides a strong basis for the formation of supramolecular polymeric systems with highly variable length, stability, and reversibility. These metallosupramolecular structures could be applied as functional materials, especially for light-emitting diodes, charge transport, organic solar cells, and sensors.[28,30] As in the above-mentioned review[28] and in the PhD thesis of R. Dobrawa[29] the literature on metallosupramolecular polymers is covered until 2004, only recent advances in the field of metallosupramolecular polymeric assemblies are represented here.

The interesting concept for the formation of neutral metallosupramolecular polymers has been reported by Lehn and co-workers.[31] The coordination polymers **38** based on acyl hydrazone containing metal ion coordination centers such as $Co^{2+}$, $Ni^{2+}$, $Zn^{2+}$, and $Cd^{2+}$ were obtained by self-assembly polymerization. Three different processes are involved in this: 1) Subunit condensation to form the tridentate coordination moiety; 2) multiple metal ion-ligand coordination to connect the ligand monomers; 3) simultaneous deprotonation to form neutral coordination centers. The combination of metal ions and ligands leads to different morphologies of the metallosupramolecular polymers. These novel neutral supramolecular polymers exhibit specific optical and mechanical properties, which can vary by the occurrence

of cross-over ligand exchange due to the reversibility of the coordination bonds. $^{1}H$ NMR spectroscopic analysis was performed to study the kinetics of the dynamic ligand-exchange reaction between homopolymers. By interchanging the ligand components and metal ions in coordination centers of polymers in solution and in the neat phase interesting optical and mechanical properties can be introduced, a particularly attractive feature of such functional dynamic materials.

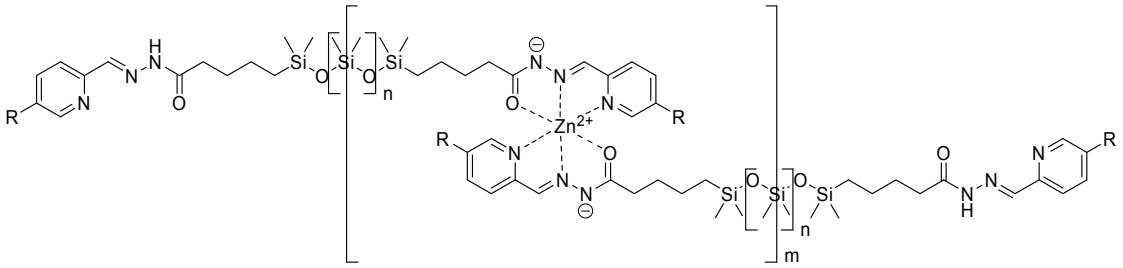

R = H or $CH_3(CH_2)_9O$

**38a**

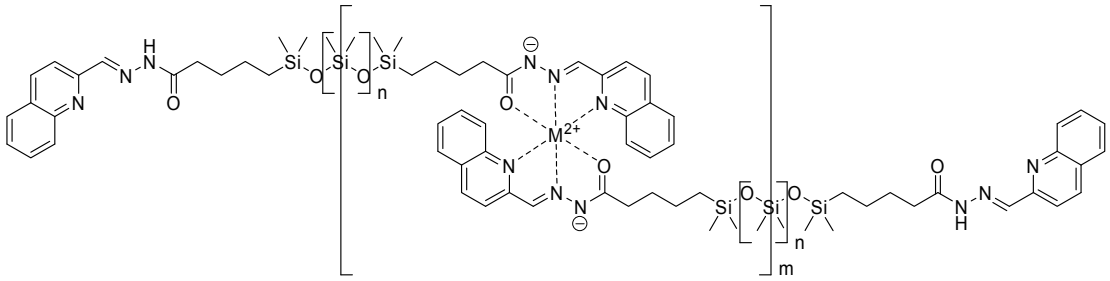

M = $Zn^{2+}$, $Co^{2+}$, $Ni^{2+}$, $Cd^{2+}$

**38b**

Oh and Mirkin have used a homochiral carboxylate-functionalized binaphtyl bis-metallotridentate Schiff base (BMSB) as a building block to form colloidal particles from coordination polymers **39**.[32] The process of particle formation is reversible, as evidenced by the formation of the starting materials upon the addition of excess pyridine. By adjusting the electronic nature of the metal ions, the physical and chemical properties of polymeric particles could be controlled. It is interesting to note that the particles are stable in water and common organic solvents. The inclusion of binaphtyl in the ligand affords fluorescence from the complex as well as from the particles. The ancillary ligands (L) also allow the manipulation of the electronic nature of the metal ions. For instance, increasing the σ-donor capability of the ancillary ligand induces a red-shift of the absorption maximum. As these

materials can be obtained in enantiopure form, they are attractive for asymmetric catalysis and chiral resolution.

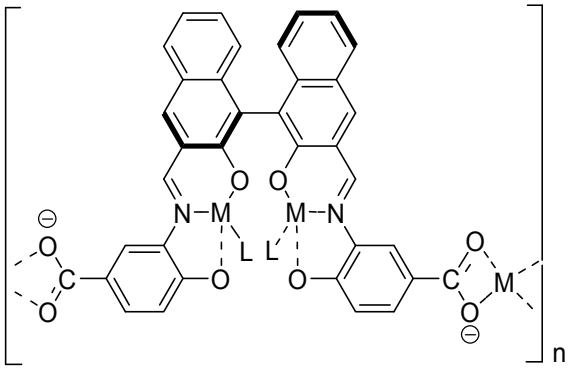


L = pyridine, water
M = $Zn^{2+}$, $Cu^{2+}$, $Ni^{2+}$

**39**

This concept has recently been used by Maeda and co-workers to obtain nanoscale architectures from dipyrrin ligands.[33] Bis(dipyrrin) ligands with various rigid phenylethynyl spacers that were prepared by cross-coupling reactions exhibited coordination behavior as indicated by change of solution color and, in some cases, formation of precipitate immediately after addition of metal salts. Self-assembled nanoscale structures of coordination polymers and oligomers based on dipyrrin ligands were observed by scanning electron microscopy (SEM). Zn(II) ion complex **40b** provided uniform nanosized spherical structures with a diameter of ca. 300 nm, while coordination polymer **40a** formed randomly shaped objects from THF solution.

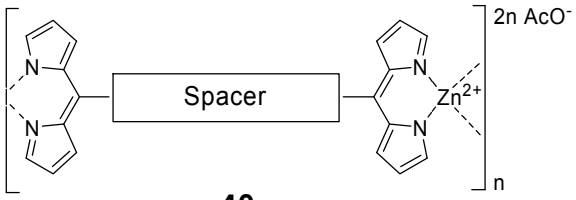


**40**

**40a**: Spacer =

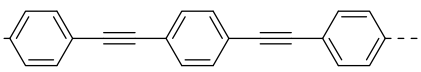

**40b**: Spacer =

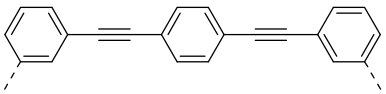

The supramolecular polymeric assemblies **41** with attractive optical properties that are formed by self-assembly of fluorescent pyridyl cruciforms with bis-Pd-pincer complexes were reported by Bunz, Weck, and co-workers.[34] This supramolecular polymeric material combines the advantages of polymers and small molecules such as optical, electronic and redox properties of cross-conjugated cruciform. Using isothermal titration calorimetry (ITC), an association constant of 5700 $M^{-1}$ was

measured for the coordination complex in dimethylformamide. The polymer properties, which are resulted from changes in the degree of polymerization (DP), could also be tailored by altering the ratios of pyridyl cruciform and bis-Pd-pincer complex.

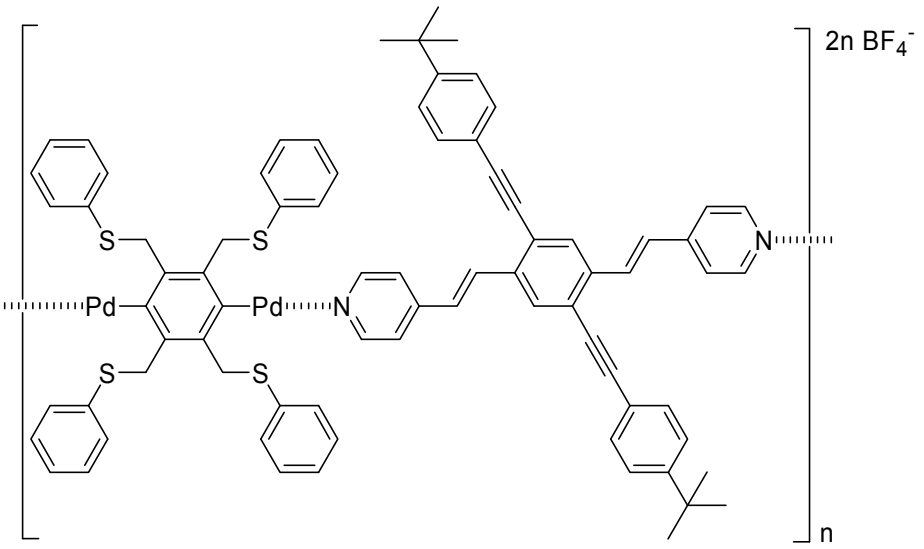


**41**

Ruben and co-workers prepared the metallosupramolecular coordination polymer **42** from new back-to-back ligand with 2:6-di(pyrazol-1-yl)pyridine as terminal binding sites and Fe(II) ion.[35] Unfortunately, the authors did not present any data on the molecular weight of this new coordination polymer. Interestingly, it was reported that a reversible spin transition (ST) above room temperature occurs at approximately 323 K with a thermal hysteresis loop of 10 K. This approach provides a general concept for achieving technologically appealing high $T_{1/2}$ systems by supramolecular interlinking of the ST-iron(II) centers. Recently, Kurth and co-workers reported on metallosupramolecular polymer system with interesting magnetic properties (see page 34).[36]

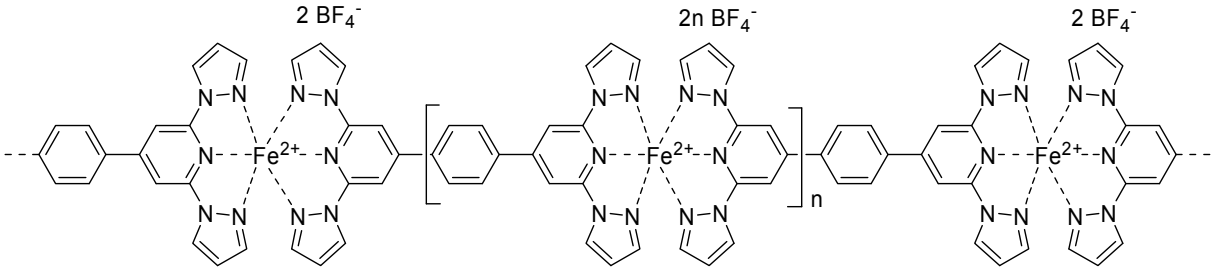


**42**

Very recently, the formation of coordination polymers **43** by self-assembly of a new type of ditopic chiral ligand bearing two azabis(oxazoline) moieties with Cu(II) ions has been reported by García and co-workers.[37] The new ligand combines the high coordinating ability of azabisoxazoline with the known ability of these kinds of ligands to form 2:1 ligand/metal ion complexes, necessary to direct the formation of the linear coordination polymer. For complexation reaction, copper (II) was chosen as the complexes of this metal ion find broad application in enantioselective catalysis.

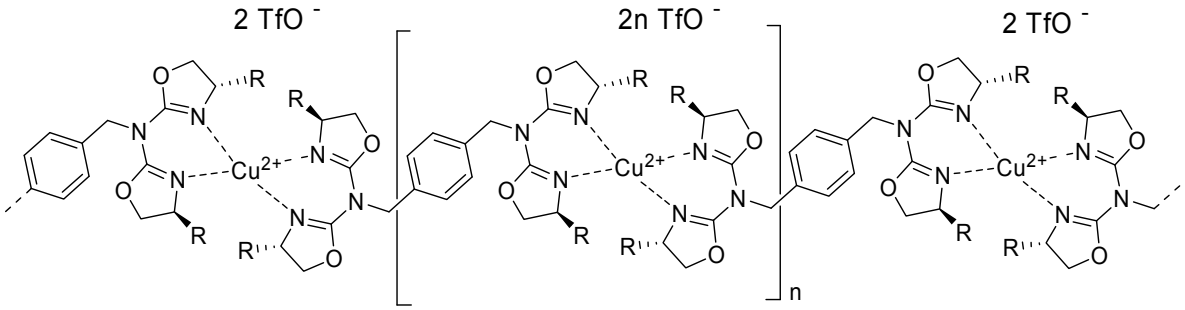


R = *tert*-Bu

**43**

Indeed, the supramolecular coordination polymer **43** could be successfully used as self-supported enantioselective catalyst, allowing a release-and-capture strategy of homogenous catalysis and heterogeneous recovery of them in the reaction medium. The self-supported catalyst has been tested in the enantioselective catalytic reaction, leading to excellent enantioselectives and allowing up to fourteen cycles without significant loss of activity or selectivity.[37]

Rowan, Beck, and co-workers have introduced multistimulus, multiresponsive metallosupramolecular coordination polymers from lanthanides and 2,6-bis(benzimidazolyl)pyridine (BIP) ligands **44**.[38] These ligands can bind transition metal ions in a 2:1 ratio as well as lanthanides in a 3:1 ratio. Therefore, the self-assembly of ligands, transition-metal ions (Co(II) or Zn(II) ions) and lanthanides (La(III) or Eu(III)) in appropriate stoichiometry results in the formation of metallosupramolecular gels. These supramolecular polyelectrolyte materials exhibit thermo, chemo, and mechanical responses as well as light-emitting properties. The nature of the response displayed by these systems depends upon the metal ion, counter-ion, and the amount of swelling solvent.[38]

The supramolecular polymerization of ditopic macromolecules **45** based on 2,6-bis(1′-methylbenzimidazyl)pyridine-endcapped poly(*p*-phenylene ethynylene) and

poly(*p*-xylene) via metal ion-ligand binding has also been reported by Rowan's group.[39] The supramolecular polymerization of these macromonomers with equimolar amounts of Zn(II) or Fe(II) ions resulted in polymers, which exhibit appreciable mechanical strength. With the objective to improve the material's mechanical properties, the authors employed minor amounts of lanthanide salts, which are well-known to bind three ligands, as a cross-linking/branching units in supramolecular polymerization of **45** and Fe(II) ion to generate the crosslinks/branch points in a **45**/metal ion system (see the schematic representation). The further addition of Fe(II) ion resulted in an instantaneous and dramatic visual increase of the solution's viscosity, illustrating the successful linear chain growth of the preformed 3:1 **45**/La(III) complexes. The formation of polymers is clearly demonstrated by an increase in the viscosity of the solutions. This approach to assemble conjugated polymers from smaller building blocks has prospects because high-molecular-weight conjugated polymers are generally difficult to process due to their high transition temperatures, limited solubility and high solution viscosities.

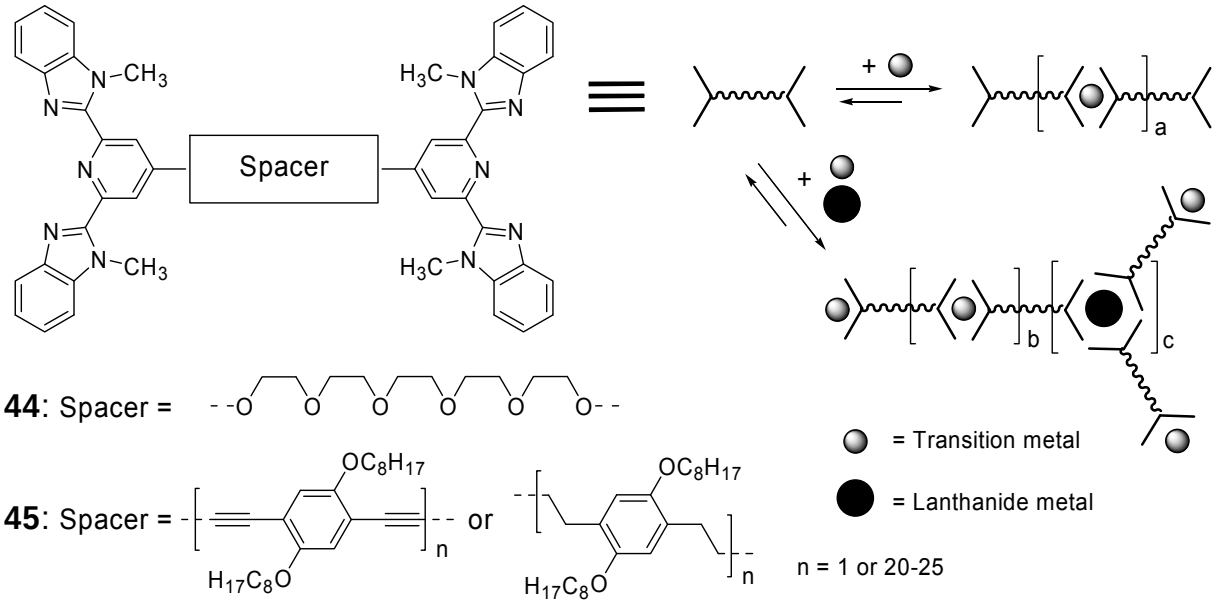


Furusho, Yashima, and co-workers reported synthesis of double-stranded metallosupramolecular helical polymers **46** consisting of two complementary metallopolymer strands that are intertwined through chiral amidinium-carboxylate salt bridges.[40] The pyridine groups are utilized for the metal coordination site to form metallosupramolecular strands. Information on the structure of the polymers **46** was

obtained by $^{1}$H NMR, DOSY NMR, absorption and CD spectroscopy. Direct evidence for the polymeric structure and their visualization were provided by AFM measurements.

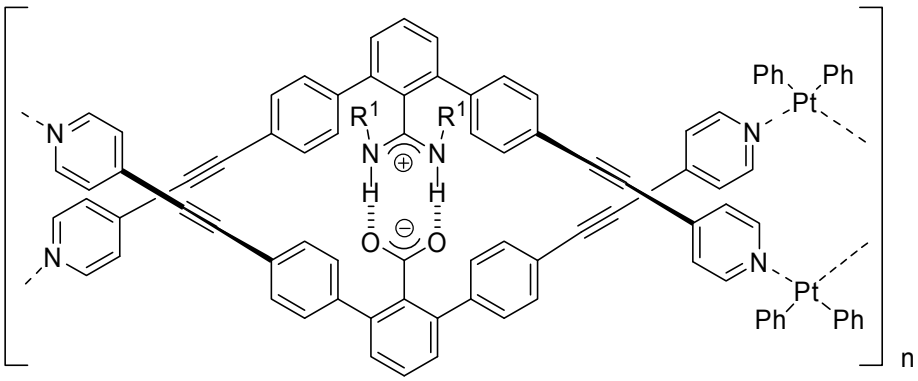


$R^1$ = (*R*)-1-phenylethyl or (*S*)-1-phenylethyl

**46**

The synthesis, characterization, and metal-ion-mediated supramolecular polymerization of diazadibenzoperylenes (DABP) **47** equipped with first to third generation Fréchet-type dendrons were reported by Würthner and co-workers.[41] Silver(I)-ion-mediated polymerization of DABP ligands was investigated by NMR spectroscopy and AFM. The supramolecular polymerization was shown to be highly dependent on the generation number of the attached dendrons; thus, first and second generation dendrimers afforded polymeric materials while the third generation resisted polymerization as a result of the shielding of the aza coordination site by dendritic wedges.

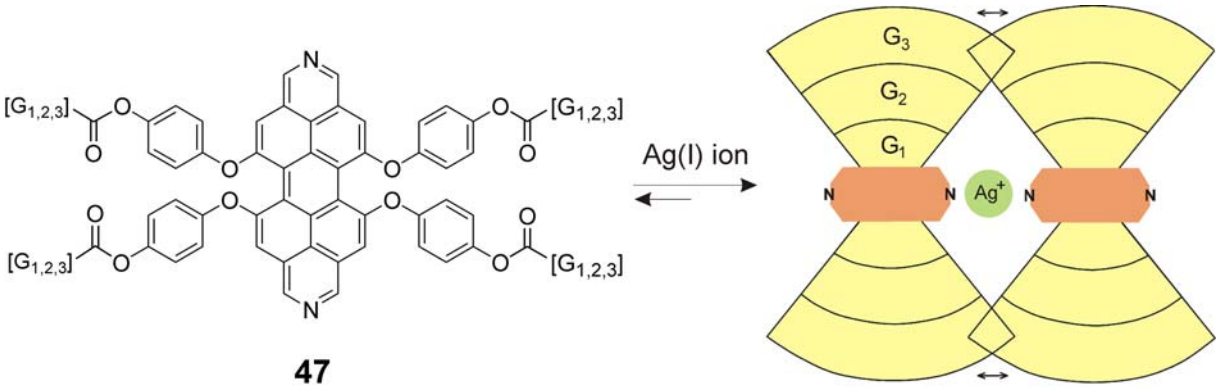


**47**

Since 2,2′:6′,2″-terpyridine (tpy) derivatives exhibit strong chelating affinity with many transition metals and use of tpy ligands affords a well-defined coordination

geometry, numerous coordination polymers containing tpy-based complexes have been reported.

Würthner and co-workers have employed the concept of metallosupramolecular polymerization to prepare a photoluminescent coordination polymer, where the metal ion serves a purely structural role.[42] Here, the photoactive tetraphenoxy-substituted PBI unit was covalently attached to tpy receptor groups that contain phenylene spacers connecting PBI and tpy. Tpy-receptors were linked together by non-covalent interactions upon formation of the corresponding bis(tpy)-zinc(II) complex. Polymer **48**, which was thermodynamically stable and kinetically labile, could be grown up to chain length of about 15 repeat units due to moderate solubility which was attributed to the extended π-system of tpy-Ph-PBI building blocks. Although the incorporation of Zn(II) ions had little effect on the fluorescence spectrum of the organic monomer, it was shown that replacement by Fe(II) resulted in a significant reduction of the fluorescence quantum yield.[42]

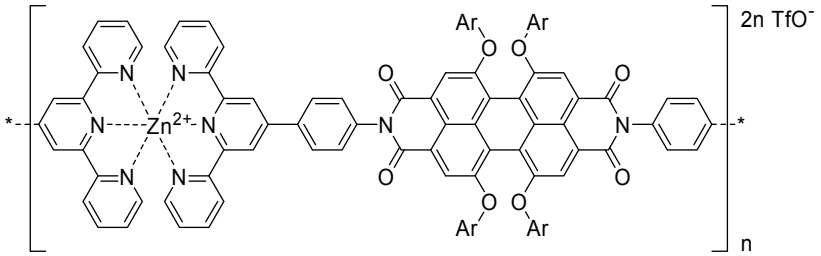


Ar = *p*-*t*BuPh, *p*-*t*OctPh

**48**

Recently, Chen and co-workers reported cadmium(II)-directed self-assembly polymerization of luminescent tpy building blocks utilizing oligofluorenes as spacers.[43] The number of repeating fluorine units in supramolecular coordination polymers **49a** influences slightly the absorption and fluorescence spectra, while the fluorescence quantum yield increases to a certain extent with increasing conjugation length of the spacers. In order to further tune the emission color, the synthesis of metallosupramolecular polymers **49b** containing a donor-accepter (D-A) structure composed of a triphenylamin electron-rich unit have also been described.[43] With D-A structure in the backbone, the absorption and fluorescence emission spectra of polymer exhibit large red-shifts compared to those of other polymers. The longer wavelength absorption and fluorescence maxima derive from intermolecular charge

transfer. The fluorescence quantum yield of coordination polymers **49** is *ca.* 0.5 in solid state, thus these polymers are promising materials for light-emitting diodes.

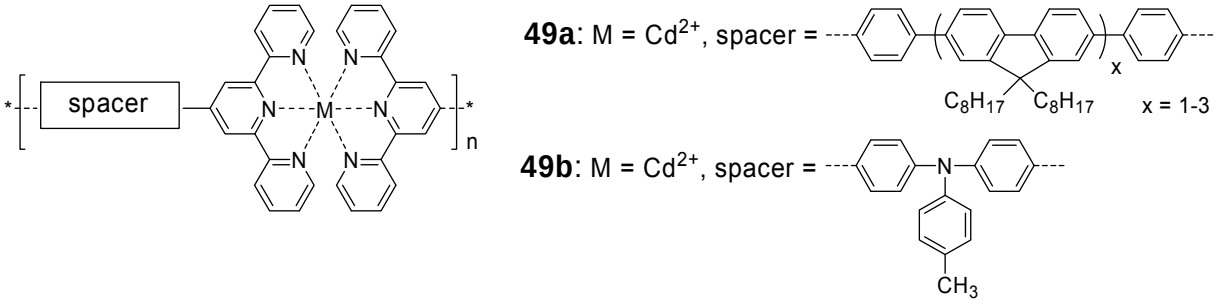


The self-assembly of amphiphilic metallosupramolecular *A-B-A* triblock copolymers **50** containing a B block of bisfunctional tpy unit and A block based on monofunctional tpy ligand has been reported by Schubert and co-workers.[44] Since the metallopolymerization of bis(tpy) ligand leads to the formation of chain-extended polymers, the addition of a macromolecular chain stopper allowed the formation of *A-B-A* architectures. The coordination polymers that have been prepared via a simple one-step polycondensation approach based on metal ion-ligand complexation can form micelles in acetone/water mixture as shown by cryo-TEM imaging.[44]

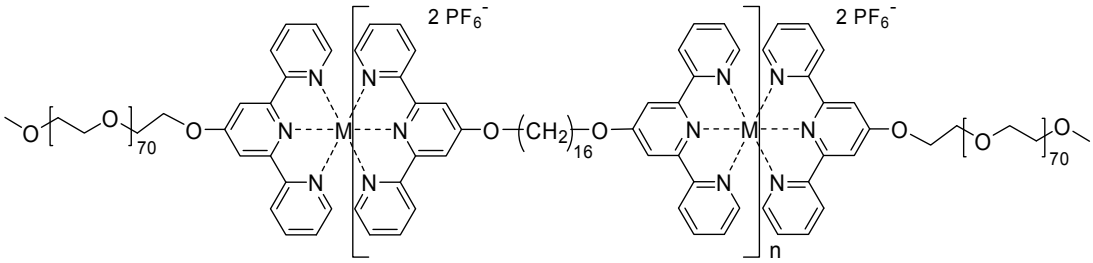


**50**: M = $Ni^{2+}$, $Fe^{2+}$, $Co^{2+}$

In the search of new electrochromic materials and to explore the structure-property relationships of metal ion-ligand-directed coordination complexes, Kurth and co-workers have investigated metallosupramolecular coordination polymers assembled from various newly synthesized bis(tpy) ligands **51**.[36] The authors have shown that optical, electrochemical, and electrochromic properties of these polymers are profoundly affected by the nature of the substituents at the peripheral pyridine rings. Metallosupramolecular polymers assembled from the electron-rich OMe group modified ligands exhibit high switching reversibility and stability and show a lower

switching potential than the unsubstituted and electron-deficient Br-substituted analogues.

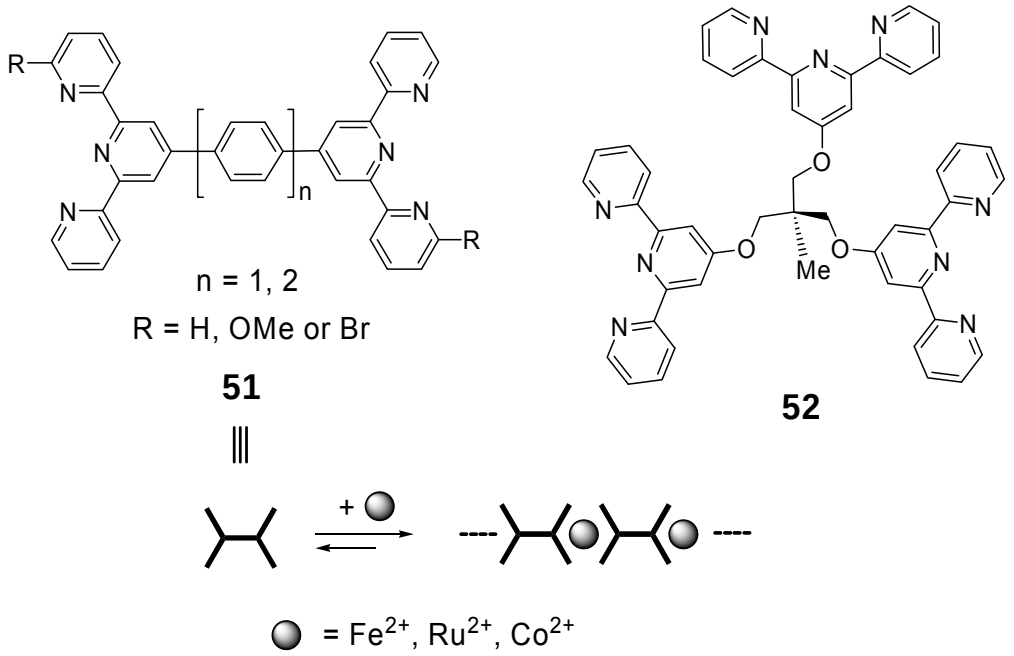


As indicated by the authors, a key feature of these materials is that the colors can be readily modified, covering the whole visible region through the design of the ligands or the choice of the metal ions, demonstrating the ease for color tuning, which is a topic of great concern in electrochromic applications. The properties of these electrochromic supramolecular materials reveal their high potential for technological applications for a broad range of purposes.[36] Kurth and co-workers have also successfully applied the layer-by-layer approach to such metallosupramolecular polymers.[45] Iron(II) ion induced self-assembly of bis(tpy) **51** (n = 1, R = H) and triterpyridine ligands **52** resulted in well-soluble cross-linked metallosupramolecular coordination polymers. UV/Vis spectroscopy, X-ray analysis, AFM, and ellipsometry showed that the film growth is linear and continuous. The incorporation of such metallosupramolecular polymers in electrochromic films seems to be a common and promising approach for the development of display-type applications.

## Conclusion

The present introductory chapter gives an overview of metallosupramolecular architectures that incorporate dye molecules. The metal-ion-directed self-assembly of chromophores mimics the fundamental assembly processes found in natural photosystems. As shown in this chapter, many fascinating supramolecular methodologies have been developed and succeeded in providing macrocyclic and polymeric arrangements. The metallocyclic dye assemblies have potential to be used in artificial light-harvesting systems. Metallosupramolecular polymeric and cyclic architectures are also useful for applications in the fields of molecular recognition, sensing, supramolecular catalysis, electronics and photonics.

Incorporation of fluorophores like perylene bisimide chromophores into coordination-based assemblies seems to be a promising approach to provide novel luminescent metallosupramolecular architectures. The application of this concept is the major objective of this PhD work and the pertinent results are described in following chapters.

## References


[1] a) R. Emerson, W. Arnold, *Gen. Physiol.* **1932**, *16*, 191-205; b) L. Stryer, *Biochemie*, 4. Aufl., Spektrum: New York, **1999**.

[2] a) G. McDermott, S. M. Prince, A. A. Freer, A. M: Hawthornthwaite-Lawless, M. Z. Papiz, R. J. Cogdell, N. W. Isaacs, *Nature* **1995**, *374*, 517-521; b) X. Hu, T. Ritz, A. Damjanović, F. Autenrieth, K. Schulten, *Q. Rev. Biophys.* **2002**, *35*, 1-62; c) A. W. Roszak, T. D. Howard, J. Southall, A. T. Gardiner, C. J. Law, N. W. Isaacs, R. J. Cogdell, *Science*, **2003**, *302*, 1969-1972.

[3] a) S. Bahatyrova, R. N. Frese, C. A. Siebert, J. D. Olsen, K. O. van der Werf, R. van Grondelle, R. A. Niedermann, P. A. Bullough, C. N. Hunter, *Nature* **2004**, *430*, 1058-1062; b) S. Scheuring, J. N. Sturgis, V. Prima, A. Bernadac, D. Lévy, J.-L. Rigaud, *Proc. Natl. Acad. Sci. U. S. A.* **2004**, *101*, 11293-11297; c) S. Scheuring, D. Lévy, J.-L. Rigaud, *Biochim. Biophys. Acta* **2005**, *1712*, 109-127.

[4] C.-C. You, R. Dobrawa, C. R. Saha-Möller, F. Würthner, *Top Curr Chem* **2005**, *258*, 39-82.

[5] a) M. Fujita, *Chem. Soc. Rev.* **1998**, *27*, 417-425; b) S. Leininger, B. Olenyuk, P. J. Stang, *Chem. Rev.* **2000**, *100*, 853-908; c) G. F. Swiegers, T. F. Malafetse, *Chem. Rev.* **2000**, *100*, 3483-3538; d) T. Imamura, K. Fukushima, *Coord. Chem. Rev.* **2000**, *133*, 133-156; e) F. Würthner, C.-C. You, C. R. Saha-Möller, *Chem. Soc. Rev.* **2004**, *33*, 133-146; f) S. J. Lee, J. T. Hupp, *Coord. Chem. Rev.* **2006**, *250*, 1710-1723; g) Y. Kobuke, *Eur. J. Inorg. Chem.* **2006**, *12*, 2333-2351; h) M. W. Cooke, D. Chartrand, G. S. Hanan, *Coord. Chem. Rev.* **2008**, *252*, 903-921.

[6] M. Fujita, J. Yazaki, K. Ogura, *J. Am. Chem. Soc.* **1990**, *112*, 5645-5647.

[7] a) P. J. Stang, D. H. Cao, *J. Am. Chem. Soc.* **1994**, *116*, 4981-4982; b) P. J. Stang, D. H. Cao, S. Saito, A. M. Arif, *J. Am. Chem. Soc.* **1995**, *117*, 6273-6283; c) P. J. Stang, B. Olenyuk, *Angew. Chem.* **1996**, *108*, 797-802; *Angew. Chem. Int. Ed. Engl.* **1996**, *35*, 732-736; d) P. J. Stang, B. Olenyuk, *Acc. Chem. Res.* **1997**, *30*, 502-518.

[8] a) F. Würthner, A. Sautter, C. Thalacker, *Angew. Chem.* **2000**, *112*, 1298-1301; *Angew. Chem. Int. Ed. Engl.* **2000**, *39*, 1243–1245; b) F. Würthner, A.

Sautter, J. Schilling, *J. Org. Chem.* **2002**, *67*, 3037–3044; c) F. Würthner, A. Sautter, *Chem. Commun.* **2000***,* 445–446; d) F. Würthner, A. Sautter, D. Schmid, P. J. A. Weber, *Chem. Eur. J.* **2001**, *7*, 894–902; e) F. Würthner, A. Sautter, *Org. Biomol. Chem.* **2003**, *1*, 240–243; f) C. You, F. Würthner, *J. Am. Chem. Soc.* **2003**, *125*, 9716–9725; g) A. Sautter, B. Kaletaş, D. G. Schmid, R. Dobrawa, M. Zimine, G. Jung, I. H. M. van Stokkum, L. De Cola, R. M. Williams, F. Würthner, *J. Am. Chem. Soc.* **2005**, *127*, 6719–6729; h) C-C. You, C. Hippius, M. Grüne, F. Würthner, *Chem. Eur. J.* **2006***,12,* 7510–7519.

[9] a) R. V. Slone, J. T. Hupp, *Inorg. Chem.* **1997,** *36,* 5422-5423; b) M. L. Merlau, M. P. Mejia, S. T. Nguyen, J. T. Hupp, *Angew. Chem.* **2001**, *113*, 4369-4372; *Angew. Chem.* **2001**, *40*, 4239-4242; c) K. E. Splan, C. L. Stern, J. T. Hupp, *Inorg. Chim. Acta* **2004**, *357*, 4005-4014.

[10] a) P. J. Stang, J. Fan, B. Olenyuk, *Chem. Commun.* **1997**, *15*, 1453-1454 ; b) J. Fan, J. A. Whiteford, B. Olenyuk, M. D. Levin, P. J. Stang, E. B. Fleischer, *J. Am. Chem. Soc.* **1999,** *121,* 2741-2752.

[11] C. M. Drain, J.-M. Lehn, *J. Chem. Soc. Chem. Commun.* **1994**, *19*, 2313-2315.

[12] a) E. Iengo, E. Zangrando, R. Minatel, E. Alessio, *J. Am. Chem. Soc*. **2002**, *124*, 1003-1013; b) E. Iengo, E. Zangrando, E. Alessio, *Eur. J. Inorg. Chem.* **2003**, *13*, 2371-2384; c) A. Prodi, C. Chiorboli, F. Scandola, E. Iengo, E. Alessio, *ChemPhysChem* **2006**, *7*, 1514-1519.

[13] a) U. S. Schubert, H. Hofmeier, G. R. Newkome, *Modern Terpyridine Chemistry*, Wiley-VCH: Weinheim, **2006**; b) E. C. Constable, *Chem. Soc. Rev.* **2007**, *36*, 246-253.

[14] S.-S. Sun, A. J. Lees, *Inorg. Chem.* **2001**, *40*, 3154-3160.

[15] a) F. M. Romero, R. Ziessel, A. Dupont-Gervais, A. Van Dorsselaer, *Chem. Commun.* **1996**, *4*, 551-553; b) R. Ziessel, *Synthesis* **1999**, *11*, 1839-1865.

[16] a) G. R. Newkome, T. J. Cho, C. N. Moorefield, G. R. Baker, R. Cush, P. S. Russo, *Angew. Chem.* **1999**, *111*, 3899-3903; *Angew. Chem. Int. Ed.* **1999**, *38*, 3717-3721; b) G. R. Newkome, T. J. Cho, C. N. Moorefield, P. P. Mohapatra, L. A. Godínez, *Chem. Eur. J.* **2004**, *10*, 1493-1500; c) S.-H. Hwang, P. Wang, C. N. Moorefield, L. A. Godínez, J. Manríquez, E. Bustos, G. R. Newkome, *Chem. Commun.* **2005**, *37*, 4672-4676; d) S.-H. Hwang, C. N. Moorefield, P. Wang, F. R. Fronczek, B. H. Courtney, G. R. Newkome, *Dalton Trans.* **2006**, *29*, 3518-3522; e) S.-H. Hwang, C. N. Moorefield, P. Wang, J.-Y. Kim, S.-W.

Lee, G. R. Newkome, *Inorg. Chim. Acta* **2007**, *360*, 1780-1784; f) I. Eryazici, P. Wang, C. N. Moorefield, M. Panzer, S. Durmus, C. D. Shreiner, G. R. Newkome, *Dalton Trans.* **2007**, *6*, 626-628; g) S. Li, C. N. Moorefield, P. Wang, C. D. Shreiner, G. R. Newkome, *Eur. J. Org. Chem.* **2008**, *19*, 3328-3334.

[17] a) B. Hasenknopf, J.-M. Lehn, N. Boumediene, A. Dupont-Gervais, A. Van Dorsselaer, B. Kneisel, D Fenske, *J. Am. Chem. Soc*. **1997**, *119*, 10956-10962; b) B. Hasenknopf, J.-M. Lehn, N. Boumediene, E. Leize, A. Van Dorsselaer, *Angew. Chem.* **1998**, *110*, 3458-3460; *Angew. Chem. Int. Ed.* **1998**, *37*, 3256-3268.

[18] a) Y. Kobuke, H. Miyaji, *J. Am. Chem. Soc*. **1994**, *116*, 4111-4112; b) Y. Kobuke, H. Miyaji, *Bull. Chem. Soc*. *Jpn.* **1996**, *69*, 3563-3569.

[19] M. Morisue, Y. Kobuke, *Chem. Eur. J.* **2008**, *14*, 4993-5000.

[20] a) C. A. Hunter, L. D. Sarson, *Angew. Chem.* **1994**, *106*, 2424-2426; *Angew. Chem. Int. Ed. Engl.* **1994**, *33*, 2313-2316; b) X. Chi, A. J. Guerin, R. A. Haycock, C. A. Hunter, L. D. Sarson, *J. Chem. Soc. Chem. Commun.* **1995**, *24*, 2563-2565; c) X. Chi, A. J. Guerin, R. A. Haycock, C. A. Hunter, L. D. Sarson, *J. Chem. Soc. Chem. Commun.* **1995**, *24*, 2567-2569; d) P. Ballester, A. Costa, P. M. Deyà, A. Frontera, R. M. Gomila, A. I. Oliva, J. K. M. Sanders, C. A. Hunter, *J. Org. Chem.* **2005**, *70*, 6616-6622; e) P. L. Bernad, Jr, A. J. Guerin, R. A. Haycock, S. L. Heath, C. A. Hunter, C. Raposo, C. Rotger, L. D. Sarson, L. R. Sutton, *New J. Chem.* **2008**, *32*, 525–532.

[21] C. A. Hunter, R. K. Hyde, *Angew. Chem.* **1996**, *108*, 2064-2067; *Angew. Chem. Int. Ed. Engl.* **1996**, *35*, 1936-1939.

[22] C. Ikeda, N. Nagahara, N. Yoshioka, H. Inoue, *New J. Chem.* **2000**, *24*, 897-902.

[23] a) K. Funatsu, A. Kimura, T. Imamura, Y. Sasaki, *Chem. Lett.* **1995**, *24*, 765-767; b) K. Funatsu, T. Imamura, A. Ichimura, Y. Sasaki, *Inorg. Chem.* **1998**, *37*, 1798-1804; c) K. Fukushima, K. Funatsu, A. Ichimura, Y. Sasaki, M. Suzuki, T. Fujihara, K. Tsuge, T. Imamura, *Inorg. Chem*. **2003**, *42*, 3187-3193.

[24] a) A. Tsuda, T. Nakamura, S. Sakamoto, K. Yamaguchi, A. Osuka, *Angew. Chem.* **2002**, *114*, 2941-2945; *Angew. Chem. Int. Ed.* **2002**, *41*, 2817-2821; b) I.-W. Hwang, T. Kamada, T. K. Ahn, D. M. Ko, T. Nakamura, A. Tsuda, A. Osuka, D. Kim, *J. Am. Chem. Soc.* **2004**, *126*, 16187-16198.

[25] a) U. Michelsen, C. A. Hunter, *Angew. Chem.* **2000**, *112*, 780-783; *Angew. Chem. Int. Ed.* **2000**, *39*, 764-767; b) R. A. Haycock, C. A. Hunter, D. A. James, U. Michelsen, L. R. Sutton, *Org. Lett.* **2002**, *2*, 2435-2438.

[26] a) R. Takahashi, Y. Kobuke, *J. Am. Chem. Soc.* **2003**, *125*, 2372-2373; b) C. Ikeda, A. Satake, Y. Kobuke, *Org. Lett.* **2003**, *5*, 4935-4938; c) R. Takahashi, Y. Kobuke, *J. Org. Chem.* **2005**, *70*, 2745-2753; d) A. Satake, H. Tanaka, F. Hajjaj, T. Kawai, Y. Kobuke, *Chem. Commun.* **2006**, 24, 2542-2544; e) F. Hajjaj, Z. S. Yoon, M.-C. Yoon, J. Park, A. Satake, D. Kim, Y. Kobuke, *J. Am. Chem. Soc.* **2006**, *128*, 4612-4623.

[27] a) Y. Kuramochi, A. Satake, Y. Kobuke, *J. Am. Chem. Soc.* **2004**, *126*, 8668-8669; b) O. Shoji, S. Okada, A. Satake, Y. Kobuke, *J. Am. Chem. Soc.* **2005**, *127*, 2201-2210; c) O. Shoji, H. Tanaka, T. Kawai, Y. Kobuke, *J. Am. Chem. Soc.* **2005**, *127*, 8598-8599; d) A. Satake, M. Yamamura, M. Oda, Y. Kobuke, *J. Am. Chem. Soc.* **2008**, *130*, 6314-6315.

[28] R. Dobrawa, F. Würthner, *J. Polym. Sci. Part A: Polym. Chem.* **2005**, *43*, 4981-4995.

[29] R. Dobrawa, *"Synthesis and Characterization of Terpyridine-based Fluorescent Coordination Polymers"*, Dissertation, Universität Würzburg **2004**.

[30] a) A. Islam, H. Sugihara, H. Arakawa*, J. Photochem. Photobiol. A: Chem.* **2003**, *158*, 131-138; b) P. Andres, U. S. Schubert, *Adv. Mater*. **2004**, *16*, 1043-1068; c) D. Hinderberger, O. Schmelz, M. Rehahn, G. Jeschke, *Angew. Chem.* **2004**, *116*, 4716-4721; *Angew. Chem. Int. Ed*. **2004**, *43*, 4616-4621; d) X. Chen, L. Ma, Y. Cheng, Z. Xie, L. Wang, *Polym. Int*. **2007**, *56*, 648-654; e) S. M. Brombosz, A. J. Zucchero, R. L. Phillips, D. Vazquez, A. Wilson, U. H. F. Bunz, *Org. Lett.* **2007**, *9*, 4519-4522; f) G. R. Whittell, I. Manners, *Adv. Mater.* **2007**, *19*, 3439-3468; g) J.-C. Eloi, L. Chabanne, G. R. Whittell, I. Manners, *Materials Today* **2008**, *11*, 28-36.

[31] a) C.-F. Chow, S. Fujii, J.-M. Lehn, *Angew. Chem.* **2007**, *119*, 5095-5098; *Angew. Chem. Int. Ed.* **2007**, *46*, 5007-5010; b) C.-F. Chow, S. Fujii, J.-M. Lehn, *Chem. Asian J.* **2008**, *3*, 1324-1335.

[32] M. Oh, C. A. Mirkin, *Nature* **2005**, *438*, 651-654.

[33] H. Maeda, M. Hasegawa, T. Hashimoto, T. Kakimoto, S. Nishio, T. Nakanishi, *J. Am. Chem. Soc.* **2006**, *128*, 10024-10025.

[34] W. W. Garhardt, A. J. Zucchero, J. N. Wilson, C. R. South, U. H. F. Bunz, M. Weck, *Chem. Commun.* **2006**, 2141-2143.

[35] C. Rajadurai, O. Fuhr, R. Kruk, M. Ghafari, H. Hahn, M. Ruben, *Chem. Commun.* **2007**, 2636-2638.

[36] a) F. S. Han, M. Higuchi, D. G. Kurth, *Adv. Mater.* **2007**, *19*, 3928-3931; b) F. S. Han, M. Higuchi, D. G. Kurth, *J. Am. Chem. Soc.* **2008**, *130*, 2073-2081; c) F. S. Han, M. Higuchi, Y. Akasaka, Y. Otsuka, D. G. Kurth, *Thin Solid Films* **2008**, *516*, 2469-2473; d) F. S. Han, M. Higuchi, T. Ikeda, Y. Negishi, T. Tsukudab D. G. Kurth, *J. Mater. Chem*. **2008**, *18*, 4555-4560.

[37] J. I. García, B. López-Sánchez, J. A. Mayoral, *Org. Lett.* **2008**, *10*, 4995-4998.

[38] a) S. J. Rowan, J. B. Beck, *Faraday Discuss.* **2005**, *128*, 43-53; b) W. Weng, J. B. Beck, A. M. Jamieson, S. J. Rowan, *J. Am. Chem. Soc.* **2006**, *128*, 11663-11672.

[39] a) D. Knapton, S, J. Rowan, C. Weder, *Macromolecules* **2006**, *39*, 651-657; b) M. Burnworth, D. Knapton, S. J. Rowan, C. Weder, *J. Inorg. Organomet. Polym. Mater.* **2007**, *17*, 91-103.

[40] M. Ikeda, Y. Tanaka, T. Hasegawa, Y. Furusho, E. Yashima, *J. Am. Chem. Soc.* **2006**, *128*, 6806-6807.

[41] F. Würthner, V. Stepanenko, A. Sautter, *Angew. Chem*. **2006**, *118*, 1973-1976; *Angew. Chem. Int. Ed*. **2006**, *45*, 1939–1942.

[42] R. Dobrawa, M. Lysetska, P. Ballester, M. Grüne, F. Würthner, *Macromolecules* **2005**, *38*, 1315–1325.

[43] X. Chen, L. Ma, Y. Cheng, Z. Xie, L. Wang, *Polym. Int.* **2007**, *56*, 648-654.

[44] M. Chiper, M. A. R. Meier, D. Wouters, S. Hoeppener, C.-A. Fustin, J.-F. Gohy, U. S. Schubert, *Macromolecules* **2008**, *41*, 2771-2777.

[45] T. K. Sievers, A. Vergin, H. Möhwald, D. G. Kurth, *Langmuir* **2007**, *23*, 12179-12184.

# Chapter 2

# Synthesis and Characterization of Regioisomerically Pure 1,7-Disubstituted Perylene Bisimide Dyes

**Abstract**: This chapter deals with the synthesis of regioisomerically pure 1,7-difunctionalized perylene bisimides. The bromination and subsequent imidization of perylene bisanhydride with cyclohexylamine, followed by multiple successive recrystallization afforded for the first time regioisomerically pure *N*,*N*'-dicyclohexyl-1,7-dibromoperylene bisimide *1,7*-**3**. By using this regioisomerically pure 1,7-dibromoperylene bisimide, symmetric and unsymmetric 1,7-dipyrrolidinylperylene bisimides **4a-d** and **7**, respectively, as well as difunctionalized unsymmetric 1-bromo-7-pyrrolidinyl- and 1-cyano-7-pyrrolidinylperylene bisimides **8** and **9** could be synthesized in good yields.

## Introduction

Perylene-3,4:9,10-tetracarboxylic acid bisimide (PBI) are of increasing interest as functional dyes[1] for applications in molecular electronic devices such as photovoltaic cells,[2] organic field-effect transistors (OFETs)[3] and light-emitting diodes (OLEDs)[4]. These dyes were also used in electrophotography (xerographic photoreceptors),[5] fluorescent light collectors,[6] and lasers.[7] Furthermore, liquid crystallinity of PBIs has been recently demonstrated[8] as well as nano- and mesoscopic supramolecular architectures have been revealed.[9]

Distinct optical and electronic properties are required for the application of perylene bisimides in optoelectronics. The desired properties may be achieved by proper functionalization of perylene bisimide. The chemical modifications at imide group do not significantly effect the optical and electronic properties of this chromophore because of nodes in the HOMO and LUMO at the imide nitrogen atoms.[10,11] However, these properties are drastically changed on functionalization of the perylene core with electron donor or acceptor groups. Such core-functionalized PBIs are usually synthesized from the respective halogenated, in particular brominated derivatives in the case of difunctionalized PBIs. In one of the patents in the year 1997,[12] BASF disclosed a procedure for the bromination of perylene bisanhydride **1** and subsequent imidization of the brominated product as well as the exchange of bromine atoms in bisimides by phenoxy and alkyne groups. This patent claimed that the bromination of perylene bisanhydride **1** under the conditions applied forms selectively 1,7-dibromoperylene bisanhydride *1,7*-**2** (Scheme 1) and, the subsequent imidization leads to isomerically pure 1,7-dibrominated PBIs. In the past years, numerous disubstituted perylene bisimides (PBIs) with interesting functionalities[13] including liquid crystalline[14,15] PBIs, dendrimers,[16] and polymers,[17] were synthesized from 1,7-dibrominated perylene bisimides according to the patent procedure[12] and have been applied in light-harvesting systems,[18] LEDs,[15b,18a,c,19] OFETs,[20] molecular switches,[21] wires,[22] and logic gates.[23]

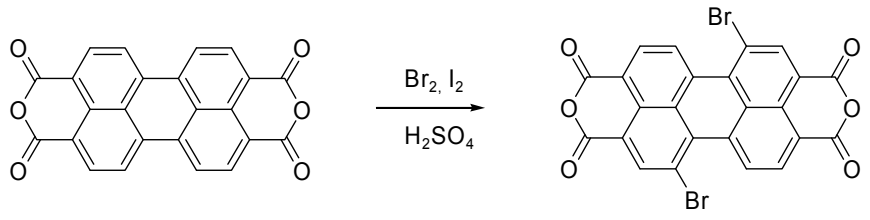


**1** *1,7*-**2**

***Scheme 1.*** Bromination of perylene bisanhydride (**1**) according to the BASF patent.[12]

Apparently the previously reported difunctionalized PBIs are apparently mixtures of 1,7 and 1,6 regioisomers rather than isomerically pure compounds. Surprisingly, only one of the above-cited publications has drawn attention to this problem, while the others have reported only 1,7-disubstituted perylene bisimides.[14b] A possible reason for this may be the fact that on the one hand, the precursor of difunctionalized perylene bisimides, *i.e*., 1,7-dibromoperylene bisanhydride *1,7*-**2**, is virtually insoluble in any organic solvent, and it could be characterized only by elemental analysis and mass spectrometry which could not differentiate the regioisomers. On the other hand, the isomeric mixtures of the subsequently synthesized perylene bisimides could only be observed by high-field (> 400 MHz) $^1$H NMR. Thus, in one of the earlier publications of our research group[15a] on liquid-crystalline PBIs, the presence of isomeric impurities was not recognized on the based of 400 MHz $^1$H NMR spectra. In the course of intensive research on perylene bisimide chemistry in our group, we became aware of this problem and have reinvestigated in detail all the steps in the synthesis of disubstituted perylene bisimides to assign unequivocally the respective isomers and to develop methods for their purification. Indeed, 1,7-dibromoperylene bisimide can be obtained in isomerically pure form and the nucleophilic replacement of bromine atoms afford pure difunctionalized bisimide derivatives.[24] Furthermore, the synthesis and characterization of new so-called green chromophores,[13a,b] such as 1,7-dipyrrolidinylperylene bisanhydride and bisimides that exhibit optical properties reminiscent of those of chlorophyll *a* (Chl *a*) are accomplished.

## Results and Discussion

**Synthesis.** The bromination of perylene bisanhydride **1** was repeated according to the patent procedure[12] (reaction conditions (a) in Scheme 2) and the crude product, which was insoluble in organic solvents, was investigated by 600 MHz $^1$H NMR spectroscopy in concentrated $D_2SO_4$ (96-98% in $D_2O$).

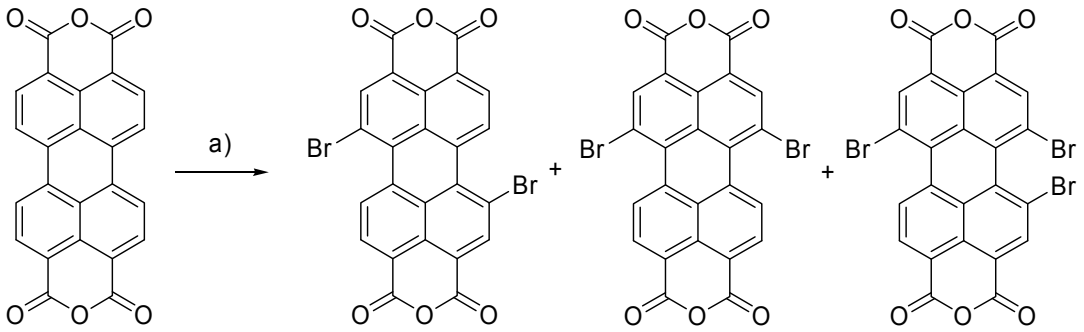


**1** *1,7*-**2** *1,6*-**2** *1,6,7*-**2´**

***Scheme 2.*** Isomeric products formed in the bromination of perylene bisanhydride **1**. Reagents and conditions: a) $Br_2$, $I_2$ (catalytic), 100% $H_2SO_4$, 85 °C, 11 h.[12]

Three sets of signals with different intensities were observed in the $^1$H NMR spectrum indicating that at least three different products are formed in the bromination of bisanhydride **1**. This signal pattern implies that 1,7- and 1,6-dibromoperylene bisanhydrides (*1,7*-**2** and *1,6*-**2**) and tribrominated perylene bisanhydride *1,6,7*-**2´** (Scheme 2) are formed in the bromination of perylene bisanhydride **1**. (Further evidence for structural assignment of these compounds is provided below).

The products of the bromination of perylene bisanhydride were insoluble in organic solvents and could not be purified by column chromatography. Therefore, the crude product mixture was used for the subsequent imidization with cyclohexylamine under the reaction conditions reported in the BASF patent (reaction conditions (b) in Scheme 3).[12] As expected, the imidization afforded a mixture of 1,7- and 1,6-dibromoperylene bisimides (*1,7*-**3** and *1,6*-**3**) and tribrominated perylene bisimide *1,6,7*-**3´**.

For the imidization of perylene bisanhydride derivatives, different reaction conditions from those used in the above-mentioned patent were employed,[16b] therefore, the imidization of brominated products of perylene bisanhydride **1** in a 2:1 mixture of $H_2O$/*n*-PrOH, instead of *N*-methylpyrrolidinone, at 80 °C (reaction conditions (c) in Scheme 3) was also carried out and similar results were obtained as under the reaction conditions (b).

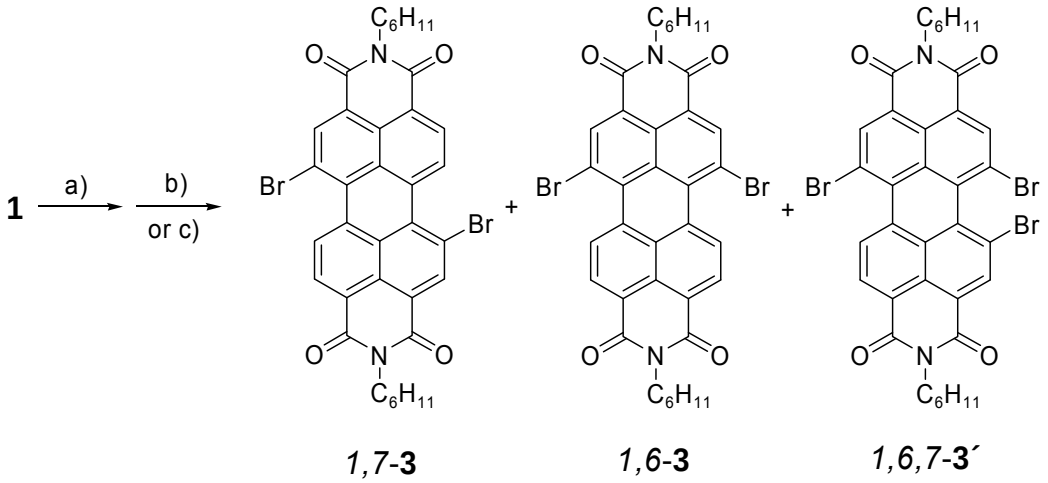


*1,7*-**3** *1,6*-**3** *1,6,7*-**3´**

***Scheme 3.*** Isomeric products formed in the bromination and subsequent imidization of perylene bisanhydride **1**. Reagents and conditions: a)[12] $Br_2$, $I_2$ (catalytic), 100% $H_2SO_4$, 85 °C, 11 h; b)[12] $H_{11}C_6$-$NH_2$, *N*-methylpyrrolidinone, 85 °C, 6 h; c) $H_{11}C_6$-$NH_2$, $H_2O$/*n*-PrOH (2:1), Ar, 80 °C, 10 h.

In contrast to brominated perylene bisanhydrides **2**, the respective perylene bisimides **3** were soluble in organic solvents facilitating their further purification. The silica-gel column chromatography of the product mixture obtained after imidization of **2** with $CH_2Cl_2$ as eluent allowed the separation of the minor component tribrominated perylene bisimide *1,6,7*-**3´**, which was obtained in ca. 1% yield and was characterized by $^1H$ and $^{13}C$ NMR, and MS. However, the regioisomeric 1,7- and 1,6-dibromoperylene bisimides (*1,7*-**3** and *1,6*-**3**) could not be separated by column chromatography and a 80:20 mixture (determined by 600 MHz $^1H$ NMR) of *1,7*-**3** and *1,6*-**3** was obtained in 61% yield. Fortunately, the major regioisomer *1,7*-**3** could be separated by recrystallization of the 80:20 mixture of *1,7*-**3** and *1,6*-**3** from $CH_2Cl_2$/MeOH (1:1). The recrystallization process was monitored by 600 MHz $^1H$ NMR spectroscopy (Figure 1) to assess the number of recrystallization steps required for complete purification. After

three successive recrystallizations, the regioisomer *1,7*-**3** could be obtained in pure form as revealed from the $^1$H NMR spectrum (Figure 1c). The mother liquor was enriched with the minor isomer *1,6*-**3** as was evident from the NMR spectrum (Figure 1d); however, the latter could not be obtained in pure form. It is noteworthy that the characteristic signals of the regioisomers *1,7*-**3** and *1,6*-**3**, in particular the doublets, were only separated in high field $^1$H NMR spectra since the chemical shifts differ very little (0.006 ppm for the doublets at 9.42-9.46 ppm, see Figure 1a), while at the lower field these signals overlap.

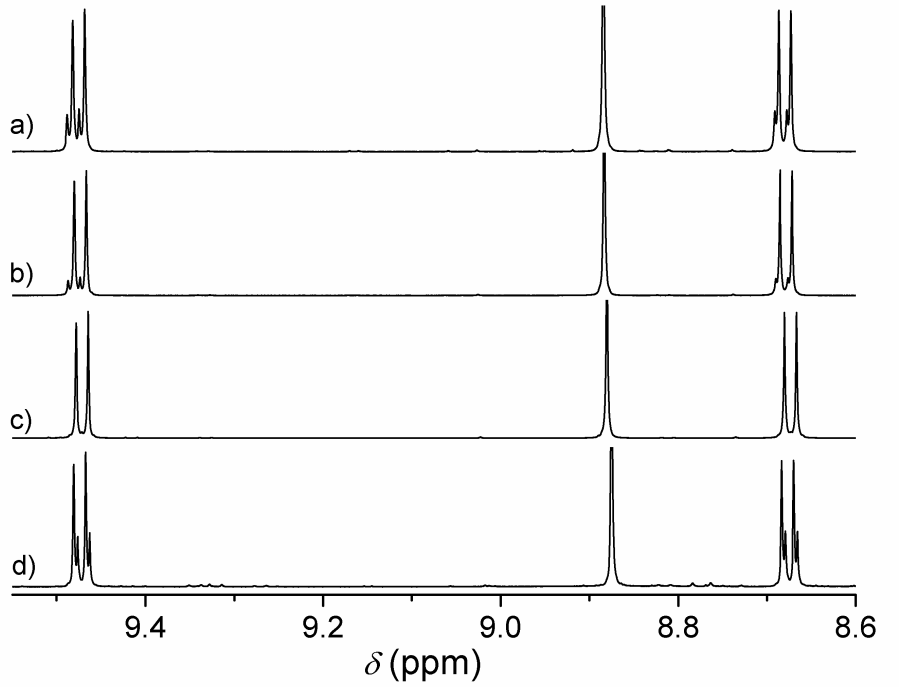


**Figure 1.** NMR spectroscopic monitoring of recrystallization; 600 MHz $^1$H NMR spectra: a) regioisomeric mixture of *1,7*-**3** and *1,6*-**3** before recrystallization; b) after one and c) after three repetitive recrystallizations; d) spectrum of mother liquor of first recrystallization.

This might be the reason why in former publications on 1,7-difunctionalized PBIs, the problem of regioisomers was not recognized. Although our NMR data are in agreement with those reported for 1,7-dibromoperylene bisimides,[14b,16b] an unequivocal assignment of the NMR signals to the individual regioisomers *1,7*-**3** and *1,6*-**3** is not possible due to the symmetry of both isomers. Fortunately, single crystals of the major

isomer, obtained after repetitive recrystallization (Figure 1c), were grown by covering its $CH_2Cl_2$ solution by MeOH layer. The crystal of 1,7-dibromo PBI *1,7*-**3** could be investigated by X-ray analysis. The crystal properties and packing information are described in our publication[24] and in the PhD thesis of Z. Chen (Universität Würzburg, 2006).

Once the reasonable amounts of isomerically pure 1,7-dibromoperylene bisimide *1,7*-**3** were obtained, this substrate was used further for the synthesis of 1,7-difunctionalized perylene bisimides and bisanhydrides. The transformations are shown in Scheme 4.

The nucleophilic substitution of regioisomerically pure 1,7-dibromoperylene bisimide *1,7*-**3** with pyrrolidine at 55 °C according to Wasielewski's method[13a] (Scheme 4, conditions (a)) afforded the corresponding dipyrrolidinyl PBI **4a** as a green solid in 67% yield after column chromatography. Once the substitution reaction was carried out at 46 °C, the monopyrrolidinyl perylene bisimide **8** was obtained in 28% yield after column chromatographic purification. The latter substrate was converted to the hitherto unknown unsymmetrically difunctionalized monocyano monopyrrolidinyl PBI **9** by cyanation with $Zn(CN)_2$ in the presence of Pd(0) catalyst according to literature procedure (Scheme 4, conditions (g)).[13e]

The saponification of **4a** in isopropanol with 100-fold excess of KOH afforded the hitherto unknown 1,7-dipyrrolidinylperylene bisanhydride **5** that could be obtained after recrystallization from tetrachloroethane / acetic ether mixture in 62% yield. This novel building block was successfully applied for the synthesis of regioisomerically pure 1,7-dipyrrolidinyl PBIs **4b**-**d**. The condensation of 1,7-dipyrrolidinylperylene-3,4:9,10-tetracarboxylic acid bisanhydride (**5**) with 4-aminopyridine in quinoline at 180 °C (Scheme 4, conditions (d)) afforded the ditopic perylene bisimide ligand **4b** (76%), which is an important building block in metal-ion-induced supramolecular chemistry.[9g,j,25] The reaction of **5** with 4-dodecylaniline and 3,4,5-tridodecyloxyaniline according to standard procedure[26] afforded the corresponding difunctionalized symmetrical PBIs **4c** and **4d** in 44% and 33% yield, respectively.

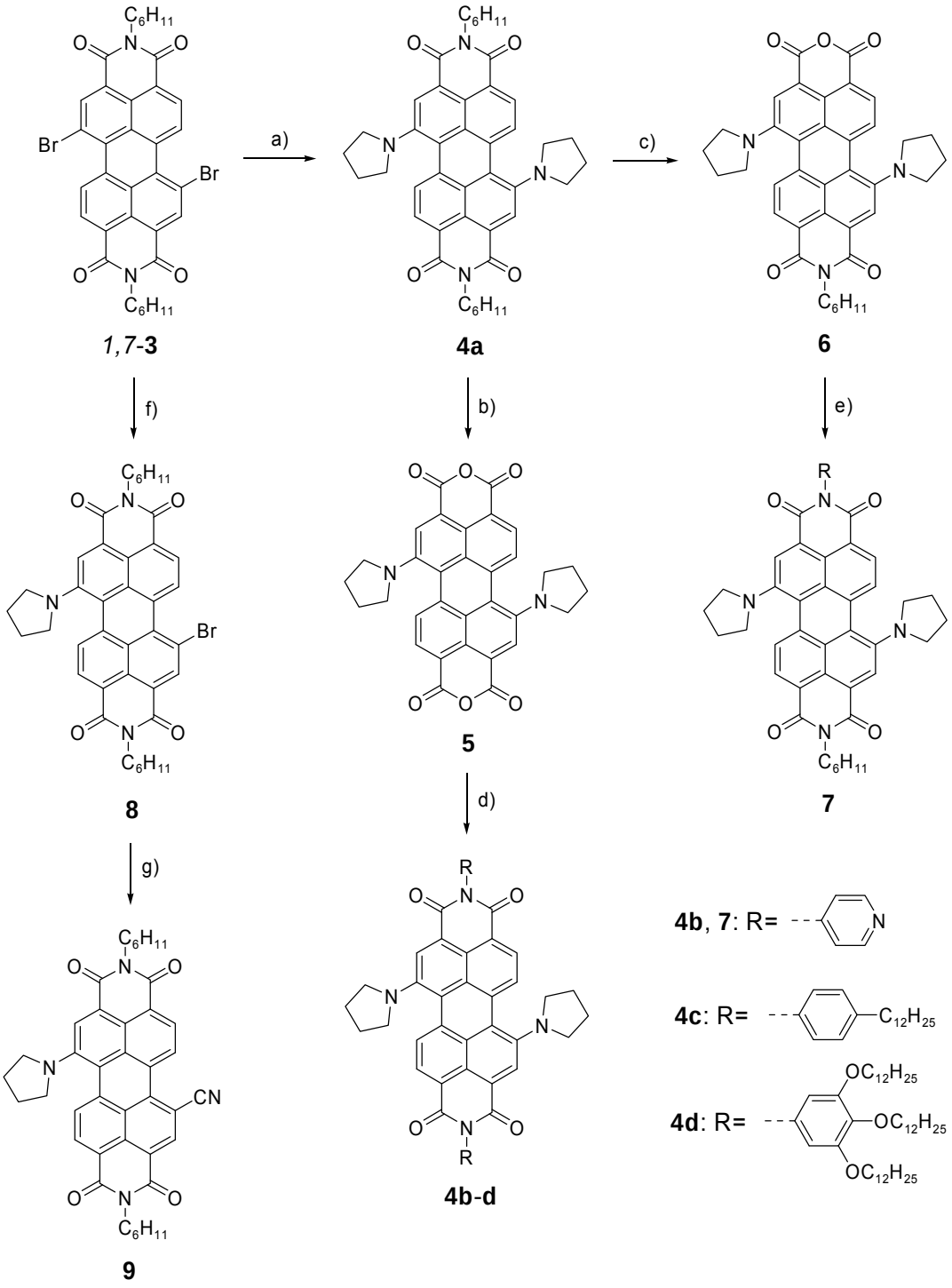


***Scheme 4.*** Chemical transformations of isomerically pure 1,7-dibromoperylene bisimide *1,7*-**3**. Reagents and conditions: a) pyrrolidine, 55 °C, Ar, 24 h, 67% of **4a**; b) KOH (100 equv.), *i*PrOH, reflux, 2 h, 62% of **5**; c) KOH (50 equv.), *i*PrOH/$H_2O$ (6:1), reflux, 2.75 h, 88% of **6**; d) 4-aminopyridine, 4-dodecylaniline or 3,4,5-tridodecyloxyaniline, $Zn(OAc)_2$, quinoline, 180 °C, 18-24 h, 76% of **4b**, 44% of **4c**, and 33% for **4d**; e) 4-aminopyridine, $Zn(OAc)_2$, quinoline, 180 °C, 4.5 h, 84% of **7**; f) pyrrolidine, 46 °C, Ar, 24 h, 28% of **8**; g) $Pd_2(dba)_3$, 1,1-bis(diphenylphosphino)ferrocene, $Zn(CN)_2$, dioxane, 110 °C, Ar, 20 h, 84% of **9**.

Since perylene monoimide monoanhydrides are important starting materials for the synthesis of unsymmetrical perylene bisimides,[27] reaction conditions for partial saponification of **4a** were searched to obtain pure dipyrrolidinyl-functionalized perylene monoimide monoanhydride **6** that may serve as a building block for the synthesis of electron-donor functionalized unsymmetrical PBIs. After optimization of the reported reaction conditions,[13b] a partial saponification of **4a** was achieved in a 6:1 mixture of isopropanol-water with 50-fold excess of KOH at 105 °C. Under these reaction conditions, after ca. 2.75 h bisimide **4a** was converted up to 45% and only monoimide monoanhydride **6** was formed. Prolonged reaction time led to the generation of bisanhydride **5**, hence the reaction was terminated after this time, followed by column chromatographic purification of the crude mixture that afforded **6** in analytically pure form in 88% yield (relative to the converted amount of **4a**) and the unreacted starting material **4a** was recovered in ca. 50% yield. The unsymmetrical, monotopic building block **7** could be obtained in 84% yield by condensation reaction of **6** with 4-aminopyridine (Scheme 4, conditions (e)).

The present 1,7-disubstituted perylene bisimides were fully characterized by $^{1}H$ and $^{13}C$ NMR, high resolution mass spectrometry, and elemental analysis (for synthetic details and characterization data, see Experimental Section).

**Optical and Electrochemical Properties.** The optical properties of present compounds in dichloromethane have been explored by UV/Vis absorption and fluorescence spectroscopy. The nucleophilic substitution of 1,7-dibromoperylene bisimide with pyrrolidine afforded a green perylene compound (**4a**) that exhibit intense optical absorption band near 700 nm.[13a,b] The introduction of secondary cyclic amine induced dramatic bathochromic shifts relative to the lowest energy optical transition of *1,7*-**3** ($\lambda_{max}$ = 527 nm in $CHCl_2$) due to a charge-transfer (CT) from electron donating amine into perylene core (see Figure 2). The maximum of the longest wavelength absorption band of **4a** is at $\lambda_{max}(\varepsilon)$ = 700 nm (38700 $M^{-1}cm^{-1}$). The optical properties of 1,7-dipyrrolidinyl-substituted perylene bisanhydride and bisimide are summarized in Table 1.

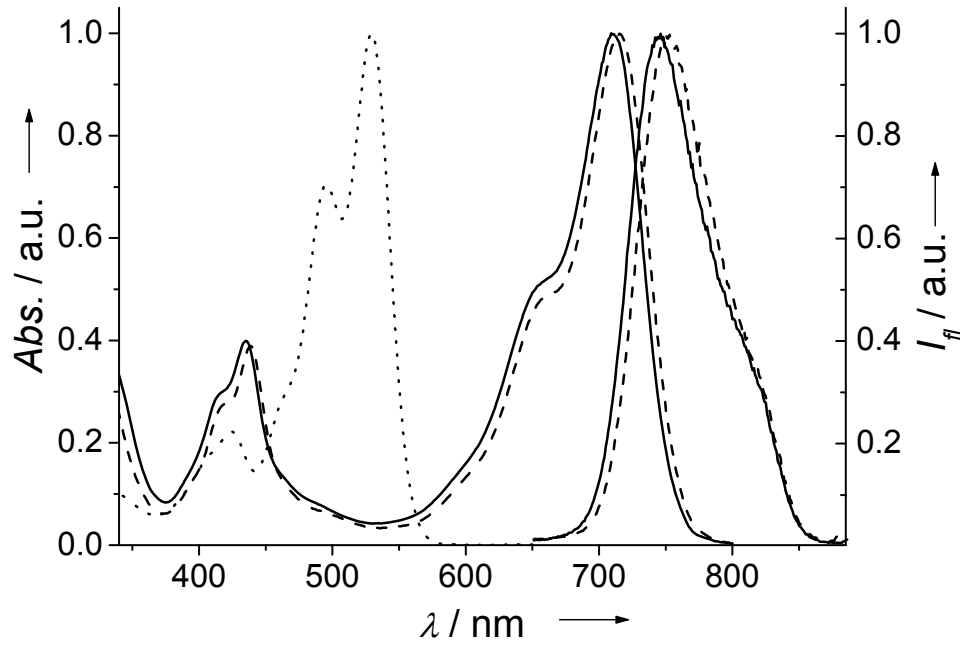


***Figure 2.*** UV/Vis absorption spectra of 1,7-dibromoperylene bisimide *1,7*-**3** (dotted line), 1,7-dipyrrolidinylperylene bisanhydride **5** (solid line) and bisimide **4b** (dashed line), and fluorescence spectra of **5** (solid line) and **4b** (dashed line) in dichloromethane at 20 °C.

***Table 1.*** Optical properties in dichloromethane.

| Compound | UV/Vis absorption | | Fluorescence emission | |
|---|---|---|---|---|
| | $\lambda_{max}$/nm | $\varepsilon$/M$^{-1}$cm$^{-1}$ | $\lambda_{max}$/nm[a] | $\Phi_{fl}$[b] |
| *1,7*-**3** | 527 | 49800 | 543 | 0.94 |
| **4a** | 700 | 38700 | 736 | 0.25 |
| **4b** | 715 | 44500 | 756 | 0.15 |
| **4c** | 706 | 45800 | 745 | 0.20 |
| **4d** | 707 | 44800 | 741 | 0.34 |
| **5** | 709 | 33500 | 744 | 0.18 |
| **6** | 708 | 35900 | 746 | 0.14 |
| **7** | 705 | 42800 | 745 | 0.25 |
| **8** | 656 | 27300 | 734 | 0.19 |
| **9** | 684 | 27600 | 754 | 0.10 |

[a] Excitation at $\lambda_{ex}$ = 500 nm for *1,7*-**3** and at $\lambda_{ex}$ = 615 nm for **4**-**9**; [b] errors for quantum yields are 0.02.

It is important to note that the replacement of the *N*-cyclohexyl substituents in perylene bisimide **4a** by other substituents (*e.g.*, 4-pyridinyl, 4-dodecylphenyl or 3,4,5-tridodecyloxyphenyl) did not affect the absorption and emission maxima of the chromophore. Upon excitation at 615 nm, perylene bisimide **4a** and anhydride **5** exhibit an intense emission at $\lambda_{max}$ = 736 and 744 nm, respectively. The fluorescence quantum yields are calculated to $\Phi_{fl}$ = 0.25 for **4a** and 0.18 for **5** in dichloromethane (see Figure 2 and Table 1).

The electrochemical properties of pyridine-functionalized 1,7-dipyrrolidinyl perylene bisimides **4b** and **7** are investigated by cyclic voltammetry (Figure 3).

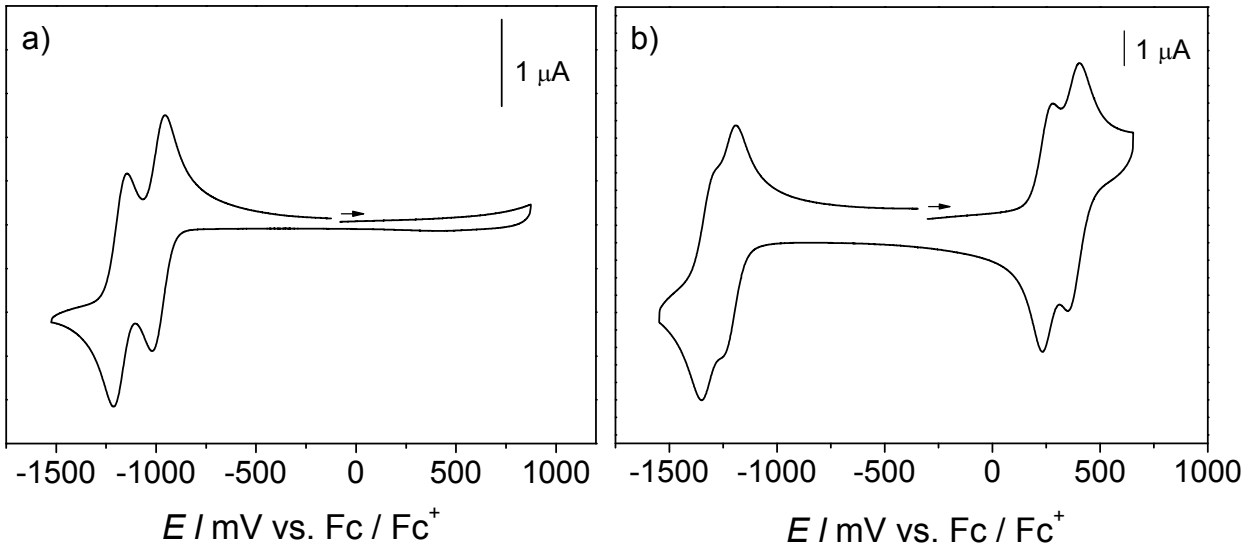


***Figure 3.*** Cyclic voltammograms of di-bromo PBI *1,7*-**3** (a) and ditopic perylene bisimide **4b** (b) in dichloromethane at RT (sweep rate 100 $mVs^{-1}$). Working electrode: platinum disk; counter electrode: platinum wire; reference electrode: Ag/AgCl; supporting electrolyte: tetrabutyl ammonium hexafluorophosphate ($NBu_4PF_6$, $1\times10^{-3}$ M).

The first and the second reduction potentials for both PBIs were detected at halfwave potentials of –1.21 V and –1.32 V vs. $Fc/Fc^+$ (for **4b**) and –1.28 V and –1.39 V vs. $Fc/Fc^+$ (for **7**) corresponding to the formation of radical anions and dianions (Figure 3b), respectively, while di-bromo perylene bisimide *1,7*-**3** possesses two reduction potentials at –0.99 and –1.17 V (Figure 3a). The substitution of bromine atoms in *1,7*-**3** by

pyrrolidinyl groups leads to little decrease in the electron affinity of the molecules. In contrast to the dibromo perylene bisimide *1,7*-**3**, which does not exhibit any oxidation waves in the available potential range (Figure 3a), two reversible oxidation waves corresponding to the formation of radical cationic and dicationic species are observed for the dipyrrolidinyl-substituted PBIs **4b** and **7** (Figure 3b). Symmetrical perylene bisimide **4b** exhibits the oxidation wave at 0.25 V corresponding to the radical cationic state of **4b**, and at 0.38 V for the second oxidation corresponding to the dicationic species. For the unsymmetrical bisimide **7**, the first and second oxidation waves occur at 0.21 V and 0.35 V, respectively. The similar redox potentials of symmetrical and unsymmetrical PBIs **4b** and **7** indicate that the electrochemical behavior of PBIs is little influenced by the substituents at the *pery* positions due to nodes at N atoms in the HOMO and LUMO.[10,11]

## Conclusions

The detailed study has shown that the bromination and subsequent imidization of perylene bisanhydride **1** with cyclohexylamine leads to a mixture of regioisomeric 1,7- and 1,6-dibromoperylene bisimides *1,7*-**3** and *1,6*-**3**, and tribrominated bisimide *1,6,7*-**3´**. Since the regioisomers *1,7*-**3** and *1,6*-**3** are only detectable by high field $^{1}$H NMR spectroscopy and cannot be separated by conventional silica-gel column chromatography, it is suspected that the previously reported 1,7-difunctionalized PBIs that were synthesized from 1,7-dibromoperylene bisimide obtained according to the BASF patent[12] are contaminated with the respective 1,6 isomers. Thus, one of the objectives of this work was to draw attention of chemists as well as material scientists to this apparently less considered problem of regioisomeric impurity in 1,7-difunctionalized PBI probes.

Isomerically pure 1,7-dibromoperylene bisimide *1,7*-**3** was obtained. Although the present purification method is rather cumbersome, to date no attractive alternative is available for the preparation of regioisomerically pure 1,7-dibromoperylene bisimides that are important precursors for the synthesis of 1,7-difunctionalized PBIs.

Regioisomerically pure 1,7-dibromoperylene bisimide *1,7*-**3** has shown to be a versatile building block for the synthesis of various pure 1,7-difunctionalized PBI derivatives. In this chapter it has been shown that the two bromine substituents can be exchanged even in a sequential manner leading to donor-acceptor substituted PBIs. Partial saponification of bisimides to imide-anhydrides is possible as well.

The 1,7-pyrrolidinyl-substituted perylene bisanhydride **5** and unsymmetrical imide-anhydride **7**, whose synthesis and characterization are given in this chapter, will be used for their subsequent chemical modification with terpyridine units to afford ditopic and monotopic PBI ligands, which were subjected to metallosupramolecular polymerization (see Chapter 3).

## Experimental Section

**General**: Solvents and reagents were obtained from commercial sources and used as received. NMR spectra were recorded at room temperature on 600 MHz ($^1$H) and 400 ($^1$H) MHz spectrometers. The solvents for spectroscopic studies were of spectroscopic grade and used as received. UV/Vis spectra were measured on a spectrophotometer equipped with a temperature controller. The steady state fluorescence spectra were measured on a conventional spectrofluorometer and fluorescence quantum yields were determined by the optically dilute method[28] with Fluorescein ($\Phi_{fl}$ = 0.92 in 1N NaOH aqueous solution),[29] Cresyl violet ($\Phi_{fl}$ = 0.54 in methanol),[30] or Nileblue ($\Phi_{fl}$ = 0.27 in ethanol)[30] as reference. Cyclic voltammetry was performed with an electrochemical workstation of BAS Epsilon in a three-electrode single-compartment cell using dichloromethane as solvent (10 mL). Working electrode: platinum disk; counter electrode: platinum wire; reference electrode: Ag/AgCl. As supporting electrolyte tetrabuthyl ammonium hexafluorophosphate ($NBu_4PF_6$, $1\times10^{-3}$ M) was used. All potentials were internally referenced to the $Fc/Fc^+$ couple. The solutions were purged with argon prior to use.

**Bromination of Perylene Bisanhydride 1**:[12] A mixture of 31.3 g (80.0 mmol) perylene-3,4:9,10-tetracarboxylic acid bisanhydride (**1**) and 472 g of 100% by weight sulfuric acid was stirred for 12 h at room temperature and subsequently $I_2$ (0.77 g, 3.0 mmol) was added. The reaction mixture was heated to 85 °C and 28.2 g (176 mmol) of bromine were added dropwise in a time period of 8 h. After bromine addition, the reaction mixture was heated for additional 10 h at 85 °C and cooled to room temperature. The excess bromine was removed by a gentle stream of $N_2$ gas and 65 mL water was added carefully. The resulting precipitate was separated by filtration through a G4 funnel, washed with 300 g of 86% sulfuric acid and a large amount of water, and dried in vacuum to give 42.0 g (95%) of a red powder. The crude product could not be purified, since it is insoluble in organic solvents. The analysis of this crude product by 600 MHz $^1$H NMR in conc. $D_2SO_4$ (96-98% in $D_2O$) revealed that 1,7- and 1,6-dibromo- and 1,7,6-tribromoperylene bisanhydrides were formed in a ratio of 76:20:4 (Figure 1).

MS (EI, 70 eV) *m/z* (%): 547.8 (45.9), 548.8 (16.0), 549.8 (92.0), 550.1 (24.2), 551.8 (45.9) [$M^+$] (calcd 550.1); HRMS (EI) calcd for $C_{24}H_6Br_2O_6$ 547.8525, found 547.8523.

**1,7-Dibromoperylene-3,4:9,10-tetracarboxylic Acid Bisanhydride (*1,7*-2)**: $^1$H NMR (600 MHz, $D_2SO_4$, calibrated for TMS): $\delta$ = 9.68 (d, 2H, *J* = 8.2 Hz), 9.01 (s, 2H), 8.79 (d, 2H, *J* = 8.3 Hz).

**1,6-Dibromoperylene-3,4:9,10-tetracarboxylic Acid Bisanhydride (*1,6*-2)**: $^1$H NMR (600 MHz, $D_2SO_4$, calibrated for TMS): $\delta$ = 9.70 (d, 2H, *J* = 8.1 Hz), 8.98 (s, 2H), 8.82 (d, 2H, *J* = 8.1 Hz).

**Imidization of Crude Bromination Product**:[12] A suspension of brominated perylene bisanhydrides (0.95 g, 1.72 mmol) obtained in the above reaction, cyclohexylamine (0.502 g, 5.07 mmol) and acetic acid (0.50 g, 8.33 mmol) in 20 mL *N*-methyl-2-pyrrolidinone was stirred at 85 °C under Ar for 6 h. After cooling to room temperature, the precipitate was separated by filtration, washed with 100 mL MeOH, and dried in vacuum. The crude product was purified by silica-gel column chromatography with $CH_2Cl_2$ as eluent. The first band was collected and after evaporation of solvent, *N,N'*-dicyclohexyl-1,7,10-tribromoperylene bisimide *1,6,7*-**3´** was obtained as a red powder (13 mg, 1%). The second band contained a mixture of *N,N'*-dicyclohexyl-1,7- and 1,6-dibromoperylene bisimide (*1,7*-**3** and *1,6*-**3**) as a red powder (755 mg, 61%) and 600 MHz $^1$H NMR analysis revealed a 80:20 ratio. The regioisomeric dibromoperylene bisimides *1,7*-**3** and *1,6*-**3** could not be separated by column chromatography.

Regioisomerically pure 1,7-dibromoperylene bisimide was obtained by repetitive crystallization. In a typical procedure, 450 mg of the 80:20 mixture of *N,N'*-dicyclohexyl-1,7- and 1,6-dibromoperylene bisimide was dissolved in 100 mL $CH_2Cl_2$. The solution was poured into a cylinder-shaped glass container (diameter: 5 cm, height: 14 cm) through a glass funnel with a filter paper and 120 mL MeOH was very carefully layered on the top of $CH_2Cl_2$ solution by a syringe. The container was sealed and kept at room temperature for 2 weeks to grow red crystals of perylene bisimide (280 mg, 62%). The

recrystallization was repeated 2 more times to obtained pure 1,7-dibromoperylene bisimide *1,7*-**3** (100 mg, 22%).

***N,N'*-Dicyclohexyl-1,7-dibromoperylene-3,4:9,10-tetracarboxylic Acid Bisimide (*1,7*-3)**: Mp > 400 °C; $^1$H NMR (600 MHz, $CDCl_3$, TMS ): $\delta$ = 9.45 (d, 2H, *J* = 8.2 Hz), 8.86 (s, 2H), 8.65 (d, 2H, *J* = 8.0 Hz), 5.02 (m, 2H), 2.54 (m, 4H), 1.20-2.00 (m, 16H); $^{13}$C NMR (100 MHz, $CDCl_3$, TMS): $\delta$ = 163.3, 162.7, 137.9, 132.7, 132.6, 129.9, 129.2, 128.4, 127.0, 123.7, 123.3, 120.7, 54.3, 29.1, 26.5, 25.4; MS (EI, 70 eV) *m/z* (%): 710.0 (20.6), 712.0 (44), 714.0 (22.9) [$M^+$] (calcd 710.0); UV/Vis ($CH_2Cl_2$): $\lambda_{max}$ ($\varepsilon$) = 527 (49800), 492 (33700), 466 (13600), 390 (5300), 276 nm (26400 $M^{-1}$ $cm^{-1}$); fluorescence ($CH_2Cl_2$, $\lambda_{ex}$ = 500 nm): $\lambda_{max}$ = 543 nm; quantum yield ($CH_2Cl_2$): $\Phi_{fl}$ = 0.94; elemental analysis: calcd (%) for $C_{36}H_{28}Br_2N_2O_4$: C, 60.69; H, 3.96; N, 3.93; found: C, 60.10; H, 4.00; N, 3.92.

***N,N'*-Dicyclohexyl-1,7,10-tribromoperylene-3,4:9,10-tetracarboxylic Acid Bisimide (*1,6,7*-3´)**: Mp > 400 °C; $^1$H NMR (400 MHz, $CDCl_3$, TMS): $\delta$ = 9.41 (d, 1H, *J* = 8.0 Hz), 8.87 (s, 1H), 8.78 (s, 2H), 8.67 (d, 1H, *J* = 8.2 Hz), 5.02 (m, 2H), 2.52 (m, 4H), 1.9-1.2 (m, 16H); $^{13}$C NMR (150 MHz, $CDCl_3$, TMS ): $\delta$ = 163.0, 162.9, 162.6, 162.5, 137.4, 136.6, 136.4, 133.3, 133.1, 131.4, 131.2, 130.8, 130.7, 129.5, 127.9, 125.9, 125.2, 124.2, 123.8, 123.7, 123.4, 123.3, 122.9, 121.3, 54.4, 54.3, 29.2, 29.1, 29.1, 29.0, 26.5, 26.5, 25.4, 25.3; MS (EI, 70 eV): *m/z* (%) = 790.0 (30.5), 791.0 (12.9), 792.0 (30.6), 793.0 (13) [$M^+$] (calcd 791.3); UV/Vis ($CH_2Cl_2$): $\lambda_{max}$ ($\varepsilon$) = 529 (36900), 495 (26000), 424 (8100), 271 nm (23000 $M^{-1}$ $cm^{-1}$).

***N,N'*-Dicyclohexyl-1,7-dipyrrolidinylperylene-3,4:9,10-tetracarboxylic Acid Bisimide (4a)**: A mixture of 95.0 mg (0.133 mmol) of *1,7*-**3** and 4.30 g (59.7 mmol) of pyrrolidine was stirred under Ar for 24 h at 55 °C. Subsequently the reaction mixture was poured into 15 mL of 10% HCl under stirring and extracted with methylene chloride (3 x 20 mL), dried over $MgSO_4$, and concentrated by rotary evaporation. The resulting precipitate was purified by column chromatography on silica gel ($CH_2Cl_2$/hexane (40/1, v/v)) to yield 62 mg (67%) of a green solid.

Mp > 400 °C; $^1$H NMR (400 MHz, $CDCl_3$, TMS): $\delta$ = 8.41 (s, 2H), 8.31 (d, *J* = 8.1 Hz, 2H), 7.56 (d, *J* = 8.1 Hz, 2H), 5.04-5.10 (m, 2H), 3.65-3.82 (m, 4H), 2.72-2.89 (m, 4H), 2.56-2.66 (m, 4H), 1.80-2.10 (m, 12H), 1.76-1.78 (m, 6H), 1.20-1.50 (m, 6H); $^{13}$C NMR (100 MHz, $CDCl_3$): $\delta$ = 163.5, 163.4, 145.4, 132.8, 128.7, 125.5, 122.6, 121.1, 119.7, 118.4, 116.9, 52.7, 51.0, 28.1, 25.6, 24.7, 24.5; MS (EI, 70 eV): *m/z* (%) = 692.3 (100) [$M^+$], 693.3 (48.8) [$M^+$+H] (calcd 692.3); HRMS (EI) calcd for $C_{44}H_{44}N_4O_4$ 692.3362, found 692.3370; UV/Vis ($CH_2Cl_2$): $\lambda_{max}$ ($\varepsilon$) = 700 (38700), 436 (15400), 346 (50600), 314 (24700), 275 nm (25300 $M^{-1}$ $cm^{-1}$); fluorescence ($CH_2Cl_2$, $\lambda_{ex}$ = 615 nm): $\lambda_{max}$ = 736 nm; quantum yield ($CH_2Cl_2$): $\Phi_{fl}$ = 0.25±0.01.

**1,7-Dipyrrolidinylperylene-3,4:9,10-tetracarboxylic Acid Bisanhydride (5)**: A mixture of 100 mg (0.15 mmol) of **4a**, 600 mg (15.0 mmol) of KOH and 5 mL of *i*PrOH was brought to reflux. The mixture was stirred for 2 h and poured under stirring into 17 mL of AcOH. The resulting green precipitate was concentrated by centrifugation, washed with water and methanol, and purified by recrystallization from tetrachloroethane/ethylacetate to give 47 mg (62%) of **5**.

Mp > 400 °C; $^1$H NMR (400 MHz, $CDCl_3$, TMS): $\delta$ = 8.47 (s, 2H), 8.42 (d, *J* = 8.1 Hz, 2H), 7.60 (d, *J* = 8.1 Hz, 2H), 3.69-3.81 (m, 4H), 2.80-2.92 (m, 4H), 2.03-2.17 (m, 8H); $^{13}$C NMR (100 MHz, tetrachlorethane[$D_2$]): $\delta$ = 160.6, 146.6, 135.2, 130.3, 129.5, 128.4, 124.1, 122.4, 118.0, 117.6, 114.7, 52.6, 25.7; MS (EI, 70 eV): *m/z* (%) = 530.1 (100) [$M^+$], 531.2 (35.9) [$M^+$+H] (calcd 530.14); HRMS (EI) calcd for $C_{32}H_{22}N_2O_6$ 530.1479, found 530.1480; UV/Vis ($CH_2Cl_2$): $\lambda_{max}$ ($\varepsilon$) = 709 (33500), 435 (13400), 318 (22400), 276 (18700), 252 nm (37300 $M^{-1}$ $cm^{-1}$); fluorescence ($CH_2Cl_2$, $\lambda_{ex}$ = 615 nm): $\lambda_{max}$ = 744 nm; quantum yield ($CH_2Cl_2$): $\Phi_{fl}$ = 0.18±0.02.

***N,N'*-Di-(4-pyridyl)-1,7-dipyrrolidinylperylene-3,4:9,10-tetracarboxylic Acid Bisimide (4b):** A mixture of 73.0 mg (0.137 mmol) of 1,7-dipyrrolidinylperylene-3,4:9,10-tetracarboxylic acid bisimide (**5**), 75.0 mg (0.792 mmol) of 4-aminopyridine and $Zn(OAc)_2$ (11.0 mg, 0.07 mmol) was heated in quinoline (3 mL) under stirring at 180 °C for 20 h under argon. After cooling to room temperature, the mixture was poured on

aqueous 2N HCl (10 mL). The resulting precipitate was separated by filtration, washed with water (5 × 40 mL) and purified by column chromatography (silica gel, $CH_2Cl_2/CH_3OH$ (40:1, v/v)) to yield 74 mg (76%) of **4b** as a dark-green powder.

Mp > 400 °C; MS (EI, 70 eV): *m/z* = 682.1 [$M^+$] calcd for $C_{42}H_{30}N_6O_4$ 682.1; $^1$H NMR (400 MHz, $CDCl_3$, TMS): $\delta$ = 8.85 (d, *J* = 6.0 Hz, 4H, $H_{Py}$), 8.53 (s, 2H, $H_{pery}$), 8.49 (d, *J* = 8.1 Hz, 2H, $H_{pery}$), 7.72 (d, *J* = 8.1 Hz, 2H, $H_{pery}$), 7.41 (d, *J* = 6.0 Hz, 4H, $H_{Py}$), 3.72-3.86 (m, 4H, $H_{Pyrrolidinyl}$), 2.80-2.92 (m, 4H, $H_{Pyrrolidinyl}$), 1.98-2.20 (m, 8H, $H_{Pyrrolidinyl}$); $^{13}$C NMR (100 MHz, $CDCl_3$): $\delta$ = 163.4, 163.3, 149.7, 146.7, 144.8, 134.8, 130.3, 127.4, 124.7, 124.2, 122.5, 121.4, 121.3, 118.6, 118.3, 52.5, 25.8; UV/Vis ($CH_2Cl_2$): $\lambda_{max}$ ($\varepsilon$) = 715 (44500), 439 (17400), 318 (25500), 248 nm (60000 $M^{-1}cm^{-1}$); fluorescence ($CH_2Cl_2$, $\lambda_{ex}$ = 615 nm): $\lambda_{max}$ = 756 nm, quantum yield ($CH_2Cl_2$) $\Phi_{fl}$ = 0.15±0.01; elemental analysis calcd for $C_{42}H_{30}N_6O_4 \times H_2O$ (700.1): C 71.91, H 4.56, N 11.98; found: C 71.37, H 4.73, N 11.34.

***N,N'*-Di-(4-dodecylphenyl)-1,7-dipyrrolidinylperylene-3,4:9,10-tetracarboxylic Acid Bisimide (4c)**: A mixture of 33.0 mg (0.062 mmol) of **5**, 78.0 mg (0.30 mmol) of 4-dodecylaniline, 20.0 mg (0.10 mmol) of $Zn(OAc)_2$ and 5 mL of quinoline was heated under stirring at 180 °C for 18 h under argon. 7 mL of 15% HCl was poured into the cooled mixture under stirring. The resulting precipitate was separated by filtration, washed with 40 mL of water, dried at 40 °C/$10^{-3}$ mbar, and purified by column chromatography ($CH_2Cl_2/CH_3OH$ (50/1, v/v)) to yield 28 mg (44%) of **4b**.

Mp 116-118 °C; $^1$H NMR (400 MHz, $CDCl_3$, TMS): $\delta$ = 8.48 (s, 2H), 8.39 (d, *J* = 8.1 Hz, 2H), 7.61 (d, *J* = 8.1 Hz, 2H), 7.37 (d, *J* = 8.4 Hz, 4H), 7.25 (d, *J* = 8.4 Hz, 4H), 3.65-3.80 (m, 4H), 2.75-2.91 (m, 4H), 2.68-2.72 (m, 4H), 1.90-2.10 (m, 4H), 1.66-1.73 (m, 4H), 1.20-1.45 (m, 40H), 0.80-0.95 (m, 6H); $^{13}$C NMR (100 MHz, $CDCl_3$): $\delta$ = 164.4, 164.3, 146.6, 143.4, 134.6, 133.1, 130.2, 129.4, 128.3, 126.9, 123.9, 122.5, 121.9, 121.1, 119.3, 118.3, 52.2, 35.8, 31.9, 31.3, 29.7, 29.7, 29.6, 29.6, 29.6, 29.5, 29.4, 25.8, 22.7, 14.1; MS (EI, 70 eV): *m/z* (%) = 1016.5 (100) [$M^+$], 1017.4 (75.2) [$M^+$+H]; HRMS (EI) calcd for $C_{68}H_{80}N_4O_4$ 1016.610, found 1016.604; UV/Vis ($CH_2Cl_2$): $\lambda_{max}$ ($\varepsilon$) = 706

(45800), 435 (18000), 315 (28400), 245 nm (63600 $M^{-1}$ $cm^{-1}$); fluorescence ($CH_2Cl_2$, $\lambda_{ex}$ = 615 nm): $\lambda_{max}$ = 745 nm; quantum yield ($CH_2Cl_2$): $\Phi_{fl}$ = 0.20±0.01; elemental analysis: calcd (%) for $C_{68}H_{80}N_4O_4 \times H_2O$ (1035): C, 78.85; H, 7.77; N, 5.40; found: C, 79.21; H, 8.06; N, 5.38.

***N,N'*-Di-(3,4,5-tridodecyloxyphenyl)-1,7-dipyrrolidinylperylene-3,4:9,10-tetracarboxylic Acid Bisimide (4d)**: A mixture of 100 mg (0.188 mmol) of **5**, 518 mg (0.80 mmol) of 3,4,5-tridodecyloxyaniline, 50.0 mg (0.25 mmol) of $Zn(OAc)_2$ and 10 mL of quinoline was heated under stirring, at 180 °C for 24 h under argon. 45 mL of 15% HCl was poured into the cooled mixture under stirring. The resulting precipitate was separated by filtration, washed with 20 mL of water and 10 mL of methanol, dried at 40 °C/$10^{-1}$ mbar, and purified by column chromatography (THF/hexane (1/2, v/v)) to yield 111 mg (33%) of **4c**.

Mp 93-95 °C; $^1$H NMR (400 MHz, $CDCl_3$, TMS): $\delta$ = 8.45 (s, 2H), 8.40 (d, *J* = 8.1 Hz, 2H), 7.65 (d, *J* = 8.1 Hz, 2H), 6.59 (s, 4H), 4.03-4.06 (m, 4H), 3.94-3.97 (m, 8H), 3.65-3.75 (m, 4H), 2.73-2.81 (m, 4H), 1.95-2.04 (m, 8H), 1.75-2.04 (m, 12H), 1.20-1.52 (m, 108H), 0.84-0.90 (m, 18H); $^{13}$C NMR (100 MHz, $CDCl_3$): $\delta$ = 164.4, 164.3, 153.6, 146.7, 138.2, 130.6, 130.3, 124.2, 122.6, 121.2, 119.4, 118.4, 106.9, 73.5, 69.1, 52.3, 31.9, 30.4, 29.8, 29.7, 29.7, 29.4, 29.4, 26.2, 26.1, 25.8, 22.7, 14.1; MS (MALDI-TOF): *m/z* = 1787.5 [$M^+$], 1788.5 [$M^+$+H] (calcd 1787.7); UV/Vis ($CH_2Cl_2$): $\lambda_{max}$ ($\varepsilon$) = 707 (44800), 436 (18300), 346 (28600), 271 (38600), 245 nm (73700 $M^{-1}$ $cm^{-1}$); fluorescence ($CH_2Cl_2$, $\lambda_{ex}$ = 615 nm): $\lambda_{max}$ = 741 nm; quantum yield ($CH_2Cl_2$): $\Phi_{fl}$ = 0.34±0.02.

***N*-Cyclohexyl-1,7-dipyrrolidinylperylene-3,4:9,10-tetracarboxylic acid-3,4-anhydride-9,10-imide (6)**: A mixture of 50.0 mg (0.072 mmol) of **4a**, 200 mg (3.60 mmol) of KOH, 0.5 mL of water and 3 mL of *i*-PrOH was brought to reflux. The mixture was stirred for 2.75 h and poured under stirring into 10 mL of AcOH. The resulting green precipitate was extracted with methylene chloride, washed with water, dried over $MgSO_4$, and concentrated by rotary evaporation. Column chromatography on silica gel

(chloroform/acetone/hexane (10/1/9, v/v/v)) afforded 28 mg of the starting material **4a** and 17 mg (88%) of **6**.

Mp 300-302 °C; $^1$H NMR (400 MHz, $CDCl_3$, TMS): $\delta$ = 8.44 (s, 1H), 8.36 (s, 1H) 8.34 (d, *J* = 8.1 Hz, 1H), 8.30 (d, *J* = 8.1 Hz, 1H) 7.61 (d, *J* = 8.1 Hz, 1H), 7.43 (d, *J* = 8.1 Hz, 1H), 5.03-5.10 (m, 1H), 3.62-3.79 (m, 4H), 2.71-2.90 (m, 4H), 2.55-2.64 (m, 2H), 1.90-2.10 (m, 10H), 1.70-1.85 (m, 3H), 1.35-1.55 (m, 3H); $^{13}$C NMR (100 MHz, $CDCl_3$, TMS): $\delta$ = 164.4, 161.3, 160.8, 147.1, 146.2, 135.8, 133.4, 130.2, 130.2, 128.7, 126.4, 124.7, 124.3, 123.5, 123.1, 122.3, 122.1, 120.9, 120.4, 119.6, 117.1, 116.8, 114.2, 53.9, 52.4, 52.3, 29.2, 26.6, 25.8, 25.8, 25.5; MS (EI, 70 eV) *m/z* (%) = 611.2 (100) [$M^+$], 612.2 (41.4) [$M^+$+H] (calcd 611.2); HRMS (EI) calcd for $C_{38}H_{33}N_3O_5$ 611.2420, found 611.2420; UV/Vis ($CH_2Cl_2$): $\lambda_{max}$ ($\varepsilon$) = 708 (35900), 436 (14500), 317 (24100), 275 (21900), 250 nm (45000 $M^{-1}$ $cm^{-1}$); fluorescence ($CH_2Cl_2$, $\lambda_{ex}$ = 615 nm): $\lambda_{max}$ = 746 nm; quantum yield: $\Phi_{fl}$ = 0.14±0.02; elemental analysis: calcd (%) for $C_{38}H_{33}N_3O_5$: C, 74.53; H, 5.39; N, 6.86; found: C, 74.36; H, 5.54; N, 6.87.

***N*-Cyclohexyl-*N'*-(4-pyridyl)-1,7-dipyrrolidinylperylene-3,4:9,10-tetracarboxylic Acid Bisimide (7):** *N*-Cyclohexyl-1,7-dipyrrolidinylperylene-3,4:9,10-tetracarboxylic acid-3,4-anhydride-9,10-imide (**16**) (60.0 mg, 98.2 µmol) was reacted with 4-aminopyridine (29.0 mg, 0.29 mmol) in the presence of $Zn(OAc)_2$ (5 mg, 30.0 µmol) in quinoline (5 mL) for 4.5 h at 180 °C under argon. After cooling to room temperature, the mixture was poured on aqueous 2N HCl (5 mL). The product was extracted with 50 mL of methylene chloride, washed with water, dried over $MgSO_4$, and concentrated by rotary evaporation. Purification was achieved by column chromatography on silica gel with $CH_2Cl_2$/methanol (40:2, v/v) to yield **7** (57 mg, 84%) as a dark-green microcrystalline powder.

Mp > 330 °C; MS (EI, 70 eV): *m/z* = 687.2 [$M^+$] calcd for $C_{43}H_{37}N_5O_4$ 687.28; HR-MS (ESI pos.): *m/z* = 687.2840 [$M^+$], calcd for $C_{43}H_{37}N_5O_4$ 687.2845; $^1$H NMR (400 MHz, $CDCl_3$, TMS): $\delta$ = 8.77 (d, *J* = 6.1 Hz, 2H, $H_{Py}$), 8.39 (s, 1H, $H_{pery}$), 8.35 (s, 1H, $H_{pery}$), 8.27 (d, *J* = 8.1 Hz, 1H, $H_{pery}$), 8.24 (d, *J* = 8.1 Hz, 1H, $H_{pery}$), 7.62 (d, *J* = 8.1 Hz, 1H,

$H_{pery}$), 7.43 (d, $J$ = 8.1 Hz, 1H, $H_{pery}$), 7.33 (d, $J$ = 6.1 Hz, 2H, $H_{Py}$), 4.93-5.02 (m, 1H, $H_{Cy}$), 3.60-3.78 (m, 4H, $H_{Pyrrolidinyl}$), 2.68-2.89 (m, 4H, $H_{Pyrrolidinyl}$), 2.52-2.58 (m, 2H, $H_{Cy}$), 1.85-2.00 (m, 10H, $H_{Pyrrolidinyl}$ and $H_{Cy}$), 1.70-1.74 (m, 2H, $H_{Cy}$), 1.28-1.50 (m, 4H, $H_{Cy}$); $^{13}$C NMR (100 MHz, $CDCl_3$): $\delta$ = 164.8, 163.9, 163.8, 151.4, 147.2, 146.6, 144.2, 135.4, 134.0, 130.5, 130.2, 127.6, 126.9, 124.6, 124.6, 123.9, 123.1, 122.9, 122.5, 121.5 121.3, 121.2, 120.4, 119.4, 118.5, 117.7, 54.3, 52.7, 29.6, 27.0, 26.2, 25.9; UV/Vis ($CH_2Cl_2$): $\lambda_{max}$ ($\varepsilon$) = 705 (42800), 436 (17200), 314 (26100), 245 nm (56600 $M^{-1}cm^{-1}$); fluorescence ($CH_2Cl_2$, $\lambda_{ex}$ = 615 nm): $\lambda_{max}$ = 745 nm, quantum yield ($CH_2Cl_2$) $\Phi_{fl}$ = 0.25±0.01.

***N,N'*-Dicyclohexyl-1-bromo-7-pyrrolidinylperylene-3,4:9,10-tetracarboxylic Acid Bisimide (8)**: In a three-necked round-bottom flask equipped with a magnetic stirrer, reflux condenser and thermometer, a mixture of 95.0 mg (0.133 mmol) of *1,7*-**3** and 4.30 g (59.7 mol) of pyrrolidine was stirred under Ar for 24 h at 46 °C (inside). The mixture was poured under stirring into 10 mL of 10% HCl. The resulting green precipitate was separated by filtration, washed with water (2 x 10 mL) and 10 mL of methanol, dried at 60 °C/$10^{-3}$ mbar and purified by column chromatography ($CH_2Cl_2$) to yield 26.0 mg (28%) of **7** as a green powder.

Mp > 350 °C; $^1$H NMR (400 MHz, $CDCl_3$, TMS): $\delta$ = 9.52 (d, $J$ = 8.3 Hz, 1H), 8.87 (s, 1H), 8.63 (d, $J$ = 8.3 Hz, 1H), 8.51 (s, 1H), 8.46 (d, $J$ = 8.3 Hz, 1H), 7.43 (d, $J$ = 8.3 Hz, 1H), 4.98-5.10 (m, 2H), 3.69-3.75 (m, 2H), 2.75-2.85 (m, 2H), 2.50-2.64 (m, 4H), 1.98-2.18 (m, 4H), 1.89-1.93 (m, 4H), 1.72-1.77 (m, 6H), 1.30-1.47 (m, 6H); $^{13}$C NMR (100 MHz, $CDCl_3$): $\delta$ = 164.3, 164.2, 163.9, 163.2, 148.4, 137.5, 134.6, 134.2, 131.5, 130.5, 129.7, 129.5, 128.0, 127.3, 125.5, 123.9, 123.4, 122.5, 121.8, 121.4, 118.9, 117.3, 114.9, 54.0, 53.9, 52.7, 29.2, 29.1, 26.6, 25.9, 25.5; MS (MALDI-TOF) *m/z* = 701.2 [$M^+$] (calcd 701.2); UV/Vis ($CH_2Cl_2$): $\lambda_{max}$ ($\varepsilon$) = 656 (27300), 437 (15000), 296 nm (25900 $M^{-1}$ $cm^{-1}$); fluorescence ($CH_2Cl_2$, $\lambda_{ex}$ = 615 nm): $\lambda_{max}$ = 734 nm; quantum yield ($CH_2Cl_2$): $\Phi_{fl}$ = 0.19±0.01; elemental analysis: calcd (%) for $C_{40}H_{36}BrN_3O_4$: C, 68.38; H, 5.16; N, 5.98; found: C, 68.15; H, 5.16; N, 6.06.

***N,N'*-Dicyclohexyl-1-cyano-7-pyrrolidinylperylene-3,4:9,10-tetracarboxylic Acid Bisimide (9)**: *N,N'*-Dicyclohexyl-1-bromo-7-pyrrolidinylperylene bisimide **7** (100 mg, 0.142 mmol), zinc cyanide (67.0 mg, 0.568 mmol), 1,1´-bis(diphenylphosphino)ferrocene (5.0 mg, 0.01 mmol) and tris(dibenzylideneacetone)dipalladium(0) (10.0 mg, 0.010 mmol) were refluxed in 6 mL dioxane for 20 h under argon. The reaction mixture was diluted with 20 mL chloroform, filtered through Celite, and the solvent was removed on a rotary evaporator. The crude product was purified by silica-gel column chromatography (with $CHCl_3$ as eluent) to yield 77 mg (84%) of **8**.

Mp > 350 °C; $R_f$ = 0.19 ($CHCl_3$); $^1$H NMR (400 MHz, $CDCl_3$, TMS): $\delta$ = 9.50 (d, $J$ = 8.3 Hz, 1H), 8.85 (s, 1H), 8.74 (d, $J$ = 8.1 Hz, 1H), 8.56 (s, 1H), 8.55 (d, $J$ = 7.7 Hz, 1H), 7.34 (d, $J$ = 8.1 Hz, 1H), 5.01-5.07 (m, 2H), 3.70-3.90 (m, 2H), 2.62-2.82 (m, 2H), 2.54-2.60 (m, 4H), 2.10-2.20 (m, 2H), 2.00-2.10 (m, 2H), 1.90-1.93 (m, 4H), 1.73-1.76 (m, 6H), 1.32-1.49 (m, 6H); $^{13}$C NMR (100 MHz, $CDCl_3$): $\delta$ = 164.3, 164.2, 164.0, 163.3, 149.8, 144.2, 138.5, 136.1, 135.8, 133.8, 132.9, 130.4, 129.9, 129.3, 128.5, 126.6, 125.1, 124.6, 122.9, 122.5, 122.0, 120.7, 118.9, 117.8, 103.9, 54.6, 54.4, 53.4, 29.6, 29.4, 26.9, 26.2, 25.8; MS (EI, 70 eV): *m/z* (%) = 648.2 (32.4) [$M^+$], 649.2 (16.5) [$M^+$+H] (calcd 648.3); HRMS (EI) calcd for $C_{41}H_{36}N_4O_4$ 648.2739, found 648.2733; UV/Vis ($CH_2Cl_2$): $\lambda_{max}$ ($\varepsilon$) = 684 (27600), 476 (6600), 425 (15800), 300 nm (23100 $M^{-1}$ $cm^{-1}$); fluorescence ($CH_2Cl_2$, $\lambda_{ex}$ = 615 nm): $\lambda_{max}$ = 754 nm; quantum yield ($CH_2Cl_2$): $\Phi_{fl}$ = 0.10±0.01; elemental analysis: calcd (%) for $C_{41}H_{36}N_4O_4$: C, 75.90; H, 5.59; N, 8.64; found: C, 75.27; H, 5.75; N, 8.54.

## References


[1] F. Würthner, *Chem. Commun.* **2004**, 1564-1579.

[2] a) A. J. Breeze, A. Salomon, D. S. Ginley, B. A. Gregg, H. Tillmann, H.-H. Hörhold, *Appl. Phys. Lett*. **2002**, *81*, 3085-3087; b) A. Yakimov, S. R. Forrest, *Appl. Phys. Lett.* **2002**, *80*, 1667-1669; c) L. Schmidt-Mende, A. Fechtenkötter, K. Müllen, E. Moons, R. H. Friend, J. D. MacKenzie, *Science* **2001**, *293*, 1119-1122; d) C. Zafer, M. Kus, G. Turkmen, H. Dincalp, S. Demic, B. Kuban, Y. Teoman, S. Icli, *Sol. Energy Mater. Sol. Cells* **2007**, *91*, 427-431; e) H. Graaf, T. Unold, C. Mattheus, D. Schlettwein, *J. Phys. D: Appl. Phys*. **2008**, *41*, 105112; f) R. Bai, M. Ouyang, R.-J. Zhou, M.-M. Shi, M. Wang, H.-Z. Chen, *Nanotechnology* **2008**, 19, 055604; g) L. Flamigni, B. Ventura, M. Tasior, T. Becherer, H. Langhals, D. T. Gryko, *Chem. Eur. J.* **2008**, *14*, 169-183.

[3] a) H. E. Katz, Z. Bao, S. L. Gilat, *Acc. Chem. Res.* **2001**, *34*, 359-369; b) F. Würthner, *Angew. Chem.* **2001**, *113*, 1069–1071; *Angew. Chem. Int. Ed.* **2001**, *40*, 1037-1039; c) Th. B. Singh, S. Erten, S. Günes, C. Zafer, G. Turkmen, B. Kuban, Y. Teoman, N.S. Sariciftci, S. Icli, *Organic Electronics* **2006**, *7*, 480-489; d) R. Schmidt, M. M. Ling, J. H. Oh, M. Winkler, M. Könemann, Z. Bao, F. Würthner, *Adv. Mat.* **2007**, *19,* 3692-3695; e) J. Hak Oh, S. Liu, Z. Bao, R. Schmidt, F. Würthne, *Appl. Phys. Lett.* **2007**, *91*, 212107; f) C-C. You, P. Espindola, C. Hippius, J. Heinze, F. Würthner, *Adv. Funct. Mat*. **2007**, *17*, 3764-3772; g) R. T. Weitz, K. Amsharov, U. Zschieschang, E. B. Villas, D. K. Goswami, M. Burghard, H. Dosch, M. Jansen, K. Kern, H. Klauk, *J. Am. Chem.Soc.* **2008**, *130*, 4637-4645.

[4] a) M. A. Angadi, D. Gosztola, M. R. Wasielewski, *Mater. Sci. Eng. B* **1999**,*63*, 191-194; b) A. Kraft, A. C. Grimsdale, A. B. Holmes, *Angew. Chem.* **1998**, *110*, 416-443; *Angew. Chem. Int. Ed.* **1998**, *37*, 402-428; c) P. Ranke, I. Bleyl, J. Simmerer, D. Haarer, A. Bacher, H. W. Schmidt, *Appl. Phys. Lett*. **1997**, *71*, 1332-1334; d) L. Fan, W. Zhu, J. Li, H. Tian, *Syn. Met.* **2004**, *145*, 203-210; e) J. Pan, W. Zhu, S. Li, W. Zeng, Y. Cao, H. Tian, *Polymer* **2005**, *46*, 7658-7669; f) J. Hua, F. Meng, J. Li, P. Zhao, Y. Qu, *J. Appl. Polym. Sci.* **2007**, *110*, 1778-1783.

[5] a) K.-Y. Law, *Chem. Rev*. **1993**, *93*, 449-486; b) J. M. Duff, A.-M. Hor, C. G. Allen, *U.S. Pat*., US 5853933, **1998**; c) C.-K. Hsiao, A.-M. Hor, G. Baranyi, H. B. Goodbrand, *U.S. Pat*., US 6194110, **2001**.

[6] a) G. Seybold, G. Wagenblast, *Dyes Pigm.* **1989**, *11*, 303-317; b) G. Seybold, A. Stange, (BASF AG), *German Pat.*, DE 3545004, **1987**; *Chem. Abstr.* **1988**, *108*, 77134c; c) H. Langhals, S. Saulich, *German Pat.*, DE 10212358, **2003**; d) L. Flamigni, B. Ventura, C-C. You, C. Hippius, F. Würthner, *J. Phys. Chem. C* **2007**, *111*, 622-630.

[7] a) R. Gvishi, R. Reisfeld, Z. Burshtein, *Chem. Phys. Lett.* **1993**, 213, 338-344; b) R. Reisfeld, G. Seybold, *Chimia* **1990**, *44*, 295-297; c) H.-G. Löhmannsröben, H. Langhals *Appl. Phys.* **1989**, *B48*, 44-452.

[8] a) C. W. Struijk, A. B Sieval, J. E. J. Dakhorst, M. van Dijk, P. Kimkes, R. B. M. Koehorst, H. Donker, T.J. Schaafsma, S. J. Picken, A. M. van de Craats, J. M. Warman, H. Zuilhof, E. J. R. Sudhölter, *J. Am. Chem. Soc.* **2000**, *122*, 11057-11066; b) S. Alibert-Fouet, S. Dardel, H. Bock, M. Oukachmih, S. Archambeau, I. Seguy, P. Jolinat, P. Destruel, *ChemPhysChem.* **2003**, *4*, 983-985; c) Z. An, J. Yu, S. C. Jones, S. Barlow, S. Yoo, B. Domercq, P. Prins, L. D. A. Siebbeles, B. Kippelen, S. R. Marder, *Adv. Mater.* **2005**, *17*, 2580-2583; d) M. G. Debije, Z. Chen, J. Piris, R. B. Neder, M. M. Watson, K. Müllen, F. Würthner, *J. Mater. Chem.* **2005**, *15*, 1270-1276; e) D. Franke, M. Vos, M. Antonietti, N. A. J. M. Sommerdijk, C. F. J. Faul, *Chem. Mater.* **2006**, *18,* 1839-1847; f) Z. Chen, V. Stepanenko, V. Dehm, P. Prins, L. D. A. Siebbeles, J. Seibt, P. Marquetand, V. Engel, F. Würthner, *Chem. Eur. J.* **2007***, 13,* 436-449; g) V. Dehm, Z. Chen, U. Baumeister, P. Prins, L. D. A. Siebbeles, F. Würthner, *Org. Lett.* **2007**, *9*, 1085-1088; h) Y. Xu, S. Leng, C. Xue, R. Sun, J. Pan, J. Ford, S. Jin, *Angew. Chem.* **2007**, *119*, 3970-3973; *Angew. Chem. Int. Ed.* **2007**, *46*, 3896-3899.

[9] a) F. Würthner, C. Thalacker, A. Sautter, *Adv. Mater.* **1999**, *11*, 754-758; b) F. Würthner, A. Sautter, *Chem. Commun.* **2000**, 445-446; c) A. P. H. J. Schenning, J. van Herrikhuyzen, P. Ionkheijm, Z. Chen, F. Würthner, E. W. Meijer, *J. Am. Chem. Soc.* **2002**, *124*, 10252-10253; d) R. Dobrawa, F. Würthner, *Chem. Commun.* **2002**, *17*, 1878-1879; e) T. van der Boom, R. T. Hayes, Y. Zhao, P. J.

Bushard, E. A. Weiss, M. R. Wasielewski, *J. Am. Chem. Soc.* **2002**, *124*, 9582-9590; f) E. Peeters, P. A. van Hal, C. J. Meskers, R. A. J. Janssen, E. W.Meijer, *Chem. Eur. J.* **2002**, *8*, 4470-4474; g) C.-C. You, F. Würthner, *J. Am. Chem. Soc.* **2003**, *125*, 9716-9725; h) R. Dobrawa, M. Lysetska, P. Ballester, M. Grüne, F. Würthner, *Macromolecules* **2005**, *38*, 1315–1325; i) F. Würthner, *Pure Appl. Chem*. **2006**, *78,* 2341-2350; j) C-C. You, C. Hippius, M. Grüne, F. Würthner, *Chem. Eur. J.* **2006***,12,* 7510-7519; k) T. Seki, S. Yagai, T. Karatsu, A. Kitamura, *J. Org. Chem.* **2008**, *73*, 3328-3335.

[10] H. Langhals, S. Demmig, H. Huber, *Spectrochim. Acta* **1988**, *44A*, 1189-1193.

[11] J. Salbeck, H. Kunkely, H. Langhals, R. W. Saalfrank, J. Daub, *Chimia* **1989**, *43*, 6-9.

[12] A. Böhm, H. Arms, G. Henning, P. Blaschka, (BASF AG), *German Pat.* DE 19547209 A1, **1997**; *Chem. Abstr.* **1997**, *127*, 96569g.

[13] a) Y. Zhao, M. R. Wasielewski, *Tetrahedron Lett.* **1999**, *40*, 7047-7050; b) A. S. Lukas, Y. Zhao, S. E. Miller, M. R. Wasielewski, *J. Phys. Chem. B* **2002**, *106*, 1299-1306; c) T. van der Boom, R. T. Hayes, Y. Zhao, P. J. Bushard, E. A. Weiss, M. R. Wasielewski, *J. Am. Chem. Soc.* **2002**, *124*, 9582-9590; d) M. J. Fuller, C. J. Walsh, Y. Zhao, M. R. Wasielewski, *Chem. Mater.* **2002**, *14*, 952-953; e) M. J. Ahrens, M. J. Fuller, M. R. Wasielewski, *Chem. Mater.* **2003**, *15*, 2684-2686; f) Z. E. X. Dance, Q. Mi, D. W. McCamant, M. J. Ahrens, M. A. Ratner, M. R. Wasielewski, *J. Phys. Chem. B* **2006,** *110,* 25163-25173; g) H. Wang, T. E. Kaiser, S. Uemura, F. Würthner, *Chem.Commun*. **2008**, 1181-1183; h) R. H. Goldsmith, O. DeLeon, T. M. Wilson, D. Finkelstein-Shapiro, M. A. Ratner, M. R. Wasielewski, *J. Phys. Chem. A* **2008**, *112,* 4410-4414; i) J. M. Giaimo, J. V. Lockard, L. E. Sinks, A. M. Scott, T. M. Wilson, M. R. Wasielewski, *J. Phys. Chem. A* **2008,** *112,* 2322-2330.

[14] a) U. Rohr, P. Schlichting, A. Böhm, M. Gross, K. Meerholz, C. Bräuchle, K. Müllen, *Angew. Chem.* **1998**, *110*, 1463-1467; *Angew. Chem. Int. Ed.* **1998**, *37*, 1434-1437; b) U. Rohr, K. Christopher, K. Müllen, A. van de Craats, J. Warman, *J. Mater. Chem.* **2001**, *11*, 1789-1799.

[15] a) F. Würthner, C. Thalacker, S. Diele, C. Tschierske, *Chem. Eur. J.* **2001**, *7*, 2247-2253; b) Z. Chen, U. Baumeister, C. Tschierske, F. Würthner, *Chem. Eur. J.* **2007**, *13*, 450-465.

[16] a) J. M. Serin, D. W. Brousmiche, J. M. J. Fréchet, *Chem. Commun.* **2002**, *22*, 2605-2607; b) J. M. Serin, D. W. Brousmiche, J. M. J. Fréchet, *J. Am. Chem. Soc.* **2002**, *124*, 11848-11849.

[17] a) M. Thelakkat, P. Pösch, H.-W. Schmidt, *Macromolecules* **2001**, *34*, 7441-7447; b) C. Ego, D. Marsitzky, S. Becker, J. Zhang, A. C. Grimsdale, K. Müllen, J. D. MacKenzie, C. Silva, R. H. Friend, *J. Am. Chem. Soc.* **2003**, *125*, 437-443; c) S. P. Dudek, M. Pouderoijen, R. Abbel, A. P. H. J. Schenning, E. W. Meijer, J. Am. *Chem. Soc.* **2005**, *127*, 11763-11768; d) H.-Y. Wang, B. Peng, W. Wei, *J. Polym. Sci. Part B: Polym. Phys.* **2008**, *46*, 1932-1938.

[18] a) K. Sugiyasu, N. Fujita, S. Shinkai, *Angew. Chem.* **2004**, *116*, 1249-1253; *Angew. Chem. Int. Ed.* **2004**, *43*, 1229-1233; b) R. F. Kelley, W. S. Shin, B. Rybtchinski, L. E. Sinks, M. R. Wasielewski, *J. Am. Chem. Soc.* **2007**, *129*, 3173-3181; c) C. Hippius, I. H. M van Stokkum, E. Zangrando, R. M .Williams, M. Wykes, D. Beljonne, F. Würthner, *J. Phys. Chem. C* **2008**, *112*, 14626–14638.

[19] F. Würthner, P. Osswald, R. Schmidt, T. E. Kaiser, H. Mansikkamäki, M. Könemann, *Org. Lett*. **2006**, *8, 17*, 3765-3768.

[20] a) B. Yoo, T. Jung, D. Basu, A. Dodabalapur, B. A. Jones, A. Facchetti, M. R. Wasielewski, T. J. Marks, *Appl. Phys. Lett.* **2006**, *88*, 082104; b) Y. Wang, Y. Chen, R. Li, S. Wang, W. Su, P. Ma, M. R. Wasielewski, X. Li, J. Jiang, *Langmuir* **2007**, *23*, 5836-5842; c) B. A. Jones, A. Facchetti, M. R. Wasielewski, T. J. Marks, *J. Am. Chem. Soc.* **2007**, *129*, 15259-15278; d) B. A. Jones, A. Facchetti, M. R. Wasielewski, T. J. Marks, *Adv. Funct. Mater.* **2008**, *18*, 1329-1339.

[21] a) J. M. Giaimo, A. V. Gusev, M. R. Wasielewski, *J. Am. Chem. Soc.* **2002**, *124*, 8530-8531; b) M. Berberich, A-M. Krause, M. Orlandi, F. Scandola, F. Würthner, *Angew. Chem.* **2008**, *120*, 6718-6721; *Angew. Chem. Int. Ed*. **2008**, *47*, 6616-6619.

[22] E. A. Weiss, M. J. Ahrens, L. E. Sinks, A. V. Gusev, M. A. Ratner, M. R. Wasielewski, *J. Am. Chem. Soc.* **2004**, *126*, 5577-5584.

[23] X. Guo, D. Zhang, D. Zhu, *Adv. Mater*. **2004**, *16*, 125-130.

[24] The major part of this chapter is published: F. Würthner, V. Stepanenko, Z. Chen, C. R. Saha-Möller, N. Kocher, D. Stalke, *J. Org. Chem.* **2004**, *69*, 7933-7939.

[25] A. Sautter, B. Kaletaş, D. G. Schmid, R. Dobrawa, M. Zimine, G. Jung, I. H. M. van Stokkum, L. De Cola, R. M. Williams, F. Würthner, *J. Am. Chem. Soc.* **2005**, *127*, 6719–6729.

[26] F. Würthner, A. Sautter, D. Schmid, P. J. A. Weber, *Chem. Eur. J.* **2001**, *7*, 894-902.

[27] Y. Nagao, T. Naito, Y. Abe, T. Misono, *Dyes Pigm.* **1996**, *32*, 71-83.

[28] J. R. Lakowicz, *Principles of Fluorescence Spectroscopy*, 2nd ed., Kluwer Academic Plenum: New York, 1999.

[29] J. N. Demas, G. A. Grosby, *J. Phys. Chem.* **1971**, *75*, 991-1024.

[30] R. Sens, K. H. Drexhage, *J. Luminesc.* **1981**, *24*, 709-712.

# Chapter 3

## Metal-Ion Mediated Self-Assembly of Terpyridine-anchored Perylene Bisimides into Extended Rigid Polymers

**Abstract.** Red and green 2,2′:6′,2″-terpyridine (tpy)-functionalized perylene bisimide (PBI) building blocks have been synthesized and their metal-ion directed self-assembly has been studied in details by $^{1}$H NMR, DOSY NMR, and UV/Vis spectroscopy. These studies revealed that the newly synthesized ditopic bis(tpy)-PBI ligands, in which the tpy units are directly connected to PBI moieties at the imide positions, form coordination polymers upon addition of Zn(II) ion in a reversible manner. Atomic force microscopy (AFM) investigations have shown formation of extended rigid polymers which coat closely packed film with linear arrangement on graphite surface. Multilayer film of two different coordination polymers in alternate fashion could be prepared by layer-by-layer deposition technique and surface density Γ of perylene bisimide chromophores in film could be estimated.

## Introduction

Since the end of nineteenth century, polymer chemistry has been playing a significant role in natural and applied sciences.[1] Till present time, the concepts of covalent chemistry are the dominant tools for the synthesis of polymers. However, with the vigorous development of supramolecular chemistry since 1980s,[2] the utilization of reversible and highly directional noncovalent interactions has become increasingly more popular for the construction of supramolecular polymers.[3] The noncovalent interactions that have been amply applied for supramolecular polymers are hydrogen bonding,[4] dipolar,[5] solvophobic,[4e,6] π-π-interactions,[7] and metal ion-ligand coordinations.[8] Compared to the relatively weak hydrogen bonding, ionic and π-π-interactions, the metal ion coordination is a significantly stronger binding interaction and the thermodynamic and kinetic stability of coordination bond can be fine-tuned by choosing proper combination of ligand types and metal ions. Thus, metal ion-ligand coordination is a versatile tool for the preparation of coordination polymers by supramolecular approach.[8]

The fact that a large number of pyridine-based ligands are commercially available and many of them can be structurally modified by simple chemical transformation, the pyridine-functionalized building blocks are very suitable and prominent for investigating the polymerization through metal ion coordination. In particular, bipyridine and terpyridine ligands are of interest as they can coordinate a large variety of metal ions. Specifically, the 2,2′:6′,2″-terpyridine (tpy) derivatives exhibit strong chelating affinity with many transition metals.[9] A broad structural variation of tpy ligand has been utilized to tailor the properties of its metal complexes, which possess distinct optical, photophysical, electrochemical and magnetic properties,[9a,10] and are valuable functional materials for light-emitting diodes, solar cells and sensors.[8c-f,11]

Perylene bisimide (PBI) dyes are an important class of chromophores with excellent optical and electronic properties,[12] and they have been amply applied to create supramolecular assemblies by metal ion-ligand coordination,[8e,j,13] hydrogen binding[14] and π-π-interactions[15]. Furthermore, PBI dyes have been successfully incorporated in conventional covalent polymers and block copolymers.[16]

Our group has recently reported that metal-ion directed self-assembly of tpy-functionalized red tetraphenoxy-substituted perylene bisimides (tpy-Ph-PBI in Chart 1) that contain phenylene spacers connecting the imide groups with tpy ligand leads to the formation of coordination polymers with chain lengths of about 15 repeat units.[8e] One of the limitations of tpy-Ph-PBI building blocks was an only moderate solubility which was attributed to the extended π-system. For this reason only perylene bisimides with bulky bay substituents could be achieved in high purity and transformed to supramolecular coordination polymers by addition of zinc(II) and iron(II) salts. It appeared to us that a direct attachment of terpyridine receptor groups to the perylene bisimide chromophore should afford better soluble dyes owing to a less flexible receptor unit that cannot form a planar arrangement with the perylene unit for steric reasons (Chart 1).

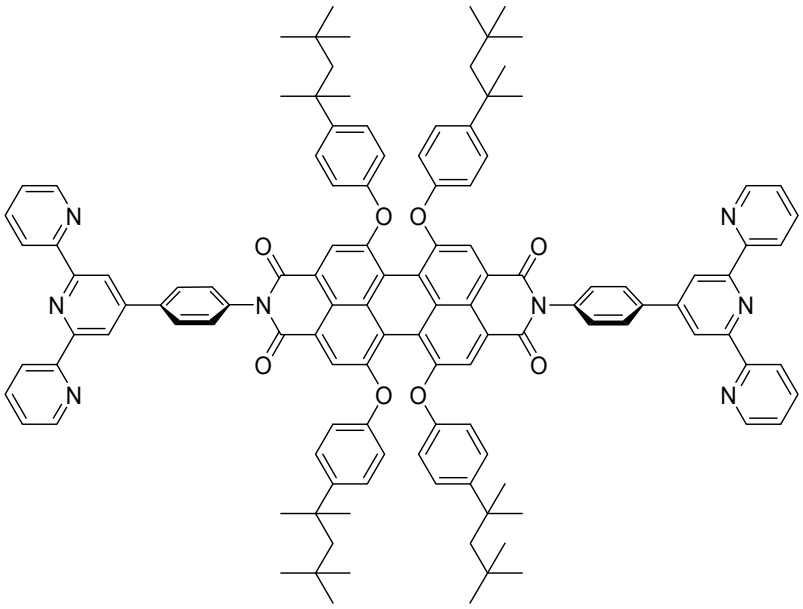

**tpy-Ph-PBI**

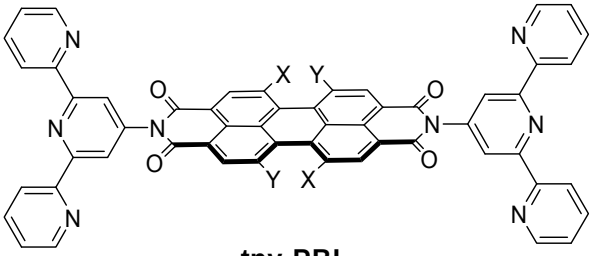

**tpy-PBI**

***Chart 1.*** General structures of previously investigated **tpy-Ph-PBI**[8e] and newly designed building blocks **tpy-PBI**.

This Chapter introduces the newly designed well soluble red and green[17] PBI building blocks, that do not contain phenylene spacers (for general structure, see tpy-PBI in Chart 1). Upon metal ion coordination of there red and green PBIs extended rigid metallosupramolecular polymers with chain length of up to 35 repeat units are formed that cover the whole visible absorption range and can be deposited in alternate fashion by layer-by-layer technique.

## Results and Discussion

**Synthesis of Tpy-anchored PBI Ligands.** The ditopic bis(terpyridine)-functionalized perylene bisimide **3** and **4a**,**b** were synthesized by imidization of the respective perylene-3,4:9,10-tetracarboxylic acid bisanhydride **1**[17c] and **2a**, **b**[14a,16a] with 4'-amino-2,2':6',2''-terpyridine[18] in pyridine/imidazole mixture in 46-59% isolated yield (Schema 1).

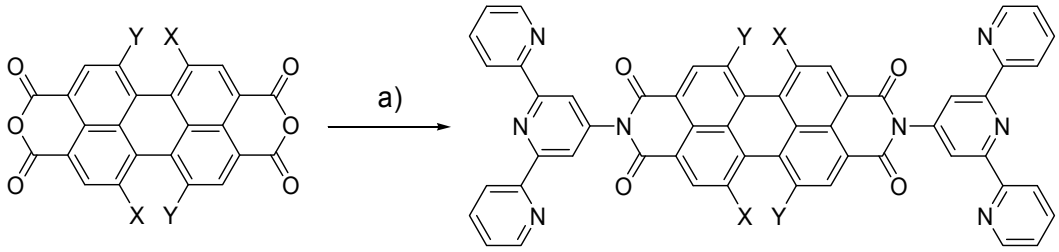


**1**: X = H, Y = (= Pyr) **3**: X = H, Y = Pyr

**2a**: X, Y = (= *p*-*t*OctPhO) **4a**: X, Y = *p*-*t*OctPhO

**2b**: X, Y = (= *p*-*t*BuPhO) **4b**: X, Y = *p*-*t*BuPhO

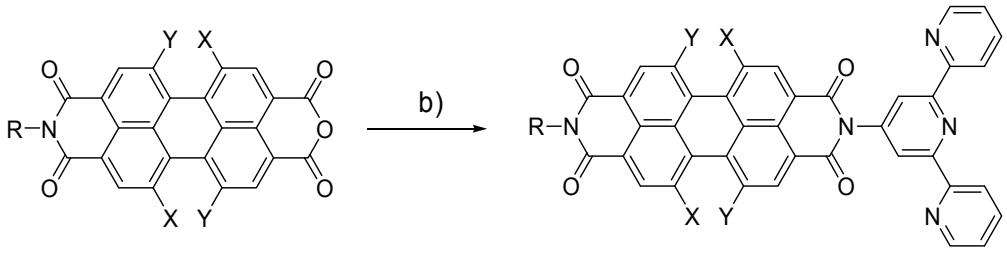


**5**: R = (= Cy); X = H, Y = Pyr **7**: R = Cy, X = H, Y = Pyr

**6**: R = *n*-$C_4H_9$; X, Y = *p*-*t*BuPhO **8**: R = *n*-$C_4H_9$; X, Y = *p*-*t*BuPhO

***Scheme 1.*** Synthesis of bis(tpy)-PBI ligands **3** and **4a**,**b**, and monotopic reference compounds **7** and **8**: a) 4′-amino-2,2′:6′,2″-terpyridine, pyridine/imidazol (2:1) mixture, argon, 120 °C, 48 h, 59% yield for **3**; 24 h, 46% yield for **4a** and 50% yield for **4b**; b) 4′-amino-2,2′:6′,2″-terpyridine. pyridine/imidazol (2:1) mixture, argon, 120 °C, 50 h, 68% yield for **7**; 48 h, 50% yield for **8**.

The monotopic reference compounds **7** and **8** were prepared similarly by condensation of 4'-amino-2,2':6',2''-terpyridine with the corresponding perylene-3,4:9,10-tetracarboxylic

acid-3,4-anhydride-9,10-imide **5**[17c] and **6**[14a] in 50 - 68% yield. The newly synthesized terpyridine-functionalized PBI building blocks were properly characterized by $^1$H NMR, MS, and in same cases also by elemental analysis.

**Complexation of Monotopic Ligands with Zn(II) Ion.** Prior to investigating the self-assembly properties of bis(tpy)-PBI ligands under metal-ion mediation, the complexation of monotopic reference compounds **7** and **8** with Zn(II) ion was studied as these ligands should form dimeric complexes at a 2:1 ratio of ligand and Zn(II) ion,[8e] and the spectroscopic data, in particular $^1$H NMR data, of such dimers will be helpful for the elucidation of supramolecular polymerization of ditopic ligands.

Indeed, the addition of zinc triflate ($Zn(OTf)_2$) to ligands **7** and **8** in chloroform/methanol (60:40) mixture led to the formation of respective dimer complexes (Scheme 2) as confirmed by $^1$H NMR and MALDI-TOF mass spectrometry.

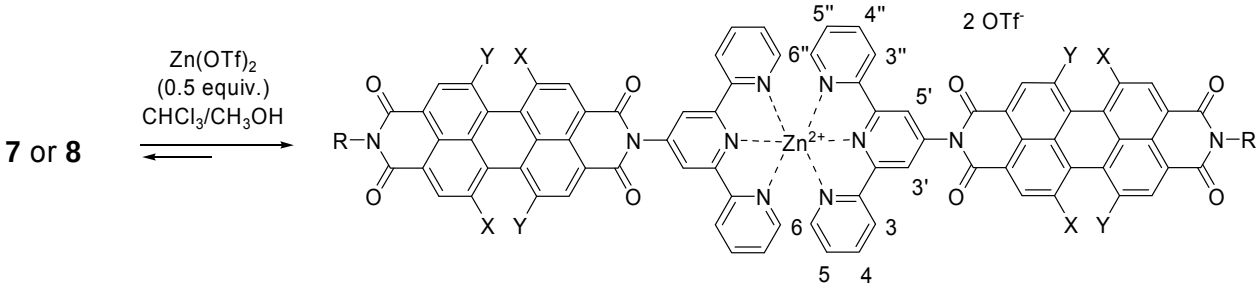


($\mathbf{7}$)$_2$Zn(OTf)$_2$: R = Cy, X = H, Y = Pyr

($\mathbf{8}$)$_2$Zn(OTf)$_2$: R = *n*-$C_4H_9$; X, Y = *p*-*t*BuPhO

***Scheme 2.*** Formation of metallodimers ($\mathbf{7}$)$_2$Zn(OTf)$_2$ and ($\mathbf{8}$)$_2$Zn(OTf)$_2$ by Zn(II)-ion-mediated self-assembly of mono(terpyridyl)-PBI ligands **7** and **8** at a 2:1 stoichiometry of ligand/Zn(OTf)$_2$ in chloroform/methanol (60:40) mixture.

The $^1$H NMR spectra measured for different ratios of ligand **7** or **8** and Zn(OTf)$_2$ provide clear indication for the formation of corresponding metallodimer ($\mathbf{7}$)$_2$Zn(OTf)$_2$ and ($\mathbf{8}$)$_2$Zn(OTf)$_2$ at an exact 2:1 ratio of ligand/Zn(II) ion (Figure 1). After achieving a 2:1 ratio of tpy-ligand/Zn(II) ratio, the signals of free terpyridine ligands disappeared and a new set of sharp signals arise with a strong upfield shift of 6,6'' protons from 8.65 and

8.72 ppm to 7.87 and 8.07 ppm compared with those of the free ligands **7** and **8**, respectively. Due to the different chemical environment of the 6,6'' protons in complex compared to those of the free ligand, the upfield shift of the 6,6'' signals, which is mainly caused by the aromatic shielding effect of the neighboring second tpy unit, is characteristic for di(terpyridine) metal complexes,[8e,19] thus the observed NMR properties confirm formation of coordination dimer complexes $(\mathbf{7})_2Zn(OTf)_2$ and $(\mathbf{8})_2Zn(OTf)_2$.

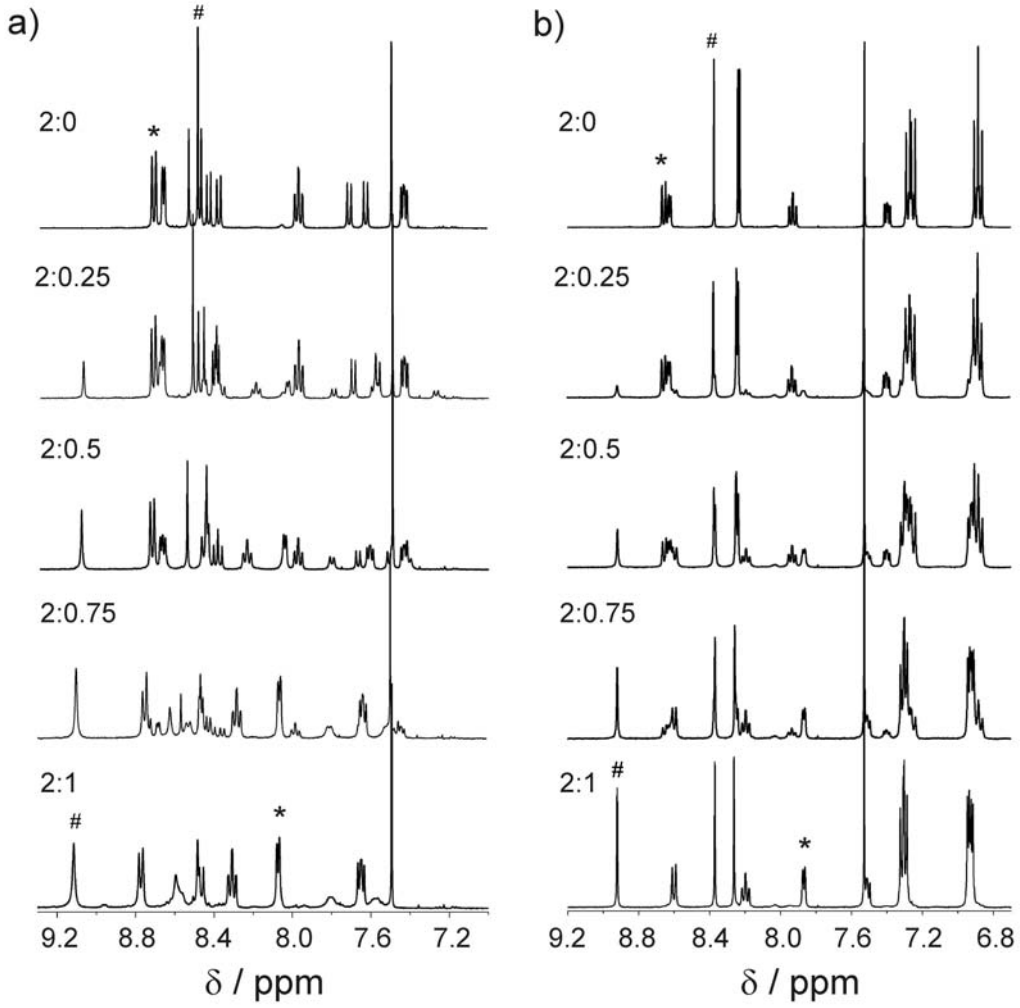


***Figure 1.***Aromatic region of $^1$H NMR spectra at different ligand/Zn(II) ion ratios (2:0 to 2:1): a) for the monotopic ligand **7** and zinc triflate in $CDCl_3/CD_3OD$ (60:40, 5 mM) from free **7** (upper spectrum) to dimer $(\mathbf{7})_2Zn(OTf)_2$ (bottom); b) for the monotopic ligand **8** and zinc triflate in $CDCl_3/CD_3OD$ (60:40, 3.5 mM) from free **8** (upper spectrum) to dimer $(\mathbf{8})_2Zn(OTf)_2$ (bottom). Ratio of **7**:Zn(II) ion (a) and **8**:Zn(II) ion (b) is given on the respective spectrum. Signals for H3',5' protons are marked with # and that of H6,6'' protons with *****.

Further evidence for the formation of dimer complexes was obtained by MALDI-TOF mass spectrometry.[13b,e,20] In Figure 2 the MALDI-TOF mass spectra of complexes $(\mathbf{7})_2Zn(OTf)_2$ and $(\mathbf{8})_2Zn(OTf)_2$ are shown.

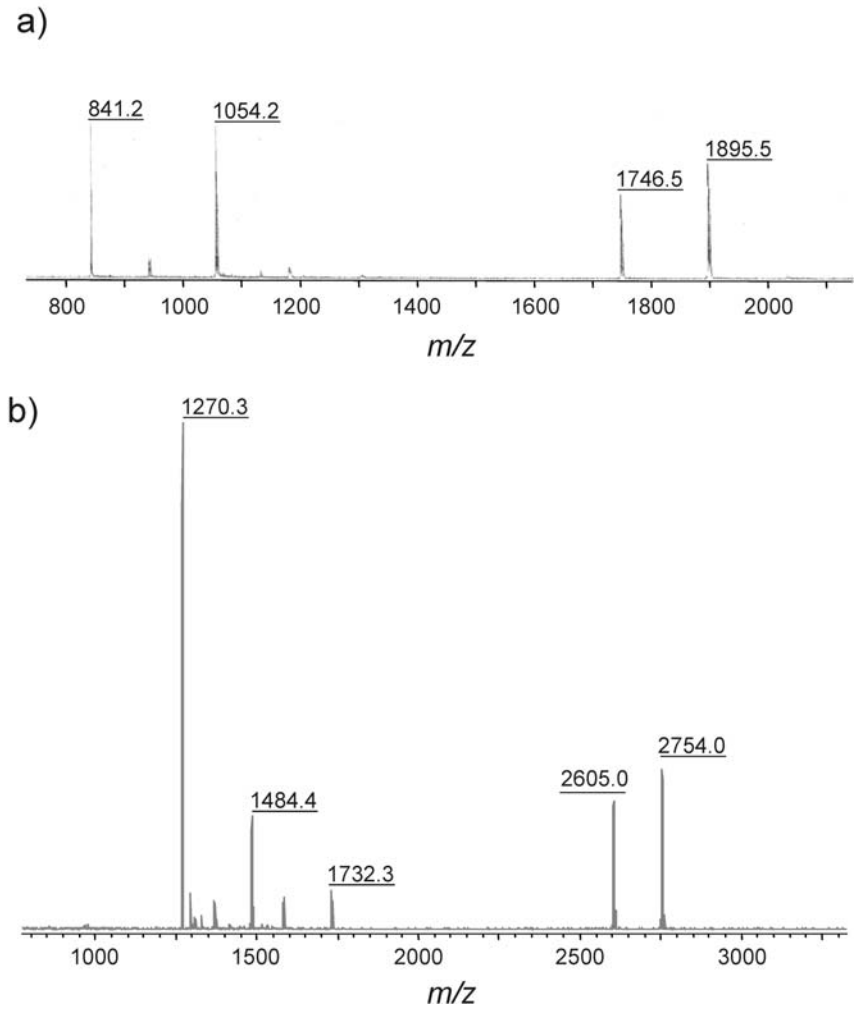


***Figure 2.*** MALDI-TOF mass spectra of Zn(II) ion complexes of monotopic ligands **7** (a, dithranol matrix[21]) and **8** (b, DCTB matrix[21]) showing the mass peaks (*m/z* = 1895.5) for $(\mathbf{7})_2Zn(OTf)$ and (*m/z* = 2754.0) for $(\mathbf{8})_2Zn(OTf)$. The peaks at *m/z* = 1746.5, 1054.2, and 841.2 correspond to $(\mathbf{7})_2Zn$, (**7**)Zn(OTf), and ligand **7**, respectively. The peaks at *m/z* = 2605.0, 1732.3, 1484.4, and 1270.3 correspond to $(\mathbf{8})_2Zn$, (**8**)Zn(OTf)(DCTB), (**8**)Zn(OTf), and ligand **8**, respectively.

The two peaks observed at *m/z* = 1895.5 and 1746.4 in upper spectrum (Figure 2a) can be assigned to charged dimeric species $[(\mathbf{7})_2(Zn)(OTf)]^+$ and $[(\mathbf{7})_2(Zn)]^{2+}$, respectively. The additional two prominent peaks in the lower *m*/*z* region of the this spectrum at *m*/*z* = 841.2 and 1054.2 correspond to the fragmented species $[(\mathbf{7})(Zn)(OTf)]^+$ and free

ligand **7**. The major peaks in the higher range of mass spectrum of $(\mathbf{8})_2Zn(OTf)_2$ (Figure 2b) at *m/z* = 2754.0 and 2605.0 correspond to the singly and doubly charged ions $[(\mathbf{8})_2(Zn)(OTf)]^+$ and $[(\mathbf{8})_2(Zn)]^{2+}$, respectively. The three most prevalent peaks in the lower *m*/*z* region of this spectrum, namely *m*/*z* = 1270.3, 1484.4, and 1732.3, agree well with the smaller species that are most likely originated from the fragmentation of the dimer complex $(\mathbf{8})_2Zn(OTf)_2$ in the gas phase.

**Supramolecular Polymerization of Ditopic Ligands by Zn(II) Ion Coordination.** Since the monotopic tpy-PBI ligands form dimeric complexes with Zn(II) ion at a 2:1 ratio as described above, it is expected that the ditopic bis(tpy)-PBI ligands **3** and **4** will form metallosupramolecular polymers with one equivalent of Zn(II) ion. Since the ligand **4a** and **4b** are very similar, except the former contains better soluble *tert*-octyl side chains while the latter *tert*-butyl groups, ligand **4a** was chosen for detailed investigations. To study the complexation of bis(tpy)-PBI ligands **3** and **4a** with Zn(II) ion $^1$H NMR titration experiments were performed in a mixture of chloroform[D]/methanol[$D_4$] (60:40) using 0.2 to 2.2 equivalents of zinc(II) triflate (in portions of 0.2, 0.4 or 0.5 equiv.) under ambient conditions. The $^1$H NMR spectra obtained for different ratios of ligand **3**/Zn(II) ion and ligand **4a**/Zn(II) ion are shown in Figure 3. For both ligands, upon addition of the first batches of zinc triflate a significant signal broadening of the characteristic proton signals of terpyridine ligand was observed. At an exact 1:1 stoichiometry of ligand/Zn(II) ion, the signals of uncomplexed ligands disappeared totally, as it was the case for reference monotopic ligands **7** and **8** at 2:1 ligand/Zn(II) ion ratio, and a new set of broad but defined signals arisen with a upfield shift of the tpy H6,6'' signals of ditopic ligands **3** and **4a** from 8.71 and 8.66 ppm to 8.07 and 7.92 ppm, respectively. These $^1$H NMR observation indicate the formation of coordination polymers **9** and **10** from ditopic ligands **3** and **4a**, respectively (Scheme 3).

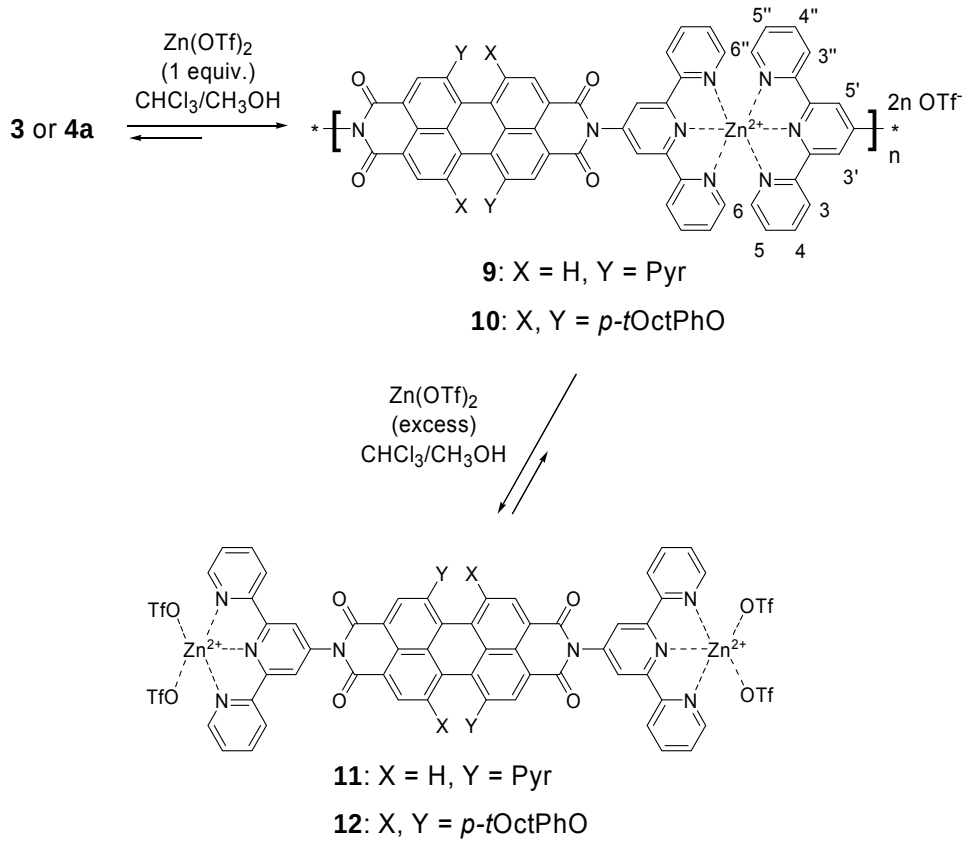


***Scheme 3.*** Formation of coordination polymers **9** and **10** by Zn(II)-ion-mediated self-assembly of ditopic (tpy)-PBI ligands **3** and **4a**, respectively, at a 1:1 stoichiometry of ligand/$Zn(OTf)_2$ in chloroform/methanol (60:40) mixture, and dissociation of the metallopolymers into monomeric complexes **11** and **12**, and oligomeric species upon addition of excess amounts of zinc(II) triflate.

Once the 1:1 stoichiometry is exceeded upon further addition of $Zn(OTf)_2$, the intensity of proton signals of polymers is decreased and a new set of signals comes up that become fairly sharp at a ratio of around 1:2 (see right panels in Figure 3) which is indicative for reversible complexation of ditopic ligands to Zn(II)-ion, resulting in fragmentation of polymers to oligomeric or monomeric species such as **11** and **12** (Scheme 3).

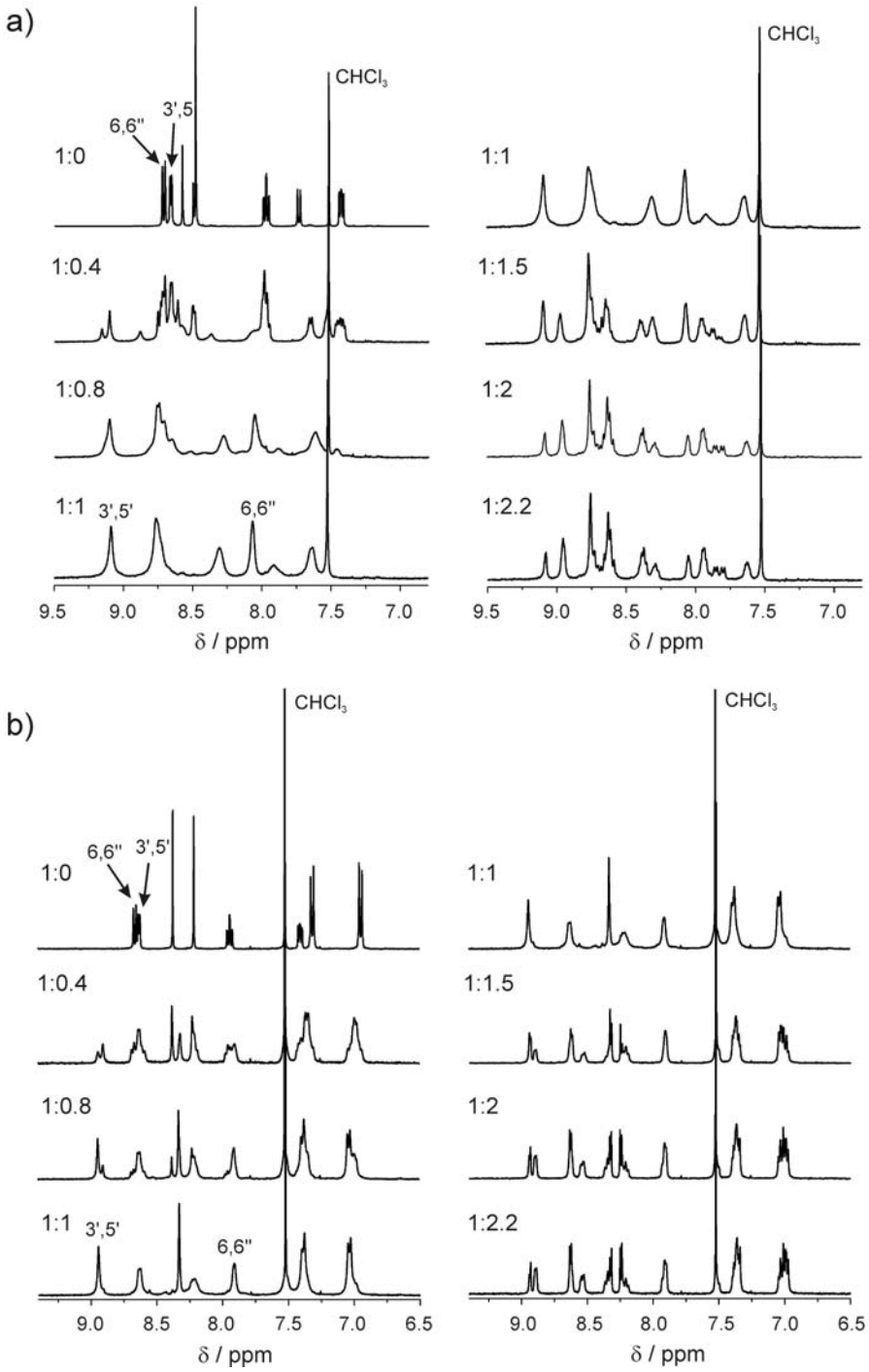


***Figure 3.*** $^{1}$H NMR spectra at different ligand/Zn(II) ion ratios: a) for the ditopic ligand **3** and zinc triflate in $CDCl_3/CD_3OD$ (60:40, 5 mM) from free **3** (upper spectrum, left) to polymer **9** (bottom, left) and the fragmented decomplexed form **11** (bottom, right); b) for the bis(tpy)-PBI ligand **4a** and zinc triflate in $CDCl_3/CD_3OD$ (60:40, 3.5 mM) from free **4a** (upper spectrum, left) to polymer **10** (bottom, left) and the fragmented decomplexed form **12** (bottom, right). The ratio of ligand/Zn(II) ion is given on the respective spectrum.

**$^1$H DOSY NMR Investigations.** To provide future evidence for the formation of polymers by Zn(II)-ion mediated self-assembly of ditopic ligands **3** and **4a**, the $^1$H NMR diffusion-ordered spectroscopy (DOSY)[22] experiments were performed, since DOSY NMR spectroscopy has recently been successfully applied to characterize supramolecular coordination polymers, whose labile and dynamic nature quite often limits the success of conventional techniques for the characterization of polymers.[8e,j] The DOSY spectra were measured in chloroform[D]/methanol[$D_4$] (60:40) mixture at 25 °C first for each ditopic ligand (**3** and **4a**) alone, and then after addition of one equivalent of $Zn(OTf)_2$ to the solution of the respective monomer providing the formation of coordination polymers (**9** and **10**), and subsequently after the addition of 2 equivalents of zinc(II) triflate leading to degradation of polymer strand and formation of short oligomeric or monomeric fragments. The $^1$H DOSY NMR spectra for ditopic ligands **3** and **4a** are shown in Figure 4. The ditopic ligand **3** with a molecular weight of 991.6 g/mol shows a diffusion coefficient value of $D = 3.76\times10^{-10}$ $m^2s^{-1}$ ($\log[D/m^2s^{-1}] = -9.42$) and, as expected, the bis(tpy)-PBI ligand **4a** with a higher molecular weight of 1670.3 g/mol exhibits a little smaller diffusion coefficient value of $D = 3.47\times10^{-10}$ $m^2s^{-1}$ ($\log[D/m^2s^{-1}] = -9.46$). A significant decrease of $D$ values to $D = 7.19\times10^{-11}$ $m^2s^{-1}$ ($\log (D/m^2s^{-1}) = -10.14$) and $D = 5.84\times10^{-11}$ $m^2s^{-1}$ ($\log (D/m^2s^{-1}) = -10.23$) was observed, when one equivalent of $Zn(OTf)_2$ was added to **3** or **4a** (see Figure 4b,e). These diffusion coefficient values are one order of magnitude smaller than those of the respective ditopic monomers, indicating formation of extended polymers with high molecular weight.

Upon addition of an excess amount of Zn(II) ion to the polymer solution, a strong increase of diffusion coefficient value is observed that points the fragmentation of the coordination polymer to oligomeric species with smaller molecular weight (Figure 4c,f). When a 1:2 stoichiometry of ligand/zinc(II) ion is reached, the diffusion coefficient increased to a value of $D = 2.22\times10^{-10}$ $m^2s^{-1}$ ($\log[D/m^2s^{-1}] = -9.65$) and $D = 2.45\times10^{-10}$ $m^2s^{-1}$ ($\log[D/m^2s^{-1}] = -9.61$) which are pretty close to the values for monomeric ligands, suggesting fragmentation of polymers into monomeric complexes **11** and **12**.

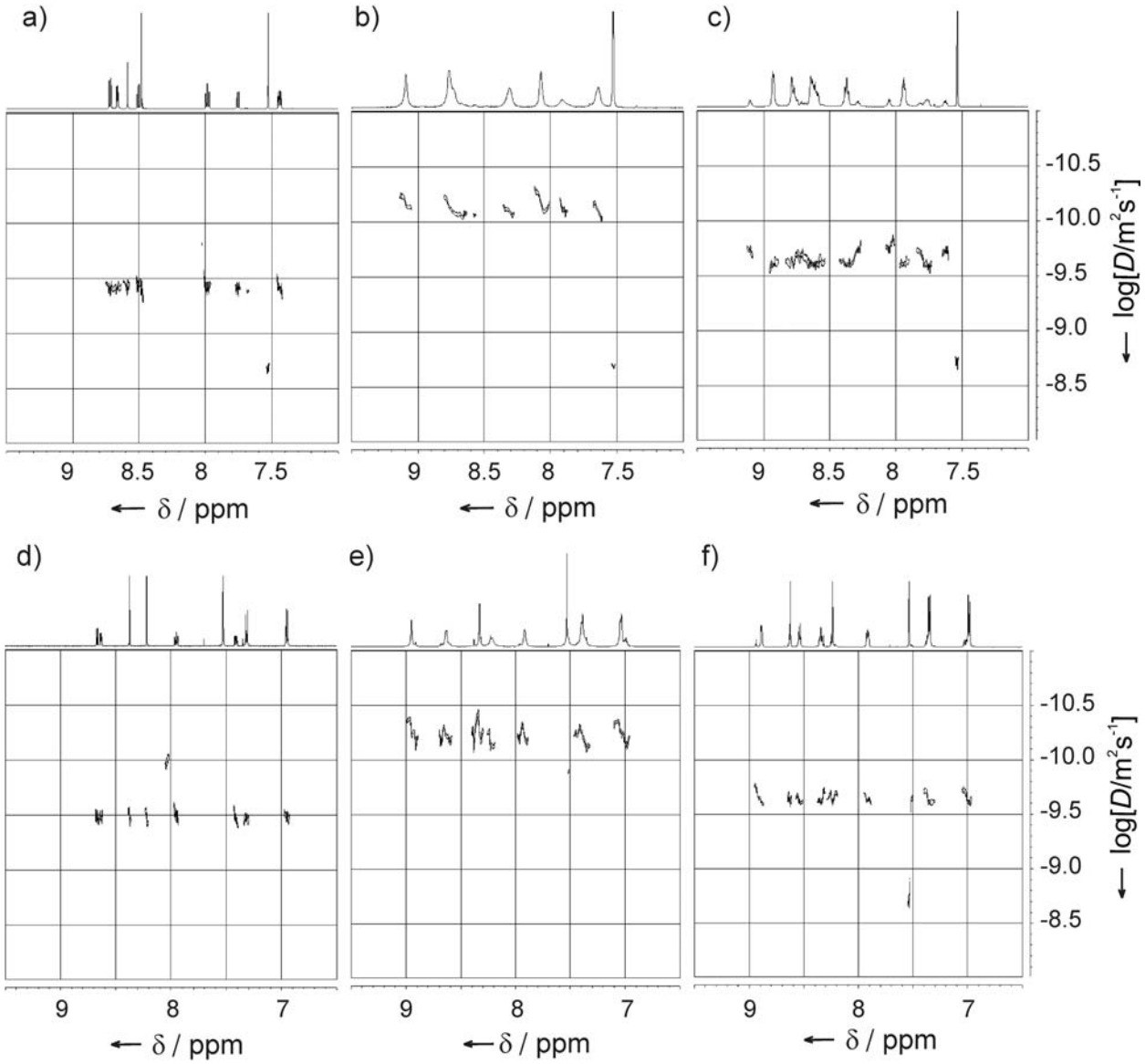


***Figure 4.*** Aromatic regions of the $^{1}$H DOSY NMR spectra for bis(tpy)-PBI ligands **3** (a) and **4a** (d), supramolecular polymers **9** (b) and **10** (e), and complexes **11** (c) and **12** (f) in chloroform[D]/methanol[$D_4$] (60:40) at 25 °C; [**3**] = $4.9\times10^{-3}$ M, [**4a**] = $3.6\times10^{-3}$ M. The diffusion coefficients $D$ [$m^2s^{-1}$] are plotted in a logarithmic scale (log[$D$/$m^2s^{-1}$]) against the chemical shift $\delta$. The signal of residual chloroform can be seen at 7.51 ppm (log[$D$/$m^2s^{-1}$] = -8.65).

**Optical Properties.** The optical properties of the present tpy-PBI ligands and their Zn(II) ion complexes have been explored by UV/Vis absorption and fluorescence spectroscopy. Uncomplexed monotopic **7** and ditopic **3** ligands show the characteristic absorption bands of the dipyrrolidinyl-substituted perylene bisimide chromophore[17] between 600

and 800 nm ($\varepsilon$ = 45000-50000 $M^{-1}cm^{-1}$) and 375-475 nm ($\varepsilon$ = 18000-20000 $M^{-1}cm^{-1}$) in dichloromethane (see Figure 5a and Figure 6).The monotopic ligand **8** containing *tert*-butyl-phenoxy substituents exhibits in dichloromethane absorption bands with maxima at $\lambda_{max}$ = 581, 541, and 453 nm reflecting the very characteristic spectral feature of tetraaryloxy-substituted perylene bisimide (Figure 5b and Figure 7).[14a,16a] An extinction coefficient of $\varepsilon$ = 46100 $M^{-1}cm^{-1}$ was found for the absorption at 581 nm. For ditopic *tert*-octyl-phenoxy-substituted ligand **4a**, the absorption maxima are marginally shifted relative to the maxima of monotopic ligand **8** and are observed at $\lambda_{max}$ ($\varepsilon$) = 588 (50800), 550 (30300) and 456 (17200 $M^{-1}cm^{-1}$) nm. Note, that the change of *tert*-butyl by *tert*-octyl groups in the periphery of chromophore does not influence its absorption properties.[8e,14c] In the case of all four tpy-PBI ligands, absorption at wavelength below 350 nm was observed for terpyridine units. It is to note that the coordination of Zn(II) ion to tpy units has slight effect on the absorption profile of chromophores (Figures 5, 6, and 7).

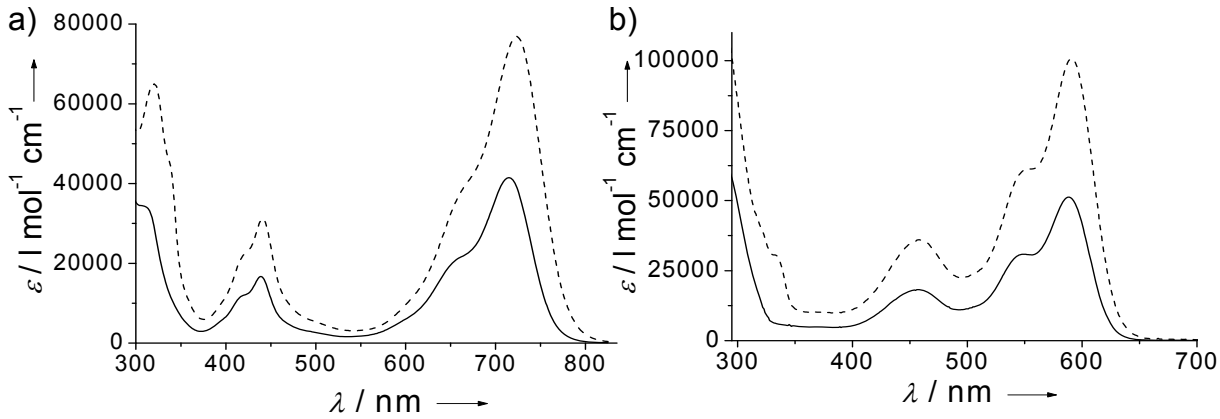


***Figure 5.*** UV/Vis absorption spectra: a) monotopic ligand **7** (solid line) and dimer $(\mathbf{7})_2Zn(OTf)_2$ (dashed line) in $CHCl_3$/MeOH (60:40) at 25 °C; b) monotopic perylene bisimide ligand **8** (solid line) and metallodimer $(\mathbf{8})_2Zn(OTf)_2$ (dashed line) in $CHCl_3$/MeOH (60:40) at 25 °C.

For dimeric complexes $(\mathbf{7})_2Zn(OTf)_2$ and $(\mathbf{8})_2Zn(OTf)_2$ in chloroform/methanol mixture (60:40), extinction coefficients of 78400 (at 723 nm) and 100700 $M^{-1}cm^{-1}$ (at 591 nm), respectively, are observed which are two-times higher than those for the respective monotopic ligands **7** (40300 $M^{-1}cm^{-1}$ at 715 nm) and **8** (51200 $M^{-1}cm^{-1}$ at 588 nm). UV/Vis titration experiments of ditopic ligands with zinc(II) triflate were carried out to explore the influence of metal-ion coordination on the absorption properties of PBI

chromophore. Figures 6 and 7 show the changes in UV/Vis spectra of the ditopic building blocks **3** and **4a**, respectively, during constant-host titration in a mixture of $CHCl_3/CH_3OH$ (60:40) by using 0.2 to 1.4 equivalents of zinc(II) triflate.

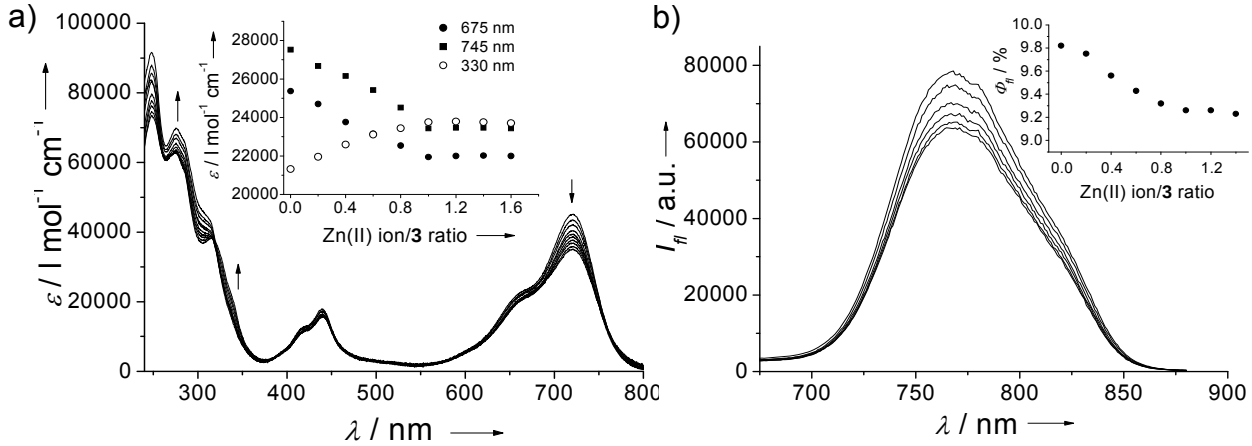


***Figure 6.*** Spectral changes upon addition of zinc(II) triflate to ditopic perylene bisimide ligand **3** in $CHCl_3$/MeOH (60:40) at 25 °C: a) absorption spectra, inset shows apparent absorption coefficient as a function of the Zn(II) ion/**3** ratio; b) fluorescence spectra, $c = 2\times10^{-6}$ M, insert shows the fluorescence quantum yields as a function of zinc(II) ion/**3** ratio. The arrows indicate the spectral changes with increasing amount of Zn(II) ion.

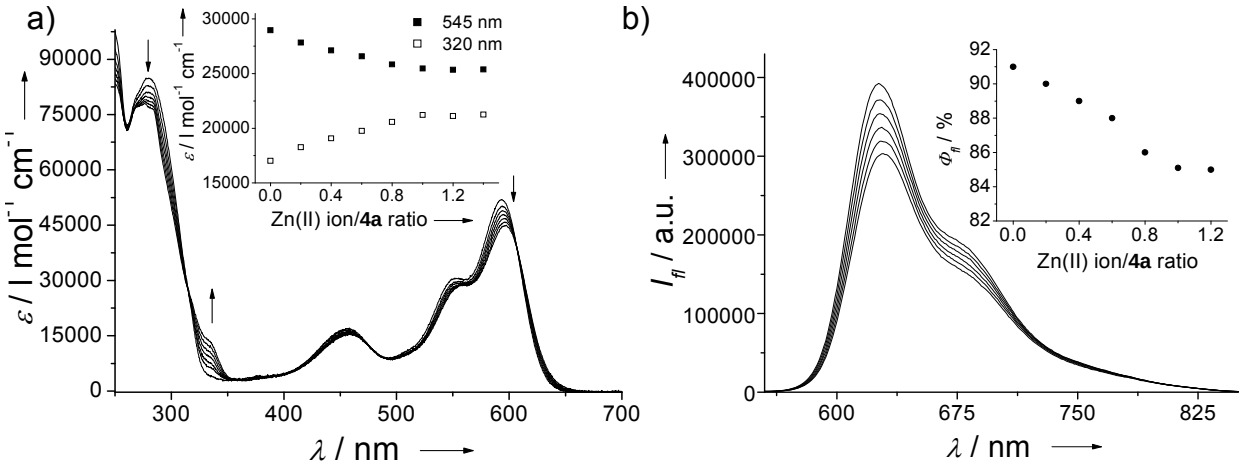


***Figure 7.*** Spectral changes upon addition of zinc(II) triflate to ditopic perylene bisimide ligand **4a** in $CHCl_3$/MeOH (60:40) at 25 °C: a) absorption spectra, inset shows apparent absorption coefficient as a function of the Zn(II) ion/**4a** ratio at 320 and 545 nm; b) change of fluorescence intensity of ditopic perylene bisimide ligand **4a** upon addition of zinc(II) ion ($c = 2\times10^{-6}$ M), insert shows the fluorescence quantum yields as a function of zinc(II) ion/**4a** ratio. The arrows indicate the spectral changes with increasing amount of Zn(II) ion.

For both ligands, upon addition of Zn(II) ion only slight changes in the absorption spectrum of the perylene bisimide chromophore are observed. When the 1:1 stoichiometry of ditopic ligand/Zn(II) ion was reached, the created polymers **9** (Figure 6) and **10** (Figure 7) exhibit a small decrease in the absorption coefficient and a red-shift of the absorption maximum from 721 and 593 nm to 722 and 596 nm, respectively. Upon addition of one equivalent of zinc(II) ion, an increase in absorbance between 300 and 350 nm, corresponding to the change in tpy absorption, is observed that can be assigned to the complexation of the tpy unit which fixes the three pyridine units in an all-cis conformation.[8c,e]

Furthermore, the fluorescence properties of ligands, dimeric complexes, and coordination polymers have been studied. Upon excitation at 550 nm, monotopic (**8**) and ditopic (**4a**) ligands exhibit an intense emission at $\lambda_{max}$ = 611 and 618 nm, respectively, which is characteristic for tetraaryloxy-substituted PBI chromophores.[14b,15a,16a] The fluorescence quantum yields are determined as $\Phi_{fl}$ = 0.89 (for **8**) and 0.96 (for **4a**) in dichloromethane. The pyrrolidinyl-substituted perylene bisimide compounds **3** and **7** exhibit fluorescence maxima at $\lambda_{max}$ = 746 and 750 nm upon excitation at 615 nm with fluorescence quantum yields of $\Phi_{fl}$ = 0.19 and 0.26, respectively, in dichloromethane.[17c] The influence of Zn(II) ion complexation on the fluorescence properties of the PBI fluorophore unit was investigated by fluorescence titration experiments. Figures 6b and 7b show the fluorescence changes for ditopic tpy-PBI ligands **3** and **4a** during titration with zinc(II) triflate in chloroform/methanol (60:40) mixture at room temperature. To notice, that the fluorescence quantum yields of ditopic ligands **3** and **4a** in titration solvent chloroform/methanol mixture, comparison with those observed in dichloromethane, are reduced from $\Phi_{fl}$ = 0.19 and 0.96 to $\Phi_{fl}$ = 0.098 and 0.91, respectively, which is apparently due to the solvent polarity. Upon addition of zinc(II) triflate, the fluorescence intensity decreases slightly once the 1:1 stoichiometry of ligand/Zn(II) ion is achieved and, accordingly, the fluorescence quantum yield of coordination polymers **9** and **10** can be determined as $\Phi_{fl}$ = 0.093 and 0.85, respectively (see insets in Figures 6b and 7b). The complexation of tpy unit with zinc(II) ion has almost no effect on the fluorescence quantum yield of perylene bisimide unit, in contrast to complexation with Fe(II) ion where the fluorescence of the perylene bisimide

fluorophore is completely quenched.[8e] Furthermore, the fluorescence lifetimes of monotopic ligands, dimeric complexes and coordination polymers have been determined. For the monotopic ligands **7** and **8**, fluorescence lifetime values of 1.6 ns ($\lambda_{ex}$ = 660 nm, $\lambda_{em}$ = 745 nm) and 7.7 ns ($\lambda_{ex}$ = 540 nm, $\lambda_{em}$ = 617 nm), respectively, in chloroform-methanol mixture are found. The complexation of ligands with Zn(II) ion, leading to formation of dimeric species (**7**)$_2$Zn(OTf)$_2$ and (**8**)$_2$Zn(OTf)$_2$, did not influence the fluorescence lifetime ($\tau$ = 1.7 and 7.5 ns for (**7**)$_2$Zn(OTf)$_2$ and (**8**)$_2$Zn(OTf)$_2$, respectively). The fluorescence lifetimes of both ditopic ligands **3** and **4a** in $CH_2Cl_2$ are determined as $\tau$ = 3.8 ns ($\lambda_{ex}$ = 660 nm, $\lambda_{em}$ = 745 nm) and 6.6 ns ($\lambda_{ex}$ = 540 nm, $\lambda_{em}$ = 617 nm), respectively. In more polar solvent DMF, a slight decrease of lifetimes, compared with those in $CHCl_2$, is observed ($\tau$ = 2.5 ns ($\lambda_{ex}$ = 660 nm, $\lambda_{em}$ = 770 nm) for **3** and $\tau$ = 4.9 ns ($\lambda_{ex}$ = 540 nm, $\lambda_{em}$ = 617 nm) for **4a**). Upon addition of zinc(II) ion the fluorescence lifetime of the ditopic ligands **3** and **4a** remains almost unchanged and at a 1:1 ratio of ligand/Zn(II) ion lifetime values of $\tau$ = 2.2 and 4.4 ns for coordination polymers **9** and **10** in DMF, respectively, are obtained.

**AFM Investigation of Coordination Polymers.** The structural properties and organization on surfaces of polymers formed by Zn(II)-ion mediated self-assembly of ditopic ligands **3** and **4a** have been investigated by atomic force microscopy (AFM). The filamentous appearance of polymers **9** and **10** on muscovite mica and highly ordered pyrolytic graphite (HOPG) can be clearly seen in AFM images (Figure 8 and 9). In contrast, for the free ditopic ligands **3** and **4a** only adlayers without any ordered structure could be observed on both substrates (not shown here). Figure 8 depicts AFM images of thin films spin-coated onto mica from diluted DMF solutions of polymers **9** and **10**.

AFM images of coordination polymer **10** revealed the presence of very long and rigid self-assembled polymeric strands with length up to several hundred nanometers (up to 400 nm, Figure 8a, b). The mean length of polymeric chains averages to 80 nm. Since the length of the respective ditopic monomer **4a** can be estimated as about 2.3 nm from structural modeling calculations (see Figure 10),[23] it is suggestive that the polymeric strand consists of more than 35 repeat units. Based on this value, the molecular weight of coordination polymer can be approximately estimated as

~ 60000 g/mol. The diameter of the polymer strand **10** was determined from molecular modeling and averages to 1.7 nm (Figure 10). From the AFM images it can be seen that the neighboring polymeric strands incline to interact with each other leading to the formation of two dimensional (2D) self-assembled film with a height of 1.5±0.3 nm. This value is in good agreement with the calculated diameter of the polymer chain. The lateral distance between neighbor strands (distance between red triangles in Figure 8c) is measured to be 4.2±0.4 nm.

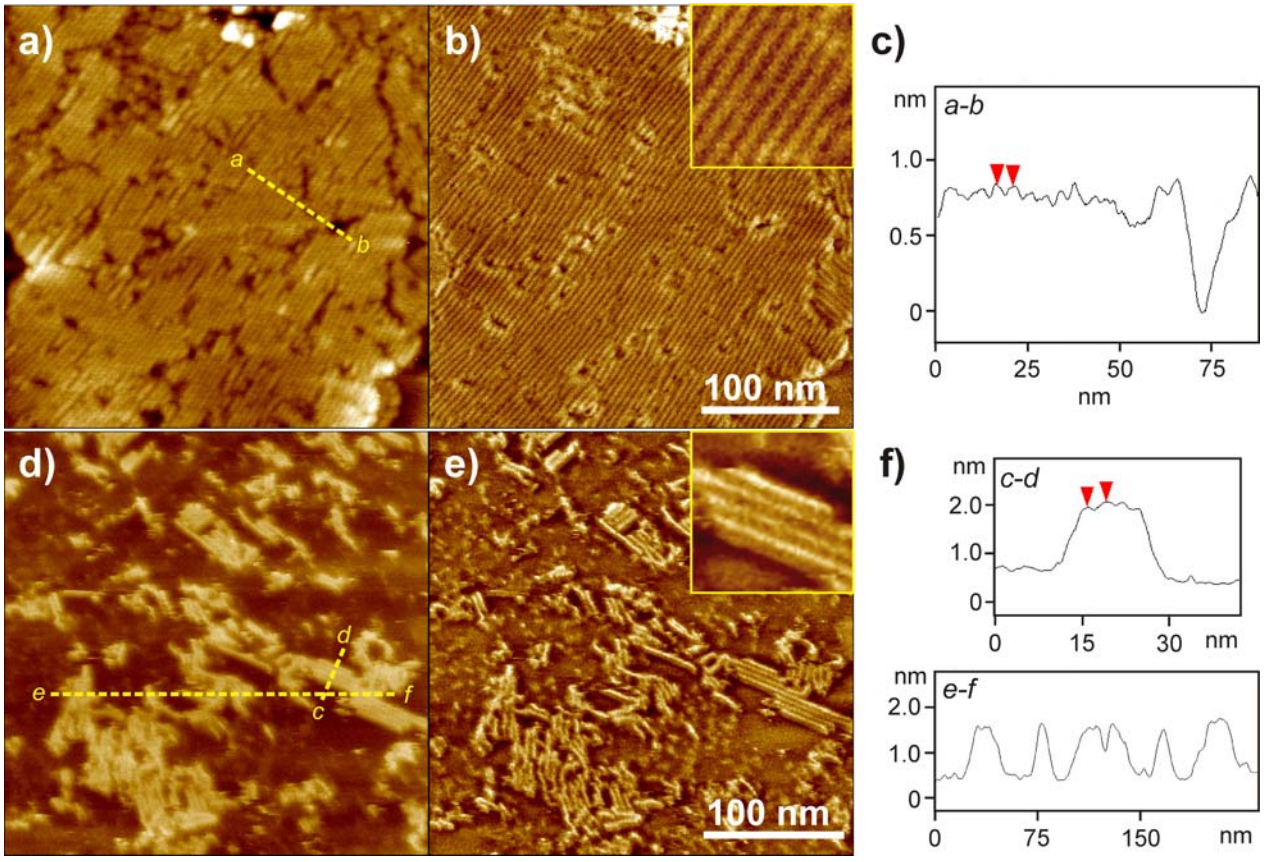


***Figure 8.*** Taping mode AFM images of coordination polymers **10** (a, b) and **9** (d, e) on mica spin-coated (4000 rpm) from DMF solution (0.05 mg/mL); (a, d) high-resolution height AFM images, (b, e) phase images, insets show magnified phase images; (c, f) cross sections along the yellow dash line *a-b* (a), *c-d* and *e-f* (d). Horizontal distance between the red triangles corresponds to the lateral distance between polymer strands **10** (c) and **9** (f, upper image). In all AFM images, the scale bar corresponds to 100 nm, the *z* data scale is 3 nm (a) and 4 nm (d).

The interaction between the coordination polymers and mica substrate is of electrostatic character because, in contrast to positively charged coordination polymers, the freshly cleaved mica bears negative charges. Mica with a chemical composition of $KAl_2(AlSi_3O_{10})(OH)_2$ has a monoclinic crystalline structure with 2/*m* symmetry and its cleaved surface is characterized by partially delocalized negative charges in combination with weakly bound, localized positive charges of $K^+$ ions.[24] The strong electrostatic interaction between positively charged polymers and negatively charged mica leads to the formation of a wide spread monolayer film, in which the polymeric chains are pressed to the surface, and hence the polymer strands appear broader. In contrast to our previously reported flexible metallosupramolecular polymers that are constructed from similar building blocks, but contain phenylene spacers (see Chart 1),[8e] the newly designed building blocks that lack such spacers indeed provide *rigid* polymeric strands.

In contrast to 2D self-assembled film of polymer **10** strands, the individual chains of coordination polymer **9** can be clearly seen on mica (Figure 8d, e). The height profile of the cross sections *c-d* and *e-f* provided a height of 1.3±0.2 nm, which is in very good agreement with calculated diameter of polymeric strand of 1.2 nm (Figure 10), and the distance between polymeric strands is estimated to be 3.4±0.3 nm (red triangles in Figure 8f). The reason, why the polymeric chain of **9** is more narrow than that of **10**, is may be the less steric demand of the pyrrolidine substituents in **9** compared to that of phenoxy substituents in **10**. The individual fibers appear to be flexible and have contour lengths in the order of up to 75 nm. Molecular modeling revealed a length of 2.3 nm for monomeric building block **3** (Figure 10). Comparison of the measured length with the calculated model suggests that a single polymeric chain is consisted of approximately 30 repeat units, corresponding to a maximal molecular weight of ~ 30000 g/mol. Despite the fact that both polymer samples are prepared under the same conditions, the chains of coordination polymer **9** are a bit shorter than those of polymer **10**. This difference, however, might be explained by slightly imbalanced ligand/metal ion stoichiometry and/or the disassembling and spreading of the polymeric fibers on the surface during the sample preparation by the spin-coating process.

Figure 9 depicts the AFM images of thin films prepared by spin-coating of solutions of polymers **9** and **10** in DMF onto HOPG. So called adlayer with average height of 0.4±0.2 nm could be observed for both polymers on the graphite surface.

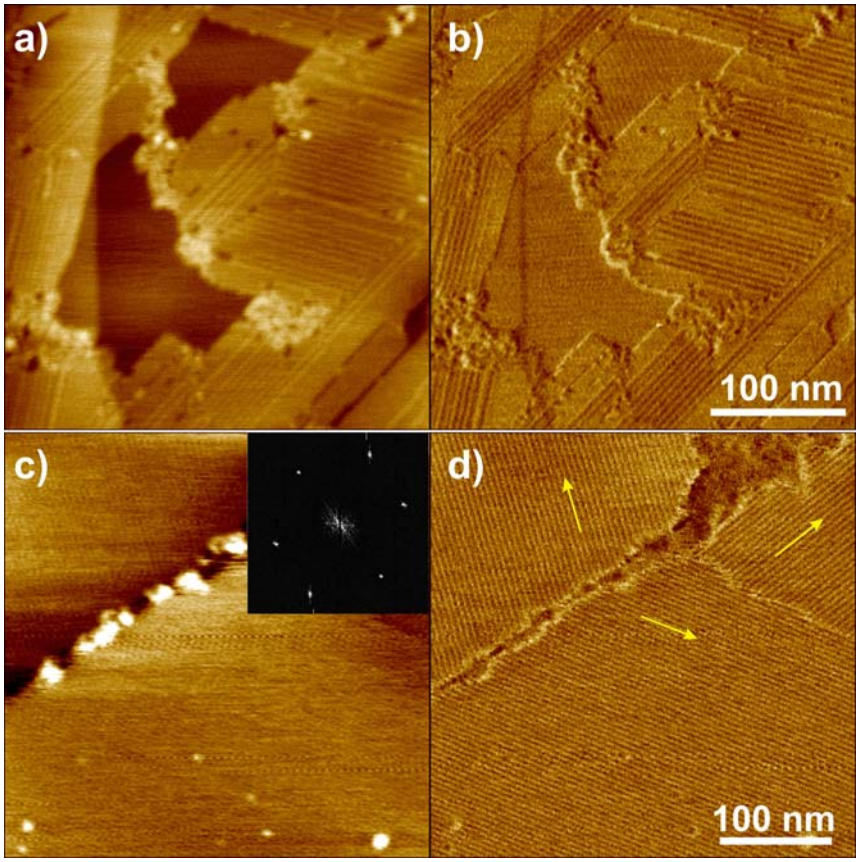


***Figure 9.*** AFM images of thin films prepared by spin-coating (4000 rpm) of DMF solutions (0.05 mg/mL) of coordination polymers **10** (a, b) and **9** (c, d) on HOPG. (a, c) Topography AFM images; (b, d) phase images. Insert in (c) shows FFT analysis spectrum of linear arrangement in image (c). Directions of linear structures (d) are indicated with yellow arrows. In all AFM images, the scale bar corresponds to 100 nm, the *z* data scale is 2 nm (a) and 1 nm (c).

The rigid polymeric strands that stretch up to several hundred nanometers formed close-packed film with linear arrangement under the influence of HOPG basal plane, while the respective free ditopic ligands **3** and **4a** form unordered ad-layers on graphite. Furthermore, 2D fast Fourier transformation (FFT) method was used for the determination of specific frequencies. FFT analysis revealed a frequency of 4.6±0.5 nm for the linear arrangement of coordination polymer **9** and 5.0±0.5 nm for polymer **10**.

It is important to note that in the linear structures, three orientations with an angle of 60° were found (yellow arrows in Figure 9d). This indicates an alignment of the self-assemblies of coordination polymers along the graphite axes as the HOPG has a hexagonal crystalline structure with 6/*m* and 2/*m* symmetry.[24] Its crystals have lamellar structure with a perfect cleavage in one direction, similar to the mica. However, the important difference to mica is that no free charges appear after the cleavage of HOPG. Thus, whilst individual polymeric chains are attached to mica in a strongly bound irreversible manner, well-ordered self-assembled two-dimensional adlayers are formed on the HOPG template. In view of the adsorption orientation, the association between the coordination polymer and the graphite surface is dominated by weak van-der-Waals forces between the both perylene bisimide π-system and alkyl residues with the basal plane of HOPG. In addition, the molecular film may also be stabilized through intermolecular interactions between the individual polymeric chains.

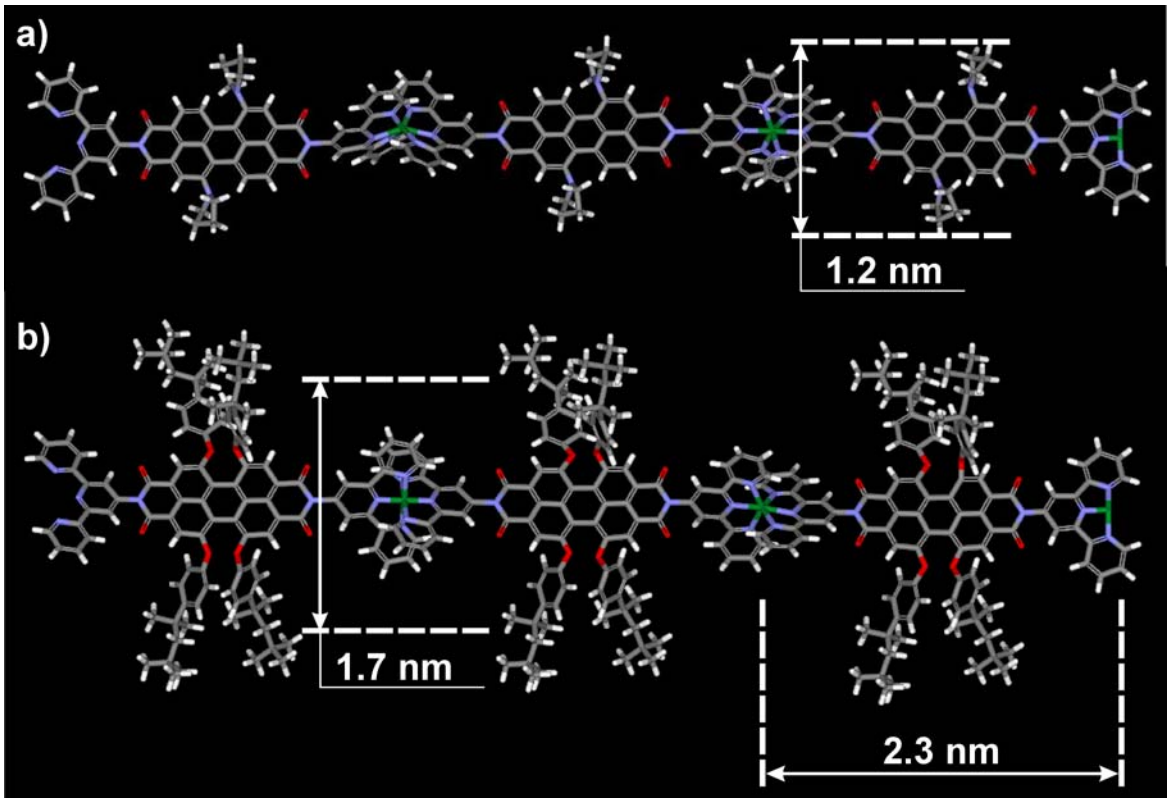


***Figure 10.*** Molecular modeling of coordination polymers **9** (a) and **10** (b).[23] Three repeat units are shown, carbon atoms are presented in grey, nitrogen and oxygen in blue are red, respectively, and zinc atoms in green.

**Electrostatic Self-Assembly of Coordination Polymers.** The layer-by-layer (LBL) deposition technique developed by Decher et al. in 1991[25] has been applied to fabrication of many polyelectrolyte films including those that incorporate water-soluble PBI dyes[26] and a first example for PBI coordination polymers.[27] In our study, the different metallosupramolecular coordination polymers were used for the preparation of multilayer film in alternate fashion. LBL films were prepared by repetitive cycles of immersion of the quartz plate, which was before processed with poly(ethylene imine) (PEI) solution to ensure the contact between the quartz substrate and the subsequent layers, into solutions in the following order: an aqueous solution of poly(styrene sulfonate) (PSS), water, a polymer solution (**9** or **10** alternately) in DMF with a concentration of 1 mM, a DMF/water mixture (50:50), and again water. The growth of the multilayer on the quartz surface was monitored by UV/Vis spectroscopy. The spectra were recorded after each step in the assembly process of coordination polymer on PSS layer. Figure 11a shows a series of absorption spectra for the formation of films on quartz plate. The inset depicts the absorbance at 330, 480, 590, and 700 nm as a function of the number of layers of polymers **9** (odd-numbered) and **10** (even-numbered). The construction of multilayer film begins with electrostatic adsorption of positively charged coordination polymer **9** on negatively charged PSS layer and, further, alternate adsorption of PSS and second polymer **10**. The growth of LBL film can be determined by the increase in the UV/Vis absorption intensity in spectral region for the corresponding polymer (Figure 11a). The broad bands in the range 650-800 nm and 520-620 nm correspond to the electronic transitions $S_0 \rightarrow S_1$ in the pyrrolidinyl- and *tert*-octyl-phenoxy-substituted perylene bisimide, respectively, while the complexed terpyridine units absorb in the spectral region between 300-350 nm (Figure 11a). The absorption profile of alternate multilayer film exhibits the combined absorption spectra of both coordination polymers.[28] No significant shift of absorption maxima of chromophores in film could be observed compared to those in the solution. But, in contrast to UV/Vis spectra of coordination polymers in solution (see Figures 6a and 7a), in LBL film the shape of UV/Vis bands are significantly broadened, which is indicative for the aggregation of polymers on surface.

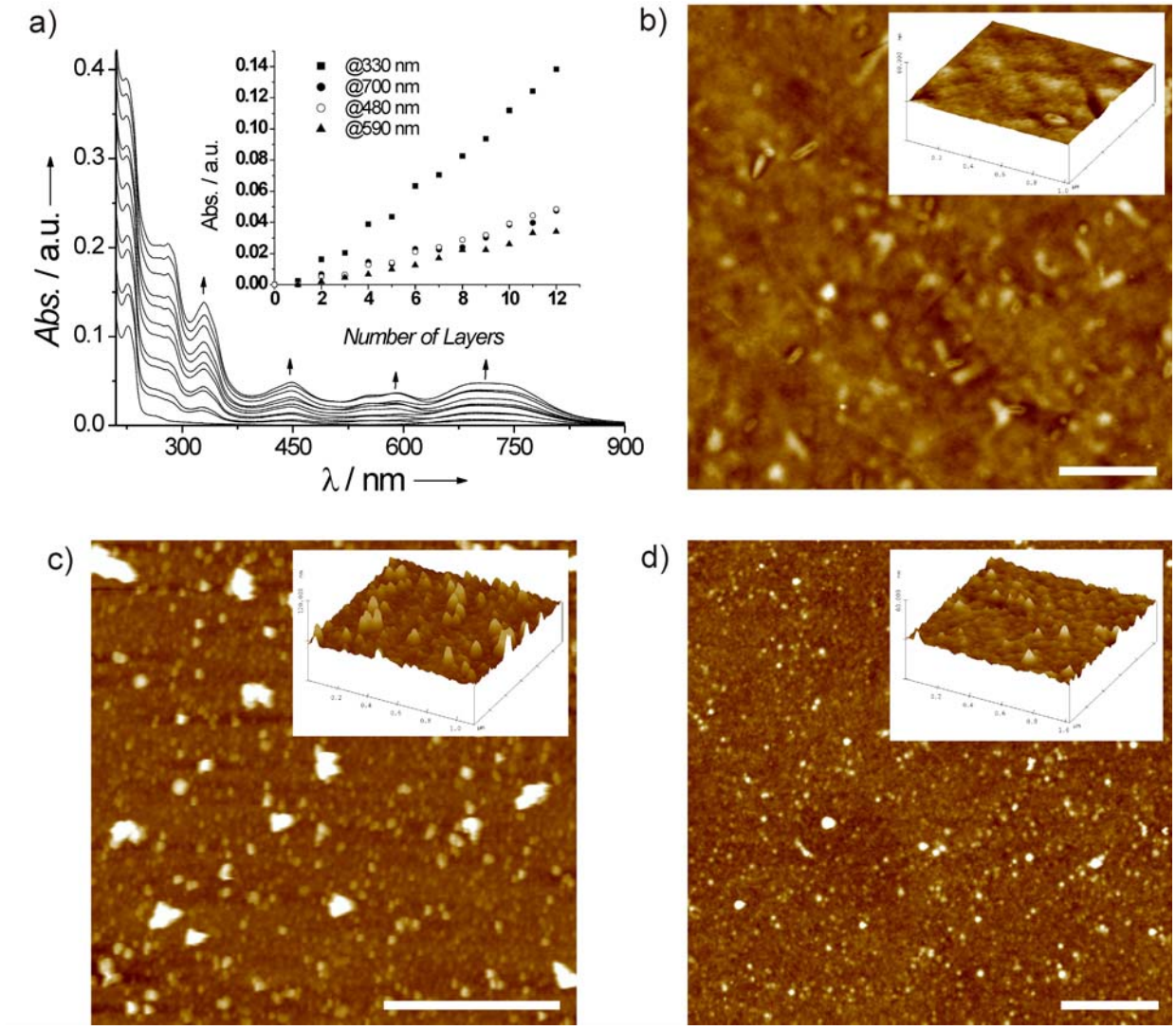


***Figure 11.*** (a) UV/Vis spectra of self-assembled alternate multilayers [Quartz/PEI/(PSS/**9**)$_6$/(PSS/**10**)$_6$]. The inset shows the absorbance at the absorption peaks 330 (■), 480 (○), 590 (▲), and 700 nm (●) as a function of the number of layers of coordination polymers **9** and **10**. The arrows indicate the change of absorbance with increasing number of layers. (b-d) Height AFM images of quartz substrate (b), PEI/PSS layer (c) and film after deposition of coordination polymers (d); white scale bar in all images is 1 *μ*m; *z* data scales are 15 (b), 70 (c), and 25 nm (d). The insets depict AFM angle view images.

The surface density Γ of the perylene chromophore films for every deposition step can be calculated according to the equation $\Gamma = [A_\lambda \cdot \varepsilon_\lambda^{-1} \cdot i^{-1}]/2$, where $A_\lambda$ is the absorbance of the film at $\lambda$, $\varepsilon_\lambda$ is the molar extinction coefficient of perylene bisimide chromophore, and *i* is the number of layers in film. It is to note that the calculation of surface coverage is an approximation since only the molar extinction coefficient of the isotopic solution in

$CH_2Cl_2$ is known. Using the average molar extinction coefficient of 48200 $M^{-1}cm^{-1}$ at 714 nm for ligand **3** and 50800 $M^{-1}cm^{-1}$ at 588 nm for ligand **4a**, the values for the surface coverage can be estimated as 0.8 and 0.6 monomer units/$nm^2$ that correspond to a space requirement of 1.2 and 1.6 $nm^2$/monomer units for **3** and **4a**, respectively. However, from molecular modeling studies[23] (Figure 10) the space requirement of monomeric perylene bisimide building block can be estimated as about 2–3 $nm^2$ for **3** and about 3–5 $nm^2$ for **4a** depending on the conformation of the *tert*-octyl-phenoxy substituents and the density of the packing provided that the units are aligned parallel to the surface. Therefore, one layer of the coordination polymer **9** consists of two polymer strands, while the layer of the coordination polymer **10** contains approximately three polymer strands. These approximate values of the surface coverage indicate aggregation of the polymer fibers on the substrate surface.

The investigation of the substrates under an optical microscope revealed a homogeneous film. Furthermore, the AFM investigations of quartz substrate before and after deposition of coordination polymers were carried out. The topography and the surface roughness of the quartz substrate, PSS sample, and a six double layer sample of PSS/coordination polymer **10** was examined. In Figure 11b-d, three tapping mode images with insets showing AFM angle view images are presented. The very flat quartz substrate became rough-textured surface after deposition of PEI/PSS layers. Once polymers are adsorbed on top of the PSS films, the surface becomes again smooth. In the case of a negatively charged PSS layer, the positively charged polymers with extended aromatic system of the perylene bisimide are concentrated at the surface and can jointly aggregate by $\pi$-$\pi$ interaction forming the plane film. The AFM measurements reveal that the surface roughness of PEI/PSS multilayer is a factor of 4 larger than that for PSS/polymer multilayer film. The root mean square (RMS) value of the surface roughness was determined to be 1.2, 9.2, and 2.1 nm for the quartz substrate (b), PEI/PSS film (c), and PSS/coordination polymer multilayer film after deposition of twelve polymer layers (d), respectively.

## Conclusions

With new red and green tpy-PBI building blocks highly soluble, extended rigid supramolecular coordination polymers could be obtained by zinc(II)-ion directed self-assembly of bis(2,2′:6′,2″-terpyridine)-anchored perylene bisimide dyes. $^{1}$H DOSY NMR technique was used to examine the change of diffusion coefficient of the bis(tpy)-PBI system upon stepwise addition of Zn(II) ion that leads first to the formation of coordination polymer and subsequently to their fragmentation, revealing a dynamic and reversible self-assembly process. The complexation of ligand monomers with zinc(II) ion is shown to be useful to preserve the fluorescence properties of PBI chromophores in polymer. The polymer formation could be visualized by AFM and their self-organization on surfaces could be explored. The present design principle to connect tpy unit directly to perylene bisimide without any spacer provided rigid supramolecular polymers with significantly longer average chain length than that observed previously for tpy-PBI ligands containing phenylene spacers.[8e] The average chain length for the present coordination polymers is estimated as to 35 repeat units that correspond to a molecular weight of ~ 30.000 to 60.000 g/mol. AFM also revealed the formation of a homogeneous monolayer on negatively charged mica and neutral HOPG substrate as well. Alternate multilayer films of coordination polymers with different optical properties could be constructed by electrostatic self-assembly. The present rigid, highly soluble and fluorescent coordination polymers supplement the family of metallosupramolecular polymers based on bis(tpy)-perylene bisimide dyes. Due to their advantageous optical properties and the possibility to form homogeneous monolayers on different surfaces, these new supramolecular polymers can be proposed for application in optoelectronic devices and as artificial light harvesting systems.

## Experimental Section

**General:** Solvents were purified and dried according to standard procedures.[29] Column chromatography was performed with silica gel (0.035-0.070 mm) and basic alumina, the latter was deactivated with 4 weight % of water to activity II. Zinc trifluoromethane sulfonate salt was obtained from commercial sources. MALDI-TOF mass spectra were measured using a Bruker Autoflex II spectrometer in reflector mode. $^{1}$H NMR spectra were recorded at 298 K on a Bruker Avance 400 spectrometer (400 MHz) and chemical shifts $\delta$ (ppm) were calibrated against tetramethylsilane (TMS) as internal reference. $^{1}$H DOSY experiments were carried out at 298 K on a Bruker DMX 600 spectrometer (600 MHz) equipped with a BGPA 10 gradient generator, a BGU II control unit, and a conventional 5 mm broadband ($^{15}$N-$^{31}$P)/$^{1}$H probe with automatic tune/match accessory and *z* axis gradient coil capable of producing pulsed magnetic field gradients in the *z* direction of 52 G cm$^{-1}$. For the measurement of UV/Vis spectra, PerkinElmer Lambda 950 spectrometer was used. The steady-state fluorescence spectra were measured on a PTI QM-4/2003 spectrometer and fluorescence quantum yields were determined by the optically dilute method[30] (A < 0.05) using *N*,*N*′-di(2,6-diisopropylphenyl)-1,6,7,12-tetraphenoxyperylene-3,4:9,10-tetracarboxylic acid bisimide ($\Phi_{fl}$ = 0.96 in chloroform)[31] and Nileblue *a* ($\Phi_{fl}$ = 0.27 in ethanol)[32] as standards. The solvents for spectroscopic studies were of spectroscopic grade and used as received. Fluorescence lifetimes were determined with a fluorescence lifetime system using a PTI GL330 nitrogen laser (337 nm) and a PTI GL302 dye laser. Fluorescence decay curves were evaluated using the software supplied with the instrument. AFM measurements were carried out under ambient conditions by using a Veeco MultiMode$^{TM}$ Nanoscope IV system operating in tapping mode in air.

## Synthesis of Perylene Bisimide Building Blocks

***N,N'*-Bis(4'-2,2':6',2''-terpyridyl)-1,7-dipyrrolidinylperylene-3,4:9,10-tetracarboxylic acid bisimide (3):** A mixture of 50.0 mg (0.094 mmol) of 1,7-dipyrrolidinylperylene-3,4:9,10-tetracarboxylic acid bisimide[17c] (**1**) and 70.3 mg (0.28 mmol) of 4'-amino-2,2':6',2''-terpyridine[18] was heated in pyridine/imidazole (2:1) under stirring at 120 °C for 48 h under argon. After cooling to room temperature, the mixture was poured into aqueous HCl (10 mL, 1 M). The resulting precipitate was separated by filtration, washed with water (6 × 50 mL) and purified by column chromatography with dichloromethane/acetone (70:2 v/v) to yield 55 mg (59%) of **3** as a dark-green powder.

Mp > 350 °C; MS (FAB): *m/z* = 991.59 [$M^+$], 992.60 [$M^+$+*H*] calcd for $C_{62}H_{42}N_{10}O_4$ 991.06; HRMS (ESI, pos.): *m/z* = 990.3385 [$M^+$] calcd for $C_{62}H_{42}N_{10}O_4$ 990.3390; $^1$H NMR (400 MHz, $CDCl_3$, TMS): $\delta$ = 8.71 (d, *J* = 6.9 Hz, 4H, H6,6''), 8.68 (d, *J* = 5.6 Hz, 4H, H3,3''), 8.57 (s, 2H, $H_{pery}$), 8.55 (s, 4H, H3',5'), 8.53 (d, *J* = 8.0 Hz, 2H, $H_{pery}$), 7.87-7.91 (m, 4H, H4,4''), 7.80 (d, *J* = 8.0 Hz, 2H, $H_{pery}$), 7.32-7.35 (m, 4H, H5,5''), 3.72-3.91 (m, 4H, $H_{Pyrrolidinyl}$), 2.87-3.02 (m, 4H, $H_{Pyrrolidinyl}$), 1.97-2.18 (m, 8H, $H_{Pyrrolidinyl}$); UV/Vis ($CH_2Cl_2$): $\lambda_{max}$ ($\varepsilon$) = 714 (48200), 437 (18900), 279 (67000), 250 nm (89200 $M^{-1}cm^{-1}$); fluorescence ($CH_2Cl_2$, $\lambda_{ex}$ = 660 nm): $\lambda_{max}$ = 750 nm, quantum yield ($CH_2Cl_2$): $\Phi_{fl}$ = 0.26; fluorescence lifetime ($CH_2Cl_2$, $\lambda_{ex}$ = 660 nm, $\lambda_{em}$ = 745 nm): $\tau$ = 3.8±0.2 ns.

***N,N'*-Bis*(*4'-2,2':6',2''-terpyridyl)-1,6,7,12-tetra(4-*t*-octylphenoxy)perylene-3,4:9,10-tetracarboxylic acid bisimide (4a):** 1,6,7,12-Tetra(4-*t*-octylphenoxy)perylene-3,4:9,10-tetracarboxylic acid bisanhydride[14a,16a] (**2a**) (0.13 mg, 0.11 mmol) was reacted with 4'-amino-2,2':6',2''-terpyridine (0.79 g, 0.32 mmol) in pyridine/imidazole (2:1) for 24 h at 120 °C under argon. After cooling to room temperature, the mixture was poured into aqueous HCl (70 mL, 1 M); the resulting precipitate was isolated by filtration and subsequently washed with water (20 mL) and methanol (20 mL). Purification was achieved by column chromatography on aluminium oxide (basic, activity II) with $CH_2Cl_2$/*n*-hexane (4:1 v/v) to yield **4a** (83 mg, 46%) as a dark-red microcrystalline powder.

Mp > 350 °C; MS (FAB): *m/z* = 1670.3 [$M^+$], 1671.3 [$M^+$+*H*], calcd for $C_{110}H_{108}N_8O_8$ 1670.08; $^1$H NMR (400 MHz, $CDCl_3$, TMS): $\delta$ = 8.65 (d, *J* = 6.9 Hz, 4H, H6,6''), 8.64 (d, *J* = 4.8 Hz, 4H, H3,3''), 8.45 (s, 4H, H3',5'), 8.21 (s, 4H, $H_{pery}$), 7.81-7.86 (m, 4H, H4,4''), 7.25-7.31 (m, 12H, $H_{Ar}$, H5,5''), 6.91 (d, *J* = 8.7 Hz, 8H, $H_{Ar}$), 1.70-2.18 (s, 12H, $CH_2$), 1.33 (s, 24H, $CH_3$), 0.74 (s, 36H, $CH_3$); UV/Vis ($CH_2Cl_2$): $\lambda_{max}$ ($\varepsilon$) = 588 (50800), 550 (30300), 456 (17200), 283 (82200), 239 nm (106800 $M^{-1}cm^{-1}$); fluorescence ($CH_2Cl_2$, $\lambda_{ex}$ = 540 nm): $\lambda_{max}$ = 618 nm, quantum yield ($CH_2Cl_2$): $\Phi_{fl}$ = 0.96±0.01; fluorescence lifetime ($CH_2Cl_2$, $\lambda_{ex}$ = 540 nm, $\lambda_{em}$ = 617 nm): $\tau$ = 6.6±0.2 ns; elemental analysis calcd (%) for $C_{110}H_{108}N_8O_8$ (1670.3): C 79.11, H 6.52, N 6.71; found: C 78.73, H 6.81, N 6.55.

***N*,*N'*-Bis*(*4'-2,2':6',2''-terpyridyl)-1,6,7,12-tetra(4-*t*-butylphenoxy)perylene-3,4:9,10-tetracarboxylic acid bisimide (4b):** This compound was synthesized and purified according to procedure as described for **4a** from 1,6,7,12-tetra(4-*t*-butylphenoxy)perylene-3,4:9,10-tetracarboxylic acid bisanhydride[14a,16a] (**2b**) (0.15 g, 0.15 mmol) and 4'-amino-2,2':6',2''-terpyridine (0.15 g, 0.61 mmol), to give **4b** (0.11 g, 50%) as a bright-red powder.

Mp > 350 °C; MS (FAB): *m/z* = 1445.5 [$M^+$], calcd for $C_{94}H_{76}N_8O_8$ 1445.6; HR-MS (ESI pos.): *m/z* = 1445.5859 [$M^+$], calcd for $C_{94}H_{76}N_8O_8$ 1445.5820; $^1$H NMR (400 MHz, $CDCl_3$, TMS): $\delta$ = 8.65 (d, *J* = 6.9 Hz, 4H, H6,6''), 8.64 (d, *J* = 4.8 Hz, 4H, H3,3''), 8.46 (s, 4H, H3',5'), 8.28 (s, 4H, $H_{pery}$), 7.82-7.88 (m, 4H, H4,4''), 7.29-7.33 (m, 4H, H5,5''), 7.24 (d, 8H, *J* = 8.7 Hz, $H_{Ar}$), 6.88 (d, *J* = 8.7 Hz, 8H, $H_{Ar}$), 1.26 (s, 36H, $CH_3$); UV/Vis ($CH_2Cl_2$): $\lambda_{max}$ ($\varepsilon$) = 585 (54200), 544 (32500), 454 (18400), 281 nm (89400 $M^{-1}cm^{-1}$); fluorescence ($CH_2Cl_2$, $\lambda_{ex}$ = 540 nm): $\lambda_{max}$ = 615 nm, quantum yield ($CH_2Cl_2$): $\Phi_{fl}$ = 0.97±0.01.

***N*-Cyclohexyl-*N'*-(4'-2,2':6',2''-terpyridyl)-1,7-dipyrrolidinylperylene-3,4:9,10-tetracarboxylic acid bisimide (7):** *N*-Cyclohexyl-1,7-dipyrrolidinylperylene-3,4:9,10-tetracarboxylic acid-3,4-anhydride-9,10-imide[17c] (**5**) (150 mg, 0.25 mmol) was reacted with 4'-amino-2,2':6',2''-terpyridine (91.3 g, 0.37 mmol) in pyridine/imidazole (2:1) for

50 h at 120 °C under argon. After cooling to room temperature, the mixture was poured ointo aqueous HCl (20 mL, 1 M); the resulting precipitate was extracted with 90 mL of methylene chloride, washed with water, dried over $MgSO_4$, and concentrated by rotary evaporation. Purification was achieved by column chromatography on silica gel with $CH_2Cl_2$/methanol (100:1 v/v) to yield **7** (140 mg, 68%) as a dark-green microcrystalline powder.

Mp > 330 °C; MS (MALDI-TOF, dithranol): *m/z* = 841.18 [$M^+$], 842.18 [$M^+$+*H*] calcd for $C_{53}H_{43}N_7O_4$ 841.95; $^1$H NMR (400 MHz, $CDCl_3$, TMS): $\delta$ = 8.70 (d, *J* = 7.9 Hz, 2H, H6,6''), 8.67 (d, *J* = 4.4 Hz, 2H, H3,3''), 8.54 (s, 1H, $H_{pery}$), 8.54 (s, 2H, H3',5'), 8.51 (s, 1H, $H_{pery}$), 8.49 (d, *J* = 9.4 Hz, 1H, $H_{pery}$), 8.44 (d, *J* = 8.1 Hz, 1H, $H_{pery}$), 7.85-7.89 (m, 2H, H4,4''), 7.80 (d, *J* = 8.0 Hz, 1H, $H_{pery}$), 7.75 (d, *J* = 8.0 Hz, 1H, $H_{pery}$), 7.32-7.35 (m, 2H, H5,5''), 5.00-5.14 (m, 1H, $NCH_2$), 3.70-3.90 (m, 4H, $H_{Pyrrolidinyl}$), 2.80-3.00 (m, 4H, $H_{Pyrrolidinyl}$), 2.56-2.67 (m, 2H, $H_{Cy}$), 1.89-2.10 (m, 10H, $H_{Pyrrolidinyl}$, $H_{Cy}$), 1.72-1.80 (m, 2H, $H_{Cy}$), 1.33-1.50 (m, 4H, $H_{Cy}$); $^{13}$C NMR (100 MHz, $CDCl_3$): $\delta$ = 164.6, 164.5, 163.6, 163.5, 157.1, 155.7, 149.1, 146.8, 146.4, 145.9, 136.8, 135.1, 134.0, 130.3, 130.0, 127.3, 126.6, 124.2, 123.9, 123.8, 122.8, 122.7, 122.3, 121.6, 121.4, 121.3, 121.2, 120.8, 119.9, 118.9, 118.7, 117.7 53.8, 52.3, 29.2, 26.7, 25.8, 25.6; UV/Vis ($CH_2Cl_2$): $\lambda_{max}$ ($\varepsilon$) = 706 (41800), 436 (16600), 309 (35600), 278 (44300), 246 nm (69500 $M^{-1}cm^{-1}$); fluorescence ($CH_2Cl_2$, $\lambda_{ex}$ = 660 nm): $\lambda_{max}$ = 746 nm, quantum yield ($CH_2Cl_2$): $\Phi_{fl}$ = 0.19; fluorescence lifetime ($CH_2Cl_2$, $\lambda_{ex}$ = 660 nm, $\lambda_{em}$ = 745 nm): $\tau$ = 3.7±0.2 ns; elemental analysis calcd for $C_{53}H_{43}N_7O_4 \times H_2O$ (859.9): C 73.95, H 5.01, N 11.30; found: C 73.86, H 5.36, N 11.42.

***N*-Butyl-*N'*-(4'-2,2':6',2''-terpyridyl)-1,6,7,12-tetra(4-*t*-butylphenoxy)perylene-3,4:9,10-tetracarboxylic acid bisimide (8):** *N*-Butyl-1,6,7,12-tetra(4-*t*-butylphenoxy)perylene-3,4:9,10-tetracarboxylic acid-3,4-anhydride-9,10-imide[14a,16a] (**6**) (0.14 mg, 0.13 mmol) was reacted with 4'-amino-2,2':6',2''-terpyridine (0.50 g, 0.20 mmol) in pyridine/imidazole (2:1) for 48 h at 120 °C under argon. After cooling to room temperature, the mixture was poured into aqueous HCl (20 mL, 1 M); the resulting precipitate was isolated by filtration and subsequently washed with water (30 mL) and

methanol (20 mL). Purification was achieved by column chromatography on aluminium oxide (basic, activity II) with $CH_2Cl_2$/*n*-hexane (4:1 v/v) to yield **6** (84 mg, 50%) as a dark-red microcrystalline powder.

Mp > 320 °C; MS (ESI-TOF, pos.): *m/z* = 1270.56 [$M^+$], calcd for $C_{83}H_{75}N_5O_8$ 1270.55; $^1$H NMR (400 MHz, $CDCl_3$, TMS): $\delta$=8.58 (m, 4H, H6,6'', H3,3''), 8.39 (s, 1H, H3',5'), 8.18 (s, 2H, $H_{pery}$), 8.17 (s, 2H, $H_{pery}$), 7.79 (m, 2H, H4,4''), 7.25 (m, 2H, H5,5''), 7.17 (m, 8H, $H_{Ar}$), 6.78 (m, 8H, $H_{Ar}$), 4.05 (m, 2H, $NCH_2$), 1.61 (m, 2H, $CH_2$), 1.34 (m, 2H, $CH_2$), 1.22 (s, 18H, $CH_3$), 1.18 (s, 18H, $CH_3$); UV/Vis ($CH_2Cl_2$): $\lambda_{max}$ ($\varepsilon$) = 581 (46100), 541 (27800), 453 (16600), 285 nm (64000 $M^{-1}cm^{-1}$); fluorescence ($CH_2Cl_2$, $\lambda_{max}$ = 540 nm): $\lambda_{max}$ = 611 nm, quantum yield ($CH_2Cl_2$): $\Phi_{fl}$ = 0.89±0.01; fluorescence lifetime ($CH_2Cl_2$, $\lambda_{ex}$ = 540 nm, $\lambda_{em}$ = 617 nm): $\tau$ = 7.2±0.2 ns; elemental analysis calcd (%) for $C_{83}H_{75}N_5O_8$ (1270.56): C 78.46, H 5.95, N 5.51; found: C 78.18, H 5.86, N 5.42.

## Metal-Ion Mediated Self-Assembly of Perylene Bisimide Building Blocks

**Metallodimer $(7)_2Zn(OTf)_2$:** To a solution of *N*-cyclohexyl-*N'*-(4'-2,2':6',2''-terpyridyl)-1,7-dipyrrolidinylperylene-3,4:9,10-tetracarboxylic acid bisimide (**7**) (10.0 mg, 11.8 µmol) in $CHCl_3$-$CH_3OH$ (60:40, 0.65 mL) a stock solution of zinc triflate (16.8 mM, 350 µL, 5.9 µmol) was added and the solution was stirred for 10 min at room temperature. The solution was concentrated using rotary evaporator; the product was precipitated by addition of acetonitrile (10 mL) and isolated quantitatively by centrifugation. Exact 2:1 stoichiometry of **7** and zinc triflate was confirmed by $^1$H NMR.

MS (MALDI-TOF, dithranol): *m/z* = 1895.50 [*M-OTf*]$^+$, 1746.50 [*M-2OTf*]$^{2+}$, 1054.20 [**8**+Zn+OTf]$^+$ calcd for $C_{108}H_{86}F_6N_{14}O_{14}S_2Zn$ 2045.51; $^1$H NMR (400 MHz, chloroform[$D_3$]-methanol[$D_4$] (60:10, v/v), TMS): $\delta$ = 9.11 (bs, 4H, H3',5'), 8.76 (d, *J* = 8.1 Hz, 4H, H3,3''), 8.58 (bs, 4H, $H_{pery}$), 8.42-8.49 (m, 4H, $H_{pery}$), 8.25-8.35 (m, 4H, H4,4''), 8.07 (d, *J* = 4.7 Hz, 4H, H6,6''), 7.75-7.85 (m, 2H, $H_{pery}$), 7.61-7.67 (m, 4H, H5,5''), 7.53-

7.61 (m, 2H, $H_{pery}$), 5.08-5.15 (m, 2H, $NCH_2$), 3.68-3.87 (m, 8H, $H_{Pyrrolidinyl}$), 2.73-2.92 (m, 8H, $H_{Pyrrolidinyl}$), 2.61-2.72 (m, 4H, $H_{Cy}$), 1.77-2.16 (m, 28H, $H_{Pyrrolidinyl}$, $H_{Cy}$), 1.38-1.56 (m, 4H, $H_{Cy}$); UV/Vis ($CHCl_3$/MeOH, 60:40, v/v): $\lambda_{max}$ ($\varepsilon$) = 723 (78400), 441 (32000), 320 (66800), 285 nm (90200 $M^{-1}cm^{-1}$); fluorescence (dimethylformamide, $\lambda_{ex}$ = 660 nm): $\lambda_{max}$ = 764 nm, quantum yield (dimethylformamide): $\Phi_{fl}$ = 0.10±0.01; fluorescence lifetime ($CHCl_3$/MeOH, 60:40 v/v, $\lambda_{ex}$ = 660 nm, $\lambda_{em}$ = 770 nm): $\tau$ = 1.8±0.2 ns.

**Metallodimer $(8)_2Zn(OTf)_2$:** To a solution of *N*-butyl-*N'*-(4'-2,2':6',2''-terpyridyl)-1,6,7,12-tetra(4-*t*-butylphenoxy)perylene-3,4:9,10-tetracarboxylic acid bisimide (**8**) (4.94 mg, 3.88 µmol) in $CHCl_3$-$CH_3OH$ (60:40, 0.70 mL) a stock solution of zinc triflate (4.85 mM, 400 µL, 1.94 µmol) was added and the solution was stirred for 10 min at room temperature. The solution was concentrated using rotary evaporator; the product was precipitated by addition of acetonitrile (10 mL) and isolated quantitatively by centrifugation. Exact 2:1 stoichiometry of ligand **8** and Zn(II) triflate was confirmed by $^1H$ NMR.

MS (MALDI-TOF, DCTB matrix): *m/z* = 2754.0 $[M\text{-}OTf]^+$, 2605.0 $[M\text{-}2OTf]^{2+}$ calcd for $C_{168}H_{150}F_6N_{10}O_{22}S_2Zn$ 2904.5; $^1H$ NMR (400 MHz, $CDCl_3$/$CD_3OD$, 60:40 v/v, TMS): $\delta$ = 8.92 (s, 4H, H3',5'), 8.59 (d, *J* = 8.1 Hz, 4H, H3,3''), 8.37 (s, 4H, $H_{pery}$), 8.26 (s, 4H, $H_{pery}$), 8.16-8.22 (m, 4H, H4,4''), 7.87 (d, *J* = 5.6 Hz, 4H, H6,6''), 7.47-7.54 (m, 4H, H5,5''), 7.27-7.33 (m, 16H, $H_{Ar}$), 6.90-6.95 (m, 16H, $H_{Ar}$), 4.11-4.17 (m, 4H, $NCH_2$), 1.66-1.72 (m, 4H, $CH_2$), 1.38-1.46 (m, 4H, $CH_2$), 1.32 (s, 36H, $CH_3$), 1.29 (s, 36H, $CH_3$), 0.93-0.99 (m, 6H, $CH_3$); UV/Vis ($CHCl_3$/MeOH (60:40, v/v)): $\lambda_{max}$ ($\varepsilon$) = 591 (100700), 552 (61200), 458 (36100), 332 (30600), 285 (136000), 267 nm (133100 $M^{-1}cm^{-1}$); fluorescence ($CHCl_3$/MeOH, 60:40 v/v, $\lambda_{ex}$ = 540 nm): $\lambda_{max}$ = 625 nm, quantum yield ($CHCl_3$/MeOH, 60:40, v/v): $\Phi_{fl}$ = 0.82±0.02; fluorescence lifetime ($CHCl_3$/MeOH, 60:40 v/v, $\lambda_{ex}$ = 540 nm, $\lambda_{em}$ = 617 nm): $\tau$ = 7.6±0.2 ns.

**Coordination Polymer 9:** To a solution of *N,N'*-bis(4'-2,2':6',2''-terpyridyl)-1,7-dipyrrolidinylperylene-3,4:9,10-tetracarboxylic acid bisimide (**3**) (3.95 mg, 3.98 µmol) in $CHCl_3$/$CH_3OH$ (60:40 v/v, 700 µL) a stock solution of zinc(II) triflate (136.5 µL, 3.98

µmol) was added and the solution was stirred for 10 min at room temperature. The exact 1:1 stoichiometry of **3** and zinc triflate was checked by $^1$H NMR and, if necessary, was adjusted until no residual signals of uncomplexed tpy ligand was observed. Upon addition of acetonitrile (5 mL) the product is precipitated and isolated quantitatively by centrifugation.

$^1$H NMR (400 MHz, $CDCl_3/CD_3OD$, 60:40 v/v, TMS): $\delta$ = 9.08 (br), 8.76 (br), 8.31 (br), 8.07 (br), 7.91 (br), 7.63 (br), 3.92 (br, $H_{Pyrrolidinyl}$), 3.05 (br, $H_{Pyrrolidinyl}$), 2.00-2.40 (br, $H_{Pyrrolidinyl}$); UV/Vis ($CHCl_3$/MeOH (60:40, v/v)): $\lambda_{max}$ ($\varepsilon$ value per perylene bisimide unit) = 722 (35200), 439 (15700), 315 (38300), 275 (62800), 248 nm (73600 $M^{-1}cm^{-1}$); fluorescence ($CHCl_3$/MeOH, 60:40 v/v, $\lambda_{ex}$ = 660 nm): $\lambda_{max}$ = 768 nm, quantum yield ($CHCl_3$/MeOH, 60:40 v/v): $\Phi_{fl}$ = 0.09±0.01; fluorescence lifetime (DMF, $\lambda_{ex}$ = 660 nm, $\lambda_{em}$ = 770 nm): $\tau$ = 2.2±0.2 ns.

**Coordination Polymer 10:** To a solution of *N*,*N'*-bis(4'-2,2':6',2''-terpyridyl)-1,6,7,12-tetra(4-*t*-octhylphenoxy)perylene-3,4:9,10-tetracarboxylic acid bisimide (**4a**) (2.53 mg, 1.52 µmol) in $CHCl_3/CH_3OH$ (60:40 v/v, 700 µL) a stock solution of zinc(II) triflate (52.5 µL, 1.52 µmol) was added and the solution was stirred for 10 min at room temperature. The exact 1:1 stoichiometry of **4a** and zinc triflate was checked by $^1$H NMR and, if necessary, was adjusted until no residual signals of uncomplexed tpy ligand was observed. By addition of acetonitrile (5 mL) the product is precipitated and isolated quantitatively by centrifugation.

$^1$H NMR (400 MHz, $CDCl_3/CD_3OD$, 60:40 v/v, TMS): $\delta$ = 8.95 (br), 8.63 (br), 8.33 (br), 8.21 (br), 7.92 (br), 7.38 (br, $H_{Ar}$), 7.03 (br, $H_{Ar}$), 1.78 (br, $CH_2$), 1.35 (br, $CH_3$), 0.79 (br, $CH_3$); UV/Vis ($CHCl_3$/MeOH (60:40, v/v)): $\lambda_{max}$ ($\varepsilon$ value per perylene bisimide unit) = 596 (44900), 553 (28100), 458 (15600), 334 (13500), 277 nm (77900 $M^{-1}cm^{-1}$); fluorescence ($CHCl_3$/MeOH, 60:40 v/v, $\lambda_{ex}$ = 540 nm): $\lambda_{max}$ = 626 nm, quantum yield ($CHCl_3$/MeOH, 60:40 v/v): $\Phi_{fl}$ = 0.85±0.02; fluorescence lifetime (DMF, $\lambda_{ex}$ = 540 nm, $\lambda_{em}$ = 617 nm): $\tau$ = 4.4±0.2 ns.

## Atomic Force Microscopy Measurement

AFM measurements were carried out under ambient conditions by using a Veeco MultiMode$^{TM}$ Nanoscope IV system (Veeco Metrology Inc.) operating in tapping mode in air. The images were taken using a scanner with a maximum scan area of 15 × 15 μm. Silicon cantilevers with a nominal spring constant of 34.0-71.0 N/m and with resonant frequency of 300 kHz, and a typical tip radius of 7 nm (OMCL-AC160TS, Olympus) were used. To obtain the best imaging quality, the scan rate was set to 0.9 Hz (~10 min for each AFM image). All AFM images were obtained at a resolution of 512 × 512 pixels. The solutions of supramolecular polymers **9** and **10** in DMF (0.05 mg/mL) were spin-coated on a highly ordered pyrolytic graphite (HOPG, Nano Technology Instruments – Europe) or muscovite mica (Veeco Metrology Inc.) under 4000 rpm.

## Preparation of Layer-by-Layer Multifilm

Quartz substrates (Hellma GmbH, Germany) were cleaned by immersing into fresh piranha solution (7:3 v/v $H_2SO_4/H_2O_2$) for 10 min followed by intensive rinsing with water. Polyethyleneimine (PEI, branched, MW ca. 750.000) and polystyrene sulfonate (PSS, MW ca. 70.000) were applied as 0.01 M solutions in 0.5 M aqueous NaCl solution. A freshly cleaned quartz substrate was immersed into a solution of PEI for 10 min, washed with water and dried under a gentle stream of argon gas. Multilayers are formed by subsequent dipping of the substrate in solutions of PSS for 10 min and the respective coordination polymer (1 mM in DMF) for 10 min. After each adsorption step in DMF the substrate is subsequently immersed in DMF, DMF–water (1:1) and water for each 2 min. These routines were repeated until the desired number of double layers was achieved. The formation of the layers was controlled by UV/Vis spectroscopy after each adsorption step.

## References


[1] a) H.-G. Elias, *An Introduction to Polymer Science*, Wiley-VCH, Weinheim, **1997**; b) D. Braun, H. Cherdron, M. Rehahn, H. Ritter, B. Voit, *Polymer Synthesis: Theory and Practice*, 4th ed., Springer-Verlag: Heidelberg, **2005**.

[2] a) J.-M. Lehn, *Supramolecular Chemistry: Concepts and Perspectives*, VCH: New York, **1995**; b) J.-M. Lehn, *Proc. Natl. Acad. Sci. U.S.A*. **2002**, *99*, 4763-4768; c) J.-M. Lehn, *Chem. Soc. Rev.* **2007**, *36*, 151-160; d) G. M. Whitesides, J. P. Mathias, C. T. Seto, *Science* **1991**, *254*, 1312-1319; e) G. M. Whitesides, M. Boncheva, *Proc. Natl. Acad. Sci. U.S.A*. **2002**, *99*, 4769–4774.

[3] a) L. Brunsveld, B. J. B. Folmer, E. W. Meijer, R. P. Sijbesma, *Chem. Rev.* **2001**, *101*, 4071-4097; b) O. Ikkala, G. Ten Brinke, *Science* **2002**, *295*, 2407-2409 ; c) J.-M. Lehn, *Polym. Int.* **2002**, *35*, 825-839; d) C. R. South, C. Burnd, M. Weck, *Acc. Chem. Res*. **2007**, *40*, 63-74.

[4] a) C. Fouquey, J.-M. Lehn, A.-M. Levelut, *Adv. Mater.* **1990**, *2*, 254-257; b) R. P. Sijbesma, F. H. Beijer, L. Brunsveld, B. J. B. Folmer, J. H. K. Ky Hirschberg, R. F. M. Lange, J. K. L. Lowe, E. W. Meijer, *Science* **1997**, *278*, 1601-1604; c) J. H. K. Ky Hirschberg, L. Brunsveld, A. Ramzi, J. A. J. M. Vekemans, R. P. Sijbesma, E. W. Meijer, *Nature* **2000**, *407*, 167-170; d) A. T. ten Cate, R. P. Sijbesma, *Macromol. Rapid Commun.* **2002**, *23*, 1094-1112; e) A. Ajayaghosh, S. J. George, A. P. H. J. Schenning, *Top. Curr. Chem.* **2005**, *258*, 83-118; f) E. Obert, M. Bellot, L. Bouteiller, F. Andrioletti, C. Lehen-Ferrenbach, F. Boué, *J. Am. Chem. Soc.* **2007**, *129*, 15601-15605; g) L. Bouteiller, *Adv. Polym. Sci.* **2007**, *207*, 79-112.

[5] a) S. Yao, U. Beginn, T. Gress, M. Lysetska, F. Würthner*, J. Am. Chem. Soc.* **2004**, *126*, 8336-8348; b) Y. Guan, S.-H. Yu, M. Antonietti, C. Böttcher, C. F. J. Faul, *Chem.-Eur. J.* **2005**, *11*, 1305-1311; c) A. Lohr, T. Greß, M. Deppisch, M. Knoll, F. Würthner, *Synthesis,* **2007**, *19*, 3073–3082.

[6] a) M. Miyauchi, Y. Takashima, H. Yamaguchi, A. Harada, *J. Am. Chem. Soc.* **2005**, *127*, 2984-2989; b) Y. Hasegawa, M. Miyauchi, Y. Takashima, H. Yamaguchi, A. Harada, *Macromolecules* **2005**, *38*, 3724-3730.

[7] a) A. Arnaud, J. Belleney, F. Boué, L. Bouteiller, G. Carrot, V. Wintgens, *Angew. Chem.* **2004**, *116*, 1750-1753; *Angew. Chem. Int. Ed*. **2004**, *43*, 1718-1721; b) T. Haino, Y. Matsumoto, Y. Fukazawa, *J. Am. Chem. Soc.* **2005**, *127*, 8936-8937; c) G. Fernández, E. P. Pérez, L. Sánches, N. Martín, *Angew. Chem.* **2008**, *120*, 1110-1113; *Angew. Chem. Int. Ed*. **2008**, *47*, 1094-1097.

[8] a) U. S. Schubert, C. Eschbaumer, *Angew. Chem.* **2002**, *114*, 3016-3050; *Angew. Chem. Int. Ed.* **2002**, *41*, 2892-2926; b) R. Knapp, S. Kelch, O. Schmelz, M. Rehahn, *Macromol. Symp*. **2003**, *204*, 267-286; c) P. Andres, U. S. Schubert, *Adv. Mater*. **2004**, *16*, 1043-1068; d) D. Hinderberger, O. Schmelz, M. Rehahn, G. Jeschke, *Angew. Chem.* **2004**, *116*, 4716-4721; *Angew. Chem. Int. Ed*. **2004**, *43*, 4616-4621; e) R. Dobrawa, M. Lysetska, P. Ballester, M. Grüne, F. Würthner, *Macromolecules* **2005**, *38*, 1315–1325; f) R. Dobrawa, F. Würthner, *J. Polym. Sci. Part A* **2005**, *43*, 4981-4995; g) J. B. Beck, J. M. Ineman, S. J. Rowan, *Macromolecules* **2005,** *38,* 5060-5068; h) C.-C.You, R. Dobrawa, C. R. Saha-Möller, F. Würthner, *Top. Curr. Chem.* **2005**, *258*, 39-82 ; i) T. Suzuki, S. Shinkai, K. Sada, *Adv. Mater*. **2006**, *18*, 1043-1046; j) F. Würthner, V. Stepanenko, A. Sautter, *Angew. Chem.* **2006**, *118*, 1973-1976; *Angew. Chem. Int. Ed.* **2006**, *45*, 1939–1942; k) D. G. Kurth, M. Higuchi, *Soft Matter* **2006**, *2*, 915–927; l)C.-F. Chow, S. Fujii, J.-M. Lehn, *Angew. Chem.* **2007**, *119*, 5095-5098; *Angew. Chem. Int. Ed.* **2007**, *46*, 5007-5010; m) J. E. Beves, E. C. Constable, C. E. Housecroft, C. J. Kepert, D. J. Price, *CrystEngComm* **2007**, *9*, 456-459; n) M. Chiper, M. A. R. Meier, D. Wouters, S. Hoeppener, C.-A. Fustin, J.-F. Gohy, U. S. Schubert, *Macromolecules* **2008**, *41*, 2771-2777; o) F. S. Han, M. Higuchi, T. Ikeda, Y. Negishi, T. Tsukudab, D. G. Kurth, *J. Mater. Chem*. **2008**, *18*, 4555–4560.

[9] a) U. S. Schubert, H. Hofmeier and G. R. Newkome, *Modern Terpyridine Chemistry*, Wiley-VCH: Weinheim, **2006**; b) E. C. Constable, *Chem. Soc. Rev.* **2007**, *36*, 246-253.

[10] J. P. Sauvage, J. P. Collin, J. C. Chambron, S. Guillerez, C. Coudret, V. Balzani, F. Barigelletti, L. De Cola, L. Flamigni, *Chem. Rev.* **1994**, *94*, 993-1019.

[11] a) W. Ng, X. Gong, W. K. Chan, *Chem. Mater*. **1999**, *11*, 1165-1170; b) A. Islam, H. Sugihara, H. Arakawa*, J. Photochem. Photobiol. A: Chem.* **2003**, *158*, 131-

138; c) X. Chen, L. Ma, Y. Cheng, Z. Xie, L. Wang, *Polym. Int*. **2007**, *56*, 648-654; d) S. M. Brombosz, A. J. Zucchero, R. L. Phillips, D. Vazquez, A. Wilson, U. H. F. Bunz, *Org. Lett.* **2007**, *9*, 4519-4522; e) F. S. Han, M. Higuchi, D. G. Kurth, *J. Am. Chem. Soc.* **2008**, *130*, 2073-2080.

[12] For reviews on perylene bisimide dyes, see: a) H. Langhals, *Heterocycles* **1995,** *40*, 477-500; b) F. Würthner *Chem. Commun.* **2004**, *14*, 1564-1579; c) H. Langhals, *Helv. Chim. Acta* **2005**, *88*, 1309-1343.

[13] a) F. Würthner, A. Sautter, D. Schmid, P. J. A. Weber *Chem. Eur. J.* **2001**, *7*, 894–902; b) C.-C. You, F. Würthner *J. Am. Chem. Soc.* **2003**, *125*, 9716–9725; c) F. Würthner, A. Sautter, *Org. Biomol. Chem.* **2003**, *1*, 240-243; d) Y. Li, N. Wang, H. Gan, H. Liu, H. Li, Y. Li, X. He, C. Huang, S. Cui, S. Wang, D. Zhu, *J. Org. Chem.* **2005**, *70*, 9686-9692; e) C.-C. You, C. Hippius, M. Grüne, F. Würthner, *Chem. Eur. J.* **2006***,12,* 7510–7519.

[14] a) F. Würthner, C. Thalacker, A. Sautter, W. Schärtl, W. Ibach, O. Hollricher, *Chem. Eur. J.* **2000**, *6*, 3871-3886; b) C. Thalacker, F. Würthner, *Adv. Funct. Mater.* **2002**, *12*, 209-218; c) Y. Liu, J. Zhuang, H. Liu, Y. Li, F. Lu, H. Gan, T. Jiu, N. Wang, X. He, D. Zhu, *ChemPhysChem* **2004**, *5*, 1210-1215; d) T. Kaiser, H. Wang, V. Stepanenko, F. Würthner, *Angew. Chem.* **2007**, *119*, 5637–5640; *Angew. Chem. Int. Ed*. **2007**, *46*, 5541–5544; f) T. Seki, S. Yagai, T. Karatsu, A. Kitamura, *J. Org. Chem.* **2008**, *73*, 3328–3335; f) H. Wang, T. E. Kaiser, S. Uemura, F. Würthner, *Chem.Commun*. **2008**, *10*, 1181–1183; g) F. Würthner, C. Bauer, V. Stepanenko, S. Yagai, *Adv. Mater.* **2008***, 20*, 1695–1698.

[15] a) F. Würthner, C. Thalacker, S. Diele, C. Tschierske, *Chem. Eur. J.* **2001**, *7*, 2245–2253; b) Z. Chen, V. Stepanenko, V. Dehm, P. Prins, L. D. A. Siebbeles, J. Seibt, P. Marquetand, V. Engel, F. Würthner, *Chem. Eur. J.* **2007***, 13,* 43–449.

[16] a) D. Dotcheva, M. Klapper, K Müllen, *Macromol. Chem. Phys.* **1994**, *195*, 1905-1911; b) M. Thelakkat, P. Posch, H.-W. Schmidt, *Macromolecules* **2001**, *34*, 7441-7447; c) E. E. Neuteboom, S. C. J. Meskers, P. A. van Hal, J. K. J. van Duren, E. W. Meijer, R. A. J. Janssen, H. Dupin, G. Pourtois, J. Cornil, R. Lazzaroni, J.-L. Brédas, D. Beljonne, *J. Am. Chem. Soc.* **2003***, 125*, 8625-8638; d) E. E. Neuteboom, S. C. J. Meskers, E. W. Meijer, R. A. J. Janssen, *Macromol.*

*Chem. Phys.* **2004**, *205*, 217–222; e) S. Xu, Y. Jin, M. Yang, F. Bai, S Cao, *Polym. Adv. Technol.* ***2006***, *17*, 556–561; f) M. Sommer, A. S. Lang, M. Thelakkat, *Angew. Chem.* **2008**, *120*, 8019-8022; *Angew. Chem. Int. Ed*. **2008**, *47*, 7901-7904; g) C. B. Nielsen, D. Veldman, R. Martín-Rapún, R. A. J. Janssen, *Macromolecules* **2008**, *41,* 1094-1103; h) J. Hua, F. Meng, J. Li, P. Zhao, Y. Qu, *J. Appl. Polym. Sci.* **2008**, *110*, 1778-1783.

[17] a) Y. Y. Zhao, M. R. Wasielewski, *Tetrahedron Lett.* **1999**, *39*, 7047-7050; b) A. S. Lukas, Y. Zhao, S. E. Miller, M. R. Wasielewski, *J. Phys. Chem. B* **2002,** *106,* 1299-1306; c) F. Würthner, V. Stepanenko, Z. Chen, C. R. Saha-Möller, N. Kocher, D. Stalke, *J. Org. Chem.* **2004**, *69*, 7933–7939.

[18] R.-A. Fallahpour, M. Neuburger, M. Zehnder, *New J. Chem.* **1999**, *23*, 53-61.

[19] a) E. C. Constable, A. M. W. Cargill Thompson, *J. Chem. Soc. Dalton Trans.* **1994**, *9*, 1409-1418; b) H. Hofmeier, S. Schmatloch, D. Wouters, U. S. Schubert, *Macromol. Chem. Phys.* **2003**, *204*, 2197-2203.

[20] For the characterization of metallosupramolecular structures by mass spectrometry, see: C. A. Schalley, *Int. J. Mass Spectrom.* **2000**, *194*, 11-39.

[21] Matrices for MALDI-MS: dithranol = 1,8,9-anthracenetriol; DCTB = *trans*-2-(3-4-*tert*-butylphenyl)-2-methyl-2-propenylidene)-malononitrile.

[22] a) T. W. Claridge, *High-Resolution NMR Techniques in Organic Chemistry*, T. O. C. Series, Pergamon-Press: Amsterdam, **1999**; b) C. S. Johnson Jr., *Prog. Nucl. Magn. Reson. Spectrosc.* **1999**, *3*, 203-256; c) Y. Cohen, L. Avram, L. Frish, *Angew. Chem.* **2005**, *117*, 524-560; *Angew. Chem. Int. Ed*. **2005**, *44*, 520-554.

[23] Molecular modeling was carried out by Software “Fujitsu quantum CAChe 5.0” using MM3 force field.

[24] L. G. Berry, B. Mason, R. V. Dietrich, *Mineralogy: concepts, descriptions, determinations*, 2nd ed.; W.H. Freeman and Co.: New York, **1983**.

[25] a) G. Decher, J. D. Hong, *Macromol. Symp.* **1991**, *46*, 321-327; b) G. Decher, *Science* **1997**, *277*, 1232-1237.

[26] a) T. Tang, J. Qu, K. Müllen, S. E. Webber, *Langmuir* **2006,** *22,* 26-28; b) T. Tang, J. Qu, K. Müllen, S. E. Webber, *Langmuir* **2006,** *22, 7610-7616*; c) T. Tang, A. Herrmann, K. Peneva, K. Müllen, S. E. Webber, *Langmuir* **2007,** *23,* 4623-4628.

[27] R. Dobrawa, D. G. Kurth, F. Würthner, *Polym. Prepr.* **2004**, *45*, 378–379.

[28] The alternate multilayer film of polymers **9** and **10** does not exhibit any measurable fluorescence upon excitation at 550 and 650 nm. The reason for that might be the efficient quenching of fluorescence in such LBL films as reported previously.[27]

[29] D. D. Perrin, W. L. F. Armarego, *Purification of Laboratory Chemicals*, 2nd ed., Pergamon Press: Oxford, **1980**.

[30] J. R. Lakowicz, *Principles of Fluorescence Spectroscopy*, 2nd ed., Kluwer Academic Plenum: New York, **1999**.

[31] a) G. Seybold, G. Wagenblast, *Dyes Pigm.* **1989**, *11*, 303-317; b) R. Gvishi, R. Reisfeld, Z. Burshtein, *Chem. Phys. Lett.* **1993**, *213*, 338-344.

[32] R. Sens, K. H. Drexhage, *J. Luminesc.* **1981**, *24*, 709-712.

# Chapter 4

# Honeycomb-Structured 2D Nanopatterns by Metal-Ion-Directed Hierarchical Self-Assembly of Perylene Bisimide Dyes

**Abstract**: A ditopic bis(terpyridyl)perylene bisimide ligand was synthesized and its Zn(II)-ion-mediated self-assembly studied by $^{1}$H NMR titration. These studies revealed the formation of a trimeric metallomacrocycle that was characterized by DOSY NMR and MALDI-TOF mass spectrometry. Higher order organization of this perylene bisimide dye containg trimeric metallocycle afforded 2D assemblies with honeycomb structures as revealed by AFM studies. Such nanopatterns offer new opportunities to mimic natural photosynthesis reaction centers by incorporating guest molecules in holes of honeycomb structures.

## Introduction

Multichromophore arrays of circular topology are of great importance for efficient light harvesting in natural photosynthesis, e.g., LH1 and LH2 complexes of purple bacteria.[1] To ensure efficient energy transfer from LH2 to LH1 and to the photosynthetic reaction centers these cyclic dye arrays are further organized into 2D patterns within the photosynthetic membrane.[2] Inspired by the structural beauty of these natural dye assemblies, a great deal of attention has been devoted in the last decade to the synthesis of artificial counterparts.[3,4] The vast majority of reported cyclic dye assemblies are porphyrin- or metalloporphyrin-based owing to easy synthetic accessibility and structural similarity of these chromophores to natural (bacterio)chlorophylls, albeit that such porphyrin-based arrays exhibit inferior functionality. Over the last few years, the research group of Würthner has prepared a number of square assemblies based on perylene bisimide (PBI) dyes that are an outstanding class of functional chromophores with favorable optical and electronic properties for application as optoelectronic materials.[5,6] Such PBI-based square scaffolds were constructed by metal-ion coordination directed self-assembly of perylene bisimide building blocks that are decorated with pyridyl ligands at the imide positions to facilitate reversible metal-ligand ligation.[4b,5,7] These PBI-based square assemblies indeed show excellent fluorescence properties and for arrays containing additional peripheral chromophores efficient energy transfer was observed.[5d-f]

Würthner and co-workers have recently reported that perylene bisimides equipped with chelating 2,2′:6′,2″-terpyridine (tpy) ligands, which have become the most important aromatic aza ligands in metallosupramolecular chemistry,[8] at the imide positions through a *para*-phenylene spacer undergo metal-ion-mediated self-assembly into highly fluorescent coordination polymers (see Figure 1, top).[9] The concept of this work is to construct perylene bisimide based metallomacrocycles with particular geometry by proper design of angular bis(terpyridyl) PBI ligands (Figure 1, bottom). Such cyclic assemblies are expected to arrange into ordered 2D patterns on surfaces, which could not be achieved for the linear polymeric counterparts in earlier work.[9]

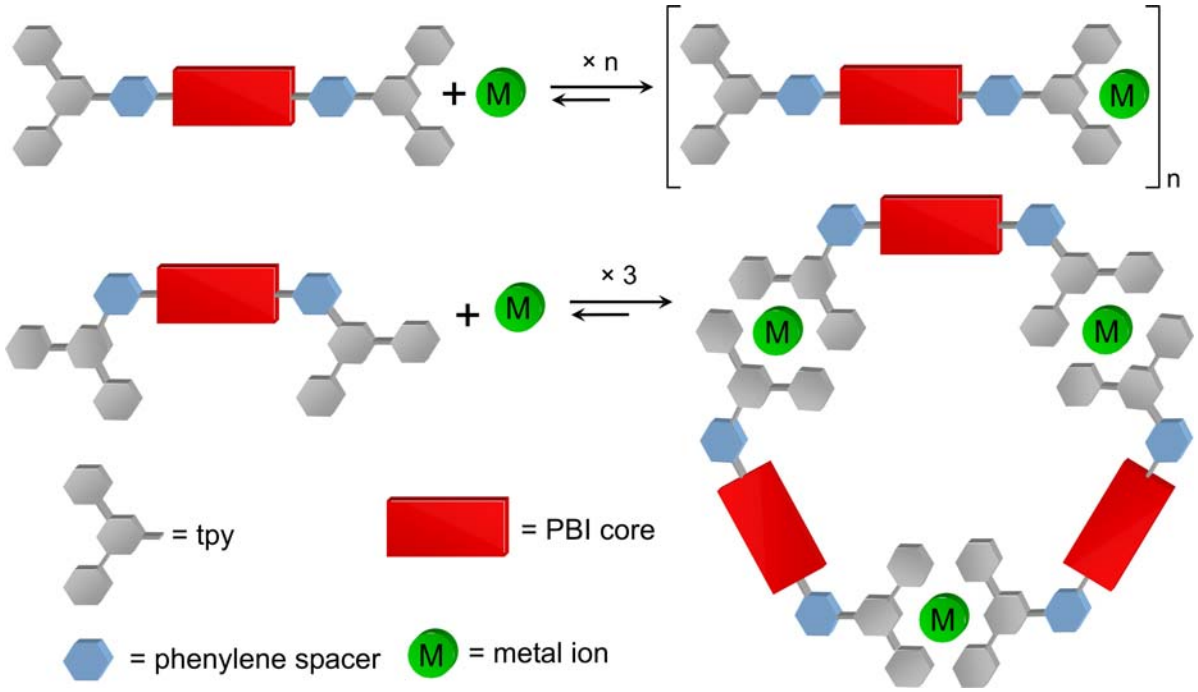


***Figure 1.*** Schematic representation of the concept of present work: The defined angular geometry (120º) of bis(terpyridyl) PBI ligands should facilitate self-assemble into trimeric metallocycle by metal-ion coordination (bottom), while linear ditopic ligands afforded coordination polymer[9] (top).

Angular bis(typ) PBI ligands with 120° angle with respect to tpy moiety and PBI core can be achieved by linking the 4′-position of tpy ligand to the meta-position of the phenylene spacer. Since 120° is the internal angle of a hexagon, metal-ion mediated self-assembly of such angular ditopic PBI ligands should lead to trinuclear metallocycles with hexagonal geometry (containing six tpy-meta-phenylene spacer units of 120º angle each),[10] as the molecular modeling study revealed that no steric constraints are to expect in the self-assembly of angular bis(tpy) PBI ligands into trimeric Zn(II)-metallocycles (Figure 2).

In this Chapter, the synthesis of ditopic bis(terpyridyl) PBI ligand **1**, which is designed by above-mentioned concept, is reported and their Zn(II)-ion-mediated self-assembly to trimeric metallomacrocycle **2** (Scheme 1). More importantly, it is shown here that these metallocyclic arrays indeed undergo higher order 2D organization into similar structures as found for their natural counterparts in the photosynthetic membrane.

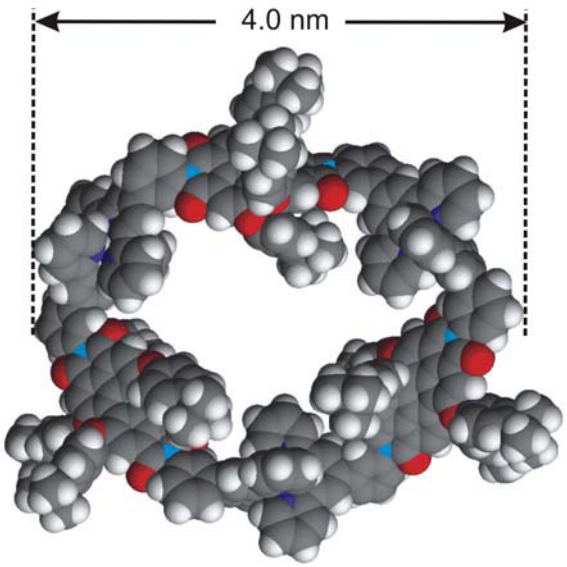


***Figure 2.*** Structure obtained by molecular modeling (Fujitsu quantum CAChe 5.0, MM3 force field) of trimeric Zn(II)-metallomacrocycle **2** (top view) possessing a diameter of 4.0 nm. The carbon atoms of PBI unites are shown in grey, oxygen atoms in red, and nitrogen atoms of tpy unites and PBIs are given in blue and light blue, respectively.

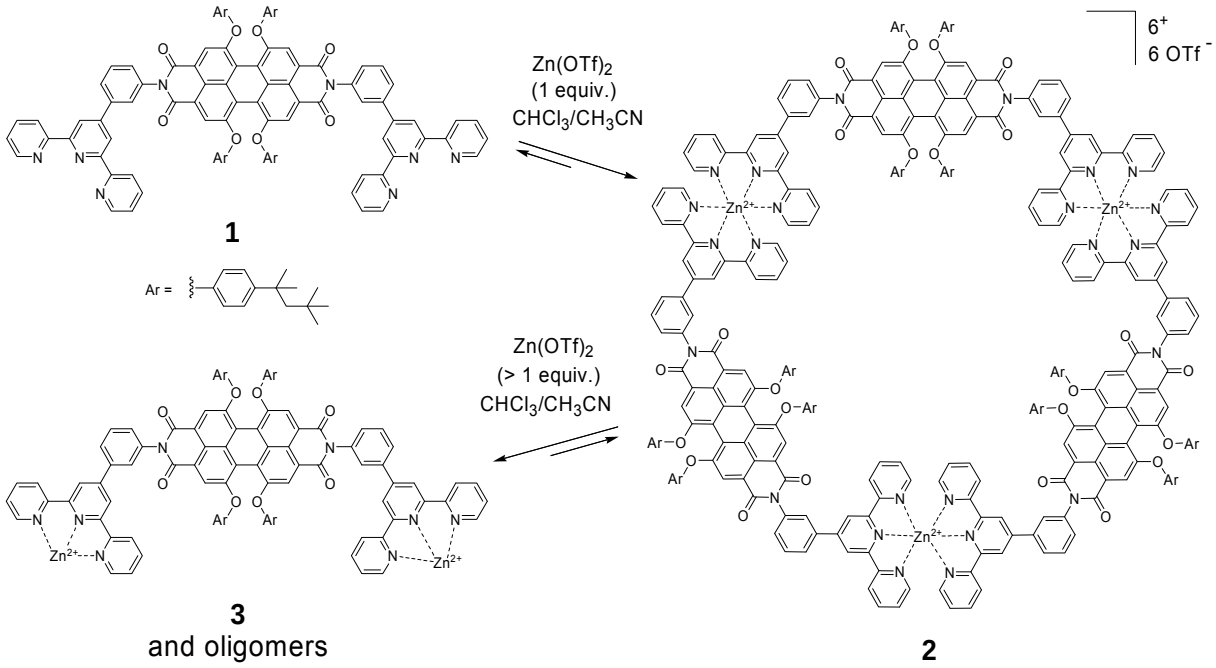


***Scheme 1.*** Formation of trimeric metallomacrocycle **2** by Zn(II)-ion-mediated self-assembly of bis(terpyridyl) PBI ligand **1** at a 1:1 stoichiometry of **1**/$Zn(OTf)_2$ in chloroform/acetonitrile mixture (60:40), and dissociation of the cyclic assembly into monomeric complex **3** and oligomeric species upon addition of excess amounts of zinc(II) triflate.

## Results and Discussion

**Synthesis.** The synthesis of bis(terpyridyl) PBI ligand **1** was achieved by the condensation of 3-(2,2′:6′,2″-terpyridin-4´-yl)aniline (**4**)[11] with 1,6,7,12-tetra(4-*t*-octyl-phenoxy)-perylene-3,4:6,10-tetracarboxylic acid bisanhydride (**5**)[12] in pyridine-imidazole mixture (2:1) in 35% isolated yield. This unknown PBI derivative **1** was fully characterized by $^1$H NMR, FAB-MS, and elemental analysis (for synthetic details and characterization data, see Experimental Section).

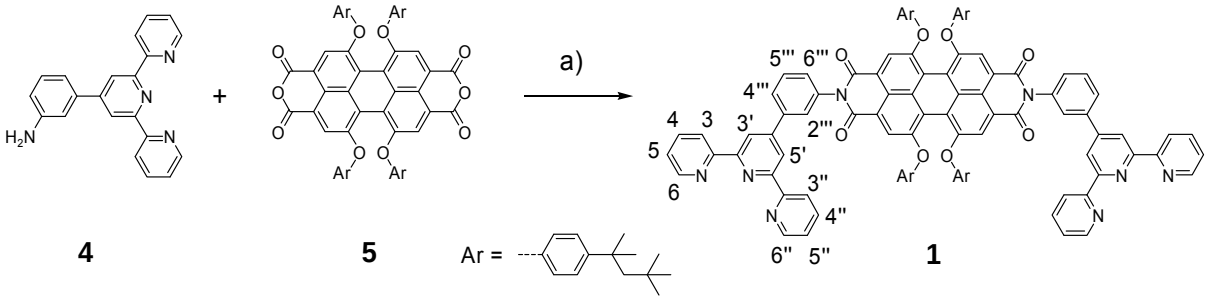


***Scheme 2*.** Synthesis of bis(tpy) PBI ligand **1**: a) pyridine/imidazol (2:1) mixture, argon, 120 °C, 5 days, 35% yield of **1**.

**Study of Complexation Reaction of Ligand with Zn(II) Ion.** Having pure bis(tpy) PBI ligand **1** in hand, the complexation reaction of this ligand with Zn(II) ion has been studied by $^1$H NMR titration in a mixture of chloroform[D]/acetonitrile[$D_3$] (60:40) using 0.2 to 2.0 equivalents of zinc(II) triflate [$Zn(OTf)_2$] (in portions of 0.2 equiv.). The $^1$H NMR spectra measured for different ratios of ligand 1/$Zn(OTf)_2$ (see Figure 3) provide clear indication for the formation of metallocyclic assembly **2** at an exact 1:1 ratio of **1**/Zn(II) ion (Scheme 1). The following observations substantiate the reversible formation of assembly **2**: Upon addition of the first batches of $Zn(OTf)_2$ a significant signal broadening and disappearance of the characteristic proton signals of terpyridine in ligand **1** at $\delta$ = 8.67 ppm for H6,6″ and at $\delta$ = 8.72 ppm for H3′,5′ are observed (see Figure 3, left panel). The spectrum obtained at a 1:1 ratio of **1**/Zn(II) ion shows a new set of sharp signals with a strong upfield shift of H6,6″ signal from 8.67 to 7.76 ppm compared with that of the free ligand **1** and a downfield shift of H3′,5′ signal from 8.72 to 8.94 ppm, confirming formation of coordination complex of Zn(II) ions with bis(terpyridyl) ligands.[9,10c] The observed sharp $^1$H NMR signals are indicative for the formation of a well-defined highly symmetric metallocycle,[10a,c] and

exclude presence of coordination polymers as in the latter case broadened signals are to expect.[9]

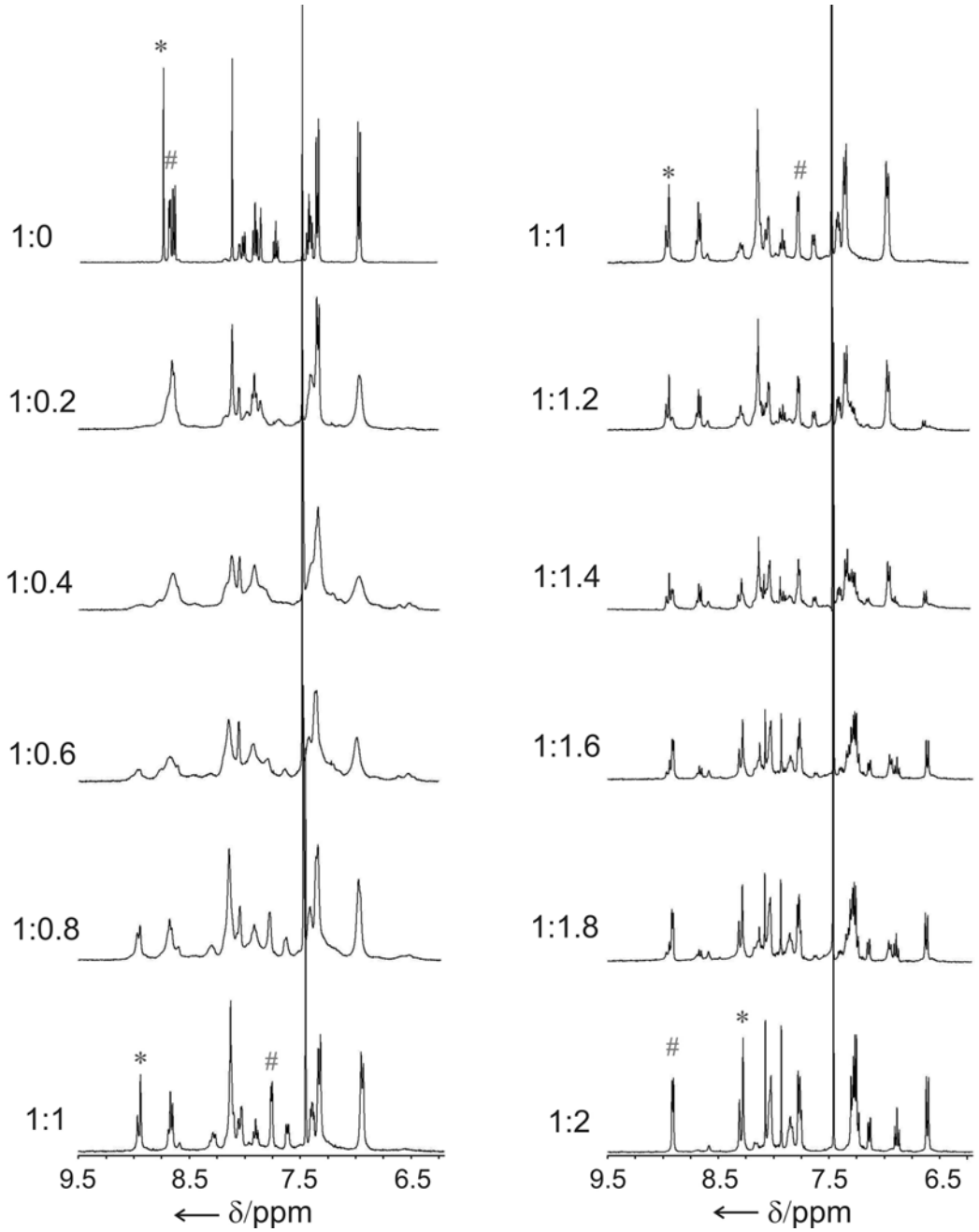


***Figure 3.*** $^{1}$H NMR titration spectra of ditopic ligand **1** with zinc(II) triflate in $CDCl_3/CD_3CN$ (60:40) at room temperature. In the left panel the spectral changes upon addition of up to 1 equivalent of $Zn(OTf)_2$ and formation of metallocycle **2** at 1:1 ratio is shown, whilst right panel depicts the changes resulted from dissociation of **2** upon addition of excess amounts of $Zn(OTf)_2$. Ratio of **1**:Zn(II) ion is indicated on the respective spectrum. Signal for H3',5' protons are marked with * and that of H6,6'' protons with #.

Indeed, $^{1}$H-$^{1}$H COSY NMR[13] analysis provides structural evidence for the trimeric metallocycle **2** self-assembled from ligand **1** and $Zn(OTf)_2$ in an equimolar ratio (see Figure 4).

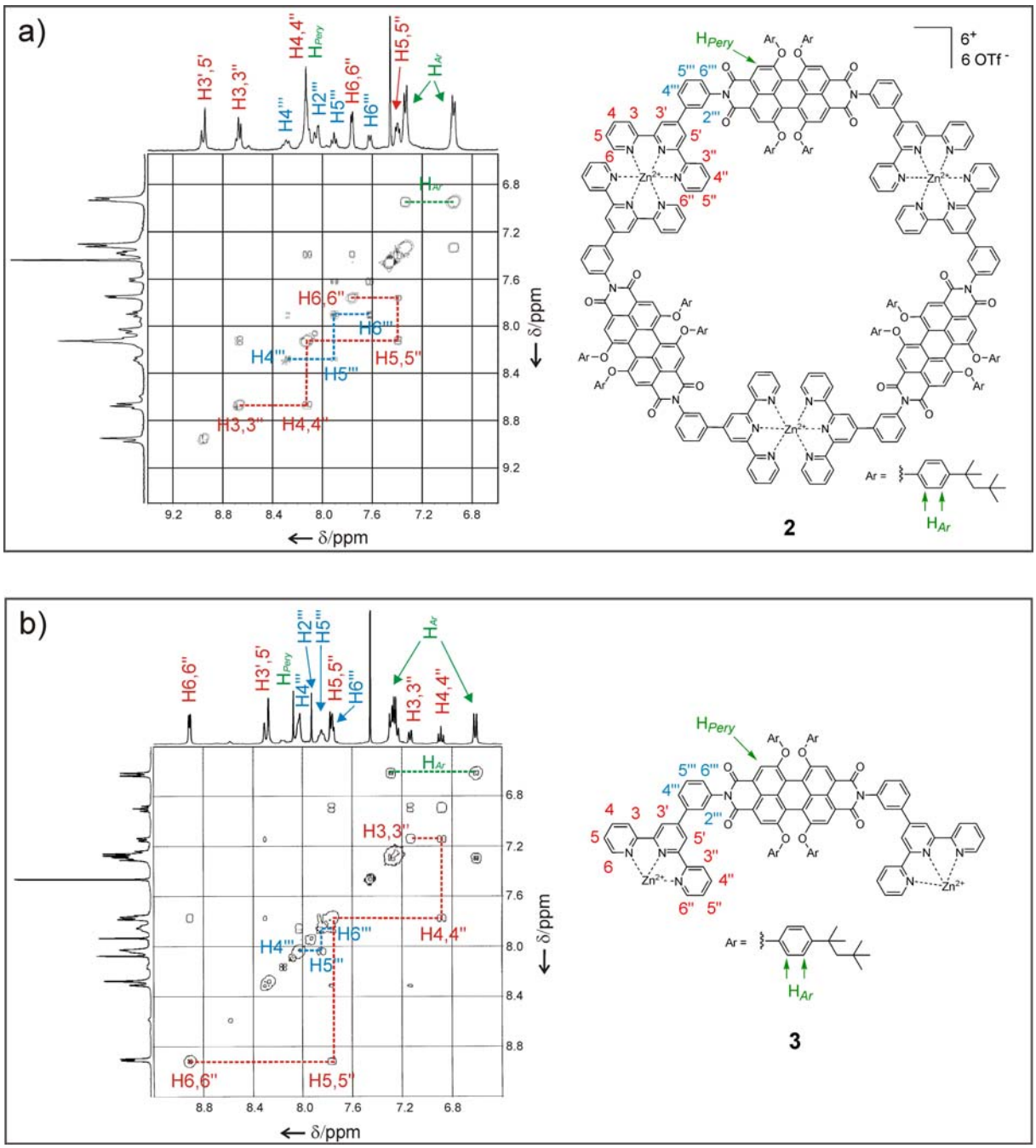


***Figure 4.*** $^{1}$H-$^{1}$H COSY NMR spectra of metallomacrocycle **2** (a) and complex **3** (b) in $CDCl_3/CD_3CN$ (60:40).

In $^{1}$H NMR titration experiments, once the 1:1 stoichiometry is exceeded by further addition of $Zn(OTf)_2$ the intensity of proton signals of metallocycle **2** is decreased and

a new set of signal arises (see Figure 3, right panel), revealing the reversibility of Zn(II)-ion-mediated self-assembly of ligand **1**. At a 1:2 ratio of **1**:Zn(II) ion a spectrum with sharp signals is obtained which is assignable to monomeric complex **3** (see also COSY spectrum in Figure 4) with the additional coordination sites of Zn(II) ions saturated either by acetonitrile molecules or triflate counterions (Scheme 1).

**$^1$H DOSY NMR Investigations.** Additional evidence for the formation of metallomacrocycle **2** by reversible Zn(II)-bis(tpy) coordination is obtained by $^1$H NMR diffusion-ordered spectroscopy (DOSY) studies. As the diffusion coefficient ($D$ [$m^2s^{-1}$]) of a spherical molecule in solution is inversely proportional to the molecular dimension, [5f,9b,14] the formation of higher molecular weight macrocycle from monomeric ligands can be substantiated by $^1$H DOSY NMR.[15] In Figure 5 the DOSY spectra of bis(tpy) PBI ligand **1** and the macrocycle formed at a 1:1 ratio of **1**:Zn(II) ion in chloroform[D]/acetonitrile[D]$_3$ (60:40) mixture are shown. Ligand **1** with a molecular weight of 1822.3 g/mol shows a diffusion coefficient value of $D = 3.8 \times 10^{-10}$ $m^2s^{-1}$ ($\log[D/m^2s^{-1}] = -9.4$), while the diffusion coefficient of the higher molecular weight (compared with ligand **1**) metallomacrocycle **2** significantly decreased to $D = 1.9 \times 10^{-10}$ $m^2s^{-1}$ ($\log[D/m^2s^{-1}] = -9.7$).

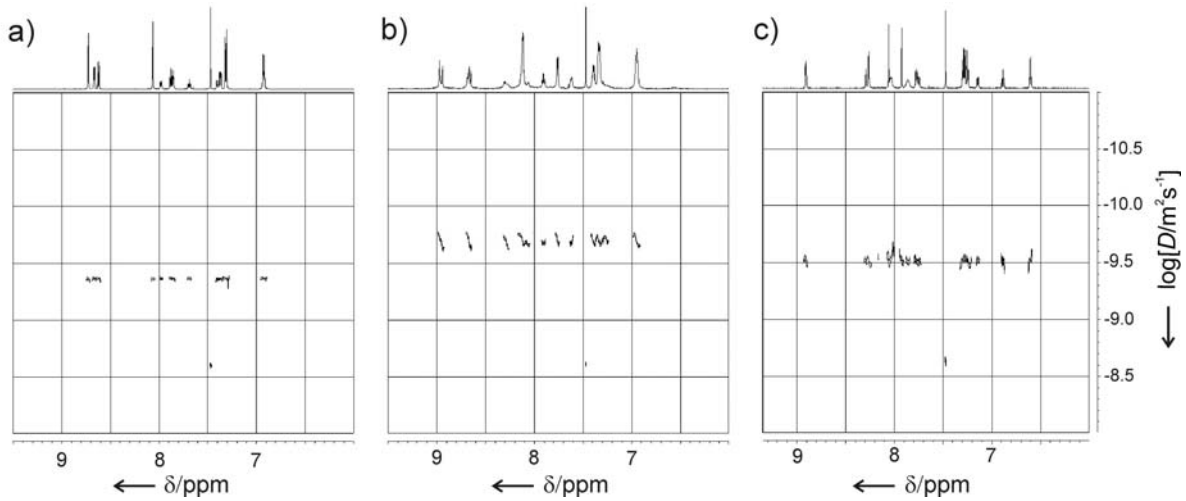


***Figure 5.*** Aromatic region of the $^1$H DOSY NMR spectra for bis(tpy) PBI ligand **1** (a), trimeric metallocycle **2** (b), and complex **3** in chloroform[D]/acetonitrile[$D_3$] (60:40) at 25 °C, [**1**] = $2.14\times10^{-3}$ M). The diffusion coefficients $D$ [$m^2s^{-1}$] are plotted in a logarithmic scale ($\log[D/m^{-1}s^{-1}]$) against the chemical shift $\delta$. The signal of residual chloroform can be seen at 7.49 ppm ($\log[D/m^2s^{-1}] = -8.65$).

Note, the formation of a coordination polymer can be excluded because in this case a much smaller diffusion coefficient is to expect.[9b] Upon addition of an excess amount of zinc(II) ion, diffusion coefficient is again increased and at a 1:2 ratio of **1**:Zn(II) ion a value of $D = 3.3 \times 10^{-10}$ $m^2s^{-1}$ ($\log[D/m^2s^{-1}] = -9.5$) is observed (see Figure 5c) which is very close to the *D* value of free ligand **1**, implying creation of a monomeric Zn(II)-complex **3** (Scheme 1) as the latter has slightly higher molecular weight. The results of a detailed investigation of diffusions coefficients at different ratios of **1**:Zn(II) ion are summarized in Table 1.

***Table 1.*** Diffusion coefficients of species formed at different ratios of **1**:Zn(II) ion.

| **1**:Zn(II) ion | $D$ [$m^2s^{-1}$] | $\log[D/m^2s^{-1}]$ |
|---|---|---|
| 1:0 | $3.8\times10^{-10}$ | -9.41 |
| 1:0.4 | $2.3\times10^{-10}$ | -9.63 |
| 1:0.8 | $2.2\times10^{-10}$ | -9.66 |
| 1:1 | $1.9\times10^{-10}$ | -9.71 |
| 1:2 | $3.3\times10^{-10}$ | -9.47 |

Once the formation of trimeric metallocycle **2** is confirmed by $^1$H NMR titration and DOSY experiments, this cyclic array was prepared on a semi-preparative scale using stoichiometric amounts of ligand **1** and zinc(II) triflate in 90% yield (for details see the Experimental Section). Macrocycle **2** is highly soluble in dimethylformamide (DMF) and chloroform/acetonitrile mixture as well, and the solutions remain clear for weeks without forming any precipitation, indicating high stability of this array in dilute solutions.

**MALDI-TOF Mass Spectrometry.** Further structural characterization of this macrocycle was achieved by MALDI-TOF MS,[16] providing expected mass peak of trimer **2** and additional peaks of multi-charged fragments (see Figure 6). The most prominent peak in higher range of mass spectrum is attributed to $(\mathbf{1})_3Zn_3(OTf)_5$ where the loss of one triflate anion provided a single charged species. The other most prevalent peaks in the lower *m*/*z* region of the MS spectrum, namely *m*/*z* = 4584.2 $[(\mathbf{1})_2Zn_3(OTf)_5]$, 4221.4 $[(\mathbf{1})_2Zn_2(OTf)_3]$, 3858.6 $[(\mathbf{1})_2Zn(OTf)]$, and 1822.2 [**1**], agree well with the smaller species, which most likely originate from the fragmentation of the macrocycle during measurement.

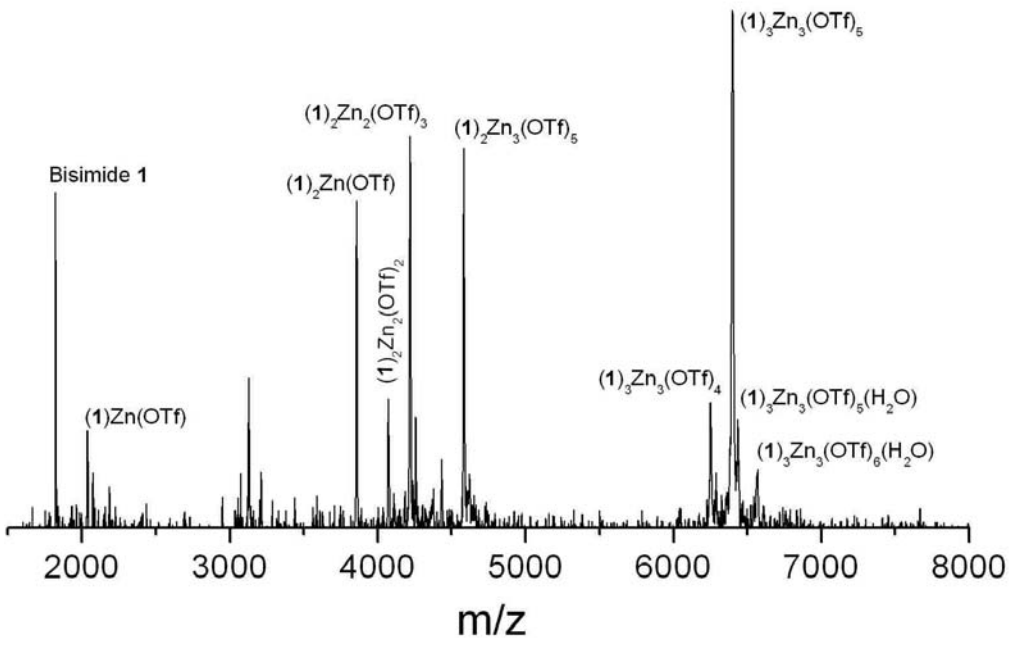


***Figure 6.*** MALDI-TOF mass spectrum (DCTB matrix) of trimeric Zn(II)-metallocycle **2** showing the mass peak (*m/z* = 6576.3) for (**1**)$_3$Zn$_3$(OTf)$_6$(H$_2$O) (**2**•H$_2$O) and fragments of **2** with triflate counterions. The source of H$_2$O molecule is apparently zinc(II) triflate monohydrate. DCTB = *trans*-2-(3-4-*tert*-butylphenyl)-2-methyl-2-propenylidene)malononitrile.

**Optical Properties.** The optical properties of ditopic PBI ligand **1** and cyclic trimer **2** in DMF have been studied by UV/Vis absorption and fluorescence spectroscopy (see Figure 7). Ligand **1** exhibits intense absorption bands with maxima at 586, 547, and 452 nm that are very characteristic for tetraaryloxy-substituted perylene bisimide chromophores.[6] The coordination of Zn(II) ion to tpy has little effect on the absorption properties of PBI unit as trimeric metallocycle **2** shows a similar absorption profile compared to that of ligand **1** with slightly shifted maxima at 580, 540, and 445 nm, respectively. For metallocycle **2**, an extinction coefficient of 143.000 $M^{-1}cm^{-1}$ at $\lambda_{max}$ = 580 nm is observed, which is nearly three-times higher than that for ligand **1** (50.700 $M^{-1}cm^{-1}$ at 586 nm). A strong increase of the absorption for tpy units is observed in the UV region (320-360 nm) upon complexation with Zn(II) ion which is in accord with literature report.[9b] As shown in Figure 7, for metallocycle **2** an intense emission at $\lambda_{max}$ = 608 nm, which is characteristic for tetraaryl-substituted PBI chromophores,[6,12] is observed upon excitation at 550 nm. From functional point of view it is quite interesting that metallocycle **2** exhibits a high fluorescence quantum yield of 75% (in DMF) which is very close to that of free ligand **1** (81%).

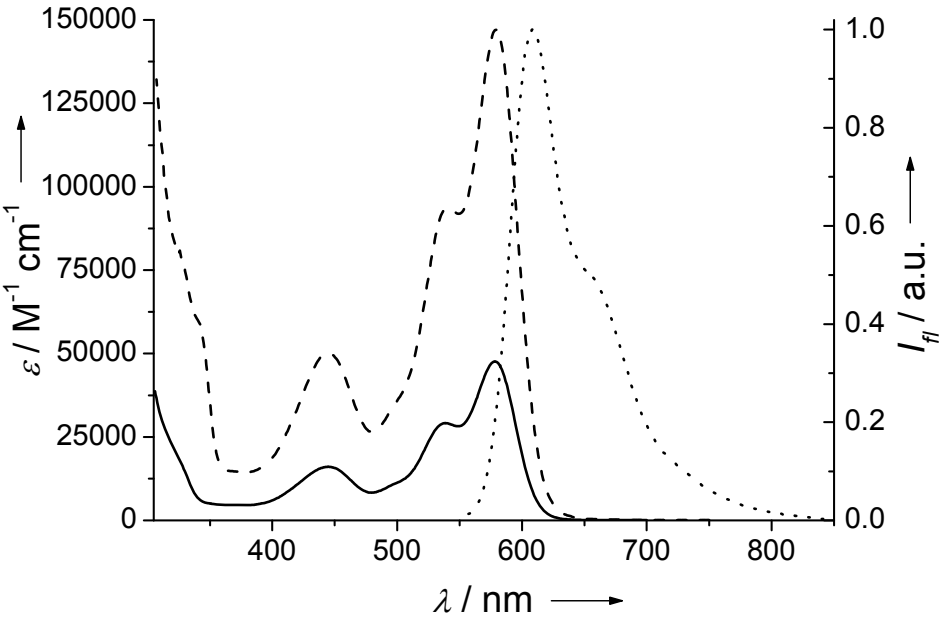


***Figure 7.*** UV/Vis absorption spectra of PBI ligand **1** (solid line) and cyclic trimer **2** (dashed line), and fluorescence emission spectrum of **2** ($\lambda_{ex}$ = 550 nm, dotted line) in DMF at 20 °C.

**Atomic Force Microscopy Investigations.** The self-assembly of cyclic array **2** on highly ordered pyrolytic graphite (HOPG) is investigated by atomic force microscopy (AFM) at ambient conditions. In contrast to metallocycle **2**, for the free ligand **1** only adlayers without any ordered structure are observed (see Figure 8).

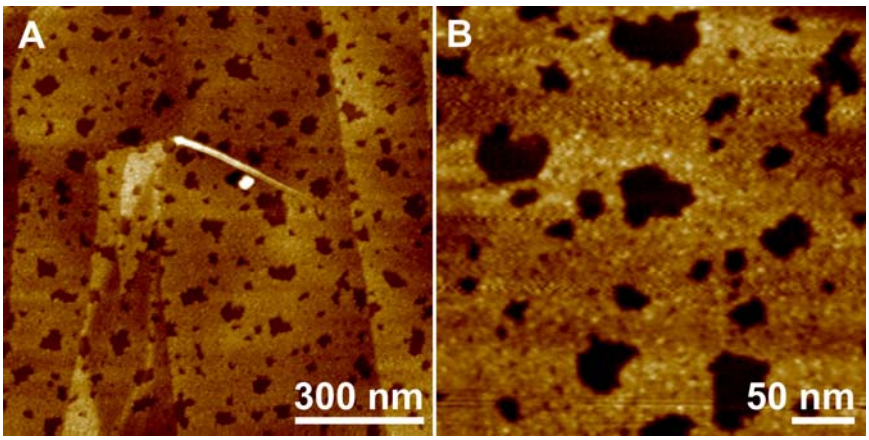


***Figure 8.*** Tapping mode height AFM images of films spin-coated from DMF solution of ligand **1** ($c$ = 2.4×10$^{-5}$ M) onto HOPG. Z scale is 2 nm (A) and 1 nm (B). No ordered structures of **1** can be seen in these images.

AFM images of samples prepared by spin-coating DMF solution of metallocycle **2** reveal highly ordered monolayers[17] with two different types of structural

arrangements, namely, linearly ordered and honeycomb structured (Figures 9 and 10). The average height of the ordered layers, both linear and honeycomb structures (the latter marked with yellow frames in Figure 9A), is estimated as 0.53±0.05 nm by cross-section analysis. For the linear structures, two orientations with an angle of 60º are observed (white arrows in Figure 9A), indicating an alignment of metallocycles **2** along the graphite axes. In height image the linearly ordered structures are clearly visible for which a periodicity of 4.7±0.2 nm is assessed by cross-section analysis which is in agreement with the frequency of 4.7 nm determined by 2D fast Fourier transformation (FFT) analysis. From high resolution phase image (Figure 9B), a diameter of 3.9±0.2 nm is estimated for metallocycle **2** that is in excellent agreement with the value (4.0 nm) obtained by molecular modeling of cyclic array **2** (see Figure 2).

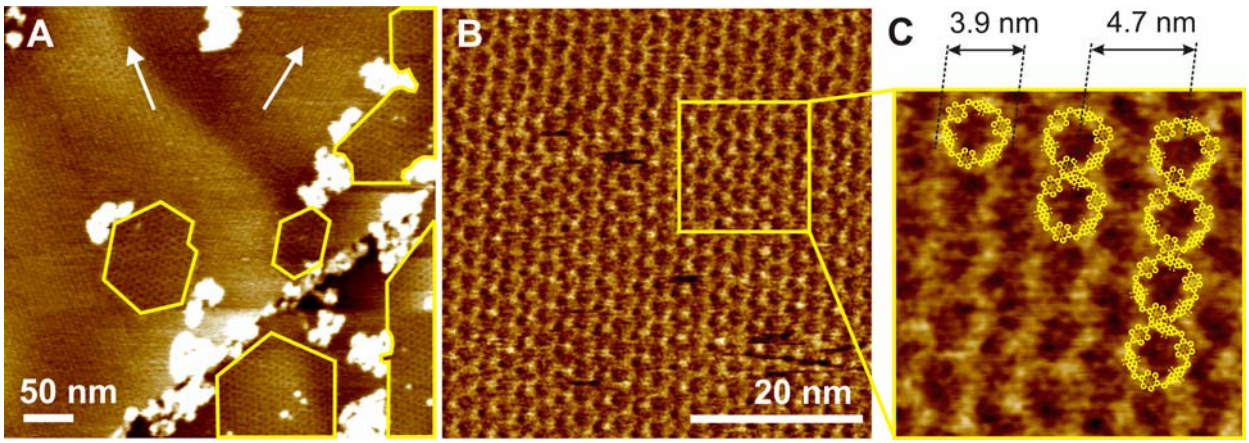


***Figure 9.*** Tapping mode AFM images of films spin-coated from DMF solution of **2** ($c$ = 2.4×10$^{-5}$ M) onto HOPG. (A) Height image; (B) high resolution phase image of a region in image A with linear structure; (C) magnification of a section in image B and proposed structural model for the linear arrangement of macrocycles **2** (for simplicity, one dimensional structures of **2** are shown here; for three dimensional structure, see Figure 2). In image A, the direction of linear structures is indicated by white arrows and the areas with honeycomb arrangement are marked with yellow frames. Not that, some unordered aggregates can be seen (bright areas in image A) that lie on the top of the ordered layers with a height of 0.55±0.05 nm with respect to the former ones.

More interestingly, the high resolution height images (Figures 10A, B) clearly reveal a second pattern, *i.e.*, honeycomb-structured 2D assemblies of metallomacrocycles **2** on HOPG. Well-ordered 2D assembled structures cover the surface up to several square micrometers. A two-dimensional FFT image (Figure 10C) shows the characteristic reflections of hexagonally packed domains of macrocycles **2**. The FFT

analysis reveals an average frequency of 6.7 nm in all directions that is indicated by the distance *d* between the bright spots in Figure 10D.

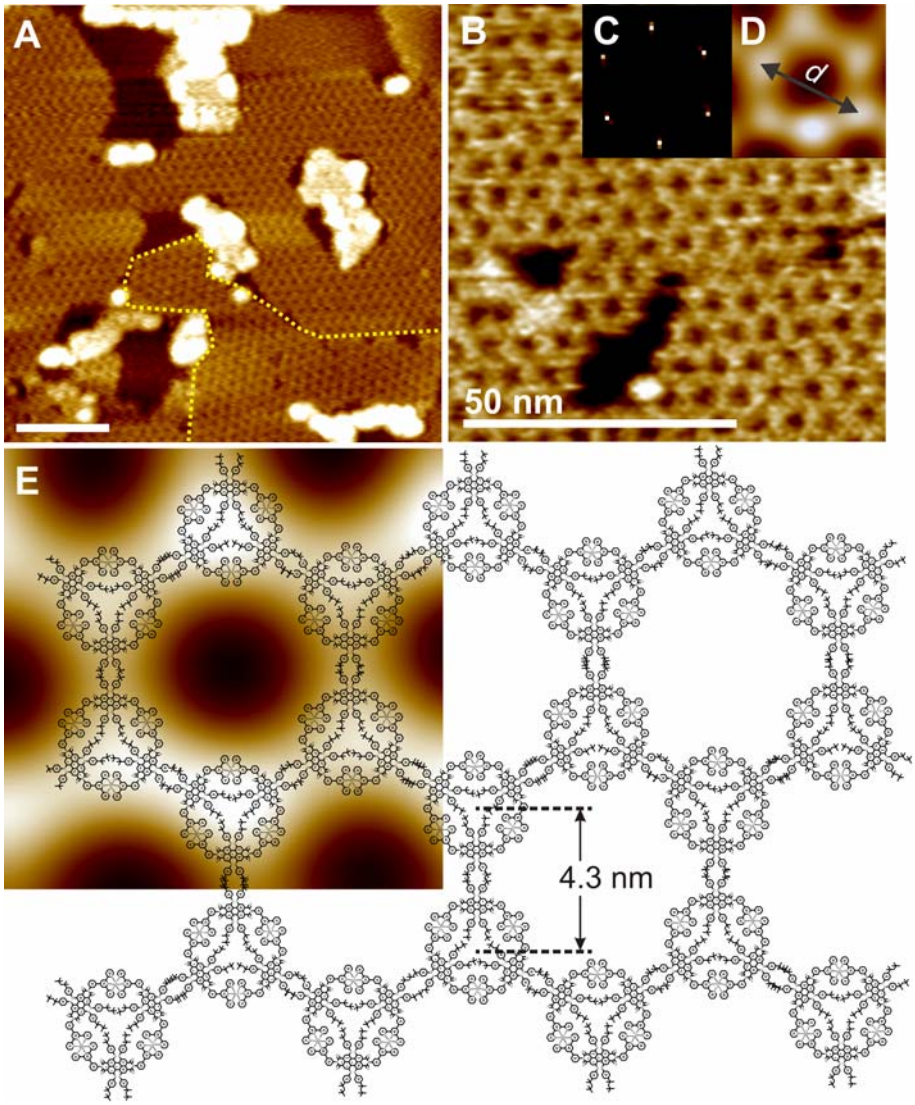


**Figure 10.** Tapping mode AFM images of films spin-coated from DMF solution of **2** ($c = 2.4\times10^{-5}$ M) onto HOPG: (A), (B) height images; (C) FFT analysis of image B; (D) a zoomed and filtered unit of the hexagonal domains in image B; (E) proposed model for the molecular arrangement of the cyclic trimers **2** (for simplicity, one dimensional structures of **2** are shown) in honeycomb structures. Scale in all images is 50 nm. In image A, the frontier of neighbor areas with honeycomb arrangement is marked with yellow dotted line.

Under the premise that each bright spot in Figure 10D equals one macrocycle, the distance between centers of two neighboring cycles is measured to 4.3±0.2 nm. On the basis of these results, a molecular model can be proposed (Figure 10E) for the honeycomb-structured nanonetwork of macrocycle **2** possessing regular holes.

According to the proposed model, the hexagonal arrangement is created by the interaction of aliphatic side chains of the adjacent macrocycles and the holes are formed by the contact of each cyclic molecule with three adjacent ones through side chains.

## Conclusion

To conclude, the newly designed angular ditopic PBI ligands **1** self-assemble in solution by Zn(II)-ion coordination into highly fluorescent hexagonal trimeric metallomacrocycles **2**. On the next level of hierarchy, these macrocycles self-organize on HOPG surface into 2D nanopatterns with structural organization reminiscent of cyclic dye arrays in the purple bacterial photosynthetic membrane. These artificial 2D patterns of cyclic dye arrays should enable energy exchange between the closely packed subunits as observed in the similarly organized natural light-harvesting complexes in purple bacteria.[1,2]

## Experimental Section

**General**: Solvents were purified and dried according to standard procedures.[18] Chromatography is performed with basic alumina, which was deactivated with 4 weight % of water to activity II. Perylene bisanhydride **5** applied in this work is accessible by literature procedures.[12] Zinc trifluoromethane sulfonate salt is commercially available. MALDI-TOF-MS were measured using a Bruker Autoflex II spectrometer in reflector mode. $^1$H NMR spectra were recorded at room temperature on a Bruker Avance 400 spectrometer (400 MHz) and chemical shifts $\delta$ (ppm) are calibrated against tetramethylsilane (TMS) as internal reference. For measurement of UV/Vis spectra PerkinElmer Lambda 950 spectrometer is used. The steady-state fluorescence spectra were measured on a a PTI QM-4/2003 spectrometer and fluorescence quantum yields were determined by the optically dilute method[19] (A < 0.05) using *N,N'*-di(2,6-diisopropylphenyl)-1,6,7,12-tetraphenoxyperylene-3,4:9,10-tetracarboxylic acid bisimide ($\Phi_{fl}$ = 0.96 in chloroform)[20] as standard. The solvents for spectroscopic studies were of spectroscopic grade and used as received.

***N,N'*-Bis-(3-(2,2':6',2''-terpyridin-4'-yl)phenyl)-1,6,7,12-(*p-t*-octylphenoxy)-perylene-3,4:9,10-tetracarboxylic acid bisimide (1)**: 1,6,7,12-Tetra(*p-t*-octylphenoxy)perylene-3,4:6,10-tetracarboxylic acid bisanhydride (**5**)[12] (0.20 mg, 0.16 mmol) was reacted with 4'-*m*-aminophenyl-2,2':6',2''-terpyridine (**4**)[11] (0.16 mg, 0.49 mmol) in a mixture of pyridine (4.2 mL) and imidazole (2.4 g) for 5 d at 120 °C under argon atmosphere. After being cooled to room temperature, the mixture was poured into aqueous HCl (150 mL, 1 M), and the resultant precipitate was separated by filtration and subsequently washed with 50 mL water. Purification was achieved by column chromatography on aluminum oxide (basic, activity II) with $CH_2Cl_2$/*n*-hexane (4:1) to yield 90.0 mg (35%) of ligand **1** as a dark-red microcrystalline powder.

Mp > 350 °C; $^1$H NMR (400 MHz, $CDCl_3$, 25 °C, TMS): $\delta$ = 8.73 (s, 4H, H3',5'), 8.69 (d, *J* = 5.6 Hz, 4H, H6,6''), 8.64 (d, *J* = 7.9 Hz, 4H, H3,3''), 8.22 (s, 4H, $H_{Pery}$), 8.08 (s, 2H, H2'''), 8.00 (d, *J* = 7.9 Hz, 2H, H4'''), 7.83-7.88 (m, 4H, H4,4''), 7.79-7.82 (m, 2H, H6'''), 7.63-7.68 (m, 2H, H5'''), 7.31-7.37 (m, 4H, H5,5''), 7.26 (d, *J* = 8.7 Hz, 8H, $H_{Ar}$),

6.90 (d, *J* = 8.7 Hz, 8H, $H_{Ar}$), 1.69 (s, 8H, $CH_2$), 1.32 (s, 24H, $CH_3$), 0.74 (s, 36H, $CH_3$); UV/Vis ($CH_2Cl_2$): $\lambda_{max}$ ($\varepsilon$) = 586 (50.700), 547 (31.400), 452 (17.700), 274 (10.2400), 248 nm (125.000 $M^{-1}\,cm^{-1}$); fluorescence (DMF, $\lambda_{ex}$ = 550 nm): $\lambda_{max}$ = 608 nm; quantum yield (DMF) $\Phi_{fl}$ = 0.81; MS (FAB): *m/z* = 1822.27 [$M^+$], 1823.29 [$M^+ + H$] (calcd: 1822.32); elemental analysis: calcd (%) for $C_{122}H_{116}N_8O_8 \cdot 2H_2O$ (1858.30): C, 78.85; H, 6.51; N, 6.03; found C, 78.44; H, 6.46; N, 5.89.

**Trimeric Zn(II)-Metallomacrocycle 2**: A stock solution of zinc(II) triflate monohydrate (6.1 µmol, 200 µL) was added to a solution of ligand **1** (11.2 mg, 6.1 µmol) in $CDCl_3/CD_3CN$ (60:40, 1 mL) and the solution was stirred for 10 min at room temperature. The exact 1:1 stoichiometry is confirmed by $^1$H NMR. The solution was then concentrated and the product was precipitated by addition of acetonitrile (3 mL) and isolated by centrifugation and subsequent filtration to yield 12.0 mg (90%) of pure metallomacrocycle **2**.

$^1$H NMR (400 MHz, $CDCl_3/CD_3CN$ (60:40), 25 °C, TMS): $\delta$ = 8.94 (s, 12H, H3',5'), 8.66 (d, *J* = 7.9 Hz, 12H, H3,3''), 8.25-8.32 (m, 6H, H4'''), 8.05-8.14 (m, 12H, H4,4''), 8.12 (s, 12H, $H_{Pery}$), 8.02 (s, 6H, H2'''), 7.87-7.93 (m, 6H, H5'''), 7.76 (d, *J* = 4.7 Hz, 12H, H6,6''), 7.61 (d, *J* = 7.6 Hz, 6H, H6'''), 7.36-7.41 (m, 12H, H5,5''), 7.32 (d, *J* = 8.6 Hz, 24H, $H_{Ar}$), 6.93 (d, *J* = 8.6 Hz, 24H, $H_{Ar}$), 1.71 (s, 24H, $CH_2$), 1.33 (s, 72H, $CH_3$), 0.74 (s, 108H, $CH_3$); UV/Vis (DMF): $\lambda_{max}$ ($\varepsilon$) = 580 (143.000), 540 (91.000), 445 nm (48.800 $M^{-1}\,cm^{-1}$); fluorescence (DMF, $\lambda_{ex}$ = 550 nm): $\lambda_{max}$ = 608 nm; quantum yield $\Phi_{fl}$ = 0.75; MS (MALDI-TOF, chloroform/acetonitrile (60:40), DCTB matrix): *m/z* = 6576.3 [(**1**)$_3Zn_3(OTf)_6(H_2O)$] (**2**•$H_2O$), 6409.3 [(**1**)$_3Zn_3(OTf)_5$], 6260.1 [(**1**)$_3Zn_3(OTf)_4$], 4584.2 [(**1**)$_2Zn_3(OTf)_5$], 4221.4 [(**1**)$_2Zn_2(OTf)_3$], 4072.6 [(**1**)$_2Zn_2(OTf)_2$], 3858.6 [(**1**)$_2$Zn(OTf)] and 2036.3 [(**1**)Zn(OTf)].

**$^1$H NMR Titration Experiment**: $^1$H NMR titration was carried out by adding 0.2 to 2.0 equivalents of $Zn(OTf)_2$ (in portions of 0.2 equiv.) to a solution of **1** (2 mM) in a mixture of chloroform[D]/acetonitrile[$D_3$] (60:40). $^1$H NMR spectra were recorded on a Bruker Avance 400 spectrometer after addition of each portion of 0.2 $Zn(OTf)_2$ using tetramethylsilane (TMS) as an internal standard.

**DOSY NMR Spectroscopy**: $^{1}$H DOSY experiments were carried out at 298 K on a Bruker DMX 600 spectrometer equipped with a BGPA 10 gradient generator, a BGU II control unit and a conventional 5 mm broadband ($^{15}$N-$^{31}$P)/$^{1}$H probe with automatic tune/match accessory and z axis gradient coil capable of producing pulsed magnetic field gradients in the z direction of 52 G cm$^{-1}$. Data were acquired and processed using the Bruker software XWIN-NMR 3.5, patch level 6. The diffusion time Δ was kept constant in each DOSY experiment, whereas the sinusoidal diffusion gradients were incremented from 2% to 95% of maximum gradient strength in 32 linear steps. Signal averaging ranged from 16 to 288 scans per increment as required for adequate signal-to-noise ratio. The $^{1}$H NMR spectra were recorded in $CDCl_3$/$CD_3CN$ (60:40) solution in 5 mm NMR tubes and referenced to interal TMS. The DOSY experiments with short bipolar gradient pulses of 4.4 ms length were performed for each sample to measure the diffusion coefficient of TMS to which the results were finally normalized to eliminate minor temperature and viscosity differences between the different systems.

**Atomic Force Microscopy (AFM)**: AFM measurements were carried out under ambient conditions by using a Veeco MultiMode$^{TM}$ Nanoscope IV system (Veeco Metrology Inc.) operating in tapping mode in air. Silicon cantilevers (Olympus Corporation) with a resonance frequency of ~ 300 kHz were used. The 512 × 512 pixel images were collected at a rate of 2 scan lines per second. Solution of ligand **1** and metallomacrocycle **2** in DMF ($c$ = 2.4×10$^{-5}$ mol/L) was spin-coated on a highly ordered pyrolytic graphite (HOPG, Nano Technology Instruments – Europe) under 7000 rpm.

## References


[1] For publications on natural cyclic light-harvesting dye arrays, see: a) G. McDermott, S. M. Prince, A. A. Freer, A. M: Hawthornthwaite-Lawless, M. Z. Papiz, R. J. Cogdell, N. W. Isaacs, *Nature* **1995**, *374*, 517-521; b) T. Pullerits, V. Sundström, *Acc. Chem. Res.* **1996**, *29*, 381-389; c) X. Hu, T. Ritz, A. Damjanović, F. Autenrieth, K. Schulten, *Q. Rev. Biophys.* **2002**, *35*, 1-62.

[2] a) S. Bahatyrova, R. N. Frese, C. A. Siebert, J. D. Olsen, K. O. van der Werf, R. van Grondelle, R. A. Niederman, P. A. Bullough, C. Otto, C. N. Hunter, *Nature* **2004**, *430*, 1058-1062; b) S. Scheuring, J. N. Sturgis, V. Prima, A. Bernadac, D. Lévy, J.-L. Rigaud, *Proc. Natl. Acad. Sci. USA* **2004**, *101*, 11293-11297.

[3] For general overviews on multichromophore dye assemblies, see: a) M.-S. Choi, T. Yamazaki, I. Yamazaki, T. Aida, *Angew. Chem.* **2003**, *116*, 152-160; *Angew. Chem. Int. Ed.* **2003**, *43*, 150-158; b) *Supramolecular Dye Chemistry*, Topics in Current Chemistry, *Vol. 258* (Ed.: F. Würthner), Springer-Verlag, Berlin, **2005**; c) F. J. M. Hoeben, P. Jonkheijm, E. W. Meijer, A. P. H. J. Schenning, *Chem. Rev.* **2005**, *105*, 1491-1546.

[4] For reviews on cyclic dye arrays, see: a) A. Satake, Y. Kobuke, *Tetrahedron* **2005**, *61*, 13-41; b) C.-C. You, R. Dobrawa, C. R. Saha-Möller, F. Würthner, *Top. Curr. Chem.* **2005**, *258*, 39-82; c) Y. Nakamura, N. Aratani, A. Osuka, *Chem. Soc. Rev.* **2007**, *36*, 831-845; recent work: d) F. Hajjaj, Z. S. Yoon, M.-C. Yoon, J. Park, A. Satake, D. Kim, Y. Kobuke, *J. Am. Chem. Soc.* **2006**, *128*, 4612-4623; e) A. Prodi, C. Chiorboli, F. Scandola, E. Iengo, E. Alessio, *ChemPhysChem* **2006**, *7*, 1514-1519; f) M. Hoffmann, C. J. Wilson, B. Odell, H. L. Anderson, *Angew. Chem.* **2007**, *119*, 3183-3186; *Angew. Chem. Int. Ed.* **2007**, *46*, 3122-3125.

[5] a) F. Würthner, A. Sautter, *Chem. Commun*. **2000**, *6*, 445-446; b) F. Würthner, A. Sautter, D. Schmid, P. J. A. Weber, *Chem. Eur. J.* **2001**, *7*, 894-902; c) C.-C. You, F. Würthner, *J. Am. Chem. Soc.* **2003**, *125*, 9716-9725; d) F. Würthner, A. Sautter, *Org. Biomol. Chem.* **2003**, *1*, 240-243; e) A. Sautter, B. K. Kaletas, D. G. Schmid, R. Dobrawa, M. Zimine, G. Jung, I. H. M. van Stokkum, L. De Cola, R. M. Williams, F. Würthner, *J. Am. Chem. Soc.* **2005**,

*127*, 6719-6729; f) C.-C. You, C. Hippius, M. Grüne, F. Würthner, *Chem. Eur. J.* **2006**, *12*, 7510-7519.

[6] For reviews on perylene bisimides, see: a) F. Würthner, *Chem. Commun.* **2004**, *14*, 1564-1579; b) F. Würthner, *Pure Appl. Chem.* **2006**, *78*, 2341-2350.

[7] For reviews on metal-ion mediated self-assembly into square scaffolds, see: a) M. Fujita, *Chem. Soc. Rev.* **1998**, *27*, 417-425; b) S. Leininger, B. Olenyuk, P. J. Stang, *Chem. Rev.* **2000**, *100*, 853-908; c) B. J. Holliday, C. A. Mirkin, *Angew. Chem.* **2001**, *113*, 2076-2097; *Angew. Chem. Int. Ed*. **2001**, *40*, 2022-2043; d) F. Würthner, C.-C. You, C. R. Saha-Möller, *Chem. Soc. Rev.* **2004**, *33*, 133-146; e) M. Schmittel, V. Kalsani, *Top. Curr. Chem.* **2005**, *245*, 1-53; f) C. H. M. Arrijs, G. P. M. van Klink, G. van Koten, *Dalton Trans.* **2006**, 308-327.

[8] For the application of 2,2′:6′,2″-terpyridine ligands in metallosupramolecular chemistry, see: a) P. R. Andres, U. S. Schubert, *Adv. Mater.* **2004**, *16*, 1043-1068; b) Y. Bodenthin, U. Pietsch, H. Möhwald, D. G. Kurth, *J. Am. Chem. Soc.* **2005**, *127*, 3110-3114; c) D. G. Kurth, M. Higuchi, *Soft Matter* **2006**, *2*, 915-927; d) *Modern Terpyridine Chemistry* (Eds.: U. S. Schubert, H. Hofmeier, G. R. Newkome), Wiley-VCH, Weinheim, **2006**; e) E. C. Constable, *Chem. Soc. Rev.* **2007**, *36*, 246-253.

[9] a) R. Dobrawa, F. Würthner, *Chem. Commun.* **2002**, *17*, 1878-1879: b) R. Dobrawa, M. Lysetska, P. Ballester, M. Grüne, F. Würthner, *Macromolecules* **2005**, *38*, 1315-1325.

[10] Newkome and co-workers have reported on metal-ion-mediated self-assembly of benzene-based bis(terpyridyl) ligands into hexameric metallomacrocycles: a) G. R. Newkome, T. J. Cho, C. N. Moorefield, G. R. Baker, R. Cush, P. S. Russo, *Angew. Chem.* **1999**, *111*, 3899-3903; *Angew. Chem. Int. Ed*. **1999**, *38*, 3717-3721; b) G. R. Newkome, P. Wang, C. N. Moorefield, T. J. Cho, P. P. Mohapatra, S. Li, S.-H. Hwang, O. Lukoyanova, L. Echegoyen, J. A. Palagallo, V. Iancu, S.-W. Hla, *Science* **2006**, *312*, 1782-1785; c) S.-H. Hwang, C. N. Moorefield, P. Wang, J.-Y. Kim, S.-W. Lee, G. R. Newkome, *Inorg. Chim. Acta* **2007**, *360*, 1780-1784. Detailed literature survey revealed that self-assembly of angular bis(terpyridyl) ligands containing functional dyes such as perylene bisimides to metallocyclic arrays has not been reported before.

[11] a) F. Krönke, *Synthesis* **1976**, 1-24; b) K. Hanabusa, A. Nakamura, T. Koyama, H. Shirai, *Polym. Int.* **1994**, *35*, 231-238.

[12] a) D. Dotcheva, M. Klapper, K. Müllen, *Macromol. Chem. Phys.* **1994**, *195*, 1905-1911; b) F. Würthner, C. Thalacker, A. Sautter, W. Schärtl, W. Ibach, O. Hollricher, *Chem. Eur. J.* **2000**, *6*, 3871-3886.

[13] T. W. Claridge, *High-Resolution NMR Techniques in Organic Chemistry*, T. O. C. Series, Pergamon-Press, Amsterdam, **1999**.

[14] For reviews on DOSY NMR, see: a) C. S. Johnson Jr., *Prog. Nucl. Magn. Reson. Spectrosc.* **1999**, *3*, 203-256; b) Y. Cohen, L. Avram, L. Frish, *Angew. Chem.* **2005**, *117*, 524-560; *Angew. Chem. Int. Ed.* **2005**, *44*, 520-554.

[15] For the characterization of metallosupramolecular assemblies by DOSY NMR, see refs. 5f, 9b and: a) A. Hori, K. Kumazawa, T. Kumazawa, D. K: Chand, M. Fujita, S. Sakamoto, K. Yamaguchi, *Chem. Eur. J.* **2001**, *7*, 4142-4149; b) T. Megyes, H. Jude, T. Grosz, I. Bako, T. Radnai, G. Tarkanyi, G. Palinkas, P. J. Stang, *J. Am. Chem. Soc.* **2005**, *127*, 10731-10738.

[16] For characterization of metallosupramolecular structures by mass spectrometry, see ref. 5 and C. A. Schalley, *Int. J. Mass Spectrom.* **2000**, *194*, 11-39.

[17] Note that, highly ordered molecular layers of flat aromatic structures were observed on HOPG surface mostly by scanning tunneling microscopy (STM), see, *e.g.*, a) S.-S. Li, H.-J. Yan, L.-J. Wan, H.-B. Yang, B. H. Northop, P. J. Stang, *J. Am. Chem. Soc.* **2007**, *129*, 9268-9269; b) M. Blunt, X. Lin, M. d. C. Gimenez-Lopez, M. Schröder, N. R. Champnes, P. H. Beton, *Chem. Commun.* **2008**, *20*, 2304-2306; c) S. Lei, K. Tahara, F. C. De Schryver, M. Van der Auweraer, Y. Tobe, S. De Feyter, *Angew. Chem.* **2008**, *120*, 3006-3010; *Angew. Chem. Int. Ed*. **2008**, *47*, 2964-2968). However, for non-planar π-systems, particularly without long alkyl chains like the present trimeric metallocycle **2** such aggregation on surfaces is rarely reported.

[18] D. D. Perrin, W. L. F. Armarego, *Purification of Laboratory Chemicals*, 2nd ed., Kluwer Academic/Plenum, Oxford, **1998**.

[19] J. R. Lakowicz, *Principles of Fluorescence Spectroscopy*, 2nd ed., Kluwer Academic/Plenum, New York, **1999**.

[20] a) G. Seybold, G. Wagenblast, *Dyes Pigments* **1989**, *11*, 303-317; b) R. Gvishi, R. Reisfeld, Z. Burshtein, *Chem. Phys. Lett.* **1993**, *213*, 338-344.

# Chapter 5

## Summary

In the recent past, metallosupramolecular assemblies of organic dyes have been of increasing interest as model systems for natural light-harvesting and photosynthetic complexes. Well-designed metal-ion-directed self-assemblies of functional materials are also investigated for application in organic solar cells, sensors, and optoelectronic devices. Perylene bisimide (PBI) dyes are an important class of chromophores with excellent perspectives for such applications due to their favorable optical and electronic properties and high photostability.

The subject of this thesis was the synthesis and characterization of PBI-based fluorescent metallosupramolecular polymers and cyclic arrays. Terpyridine receptor functionalized PBIs of predesigned geometry have been used as building blocks to construct desired macromolecular structures through metal-ion-directed self-assembly. These metallosupramolecular architectures have been investigated by NMR, UV/Vis and fluorescence spectroscopy, mass spectrometry, and atomic force microscopy (AFM).

In the introductions first chapter a brief overview on the current development in metal-ion-directed self-assembly of dyes to macrocyclic and polymeric architectures is given.

Chapter 2 reports the synthesis of regioisomerically pure 1,7-pyrrolidinyl-substituted perylene dyes **2**-**8** (Chart 1) form 1,7-dibromoperylene bisimide **1**, which was prepared for the first time in regioisomerically pure form by bromination of perylene bisanhydride, followed by imidization with cyclohexylamine and successive recrystallization.

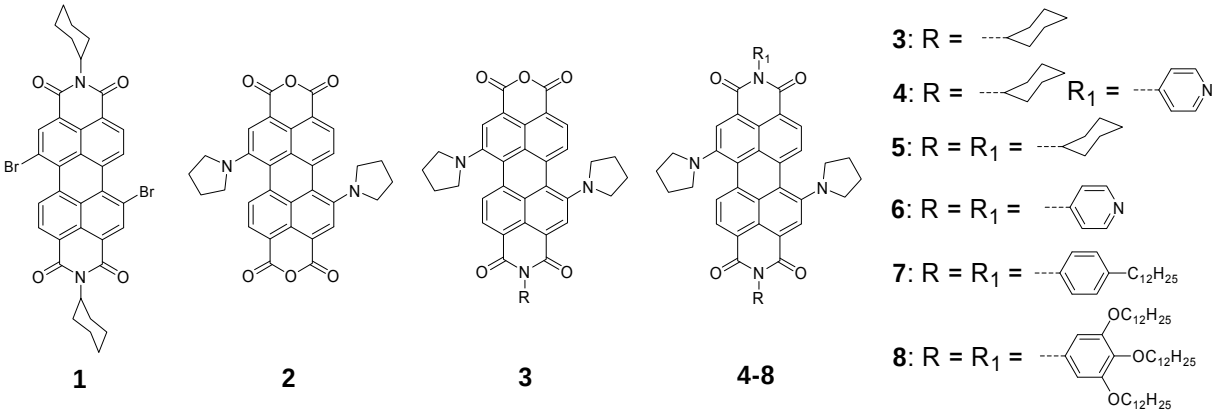


***Chart 1.*** 1,7-Dibromoperylene bisimide **1**, 1,7-Dipyrrolidinyl-substituted perylene bisanhydride **2**, unsymmetrical imide-anhydride **3** and bisimide **4**, and symmetrical bisimides **5**-**8**.

Since perylene monoimide monoanhydrides are important starting materials for the synthesis of unsymmetrical PBI, optimum reaction conditions were worked out for partial saponification of **5** to obtain pure dipyrrolidinyl-functionalized perylene monoimide monoanhydride **3** in 88% yield. The prolongation of reaction time for the saponification of **5** afforded bisanhydride **2**, which was successfully applied for the synthesis of regioisomerically pure 1,7-dipyrrolidinylperylene bisimides **6**-**8** and for the building blocks **9** (see Scheme 1) that have been used in metal-ion-mediated supramolecular polymerization (Chapter 3).

The synthesis of (2,2′:6′,2″-terpyridine)-functionalized PBI (tpy PBI) building blocks and their metal-ion-directed self-assembly is presented in Chapter 3. These studies reveal that the newly synthesized ditopic bis(tpy) PBI ligands, in which the tpy units are directly connected to PBI moieties at the imide positions, form coordination polymers upon addition of Zn(II) ion in a reversible manner. The ligands **9**-**12** (Scheme 1) have been synthesized by the reaction of the respective perylene bisanhydride or monoimide monoanhydride with 4'-amino-2,2':6',2''-terpyridine.

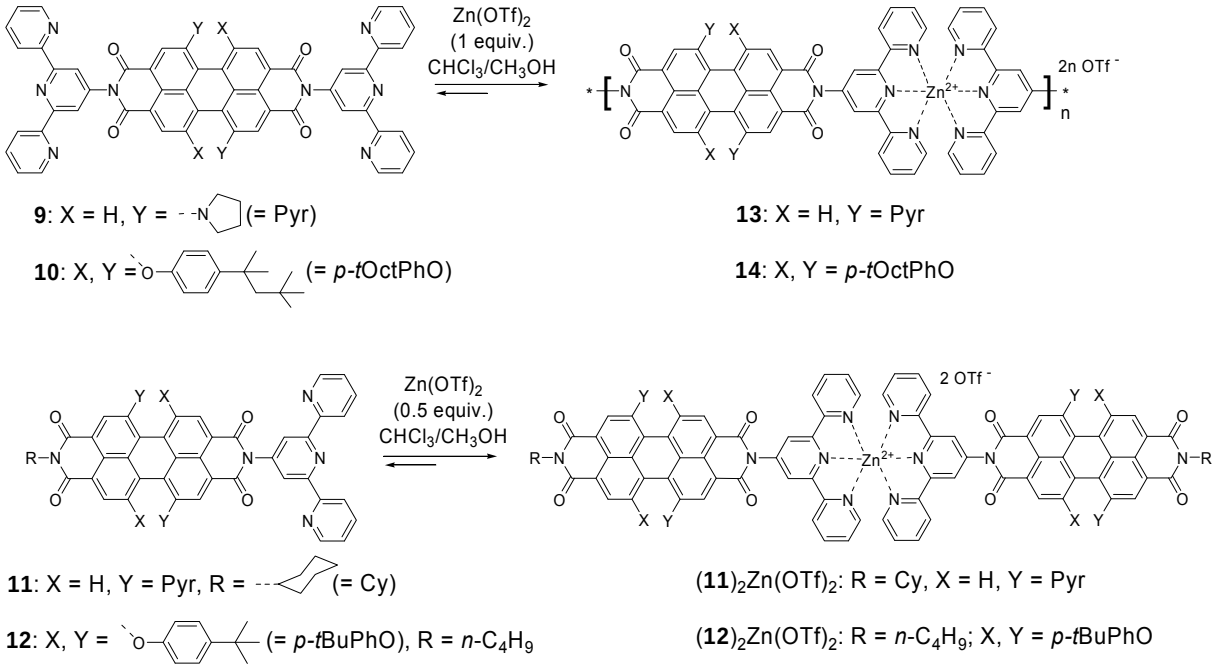


***Scheme 1.*** Novel terpyridine-based buildings blocks **9**-**12** and their metal-ion-directed self-assembly: metallosupramolecular polymers **13** and **14**, and dimeric complexes $(\mathbf{11})_2Zn(OTf)_2$ and $(\mathbf{12})_2Zn(OTf)_2$.

Prior to investigating the self-assembly properties of bis(tpy) PBI ligands **9** and **10** under metal ion mediation, the complexation of monotopic reference compounds **11** and **12** with Zn(II) ion was studied as these ligands should form dimeric complexes at a 2:1 ratio of ligand and Zn(II) ion, and the spectroscopic data, in particular $^1$H NMR data, of such dimers are helpful for the elucidation of supramolecular polymerization of ditopic ligands. Further evidence for the formation of dimer complexes was obtained by MALDI-TOF mass spectrometry. Reaction of the respective bis(tpy) PBI ligand with exactly one equivalent of Zn(II) ion led to the formation of the supramolecular coordination polymers, which have been studied in detail by $^1$H NMR, DOSY NMR, and UV/Vis spectroscopy. $^1$H DOSY NMR technique was used to examine the change of diffusion coefficient of the bis(tpy) PBI system upon stepwise addition of Zn(II) ion that leads first to the formation of coordination polymer and subsequently to their fragmentation, revealing a reversible self-assembly process. The complexation of ligand monomers with Zn(II) ion is shown to be useful to preserve the fluorescence properties of PBI chromophores in polymer. The polymer formation was visualized by atomic force microscopy (AFM) and their self-organization on surfaces was explored (Figure 1). Indeed, present design principle to connect tpy unit directly to PBI without any spacer provided rigid

supramolecular polymers with significantly longer average chain length than that observed previously for tpy PBI ligands containing additional phenylene spacers. The average chain length for the present coordination polymers is estimated as to 35 repeat units that correspond to a molecular weight of ~ 30.000 to 60.000 g/mol. AFM also revealed the formation of a homogeneous monolayer on negatively charged mica and neutral HOPG substrate as well. Multilayer film of coordination polymers with different optical properties were prepared in alternate fashion by layer-by-layer (LBL) deposition technique, the surface density Γ of PBI chromophores in these films could be estimated, and the root mean square (*RMS*) value of the surface roughness was determined by AFM measurement of the LBL multilayers.

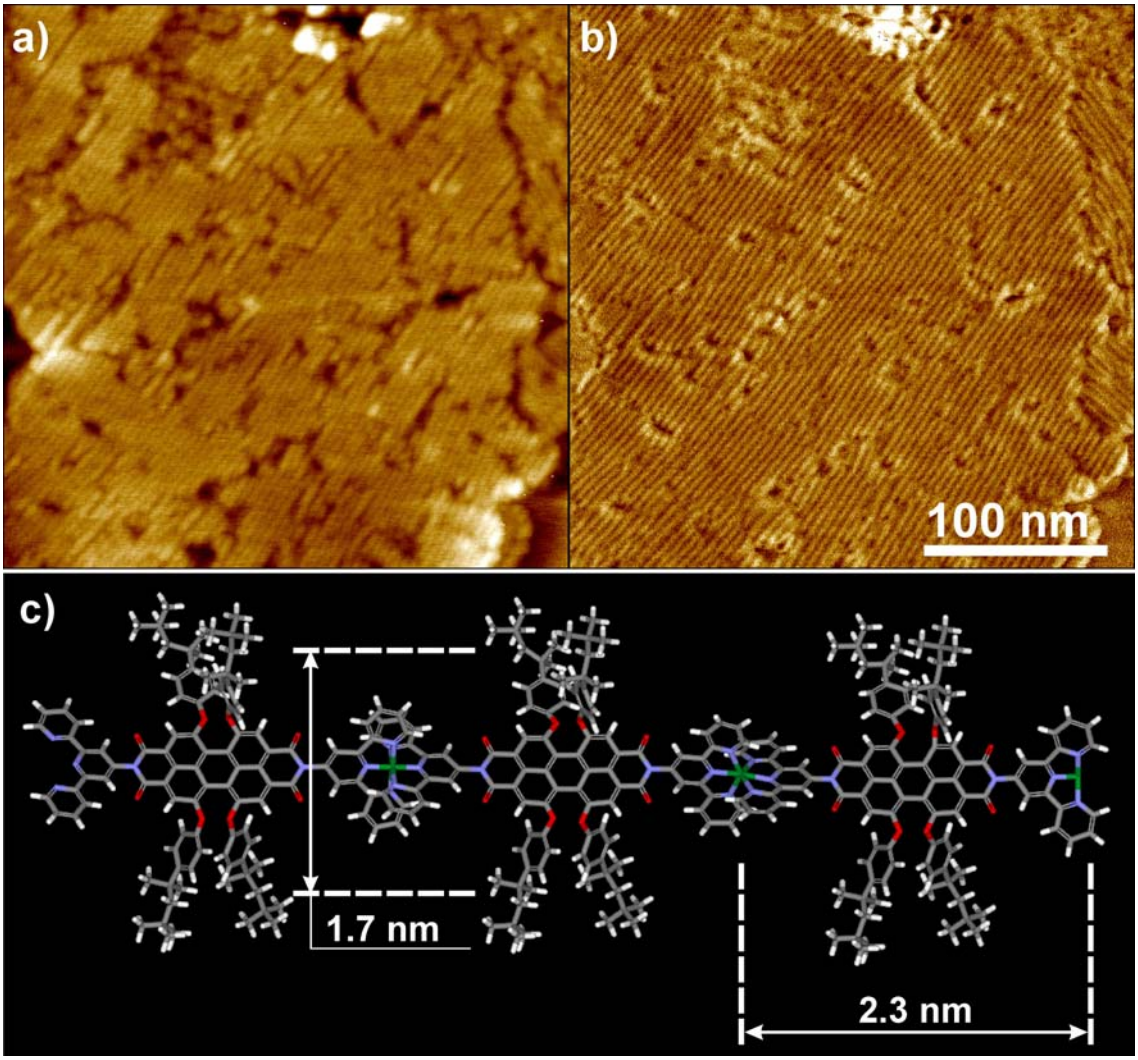


***Figure 1.*** (a,b) Taping mode AFM height (a) and phase (b) images of coordination polymers **14** on mica spin-coated (4000 rpm) from DMF solution (0.05 mg/mL). (c) Molecular modeling of coordination polymers **14**. Three repeat units are shown, carbon atoms are presented in grey, nitrogen and oxygen in blue and red, respectively, and zinc atoms in green.

Honeycomb-structured 2D nanopatterns by metal-ion-directed hierarchical self-assembly of tpy-PBI building blocks are described in Chapter 4 (Figure 2). Angular bis(tpy)-PBI ligand **15** with an angle of 120° between tpy moiety and PBI core was achieved by linking the 4′-position of tpy ligand to the meta-position of the phenylene spacer. Since 120° is the internal angle of a hexagon, metal-ion-mediated self-assembly of angular ditopic PBI ligand **15** led to the trinuclear metallocycle **16** with almost hexagonal geometry (Figure 2).

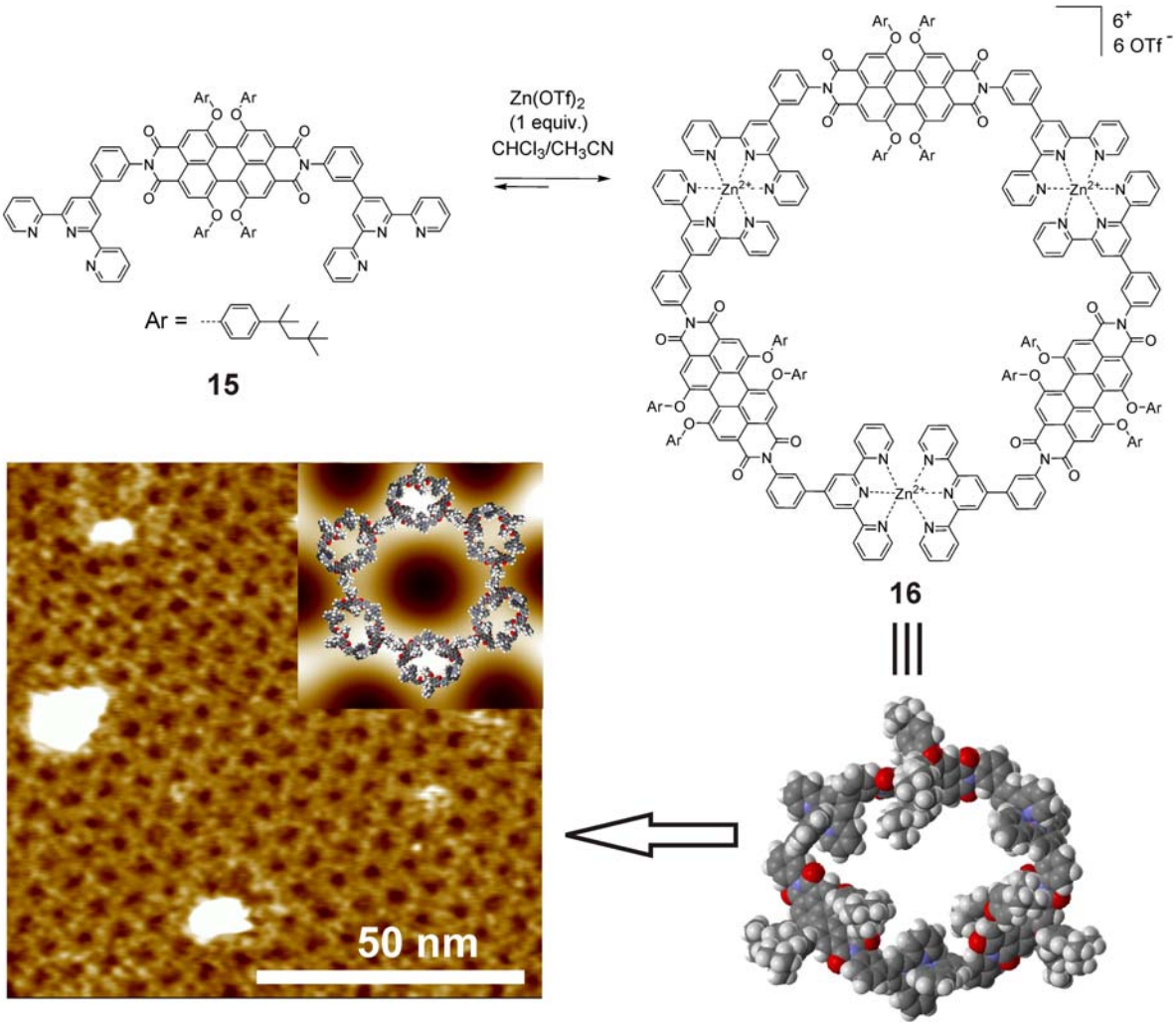


***Figure 2.*** Formation of trimeric metallomacrocycle **16** by Zn(II)-ion mediated self-assembly of bis(terpyridyl) PBI ligand **15** at a 1:1 stoichiometry of **15**/$Zn(OTf)_2$; bottom right: structure obtained by molecular modeling of trimeric Zn(II)-metallomacrocycle **16** (top view); bottom left: tapping mode AFM image of films spin-coated from DMF solution of **16** onto HOPG, inset shows a zoomed and filtered unit of the hexagonal domains and proposed model for the molecular arrangement of the cyclic trimers **16** in honeycomb structures.

Evidence for the formation of metallomacrocycle **16** at a exact 1:1 ratio of **15** and Zn(II) ion was obtained by $^1$H NMR and DOSY spectroscopy. Further structural

characterization of this macrocycle was achieved by MALDI-TOF MS providing expected mass peak of trimer **16** and additional peaks of multi-charged fragments. The optical properties of ditopic PBI ligand **15** and cyclic trimer **16** in DMF have been explored by UV/Vis absorption and fluorescence spectroscopy. The coordination of Zn(II) ion to tpy has little effect on the absorption properties of PBI unit as trimeric metallocycle **16** shows a similar absorption profile compared to that of ligand **15** with slightly shifted maxima. For metallocycle **16**, an extinction coefficient of 143.000 $M^{-1}cm^{-1}$ at $\lambda_{max}$ = 580 nm is observed, which is nearly three-times higher than that for ligand **15** (50.700 $M^{-1}cm^{-1}$ at 586 nm). From functional point of view, it is quite interesting that metallocycle exhibits a high fluorescence quantum yield of 75% (in DMF) which is very close to that of free ligand (81%). The self-assembly of cyclic array **16** on HOPG is investigated by AFM. The high resolution height AFM images clearly reveal the honeycomb-structured 2D assemblies of metallomacrocycles that cover the HOPG surface up to several square micrometers (Figure 2, bottom left).

In conclusion, new fluorescent supramolecular materials were prepared by metal-ion-directed self-assembly of tpy-functionalized PBI dyes. It was revealed that structural variation of tpy ligand can be utilized to tailor the structural properties of metallosupramolecular architectures as supramolecular polymers were obtained using linear bis(tpy)-PBI ligands and metallocycles were afforded from angular bis(tpy)-PBI ligands. Self-organization of metallocycles obtained from angular bis(tpy)-PBI building blocks led to the formation of 2D hexagonal patterns. These 2D nanopatterns are reminiscent of cyclic dye arrays in the purple bacterial photosynthetic membrane.

# Chapter 6

# Zusammenfassung

Selbstorganisierte metallsupramolekulare Assoziate organischer Farbstoffe haben in jüngster Vergangenheit zunehmend Interesse als Modellsysteme zur natürlichen Lichtsammlung und für photosynthetische Komplexe gefunden. Supramolekulare Strukturen, die durch Metallionengesteuerte Selbstorganisationsprozesse gebildet wurden, werden derzeit aber auch bereits als funktionelle Materialien in organischen Solarzellen, Sensoren und Leuchtdioden eingesetzt. Perylenbisimid (PBI)-Farbstoffe gehören zu den aussichtsreichsten Chromophor-Klassen für diese Anwendungen aufgrund ihrer hervorragenden optischen und elektronischen Eigenschaften sowie einer herausragenden Photostabilität.

Die vorliegende Arbeit beschäftigt sich mit der Synthese und Charakterisierung von fluoreszierenden metallsupramolekularen Koordinationspolymeren und Makrozyklen. Als Bausteine für die Bildung dieser makromolekularen Strukturen durch Metallionen-induzierte Selbstorganisationsprozesse wurden Terpyridin-funktionalisierte Perylenbisimide verwendet, welche die benötigte Geometrie besitzen. Die Charakterisierung der Komplexbildung und der optischen

Eigenschaften der gebildeten metallsupramolekularen Architekturen, sowie die Visualisierung der Makromoleküle und Charakterisierung ihrer Organisationseigenschaften auf verschiedenen Oberflächen wurden durchgeführt.

Das erste Kapitel der Arbeit gibt einen kurzen Überblick über die Metallionen-induzierte Selbstorganisation der Farbstoffe zu makrozyklischen und polymer Strukturen.

Kapitel 2 berichtet über Synthese der 1,7-Dipyrrolidinylperylenbisimide **2**-**8** in regioisomerenreiner Form aus 1,7-Dibromperylenbisimid **1**, welches durch Bromierung des Perylenbisanhydrids, nachfolgende Imidisierung mit Cyclohexylamin und sukzessiver Rekristallisation erhalten wurde.

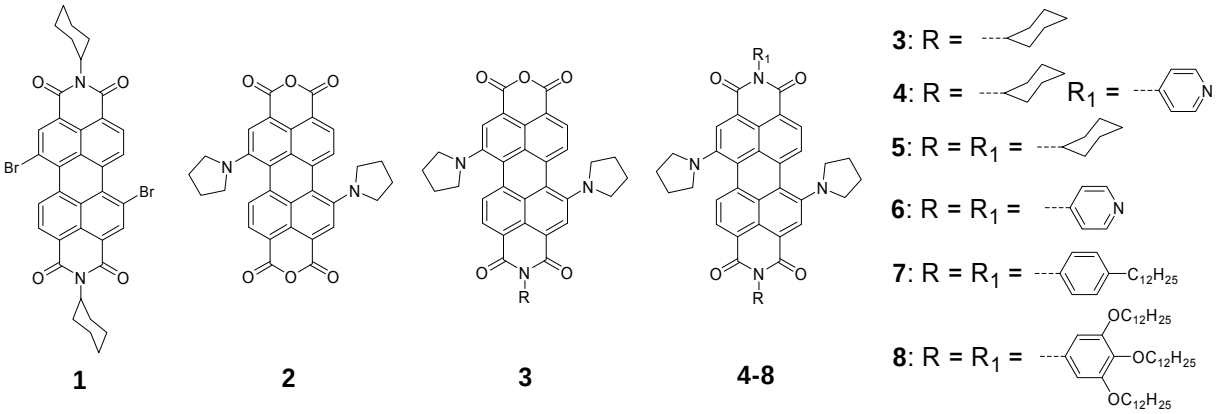


***Abbildung 1.*** 1,7-Dibromperylenbisimid **1**, 1,7-Dipyrrolidinyl-substituiertes Perylenbisanhydrid **2**, Monoimide **3** und Bisimide **4**-**8**.

Perylenmonoimide sind sehr wertvolle Synthesebausteine, weil ihre Funktionalisierung mit verschiedenen Substraten einen Zugang zu unsymmetrischen Perylenbisimiden ermöglicht. Die Reaktionsbedingungen für die partielle Verseifung von **5** wurden optimiert, um reines Dipyrrolidinyl-funktionalisiertes Perylenmonoimid **3** in hoher Ausbeute zu erhalten. Eine Verlängerung der Reaktionszeit führt zum Entstehen des Bisanhydrides **2**. Dies wurde erfolgreich auf die Synthese der regioisomerenreinen 1,7-Dipyrrolidinylperylenbisimide **6**-**8** angewendet, sowie auch auf die Synthese des neuen Bausteines **9** (Schema 1), welcher zur Bildung der metallosupramolekularen Polymere verwendet wurde (Kapitel 3).

Die Synthese von 2,2':6',2''-Terpyridin-funktionalisierten PBI (tpy-PBI) Bausteinen und ihre Metallionen-induzierte Selbstorganisation wird in Kapitel 3 vorgestellt. Diese Studien zeigen, dass die neuartigen ditopen Bis(tpy)-PBI-Liganden, in welchen die tpy-Einheiten direkt am PBI in Imidposition verknüpft sind, eine

reversible Bildung von Koordinationspolymeren bei Zugabe von Zn(II)-Ionen bewirken. Die Darstellung der Liganden **9**-**12** (Schema 1) erfolgte durch Umsetzung von 4'-Amino-2,2':6',2''-terpyridin mit dem jeweiligen Perylenbisanhydrid oder Perylenmonoimid unter Bildung des entsprechenden Perylenbisimides.

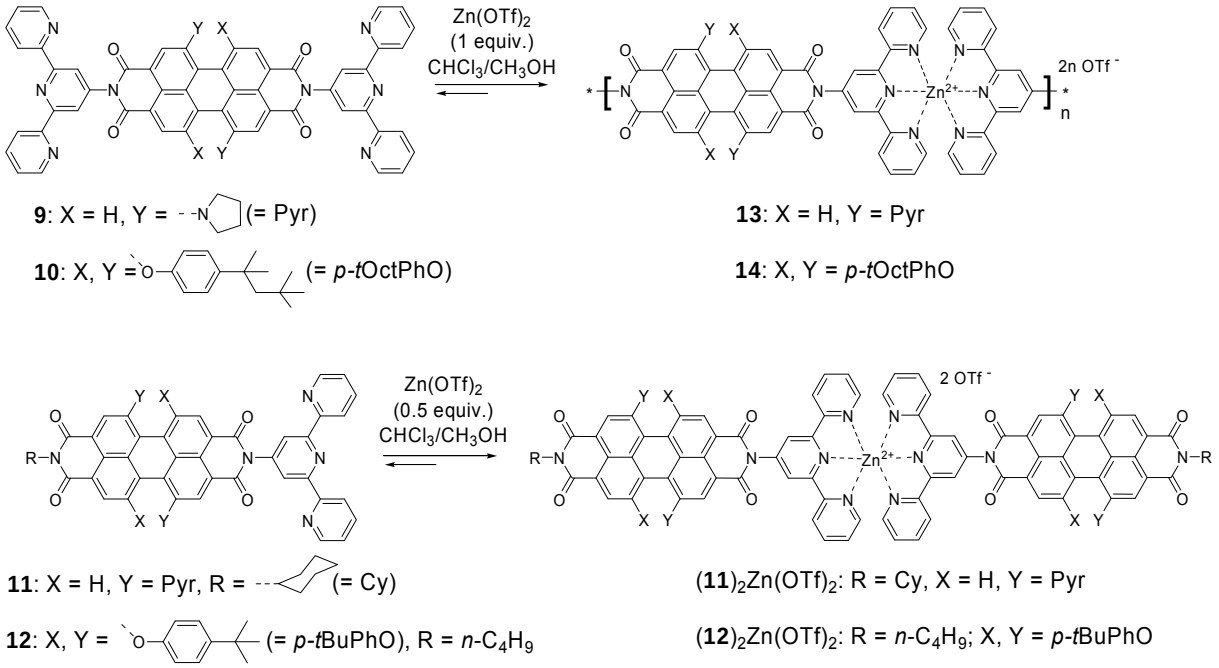


***Schema 1.*** Neue Terpyridin-funktionalisierte Bausteine **9**-**12** und ihre Metallionen-gesteuerten Architekturen: Metallsupramolekulare Polymere **13** und **14**, und Dimer-Komplexe $(\mathbf{11})_2Zn(OTf)_2$ und $(\mathbf{12})_2Zn(OTf)_2$.

Vor der Untersuchung der Selbstorganisationseigenschaften der Bis(tpy)-PBI-Liganden **9** und **10** unter Metallioneneinfluss, wurde zunächst anhand der Modellverbindungen **11** und **12**, die nur einen Terpyridin-Rezeptor tragen, die Komplexierung mit Zn(II)-Ionen untersucht, da diese Liganden Dimer-Komplexe bei einem Verhältnis von 2:1 von Ligand zu Zn(II)-Ion bilden. Die so erhaltenen spektroskopischen Daten und vor allem die Informationen aus den NMR-Titrationsexperimenten sind sehr hilfreich für die Aufklärung der supramolekularen Polymerisation der ditopen Liganden. Einen weiteren Beweis für die Bildung von Dimer-Komplexen lieferte MALDI-TOF-Massenspektrometrie. Die Umsetzung des jeweiligen Bis(tpy)-PBI-Liganden mit exakt einem Äquivalent Zn(II)-Ionen bewirkte die Bildung des supramolekularen Koordinationspolymers, welches durch $^1$H-NMR-, DOSY-NMR- und UV/Vis-Spektroskopie eingehender untersucht werden konnte.

Mittels diffusionsabhängiger NMR-Technik konnte die Änderung des Diffusionskoeffizienten des Bis(tpy)-PBI-Systems unter schrittweiser Zugabe der Zn(II)-Ionen detektiert werden. Die Zugabe von Zn(II)-Ionen führte zuerst zur Bildung des Koordinationspolymers und in der Folge zu seiner Fragmentierung, welche einen reversiblen Selbstorganisationsprozess offenbarte. Die Komplexierung des Bis(tpy)-PBI-Liganden mit Zn(II)-Ionen beeinflusste nur geringfügig die Fluoreszenzeigenschaften der Perylenbisimideinheit, so dass die optischen Eigenschaften des PBI-Chromophors im Polymer erhalten blieben.

Durch Rasterkraftmikroskopie (AFM)-Messungen konnten die metallosupramolekularen Polymere und ihre Selbstorganisation auf unterschiedlichen Oberflächen visualisiert werden (Abbildung 2).

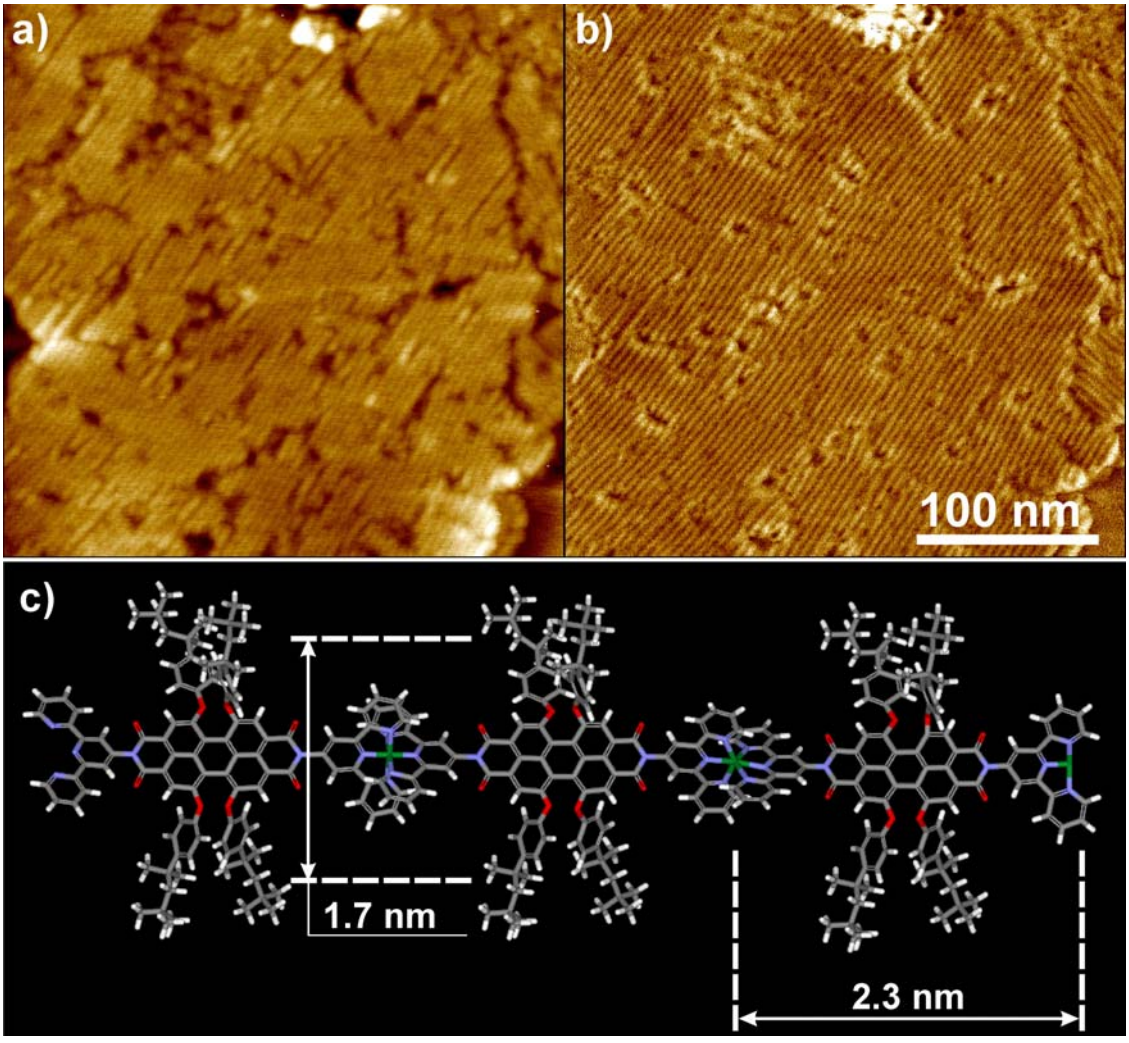


***Abbildung 2.*** (a,b) „Tapping mode“ AFM-Höhen- (a) and Phasenbilder (b) des Koordinationspolymers **14** auf Mica. (c) Molekulare Modellierung des Koordinationspolymers **14**. Drei Wiederholungseinheiten sind gezeigt, Kohlenstoffatome sind grau, Stickstoff- und Sauerstoffatome sind blau bzw. rot und Zinkatome grün abgebildet.

Das in dieser Arbeit vorgeschlagene Konzept, die tpy-Einheit direkt mit dem PBI ohne Phenylenbrücke zu verbinden, ermöglichte die Bildung der starren supramolekularen Polymere mit deutlich längerer durchschnittlicher Kettenlänge, als für Bis(tpy)-PBI-Liganden mit Phenylenbrücke. Die Auswertung der AFM-Bilder ergab eine durchschnittliche Kettenlänge von ca. 35 Wiederholungseinheiten, was einem Molekulargewicht von *ca*. 30 000 bis 60 000 g/mol entspricht. Die AFM-Messungen zeigten ebenso die Bildung einer homogenen Monoschicht auf negativ geladenem Glimmer, sowie auf neutralem hochgeordneten pyrolytischen Graphit (HOPG). Ein weiterer supramolekularer Strukturbildungsprozess wird beschrieben, in dem der polykationische Charakter der Polymere genutzt wurde, um einen polyelektrolytischen Film aus Koordinationspolymeren mit unterschiedlichen optischen Eigenschaften im alternierenden Verfahren herzustellen. Der sukzessive Aufbau der Schichten durch die „Layer-by-Layer“ (LBL)-Beschichtungsmethode ließ sich über UV/Vis-Spektroskopie verfolgen. Ferner konnten die Oberflächendichte Γ der PBI-Chromophore in diesem Film und der quadratische Mittelwert (*RMS*) der Oberflächenrauheit bestimmt werden.

Bienenwabenartige, zweidimensionale Nanostrukturen, die durch Metallionen-induzierte hierarchische Selbstorganisationsprozesse von PBI-Liganden gebildet wurden, sind in Kapitel 4 beschrieben (Abbildung 3). Der abgewinkelte Bis(tpy)-PBI-Ligand **15** weist einen Winkel von 120° zwischen tpy-Rezeptor und PBI auf, was durch eine Verbindung des tpy-Liganden an der 4'-Position mit der *meta*-Position der Phenylenbrücke erreicht werden konnte. Da der interne Winkel eines Sechseckes 120° beträgt, führte die Metallionen-induzierte Selbstorganisation solcher winkelförmiger ditoper PBI-Liganden zur Bildung eines zyklischen Trimers **16** mit nahezu hexagonaler Geometrie. Molekulare Modellierung der Assoziate zeigte, dass keine sterischen Behinderungen bei dem Selbstorganisationsprozess der PBI-Liganden mit Zn(II)-Ionen zu erwarten waren (Abbildung 3).

Den Beweis für die Bildung des Metallomakrozyklus **16** durch reversible Zn(II)-Bis(tpy)-Koordination lieferten $^{1}$H-NMR-DOSY-Untersuchungen. Eine weitere strukturelle Charakterisierung dieses zyklischen Trimers wurde durch MALDI-TOF-Massenspektrometrie erhalten. Das Massenspektrum zeigt die Anwesenheit des Zyklus **16** und seiner multigeladenen Fragmente. Die optischen Eigenschaften des PBI-Liganden **15** und zyklischen Trimers **16** in DMF wurden ebenso durch UV/Vis-Absorptions- und Fluoreszenzspektroskopie untersucht. Die Koordination der Zn(II)-

Ionen beeinflusste die exzellenten Absorptions- und Fluoreszenzeigenschaften dieses gewinkelten Liganden nur geringfügig. Der Extinktionskoeffizient des Metallmakrozykluses beträgt 143 000 $M^{-1}cm^{-1}$ bei $\lambda_{max}$ = 580 nm, welcher fast dreimal höher ist, als der des Liganden **15** (50 700 $M^{-1}cm^{-1}$ bei 586 nm). Aus funktioneller Sicht ist es sehr interessant, dass der Metallzyklus **16** eine Fluoreszenzquantenausbeute von 75% (in DMF) aufweist, die sehr nahe an der des unkomplexierten PBI-Liganden **15** liegt (81%).

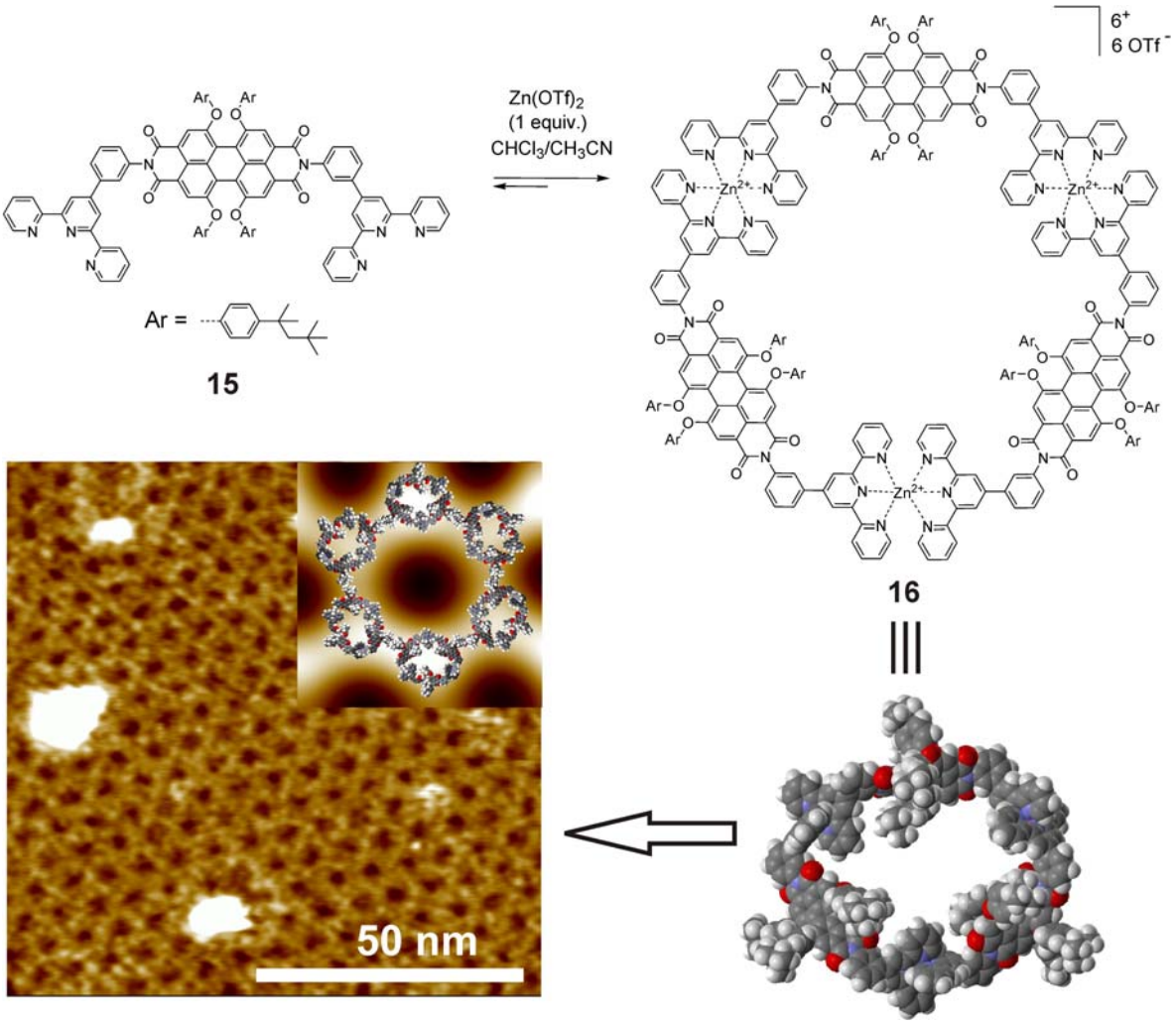


***Abbildung 3.*** Bildung eines hexagonalen Metallmakrozyklus **16** durch Zn(II)-Ionen-induzierte Selbstorganisation des Bis(tpy)-PBI-Liganden **15** bei Erreichen einer 1:1-Stöchiometrie von **15**/$Zn(OTf)_2$; unten rechts: durch molekulare Modellierung berechnete Struktur des Metallmakrozyklus **16** (Ansicht von oben); unten links: „tapping mode“ AFM-Aufnahme des Filmes, der mittels Rotationsbeschichtungsmethode der DMF-Lösung von **16** auf HOPG aufgetragen wurde; der Einschub zeigt eine vergrößerte und gefilterte Einheit der sechseckigen Domänen und das vorgeschlagene Modell der molekularen Anordnung der zyklischen Trimere **16** in den Wabenstrukturen.

Die Visualisierung und der Selbstorganisationsprozess des zyklischen Trimers **16** auf HOPG wurden durch AFM-Messungen untersucht (Abbildung 3, unten links). Die hochaufgelösten AFM-Aufnahmen zeigen eine hierarchische 2D-Anordnung des Metallmakrozyklus in einer bienenwabenförmig strukturierten Schicht, welche die Oberfläche bis zu mehreren Quadratmikrometern bedeckt.

Zusammenfassend wurden in dieser Arbeit neue fluoreszierende supramolekulare Materialien durch Metallionen-induzierte Selbstorganisations-prozesse hergestellt. Es wurde gezeigt, dass die strukturelle Änderung des tpy-Liganden für die Modifizierung der strukturellen Eigenschaften seines Metall-Komplexes genutzt werden konnte. Es konnte gezeigt werden, dass ein linearer Bis(tpy)-PBI-Ligand metallsupramolekulare Polymere liefert, während ein gewinkelter Bis(tpy)-PBI-Baustein die Bildung von zyklischen metallosupramolekularen Trimeren ermöglicht. Bei der Adsorption dieser supramolekularen Strukturen auf Substrate konnten zweidimensionale Monolagen beobachtet werden. Im Falle des gewinkelten Bis(tpy)-PBI-Liganden tritt die Bildung eines 2D-hexagonalen Musters auf. Diese 2D-Nanostrukturen erinnern an zyklische Farbstoffanordnungen in der photosynthetischen Membran von Purpurbakterien.

# Appendix

## Atomic Force Microscopy Investigations of Dye Assemblies

This *Appendix* gives a brief overview on atomic force microscopy (AFM)[1] investigations of supramolecular dye assemblies that I have carried out in cooperation with other members of our and other research groups at the Institut für Organische Chemie in Würzburg. The chemically pre-designed dye molecules form defined supramolecular self-assemblies in one, two or three dimensions by virtue of noncovalent interactions. The major objective of these investigations is to study the arrangement of special functional units with nanometer dimensions into defined molecular architectures in solution and on surfaces with potential applications of these systems in nanotechnology, for example as molecular information storage devices, diagnostic sensors, functional surfaces. This requires a precise control of the structures at very different length scales ranging from molecular size to micrometers. The visualization of nanometer-sized self-assembled structures and their self-organization on surfaces has been possible by AFM imaging that is a fundamental and an integral part of the research in supramolecular chemistry.

## Rigid-Rod Metallosupramolecular Polymers of Dendronized Diazadibenzoperylene Dyes[2]

The synthesis, characterization, and metal-ion-mediated supramolecular polymerization of diazadibenzoperylenes (DABP) **1**-**3** equipped with first to third generation Fréchet-type dendrons were reported.[2]

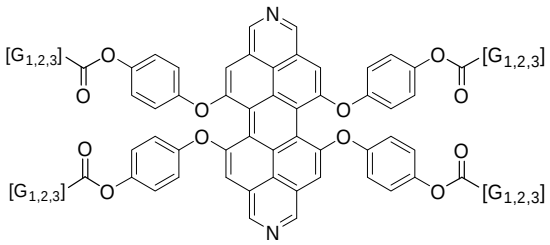

**1-3**

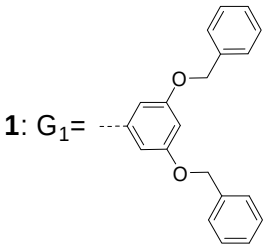

**1**: $G_1$=

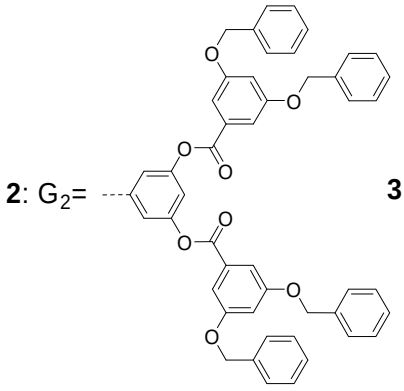

**2**: $G_2$=

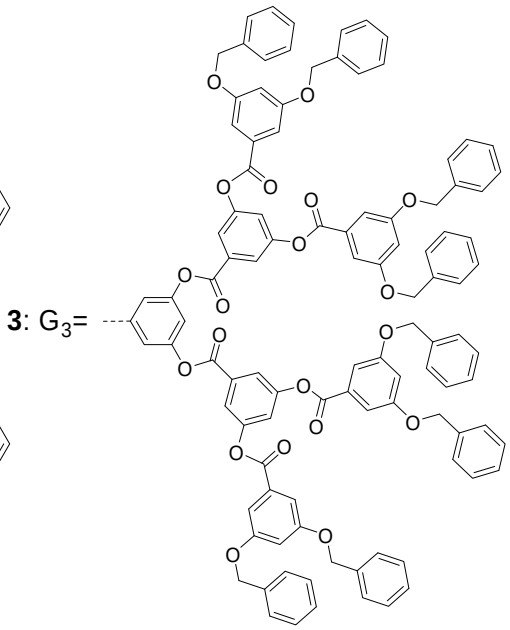

**3**: $G_3$=

Silver(I) ion-mediated polymerization of DABP dendrimers was investigated by NMR spectroscopy. To provide further evidence for metal-ion-directed polymerization and to gain insight into the structural features of the desired polymers, AFM investigations were performed. Figure 1A illustrates schematically the formation of encapsulated rigid-rod coordination polymers by metal-ion-directed self-assembly of DABP dyes and Figure 1B-D shows the tapping mode AFM images of samples prepared by spin-coating solutions of 1:1 stoichiometric mixtures of **1**-**3** with AgOTf in DMF onto HOPG. These studies provided clear evidence that dendronized diaza aromatic building

blocks can be polymerized by metal ion coordination to afford defined rigid-rod polymers.[2]

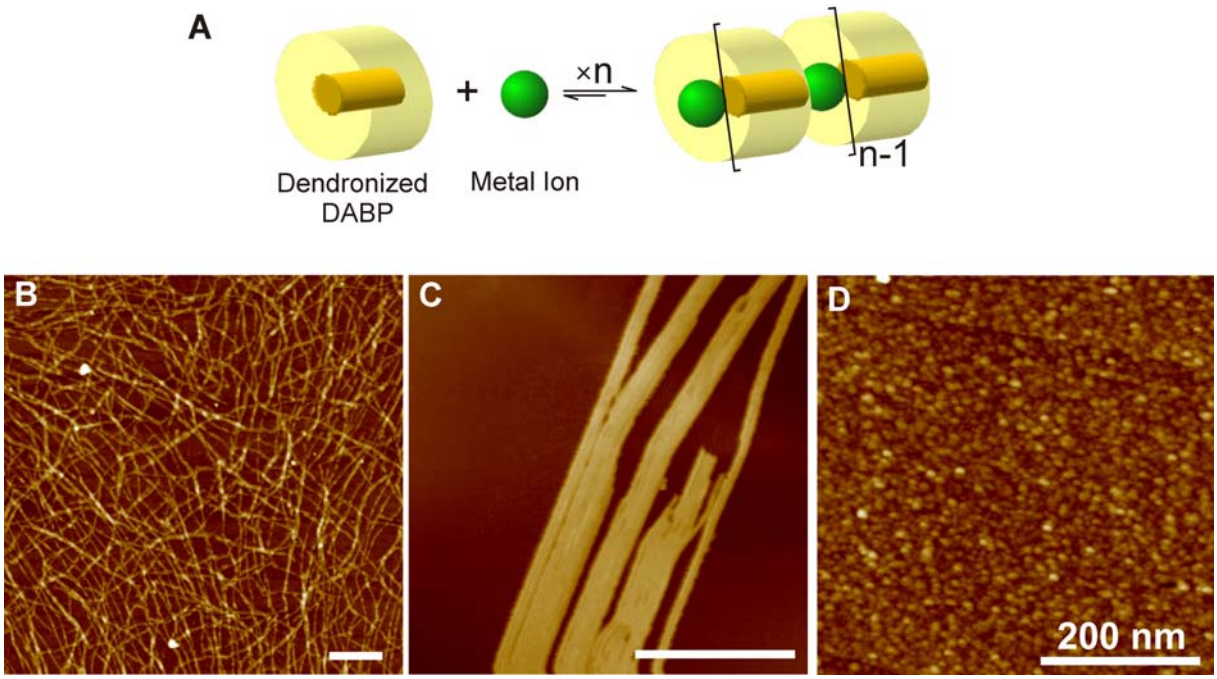


***Figure 1.*** (A) Schematically representation of the formation of coordination polymers. (B-D) AFM height images of ligands **2**, **3**, and **4** in the presence of one equivalent of AgOTf (B, C, and D, respectively) on HOPG. Scale bar: 200 nm; z scale: 12 nm. (Reprinted with permission from ref. 2. Copyright (2006) Wiley-VCH Verlag GmbH & Co. KGaA, Weinheim).[2]

The supramolecular polymerization was shown to be highly dependent on the generation number of the attached dendrons; thus, first and second generation dendrimers afforded polymeric materials (Figure 1B,C), while the third generation resisted polymerization as a result of the shielding of the aza coordination site by dendritic wedges (Figure 1D). The first and second generation, metal ion/dye-encapsulated rigid-rod polymers constitute an interesting class of π-conjugated materials.

## Functional Organogels from Highly Efficient Organogelator Based on Perylene Bisimide Semiconductor[3]

Perylene bisimide (PBI) organogelator **4** exhibits pronounced gelation capabilities leading to interpenetrating networks of PBI stacks in a broad variety of solvents, including electron-rich aromatic solvents such as thiophene.[3] AFM is the method of choice to explore the morphology on the nano- and mesoscopic scale that directs the network formation and the concomitant gelation capabilities. Remarkably, quite similar well-defined fibrous structures could be observed upon spin-coating of diluted gel solutions from different solvents (Figure 2).

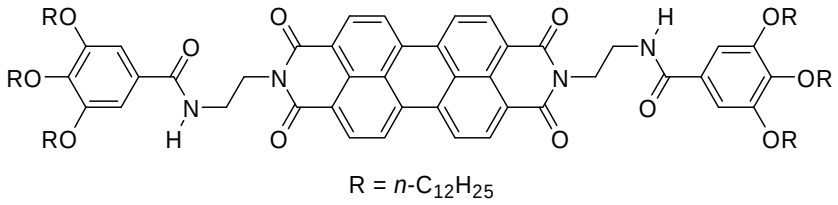


R = *n*-$C_{12}H_{25}$

**4**

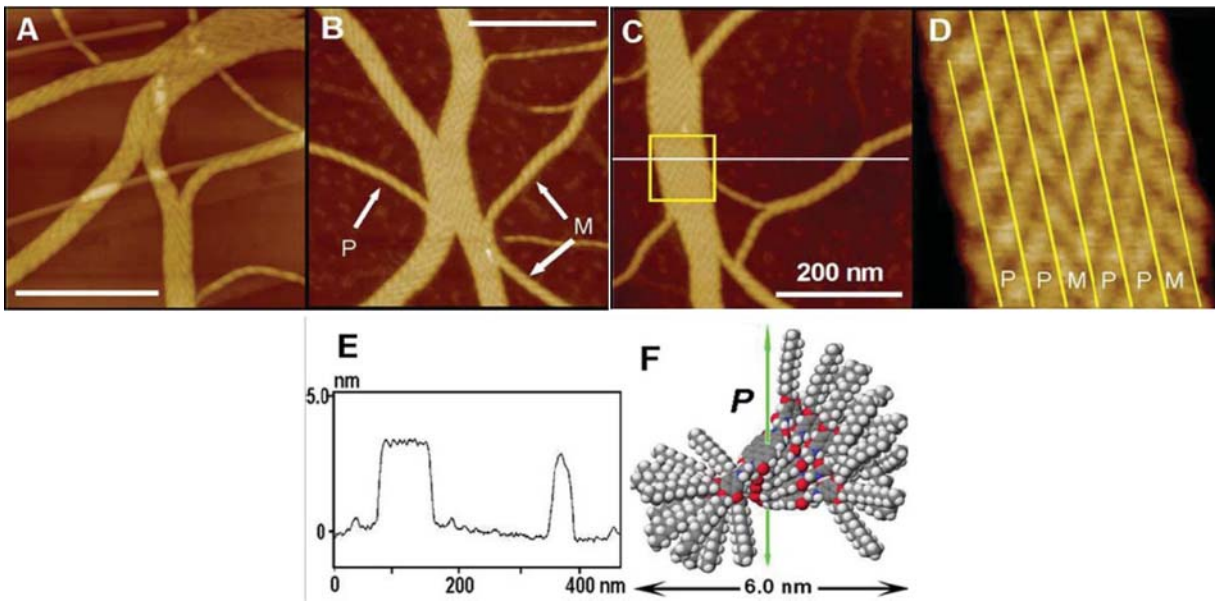


***Figure 2.*** AFM height images of films spin-coated from diluted gel solutions of **1** in toluene ($1\times10^{-4}$ M) onto HOPG (A) and mica (B and C); (D) is zoomed region image from (C). In images (A), (B) and (C) the scale bar corresponds to 200 nm and the z scale is 10 nm. (E) shows the cross-section analysis corresponding to the white line of (C) and (F) depicts a suggested packing model for self-assembled *P*-configured hydrogen-bonded aggregate with a diameter of 6.0 nm. (Reprinted with permission from ref. 3. Copyright (2006) The Royal Society of Chemistry).[3]

## One-dimensional Luminescent Nanoaggregates of Perylene Bisimides[4]

One-dimensional columnar stacking of highly photoluminescent PBI **5** was observed in the bulk sample as well as in thin films cast from methylcyclohexane (MCH) solution. AFM revealed a fingerprint-like structure composed of long and bending columns of PBI aggregates (Figure 3).

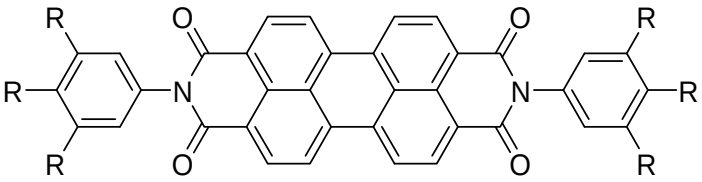


R = *n*-$C_{12}H_{25}$

**5**

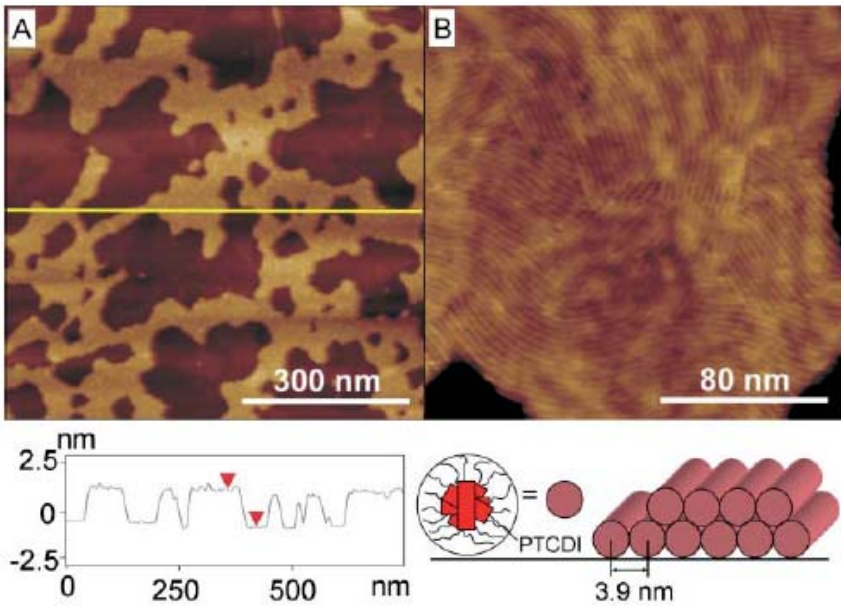


***Figure 3.*** AFM image of a thin-film spin-coated from solution of **5** in MCH ($4\times10^{-4}$ M) onto HOPG. (A) Topography image and (B) higher resolution image. Cross section analysis corresponding to the yellow line of (A) and proposed model for the packing of columnar stacks on HOPG. (Reprinted with permission from ref. 4. Copyright (2006) The Royal Society of Chemistry).[4]

The width of the column was about 3.9 nm and the height was 2.3 nm. Both values are in good agreement with molecular modelling studies, which suggest a length of 4 nm for **5** along its long axis for fully extended alkyl chains.

**Supramolecular Construction of Fluorescent J-Aggregates Based on Hydrogen-Bonded Perylene Dyes**[5]

The unprecedented packing of PBI dyes **6** in a strongly slipped arrangement could be tailored by supramolecular design through perylene core twisting enforced by bay substituents, the attachment of trialkoxyphenyl wedges, and head-to-tail alignment of the dyes through hydrogen-bonding interactions. The outstanding fluorescence properties of the chosen fluorophore provided for the first time J-aggregates that fluoresce with quantum yields of near unity.[5]

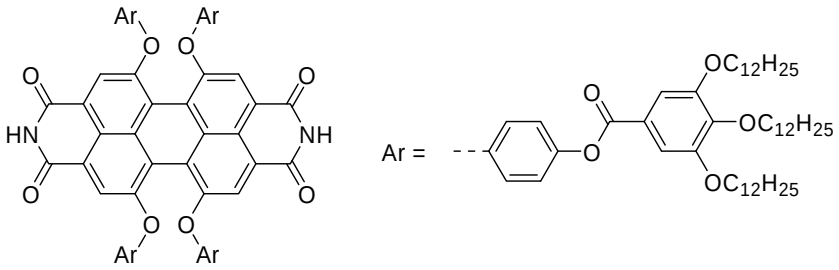


**6**

AFM was used to elucidate the size and shape of these aggregates. AFM images on silicon wafers (Figure 4) reveal a network of defined fibres whose size (height: 2.0±0.2 nm; width: 8.4±2.6 nm) is in agreement with the expected dimensions of a double string cable of the type suggested in Figure 4d. According to this model, a rigid inner core (diameter ~3.0 nm) composed of helically twisted PBIs (red) with four appended aromatic substituents (blue) and surrounded by a flexible periphery of twelve $C_{12}H_{25}$ aliphatic chains (gray).

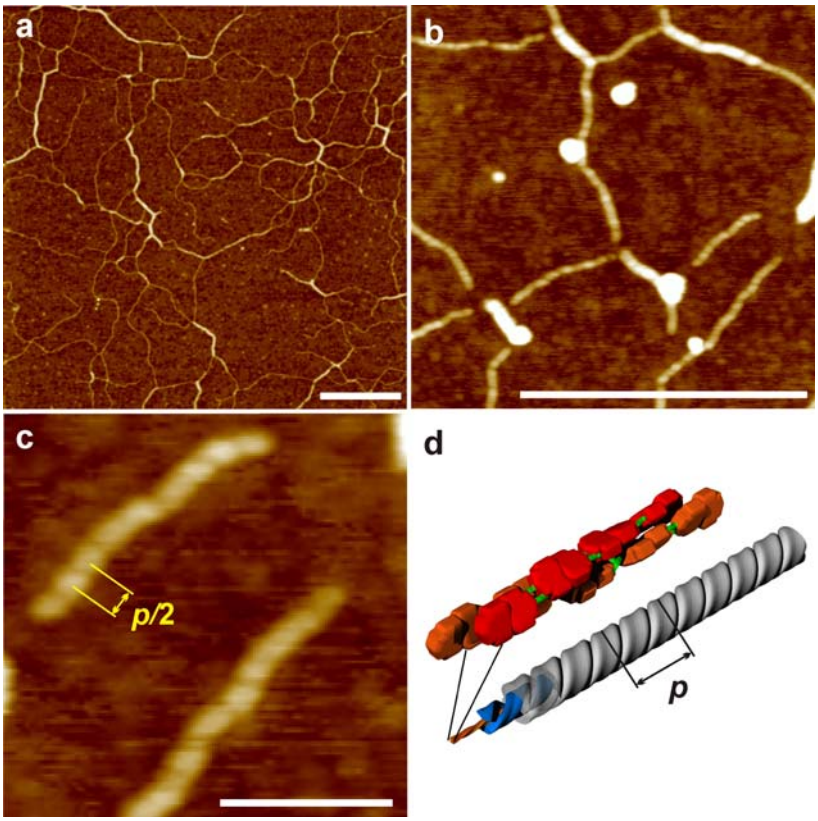


***Figure 4.*** (a, b)Tapping mode AFM images of self-assemblies of **6** on silicon wafer spin-coated (2000 rpm) from a $9\times10^{-6}$ M solution in MCH. The scale bars represent 300 nm, z scale is 6 nm. Image (c) shows a magnified section of image (b), with a scale bar representing 45 nm. In (d), the aggregate model is shown with distance *p* representing the helical pitch. The periodic top-to-top length (corresponds to the half pitch *p*/2) of the helical structures in (b,c) was measured as 6.5 ± 1.7 nm and is in good agreement with the calculated value of 6 nm. (Reprinted with permission from ref. 5. Copyright (2007) Wiley-VCH Verlag GmbH& Co. KGaA, Weinheim).[5]

## A Black Perylene Bisimide Super Gelator with an Unexpected J-Type Absorption Bank[6]

Chiral core-unsubstituted PBI **7** self-assembles into dye aggregates with strongly bathochromically shifted J-type absorption bands in solution and in the organogel state.[6] Circular dichroism (CD) spectroscopy and AFM revealed an efficient chirality transfer from the chiral peripheral side chains to the supramolecular level for these dye aggregates. Thus, the AFM images of spin-coated solutions of PBI **7** consistently showed the same characteristic nanofibers that are of left-handed helicity exclusively, irrespective of the choice of solvent or substrate (Figure 5). The

height of these fibers is 2.2–2.7 nm and the helical pitch is 6.5–6.8 nm, revealing a negligible influence of the solvent and substrate on the dimensions of fibers.

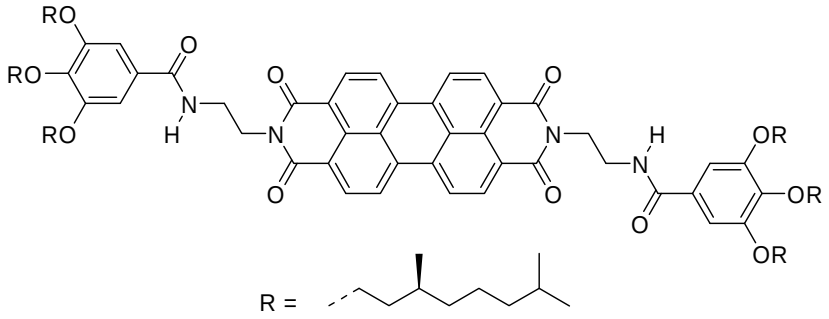


**7**

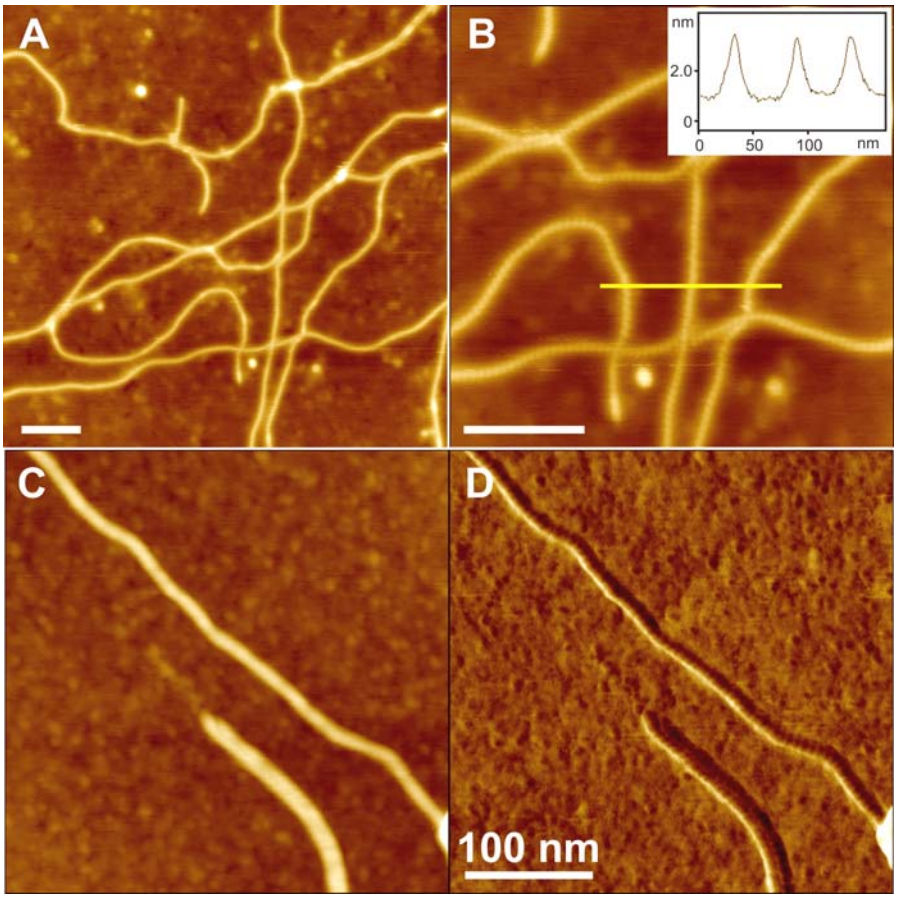


**Figure 5.** AFM height (A,B,C) and phase (D) images of films spin-coated from diluted gel solutions of PBI **7** in MCH (0.6mM) onto HOPG (A,B) and in toluene (0.2mM) onto silicon wafer (C,D). The white scale bar in images A,B and C,D corresponds to 100 and 200 nm, respectively. The z scale is 8 nm in (A,B) and 9 nm in (C,D). The inset in (B) shows the cross-section analysis along the yellow line. (Reprinted with permission from ref. 6. Copyright (2008) Wiley-VCH Verlag GmbH& Co. KGaA, Weinheim).[6]

## A New Type of Soft Vesicle-Forming Molecule: An Amino Acid Derived Guanidiniocarbonyl Pyrrole Carboxylate Zwitterion[7]

A hierarchical self-assembly of small zwitterion **8**, which does not have a classical amphiphilic structure with well-separated polar and non-polar segments, led to the formation of soft vesicles even in polar solutions.[7] AFM, dynamic light scattering (DLS), and transmission electron microscopy (TEM) were performed to investigate the self-assembly of **8**. For AFM analysis, a solution of **8** in DMSO was spin-coated onto silica wafer and analyzed in the tapping mode. Figure 6 shows spherical particles with a mean diameter of ca. 25 nm and a height of ca. 4 nm, about six times smaller than the average diameter.

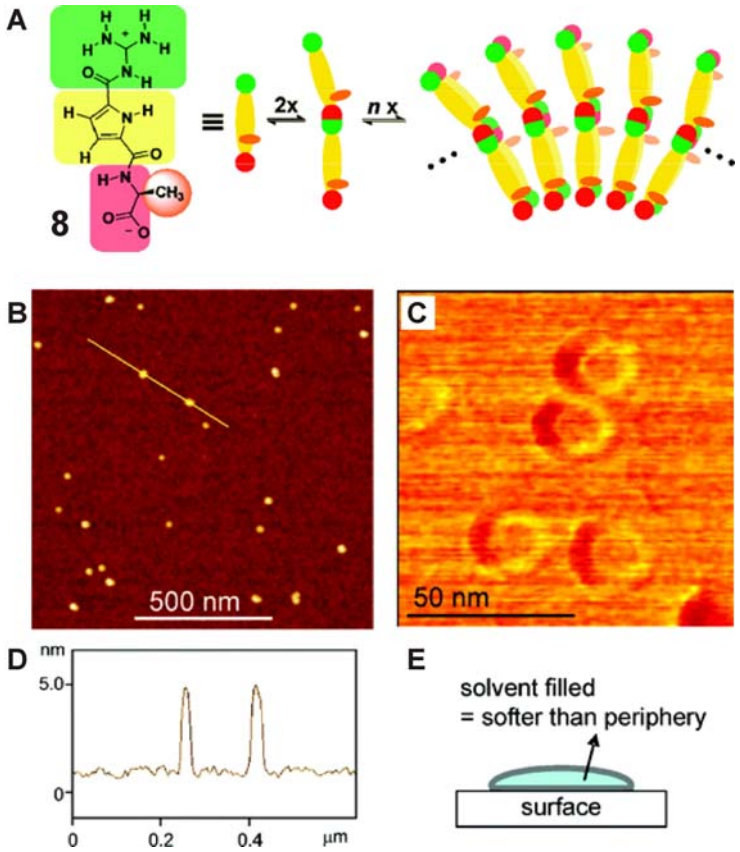


***Figure 6.*** Suggested membrane formation via the self-assembly of **8** (A). AFM height image (B) of **8** on silica wafer (Z scale is 12 nm) shows spherical aggregates. The cross section analysis along the yellow line (D) provides a mean diameter of ca. 25 nm and a height of 4 nm. The appearance of the vesicles in the phase image (C) is typical for deformed soft hollow vesicles on a surface (E). (Reprinted with permission from ref. 7. Copyright (2008) American Chemical Society).[7]

The mean diameter of 25 nm of the particles is significantly larger than the molecular dimension of zwitterion **8** (*ca.* 1.4 nm estimated from molecular modelling). Therefore, it is very unlikely that the particles are micelle-like aggregates, which generally have a diameter about twice as large as the molecular dimension. Instead, the profile of the particles in the phase image (Figure 6C) clearly indicates these particles as soft, hollow vesicles, which typically show a lower central part that is surrounded by a higher periphery in AFM experiments.

## Conclusion

Atomic force microscopy is a very important tool in modern supramolecular chemistry. Using this technique, the visualization and structural characterization of nanometer-sized self-assembled architectures are possible. Here it could be shown that AFM investigations of supramolecular dye assemblies provide information about their structural and organizational properties.

## References

[1] a) G. Binnig, C. F. Quate, C. Gerber, *Phys. Rev. Lett.* **1986**, *56*, 930-933; b) F. Giessibl, *Rev. Mod. Phys.* **2003**, *75*, 949-983.

[2] F. Würthner, V. Stepanenko, A. Sautter, *Angew. Chem.* **2006**, *188*, 1973-1976; *Angew. Chem. Int. Ed*. **2006**, *45*, 1939–1942.

[3] X.-Q. Li, V. Stepanenko, Z. Chen, P. Prins, L. D. A. Siebbeles, F. Würthner, *Chem. Commun.* **2006**, 3871–3873.

[4] a) F. Würthner, Z. Chen, V. Dehm, V. Stepanenko, *Chem. Commun.* **2006**, 1188–1190; b) Z. Chen, V. Stepanenko, V. Dehm, P. Prins, L. D. A. Siebbeles, J. Seibt, P. Marquetand, V. Engel, F. Würthner, *Chem. Eur. J.* **2007***, 13,* 436-449.

[5] T. Kaiser, H. Wang, V. Stepanenko, F. Würthner, *Angew. Chem.* **2007**, *119*, 5637-5640; *Angew. Chem. Ind. Ed.* **2007**, *46*, 5541-5544.

[6] F. Würthner, C. Bauer, V. Stepanenko, S. Yagai, *Adv. Mater.* **2008***, 20*, 1695–1698.

[7] T. Rehm, V. Stepanenko, X. Zhang, F. Würthner, F. Gröhn, K. Klein, C. Schmuck, *Org. Lett.* **2008**, *10*, *7*, 1469–1472.

## List of Publications

*"Self-Assembly and Layer-by-Layer Deposition of Metallosupramolecular Perylene Bisimide Polymers"*, **V. Stepanenko**, F. Würthner, *submitted*

*"Hierarchical Self-Assembly of Cyclic Dye Arrays into Honeycomb 2D Nanonetworks"*, **V. Stepanenko**, F. Würthner, *Small* **2008**, *4,* 2158–2161.

(DOI: 10.1002/smll.200801069)

*"Control of H- and J-Type $\pi$ Stacking by Peripheral Alkyl Chains and Self-Sorting Phenomena in Perylene Bisimide Homo- and Heteroaggregates"*, S. Ghosh, X.-Q. Li, **V. Stepanenko**, F. Würthner, *Chem. Eur. J.* **2008**, *in print*.

(DOI: 10.1002/chem.200801454)

*"A Black Perylene Bisimide Super Gelator with an Unexpected J-Type Absorption Band",* F. Würthner, C. Bauer, **V. Stepanenko**, S. Yagai, *Adv. Mater.* **2008***, 20*, 1695-1698.

(DOI: 10.1002/adma.200702935)

*"A New Type of Soft Vesicle-Forming Molecule: An Amino Acid Derived Guanidiniocarbonyl Pyrrole Carboxylate Zwitterion"*, T. Rehm, **V. Stepanenko**, X. Zhang, F. Würthner, F. Gröhn, K. Klein, C. Schmuck, *Org. Lett.* **2008**, *10*, *7*, 1469-1472.

(DOI: 10.1021/ol8002755)

*„Supramolecular Construction of Fluorescent J-Aggregates Based on Hydrogen-Bonded Perylene Dyes"*, T. Kaiser, H. Wang, **V. Stepanenko**, F. Würthner, *Angew. Chem.* **2007**, *119*, 5637-5640; *Angew. Chem. Ind. Ed*. **2007**, *46*, 5541-5544.

(DOI: 10.1002/anie.200701139)

*"Photoluminescence and Conductivity of Self-Assembled π-π Stacks of Perylene Bisimide Dyes"*, Z. Chen, **V. Stepanenko**, V. Dehm, P. Prins, L. D. A. Siebbeles, J. Seibt, P. Marquetand, V. Engel, F. Würthner, *Chem. Eur. J.* **2007***, 13,* 436-449.

(DOI: 10.1002/chem.200600889)

*„One-dimensional luminescent nanoaggregates of perylene bisimides"*, F. Würthner, Z. Chen, V. Dehm, **V. Stepanenko**, *Chem. Commun.* **2006**, 1188-1190.

(DOI: 10.1039/b517020f)

*„Rigid-Rod Metallosupramolecular Polymers of Dendronized Diazadibenzoperylene Dyes"*, F. Würthner, **V. Stepanenko**, A. Sautter, *Angew. Chem*. **2006**, *188*, 1973–1976; *Angew. Chem. Int. Ed*. **2006**, *45*, 1939-1942.

(DOI: 10.1002/ange.200503717)

*"Functional organogels from highly efficient organogelator based on perylene bisimide semiconductor"*, X.-Q. Li, **V. Stepanenko**, Z. Chen, P. Prins, L. D. A. Siebbeles, F. Würthner, *Chem. Commun*. **2006**, 3871-3873.

(DOI: 10.1039/b611422a)

*"Preparation and Characterization of Regioisomerically Pure 1,7-Disubstituted Perylene Bisimide Dyes"*, F. Würthner, **V. Stepanenko**, Z. Chen, C. R. Saha-Möller, N. Kocher, D. Stalke, *J. Org. Chem.* **2004**, *69*, 7933-7939.

(DOI: 10.1021/jo048880d)

*"Macroheterocyclic Compounds with 2,3-Pyridino(pyrazino)pyrrole and 1,3,4-Thiadiazole Residues"*, M. A. Kulikov, Yu. G. Vorobev, G. R. Berezina, **V. Stepanenko**, *Rus. J. Chem*. **2004**, *74*, 954-956.

(DOI: 10.1023/B:RUGC.0000042435.39243.5b)

*"Waste-Free and Facile Solid-State Protection of Diamines, Anthranilic Acid, Diols, and Polyols with Phenylboronic Acid"*, G. Kaupp, M. R. Naimi-Jamal, **V. Stepanenko**, *Chem. Eur. J.* **2003**, *9*, 4156-4160.

(DOI: 10.1002/chem.200304793)